Hydro-geomorphic controls on the development and distribution of acid sulfate soils in Central Java, Indonesia and robust remote sensing and GIS methods for acid sulfate soil mapping

Author:
Widyatmanti, Wirastuti

Publication Date:
2015

DOI:
https://doi.org/10.26190/unsworks/17353

License:
https://creativecommons.org/licenses/by-nc-nd/3.0/au/
Link to license to see what you are allowed to do with this resource.

Downloaded from http://hdl.handle.net/1959.4/54230 in https://unsworks.unsw.edu.au on 2024-04-28

Hydro-geomorphic Controls on the Development and Distribution of Acid Sulfate Soils in Central Java, Indonesia and Robust Remote Sensing and GIS Methods for Acid Sulfate Soil Mapping

Wirastuti Widyatmanti

Submitted in fulfillment
of the requirements for the degree of
Doctor of Philosophy
in The University of New South Wales

SCHOOL OF BIOLOGICAL, EARTH AND ENVIRONMENTAL SCIENCE
FACULTY OF SCIENCE
THE UNIVERSITY OF NEW SOUTH WALES
SYDNEY, NSW 2052, AUSTRALIA

JANUARY 2015

Acknowledgements

My thesis would never been made possible without endless contribution from many people. Some of them were directly related to my PhD work, and some others have supported me either financially or psychologically. I would like to thank God for providing me the strength, motivation, perseverance and ability to complete my study, and for sending me many people with compassionate hearth to support my five years journey for being a PhD.

The first people I would like to express my special appreciation is my supervisor, A/Prof. Jesmond Sammut. He motivated and provided me with very positive criticism which has opened my mind to deeper understanding of hydro-geomorphic processes, acid sulfate soils and scientific writing in English. His encouragement and assistance throughout my PhD has formed me to be a more perseverance person in research field.

My sincere thanks also goes to Dr. Jennifer Beer for her patience in correcting my thesis works, including my English. Her always encouraging words have supported me during the most difficult stage of my study. I would not be able to achieve this stage if she was not around.

I would also like to thank Australian Government through John Allwright Fellowship program from Australian Centre for International Agriculture Research (ACIAR), who had granted me scholarship for conducting research at the University of New South Wales for three years and three months. The University of New South Wales academic community has provided me with valuable academic experience, which can hardly found in most Indonesian universities. Thanks to Sharon Harvey from ACIAR who continuously provided assistance for me during my study. Thanks also to Ibu Mirah Nuryati and Ibu Maria Ludwina from ACIAR Indonesian Office for their great support in preparing all documents for me and my family prior departure to Australia.

I am grateful for A/Prof. Shawn Laffan for his advice in remote sensing and GIS part of my thesis and A/Prof. Rob Brander for his input in coastal geomorphology. I also have to mention Matthew Hunt, Jonathan Russel, Firoza Cooper for great assistances in administration matter, Claudette Retorick who provided me a good working spot on my first arrival, also Tamara Rouse (former AusAID liaison officer), Anna Kirkham, Tatjana, Matthew Byron, and Andre from ISS (International Student Service) who have supported me and my family during my stay in Australia.

I wish to express my gratitude to the Government of the Republic of Indonesia, who gave me opportunity to compete for obtaining AusAID scholarship in 2008 and continuously supported my stay in Australia through the Indonesian General Consulate in Sydney. I would also like to mention my employer, Gadjah Mada University (GMU) at Yogyakarta, who has supported me during my preparation for study and my stay in Australia. Special thanks to Prof. Dr. Hartono, DEA., DESS., and Prof. Dr. Suratman W. Hadiprojo, M.Sc., the former Deans of the Faculty of Geography, and Prof. Dr. Rijanta, the current Dean and all staff members of the Department of Cartography and Remote Sensing for all encouragement throughout my study.

My deep gratitude to the members of NLICC and Inner West ‘KHB’ Group at GreenSquare, the Indonesian Church Community Group, especially the family of Pastor David Widjaya, of Mr./Mrs. Edi and Rinda Suradja, of Mrs. Matrika Christianita Tanlain, Meriyantini, and Hesti Novianti and her late husband Aris Wahyu Utomo, who always supported me and my family with happiness, love, prayer, thought and exciting environment and fellowship. Many thanks for Fusion Australia family, Anne Nanscawen, Malcolm and Jenny Garvin, Elizabeth Campbell, and Perry Anderson through Fusion Sydney South who generously provide a beautiful home and environment, Rangiora, for my family to stay in Sydney for more than 3 years.

My sincere thanks to my ex-EIP friends, with whom I shared my happiness, expectation and stress during our study period in Australia: Stefani Daryanto, Robertus Purwoko, Muhammad Zahid, and Arif Hidayat. Special thanks to Matthew 14th floor friends, Indrie Miller, Celine Standfold, Lei Zhao, Moh. Chaidir Undu, Asep Permana, Michelle Jiang, Janice Liew, Christopher Setio, Jessica. My latest great friends in Room 601 Lala Wijaya, Justin Narimbi, Hatim and for great supports, specifically to Havini Vira who helped me printing my final thesis during my last stay in Sydney.

The contribution of the following people also deserves special mention. My tremendous mentor, role model, father and colleague, soon to be Professor, Projo Danoedoro, PhD, for always providing me great support, personally or through PUSPICS, and for always listening to my jeremiads. Dr. Suharyadi, who were always helping me to complete administration documents while I was away. Prof. Ahmad Mustafa, Rosiana Sabang, Dr. Tarunamulia, Kamariah, Rahmi, for their great assistance in doing soil field survey and laboratory analysis. Dimar Wahyu Anggara, Eki Yeremia Santiago, Ryan Bojes Fanani, A.M. Dwi Septiningsih, Gita Harmoni, Hayu Ratnaningtyas, for your patient and obedience in helping me to maintain high Australian standard of field soil sampling for more than total 5 months during my research. Muhammad Hafizt, Yanuar Adji Nugroho, Rif'at Darajat, and Arum Sekar for helping me to finalise many detail parts of my thesis. Mr. and Mrs. Bambang and Dewi who generously provided the accommodation during my field work in North Central Java, and Mr. Basuki and family in Southwest of Central Java. Ratna Dewadjati, the current secretary of the Agency of Regional Planning and Development (Bappeda) of Central Java Province, Prof. Slamet Budi Prayitno the former Head of Bappeda of Central Java Province, Ir. Subagyo, M.M. the former Head of Central Java Marine and Fisheries Agency for their invaluable support during my field work in Central Java. Rangiora family, Deborah Woon, Davida Ivey, Brigitte Rakow, Joshua Lee, Christopher Sewell, Nicholas Whitelock, and others, who were always ready to take over our roles to be the guardians for our kids while my husband and I needed a break.

Finally, I have to mention my family who have emotionally involved in my effort to be a PhD. My parent, Paulus Trimanto Wibowo and Sri Widayati for their unconditional love, support and pray especially, in looking after my sons very well during my completion of PhD in Indonesia. My parents in law, Mr./Mrs. Suwarno who also always pray for my success. Daniel Tri Handharkha, my beloved brother who has been patiently looking after with my sons in Sydney while I was overseas. Also Dwi Astuti Irenaningtyas and Yonathan Dri Handarkha, my other sibling, for providing me support in different kind of substances. I would also like to express my love and gratitude to my family. My husband Kurniawan Nurgoho who constantly encouraged me to complete my study, and continuously motivated me when I felt exhausted. My sons, Neo and Nino who always enlightened my days, and accompanied and motivated me to enjoy weekends in all beautiful spots of Sydney in order to escape myself from the tedious thesis works. My family's stay in Australia during the past 3 years made me enjoy and value my study.

PUBLICATIONS AND PRESENTATIONS

Widyatmanti, W. (2013). Mapping Soil Wetness Index to Assist Field Acid Sulfate Soil Survey Using Multi-resolution remotely Sensed Data. Faculty of Geography Research Grant Program. PNBP.

Widyatmanti, W., Anggara, D.W., Nugroho, Y.A. (2012). Mapping of Land Suitability for Brackish Water Aquaculture in Serayu Estuary using ALOS-AVNIR2 Data. Paper presented in JAXA Seminar. Report and Proceedings of ALOS Application and Verification Project in Indonesia, Jakarta, Indonesia.

Widyatmanti, W.; Sammut, J. (2011). Physical Characteristics of Wave-dominated Estuary with Pre-Existing Barrier. Paper, Oral Presentation in Coastal Zone 2011 Conference, Chicago, Illinois, USA.

Widyatmanti, W., Sammut, J. (2010). Estuary Classification in Central Java, Paper. Presented in Indonesian Delta Allianz Conference, Bakosurtanal – Delta Allianz; Semarang, Indonesia Result: BEST PRESENTER.

Abstract

The exploitation of coastal areas for aquaculture in Indonesia has occurred without awareness of the impact of acid sulfate soils (ASS) on the environment in which aquaculture takes place. Coastal planning policy and regulation for aquaculture has not included ASS as a consideration for or constraint on development. As a result, aquaculture is undertaken in areas of unsuitable soil and often fails after a short initial period of production. Accordingly, there is a need to provide spatial information that is able to show suitable areas for aquaculture based on an understanding of the vertical and horizontal distribution of ASS. The general aim of this study was to produce a mapping approach based on an understanding of the hydro-geomorphic controls on the distribution and formation of ASS based on hydro-, with a focus on sedimentary processes driven by hydrology. The study focussed on mapping ASS within the pyrite-bearing coastal landscapes in Central Java. The underlying approach was to identify associations between ASS development and distribution within estuarine geomorphological units. Patterns of ASS distribution and the characteristics of the soils are assumed to be associated with hydro-geomorphic processes that influence soil development.

This study utilized a multi-level methodology involving multi-resolution remotely-sensed data and GIS analysis to generate multi-scale hydro-geomorphic information (geomorphic setting, water sources and hydro-dynamics). The method includes the identification of Geo-climatic Regions (GcR), a new estuary classification system, and use of hydro-geomorphic units (HGU) for Central Java to establish a hydro-geomorphology-based classification scheme to aid mapping ASS distribution. Field and laboratory assessment of soil properties were undertaken to identify the vertical and horizontal distribution of ASS of the HGUS in each type of estuary.

This study identified four estuary types that represent two GcRs on the north coast: river-dominated estuary (Rambut Estuary); tide-dominated estuary (Jajar Estuary), and two GcRs on the south coast: wave-dominated estuary (Serayu Estuary) and one new type of estuary class which is wave-dominated estuary with pre-existing barrier (Bengawan Estuary). Fifty two HGUs were generated from different types of landforms, land-uses, vegetation types, water table depth and distance from the brackish water resources, from those four selected estuaries. Soil analytical results show that these HGUs represent different ASS physical and chemical properties in coastal sediments especially in the estuary zones of tidal shores and where river deposition occurs. The HGUs in the estuaries on the north coast have less disparity and pyrite concentration, despite their low energy environment, compared to the south coast. It was found that intensive aquaculture ponds and dredging activities were the main factors contributing to the absence of ASS in these estuaries. In contrast with some previous studies, in the south coast, the combination of high river and wave energy in wave-dominated estuaries created scattered subaqueous soil landforms. These environments comprise of a high variety of HGUs with medium to very high pyrite concentration (4-9%). The HGUs with high pyrite concentrations are mostly developed in landforms with low energy environments overlaying former high river energy environments.

Statistical analysis showed that the specific combination of river, tide and wave energy levels influenced the development and distribution of ASS. The distance of the HGUs to the river and sea, was identified as one factor that influenced the vertical distribution of pyrite concentration.

It was shown that the differing ASS properties in each HGU for each of the different estuary types, could be used to explain and map differences pyrite accumulation.

The study showed that a multi-level ASS mapping approach using geo-climatic regionalization as a basis for grouping hydro-geomorphic features catchment and their coastal marine environments indeed assist in understanding of coastal evolutionary processes in Central Java. The uses of multi-resolution remotely sensed data show the effectiveness of the approach in cost and labour, especially conducting doing field survey. The information generated for each HGU facilitated the development of a scientifically robust ASS mapping model that incorporates knowledge on the relationship between soil and landform formation in Central Java estuaries which is essential in minimizing the risk of environment degradation. The resulting maps and mapping methods will improve land capability assessment and site selection criteria for brackishwater aquaculture.

Key word: hydro-geomorphic control, acid sulfate soil, remote sensing and GIS application, geo-climatic region, estuary classification.

TABLE OF CONTENTS

LIST OF FIGURES

LIST OF TABLES

GLOSSARY OF TERMS

ACIAR - Australian Centre for International Agricultural Research.

acidity – the log hydrogen ion activity in the soil solution expressed as pH value.

aerobic – presence of oxygen in an environment.

anaerobic – absence of oxygen in an environment.

aquaculture – the cultivation of aquatic animals and plants, especially fish, shellfish, and seaweed, in natural or controlled marine or freshwater environments.

> **extensive or traditional aquaculture –** relies on wild seed supply (post larval shrimp and fish fingerlings) natural feed and tidal flows to maintain water quality.
>
> **traditional plus aquaculture** - an improvement on extensive farming practises in that pumping, regular use of artificial feed and some chemicals, principally lime and fertiliser, are used to improve production.
>
> **semi-intensive aquaculture** - still relies on a significant amount of natural feed in the early life stages but the stocked at higher density and is supplemented with other feed and fertilizers.
>
> **intensive aquaculture** - farming largely operates through the use of regular, sometimes continuous, aeration, high stocking densities and large artificial feed inputs. In intensive farms there is an almost complete dependence on pelleted feeds, although natural feed remains important to stocked post larvae.
>
> **super-intensive aquaculture –** farming based upon the culture system (stocking density and the level of inputs) and intensity of management.

ASS – acid sulfate soils; soil or sediment containing iron sulfides or products resulting from oxidation of sulfides; refers to both PASS (potential acid sulfate soil) and AASS (actual acid sulfate soil).

AASS – actual acid sulfate soils are soils containing highly acidic soil horizons or layers resulting from the aeration of soil materials that are rich in iron sulfides, primarily sulfide.

attribute data – data which describe various characteristics of the geographic objects (point, lines or polygons). They help distinguish the observation from another, even if all of them are points, in addition to using location information.

backswamp – area of low, swampy ground on the floodplain of an alluvial river between the natural levee and the bluffs.

beach - thick, wedge-shape accumulation of sand, gravel, or cobbles in the zone of breaking waves.

beach ridge – a long low, linear, even-crested rise built up by wave action at a former shoreline. Such ridges are usually modified by the wind and may occur singly or in a series of parallel ridges.

clay – sediment particles between 0.002 and 0.004 mm in diameter and having colloidal properties.

correlation coefficient – a measure of the linier relationship between two quantitative variables, indicating the degree to which they vary together; denoted by r, values range from – 1 (perpect negative correlation), trough 0 (no linear relationship) to + 1 (perfect positive correlation).

delta – an extensive area of alluvial material formed where a river enters a large body of quiterer water, such as a sea or lake. It is typically triangular in shape, and may be traversed by distributary channels.

eigen value – Eigenvalues are a special set of scalars associated with a linear system of equations (i.e., a matrix equation) that are sometimes also known as characteristic roots, characteristic values (Hoffman and Kunze 1971), proper values, or latent roots (Marcus and Minc 1988, p. 144.

eigenfactor - ranking and mapping scientific knowledge.

estuary – an open drainage adjacent to the sea typically at the mouth of a river, where the tide meets the stream.

> **tide-dominated estuary** - estuary represents a bedrock coastal embayment that has been partially infilled by sediment derived from both the catchment and marine sources, in which tidal currents, rather than waves, are the dominant force shaping the gross geomorphology.
>
> **river-dominated estuary** - estuaries that occur in the lower reaches of large rivers where the penetration of tide extends farther than, and is decoupled from, the upstream penetration of salt.
>
> **wave-dominated estuary** - the dominant energy that influenced the estuarine landform processes come from wave.

estuary zone – a zone that represent estuarine environment based on river and tidal characteristic.

floodplain - A area of low-lying ground adjacent to a river, characterized by frequently active erosion and aggradation by channeled or overbank stream flow, formed mainly of river sediments and subject to flooding.

Geo-climatic Regions (GcR) - groups of catchments with similar hydro-geomorphic characteristics (geology, geomorphology) and climatic regimes at regional level.

geographical (or spatial) data – data which represent phenomena from the real world in terms of (a) their position with respect to a known coordinate system, (b) their attributes that are unrelated to position (such as colour, cost, pH, incidence of diseas, etc.) and (c) their spatial interrelations with describe how they are linked together.

Geographical Information System (GIS) – the information technology that provides mechanism to store, analyze, manipulate and visualize geo-referenced data from the real world for particular set of purpose.

geomorphology – the branch of both physiography and geology that deals with the form of the earth, the general configuration of its surface, and the changes that take place in the evolution of landforms.

Hydro-geomorphic Units (HGUs) - detailed mapping units within selected estuaries, which are classified based upon landforms, hydrology and geomorphic processes, land-use and vegetation types related to tidal characteristics.

intertidal flat – coastal wetland that formed when mud is deposited by tides or rivers.

jarosite – sulfate of iron and potassium forming a yellowish or brownish mineral ($KFe_3(OH)_6(SO4)_2$).

land evaluation – a method/ process carried out estimate the suitability of land for a specific use such as arable farming or irrigated agriculture.

landforms – the surface features of the lands created by different type of processes.

loam – a friable soil comprising a mixture of clay, silt, sand and organic matter.

levee - A long linear rise bordering a watercourse, comprising part of the floodplain formed by deposition of sediment from overbank flow during floods. Relied is low and the outer slope very gentle.

mid-channel bar – landforms in a river that begin to form when the discharge is low in location of the lowest elevation.

mean - the arithmetic average of the data values. It is the sum of the data values divided by the number of data values.

Multistage stratified random sampling – a type of statistical soil sampling methods that dividing a region into sub-region as primary units.

parent material – the unconsolidated and more or less chemically weathered mineral or organic matter from which a soil has developed.

PCA - Principal component analysis is a statistical procedure that uses orthogonal transformation to convert a set of observations of possibly correlated variables into a set of values of linearly uncorrelated variables called principal components.

PASS – potential acid sulfate soils are soils which contain iron sulfides or sulfidic material which have not been exposed to air and oxidised. The field pH of these soils in their undisturbed state is pH 4 or more and may be neutral or slightly alkaline.

pH – the negative logarithm of the hydrogen ion activity and is the intensity factor of acidity.

process – a concept that depicts and explains how the distribution of geographic object comes to exist and may change over time.

point bar – a landform developed where stream flow is locally reduced because of friction and reduced water depth in a meandering system.

random sampling – the process of selecting observations randomly from the population without any specific predefined structure of rules. Often random numbers are used to assist the selection process.

redox potential – the reduction-oxidation potential of an environment; measures the tendency of the environment to be reducing (donate electrons) or oxidizing (accept electrons).

sand – A soil particle between 0.05 and 2.0 mm in diameter.

sand barrier – long narrow island, built largely of beach sand and dune sand, parallel with the mainland and separated from it by lagoon.

sandy shoreface – the part of beach or barrier where the ocean meets the shore of the island. It is associated with the area between high and low tide.

spatial pattern – a concept that shows how geographic object distribute at one a given time.

spatial sampling – a sampling scheme that is designed to accommodate the sampling of observations in the geographic space (involve objects that have geographic dimension).

spatial statistics – the statistics that provide useful tools for describing and analyzing how various geographic objects (or even) occur or change across the study area and over time. These statistics are strongly based upon classical statistics but have been extended to work with data that are spatially referenced.

Standard Deviation (SD) – the square root of the variance.

swale – a linear level-floor open depression excavated by wind or formed by the build-up of two adjacent ridges. Typically associated with the depression between two adjacent sand dunes.

tidal flat – A large level area of land in the littoral zone subject to inundation by water that is usually salty or brackish.

washover – a fan-like landform of sand that washed over a barrier island or spit during a storm, and then deposited sand on the landward side.

1

INTRODUCTION AND BACKGROUND

CHAPTER ONE

INTRODUCTION

1.1. Background

Throughout Indonesia, many aquaculture ponds and industries have been developed on acid sulfate soils (ASS) without an appreciation of the impacts of these soils on productivity and the environment. Acid sulfate soil is sediment containing pyrite (FeS_2) which usually forms beneath mangrove forests and other tidally-influenced environments as a result of sulfate reduction in organically-rich sediments (Dent, 1986). This pyrite remains inactive and benign under waterlogged conditions, which are typical of low-lying coastal environments. However, once it is exposed to oxygen and oxidised, it lowers the soil pH (below 4) due to the release of sulfuric acid and mineral acidity associated with metal transformations. This causes severe soil acidification if the inherent acid-neutralising capacity of the soil is exceeded. The human activities that commonly trigger pyrite oxidation in coastal lowlands are agriculture, drainage-related infrastructure, industry, tourism and aquaculture (Ahern *et al*., 1998b; Lin *et al.*, 1995; Sammut *et al.*, 1996). In most cases, the effects of development in ASS are moderate to severe (Dent, 1986; Sammut *et al*., 1996). In aquaculture, ASS not only degrades soil and water quality, but can also lead to recurrent crop failures (Golez, 1995; Gosavi *et al.*, 2004; Sammut, 1999). Consequently, many ASS-affected aquaculture ponds have been abandoned and other environments, which are susceptible to these effects, such as rivers, estuaries and possibly marine areas, have often struggled to remain commercially viable (Dieberg & Kiattisimkul, 1996; Powell & Martens, 2005; Sammut & Hanafi, 2000).

The development of ASS, and its subsequent environmental impacts, triggers conflicts between coastal development and conservation (Sammut *et al*., 1996; White *et al*., 2007). Coastal development is important for economic reasons. Brackishwater aquaculture expansion is needed to fulfill market demands, especially the supply of shrimp. On the other hand, conservation is also important to maintain the sustainability of the coastal environment, in this case to avoid the exposure of pyritic layers and ensure that economic, social and conservation needs are met in balance. These issues raise an awareness of the importance of emphasizing the need to develop without significant impacts for decision makers, local communities and aquaculture farmers who are exploiting coastal lowland environments. Because ASS mostly occurs in areas that are under pressure for development, and where population is high, environmental decision makers and all coastal stakeholders require scientifically-based spatial information to identify the location of these problematic sediments. Thus, robust mapping approaches are needed to provide simple, efficient and comprehensive maps of ASS distribution to support aquaculture land sustainability and capability, and local management and planning for coastal resources.

The Australian Centre for Agricultural Research (ACIAR) Projects FIS/97/22 and FIS/2002/076 developed mapping protocols to map ASS in coastal lowlands. However, current soil mapping is restricted to showing the presence or absence of ASS and does not identify the soil profile depth and potential severity of ASS in coastal lowlands. This information is important to determine the best management strategies for landscapes where ASS is present. Other studies on ASS mapping are mostly related to wetlands and agricultural fields, rather than focusing on aquaculture (Anda *et al.*, 2009; Fitzpatrick *et al*. 2008; Madsen, 1985). Some studies provide very useful detailed mapping methodologies for rapid assessment of ASS distribution and soil properties, and more accurate boundary assessment (Ahmed & Dent, 1987; Bregt & Gesink, 1992; Husson *et al.*, 2000; Tarunamulia, 2008). Nevertheless, few studies, specifically in relation to Indonesia, discuss the influence of soil development process and landscape evolution on soil pyrite concentration (the key soil mineral present in ASS) and its distribution in the soil profile.

In other parts of the world, the vertical distribution of pyrite is known to be controlled by hydro-geomorphic processes (Dent, 1986; Sammut *et al*., 1996). There is very little known about these hydro-geomorphic processes and their role in coastal landscape evolution and ASS distribution in Indonesia and whether the knowledge from elsewhere is transferable. Studies conducted elsewhere in the world have noted the importance of understanding how landscapes evolved in order to improve ASS mapping (Dent, 1986; Lin, 1995). Certainly in Indonesia there is nothing in the published literature concerning the relationship between landscape evolution and ASS formation.

In terms of landscape evolution, previous studies have found that ASS presence and absence is strongly associated with the context of estuary and catchment processes because the conditions for ASS formation are largely controlled by these processes (Dent, 1987; Roy, 1984a; Roy *et al.*, 2001). Estuaries are the dominant coastal feature of any coastline and are often characterized by soft-sedimentary land units (Bird & Ongkosongo, 2000). Not all estuaries are the same; they can be differentiated based on their energy conditions and resulting differences in landforms. ASS are known to form in low energy environments (Dent, 1986) and their characteristics are likely to differ between estuary types. Hence, estuary classification can provide a framework for the investigation of soil forming processes and, in particular, how sediments, such as ASS, are distributed and differ between estuary types. An understanding of ASS formation and distribution, framed in the knowledge of estuary forming processes would enable more effective mapping of ASS.

In Indonesia, unfortunately, there is no estuary classification system available (personal communication: Ongkosongo, 2010, 2012; Sunarto, 2012). The existing classification of Indonesian coastal environments is a delta classification, developed by Ongkosongo (1984). Other studies focused on individual coastal and estuary systems which were classified using existing classification systems from other countries (Bird & Ongkosongo, 2000; Hoekstra, 1988; Hoekstra *et al.*, 1989; Ongkosongo, 2010; Verstappen, 2000). The previous estuarine studies in Indonesia have concentrated more on geo- and bio-chemical properties of soils and water quality rather than the paleo-environment, geomorphology and sedimentary processes (Carbonel & Moyes, 1987; Jennerjahn *et al.*, 2004; Lin *et al.*, 1995). Applying other estuary classification systems based on different geomorphological features and hydrological and climatic conditions will not always be appropriate and suitable in a tropical country like Indonesia. Therefore, this study needed to establish a new estuary classification system appropriate for Indonesia to predict occurrences of ASS formation. This estuary classification, although developed for ASS soil-mapping purposes, will become a significant foundation for more advanced estuary classification systems in Central Java, and in Indonesia generally.

Due to this limited understanding of the relationship between estuary evolution and ASS formation, it is currently not possible to accurately map the presence of ASS in aquaculture ponds in Java. Similarly, it is not possible to estimate the depth of these soils in alluvial landscapes anywhere in Indonesia. In some cases, for instance in flood plains, good quality soils overlie ASS and they can be inadvertently excavated in pond-based aquaculture due to the depth of disturbance (generally greater than 2 m). Mapping can under or overestimate the distribution of these soils unless hydro-geomorphic controls on soil formation are understood and applied to mapping systems. Therefore, further research is needed to improve the soil-mapping component of land capability assessment protocols and thereby increase the accuracy of the land classes in the scheme, so that ASS areas can be avoided in aquaculture development.

1.2 A Brief Description of Acid Sulfate Soil

ASS are also known as catclays in other parts of the world, and were first recognized in the Netherlands around 270 years ago (Dent, 1986). Pons (1973) describes ASS as a soil, “in which as a result of processes of soil formation, sulfuric acids either will be produced, are being produced or have been produced in amounts that have a lasting effect on main soil characteristics." Most acidic soils around the world acidify due to leaching, the formation of organic acids or nitrification (van Breemen *et al*., 1983; Claff *et al.*, 2011; Nyberg *et al.*, 2011; Beucher *et al.*, 2013). By contrast, as mentioned previously, the acidity of ASS is generated by the oxidation of pyrite and associated transformation of metals (Dent, 1986; Sammut *et al.*, 1996; Larssen et al., 2011; Shi *et al.*, 2014; Oliveira *et al.*, 2012).

Raw ASS do not form from *in situ* weathering processes. Rather, they are usually formed by estuarine sedimentary processes, following sea level rise and stabilisation, creating conditions suitable for bacteria to form sulfides. Specifically, ASS forms in waterlogged environments that contain iron and are rich in both organic matter and dissolved sulfate, usually from seawater. This organic matter provides energy for sulfate-reducing bacteria to reduce sulfate in seawater and iron to iron disulfide (pyrite) under anaerobic conditions, creating low redox conditions.

The overall equation for the formation of pyrite can be expressed as (Dent, 1986):

$$Fe_2O_3(s) + 4SO_4^{2-} + 8CH_2O + ½O_2 \rightarrow 2FeS_2(s) + 8HCO^{3-} + 4H_2O \quad (\textbf{Equation 1})$$

The overall equation for the oxidation of pyrite can be expressed as:

$$FeS_2 + 15/4.O_2 + 7/2.H_2O \rightarrow Fe(OH)_3 + 2SO_4^{2-} + 4H^+ \quad (\textbf{Equation 2})$$

Pyrite usually forms in coastal lowlands, such as mangroves, saltmarsh or tidal flats, where conditions are well suited (Pons & van Breemen, 1982; Dent, 1986). The sub-aerial alluvial plains bordering riverine channels also provide an ideal setting for iron sulfide minerals to form (Roy *et al.*, 2001). The oxidation of pyrite, and the subsequent formation of acidity, will mobilize metals such as iron and aluminum. These and other metals generate further acidity and can drive the pH of the soil down to below 3 (Sammut *et al.*, 1996). Oxidation of pyrite in Indonesia often results from the excavation of ASS to build ponds. The construction of dykes, ponds and canals enables oxygen to enter the soil thereby triggering the process outlined in Equation 2. Further descriptions of ASS development processes in different type of landscapes are provided in Chapter 2.

1.3 Aquaculture in Indonesia

1.3.1 Brackishwater Aquaculture

Coastal lowlands, although subjected to erosion, sedimentation, flooding and tidal inundation, are favoured environments for urban and rural development (Carter, 1988; Roy, 1984a; White *et al.*, 1997). In Indonesia, the primary human activities in the coastal lowlands are associated with urbanisation, industry, agriculture and aquaculture. Table 1.1 shows that pond-based farming has increased over time, but along with the significant decrease of natural areas/mangrove areas.

Specifically for coastal lowland aquaculture purposes, brackishwater resources have been exploited in Indonesia for the last six centuries, and there have been promising economic opportunities for local communities (Schuster, 1952, cited in Beveridge & Brooks, 2008; Beveridge, 2007). The value of fish and shrimp, farmed in earthen ponds, exceeds that of many agricultural commodities. Therefore aquaculture has become the most popular activity for the coastal communities in Indonesia.

Table 1.1 Changing land-use over time in Java's coastal area

Type	1994 (ha)	1994 (%)	2001 (ha)	2001 (%)
Ricefields	3,800	16	4,230	18
Pond-based aquaculture	3,450	14	5,750	25
Settlements	385	2	1,100	4.7
Dryland cropping	4,190	18	4,800	20.3
Natural Area/Mangrove	11,558	50	7,580	32

(Doyde et al., 2006)

In Java, the most populated island in Indonesia, aquaculture started when the local communities, who lived in coastal areas, worked on brackishwater ponds to culture shrimp or fish to fulfil their daily food needs (Brown and Prayitno, 1987). The farmers were originally convicts who were exiled from inland areas. Convicts were forbidden to work in agriculture or shipping, therefore they moved to the coastal areas to start a new life as fishermen or pond-based farmers. Milkfish (*Chanos chanos*) and mullet (*Mugil* spp.) were the common traditional culture species during that time. Over the last 30 years, in line with culture technology development, they subsequently started to convert their ponds to more valuable commodities, such as shrimp or shrimp-fish polyculture (Nurdjana, 2006; FAO, 2007; 2013). These systems are known as 'traditional' or 'extensive' farms because they relied on wild seed supply (post larval shrimp and fish fingerlings) natural feed and tidal flows to maintain water quality.

In Indonesia, aquaculture is commonly divided into extensive or traditional, semi-intensive and intensive (USDA, 2007). More recently, super intensive systems have been developed. These classes are based upon the culture system (stocking density and the level of inputs) and intensity of management (Edwards *et al*., 1988; Pullin *et al*., 1993; Bush *et al*., 2010; Bala *et al.*, 2009; Vinatea *et al.*, 2010; Pattanaik & Prasad, 2011; Shi *et al*., 2011). The extensive farming system depends on natural feed with no food supplied from outside sources (Figure 1.A.). Traditional farmers usually own these ponds. However, in recent years traditional farmers have used hatchery-reared post larvae and artificial feed. Consequently, these systems are often called improved extensive or traditional plus. The semi-intensive system, although still relying on a significant amount of natural feed in the early life stages of the stock, is stocked at higher density and is supplemented with other feed and fertilizers (Figure 1.B). It involves the intermittent use of paddlewheels to aerate the pond waters in order to sustain the stocking intensity. By contrast, intensive farming largely operates through the use of regular, sometimes continuous, aeration, high stocking densities (Table 1.2) and large artificial feed inputs (Figure 1.C). In intensive farms there is an almost complete dependence on pelleted feeds, although natural feed remains important to stocked post larvae.

Table 1.2 Common aquaculture pond sizes and stocking density for shrimp and milkfish in Indonesia (DGA, 1994; MMAF, 2008)

Aquaculture System	Ponds Size (ha)	Stocking Density (fry/ha/crop)
Extensive/Traditional	1 - 4	7,500-12,000
Semi-intensive	1 - 2	30,000 – 60,000
Intensive	0.2.-0.1	100,000 – 150,000
Super-intensive	0.3-0.5	>150,000

Figure 1.1. Different types of aquaculture in Indonesia:
(A) extensive/traditional, (B) semi-intensive, and (C) intensive.

Today in Indonesia, the most common aquaculture farming system is traditional plus (also known as improved extensive) (DGA, 2004; DGA, 2014; Mu'tamar, *et al.*, 2013). This system is an improvement on extensive farming practises in that pumping, regular use of artificial feed and some chemicals, principally lime and fertiliser, are used to improve production. Most traditional-plus systems are located close to tidal water to minimise the need for pumping for water exchange. Traditional-plus systems usually produce less than 1 tonne of shrimp per ha per cycle. Polyculture is also attempted in these ponds, especially when shrimp production problems occur. Traditional-plus farms also produce fish such as Milkfish *(Chanos chanos*), and may also revert to the traditional system of seaweed farming.

1.3.2 Mangrove Clearance and Acid Sulfate Soil in Aquaculture Development

Mangrove forest is important as a nursery ground and source of food for many marine fish and shrimp (Primavera, 1997; Graaf & Xuan, 1998; Barbier *et al.*, 2011; Sandilyan & Kathiresan, 2012; Lee *et al*., 2014). The inshore yield of shrimp and fish has been positively correlated with mangrove areas in several tropical countries such as the Philippines, Indonesia and Malaysia (Camacho & Bagarinao, 1987; Macnae, 1974, cited in Primavera, 2005; Martosubroto *&* Naamin, 1997). Unfortunately, it is mangrove forests that have been targeted for coastal development because they are wrongly considered as cheap and marginal land. Increasing population pressure, associated with the development of coastal aquaculture ponds, has been also known to pose a threat to mangrove communities (Pons & Fiselier, 1991). Meanwhile, in some developing countries, efforts by scientists to promote sustainable coastal development and to raise awareness of the impacts of mangrove destruction and unplanned aquaculture has not changed the attitudes of local government, decision makers and the community until the last decade (Hanafi & Ahmad, 1999; Primavera, 2005; Paul & Vogl, 2011; Datta *et al*., 2012; Islam, 2014). Consequently, mangrove clearance is continuing to degrade the environment, reducing yields of inshore marine fish (Primavera, 2006; Maltby, 2014; Islam *et al.*, 2014). Research shows the area of mangrove forest cleared for the development of fish ponds in Asia, reached 2 million ha in 1996 (Ilman *et al*., 2011; Mastaller, 1996). Some unmanaged conversions have led to lower mangrove diversity and reduced productivity of aquaculture ponds (Alongi, 2002). Further development of mangroves also leads to wider environment degradation caused by ASS (Golez, 1995; Pons & Zonneveld, 1965; Stevenson, 1997). However, recent studies on sustainable aquaculture management adopted by government and local farmers have shown a shifting paradigm involving mangrove plantation on their brackishwater aquaculture development (Fitzgerald, 2000; Boyd, 2002; MoF, 2007), but ASS has not been become their concern yet.

There are about 438,000 ha of brackishwater ponds in Indonesia (FAO, 2009; Wetland International, 2002). About 63% of them are built on tidal and mangrove areas (Kongkoe, 1997, Kusumastanto & Jolie, 1998). These ponds, which were constructed on land that used to be mangrove forest, had poor water or soil quality, which was possibly the result of the pyrite oxidation. In coastal aquaculture, pyrite oxidation occurs when material excavated to form canals and ponds are used to construct the pond dykes (Gosavi *et al.*, 2004). During the construction phase, pyrite will start to oxidize in the pond bottoms and dyke walls. During the production phase most of the oxidation takes place in the dyke. Pond preparation processes, which include draining and flushing of the ponds then inevitably leaches the pyrite oxidation products (acid and metals) into the pond water and canals (Brownswijk *et al.*, 1995; Golez, 1995; Sammut & Hanafi, 2000). Over subsequent crops, these extremely acid soils significantly reduce pond water quality through the pollution of ponds with iron and other metals. The poor water quality reduces phytoplankton growth, which is needed as natural feed, and commodity yields decrease. In addition, the ASS leachate can lead to toxic discharges into river water, and trigger fish mortalities and downstream degradation (Johnston *et al*., 2005; Sammut *et al*., 1996).

Large areas of aquaculture ponds in Indonesia exist in the coastal region of Sumatra, Java, Kalimantan, Sulawesi and western Nusa Tenggara (Nurdjana, 2006). Similarly with extensive aquaculture, semi-intensive/intensive systems originally developed in the coastal areas of Java, followed by Sumatra, and Sulawesi. The rapid development of aquaculture commenced in the 1980s, during the boom in Asian shrimp farming. The

Indonesian government supported the development of these farming industries under the regional/international funding organization scheme (WRM, 2002). The expansion of the shrimp farmed area has increased aquaculture productivity. However, in some areas, increased productivity was unsustainable, due to improper planning (Poernomo, 1992).

A major difficulty has emerged in aquaculture, particularly in large shrimp ponds. Shrimp farms in the former mangrove areas tended to fail after 2-5 years of prosperity, followed by reduced productivity, ultimately leading farmers and companies to abandon ponds (Figure 1.2). These semi-intensive farms, which were widely established across Java and parts of Sumatra, also have experienced frequent crop failures largely due to disease outbreaks and water quality problems (Hanafi & Ahmad, 1999). In Central Java, shrimp disease outbreaks began in 1990, resulted in 40 % of shrimp ponds no longer operating (Hanafi & Ahmad, 1999; MMAF, 2011). Pond abandonment escalated after further clearing of mangrove forest. In 1995, disease impacts on ponds were five times greater. Often the root cause of this reduction in productivity is poorly understood, with simple causes such as “white spot” virus being blamed, without awareness of other possible environmental issues caused by mangrove clearance (WRM, 2002). In 1998, the government announced that more potential shrimp pond areas were available through conversion of 860,000 out of 2.5 million hectares of remaining mangrove areas. This announcement had ignored the risk of ASS in mangrove areas.

In 2000, Indonesia exported 144,000 tonnes (US$1,003 million) of shrimp, but from that high point, exports declined to 127,000 tonnes in 2001 (US$940 million) and 122,050 tonnes in 2002 (US$840 million) (IBS, 2003; Oktaviani, 2007). As a result, the Government of Indonesia recently initiated a revitalisation program in an effort to increase production in existing ponds and estimated the total potential area for aquaculture to be 7,231,000 ha (DGA, 2004a). This figure includes about 3,775,000 ha of mariculture (52 %), 1,225,000 ha of brackishwater aquaculture (17 %), and 2,230,500 ha of freshwater aquaculture (31 %). The existing areas used for marine, brackishwater and freshwater aquaculture were only about 0.03 %, 39.3 % and 11.2 % of the potential area, respectively (MMAF, 2011). However, the criteria for determining ‘potential area’ were not clearly expressed. On the other hand, the industry will continue to satisfy the market demands by carelessly targeting these ‘potential areas’. In order to achieve this, as in other parts of the world, the conversion of pristine coastal environments including mangrove forest to aquaculture is inevitable (Primavera, 2005).

Figure 1.2. An example of an abandoned pond in Central Java. Left unused, the pond will continue to generate acid for years. High demand for shrimps causes farmers to seek new sites to fulfill market demand.

Instead of recognizing the problem of reduced aquaculture productivity and seeking solutions to address this, the government, yet again, reported that Indonesia has about 94% of land available for aquaculture that has not yet been used (MMAF, 2009). It was also claimed that the total existing ponds in Indonesia are nothing compared to the total coastal area, specifically the mangrove forest area. This information motivates farmers and aquaculture companies to develop new areas to meet economic demand instead of remediating their old ponds. Without an awareness of ASS as a constraint to development, new ventures will continue to face the problems of the past and there will be further environmental degradation. Therefore, this current study on identifying and formulating improved and more efficient methods to accurately map ASS, will contribute to preventing these problems in future coastal planning and aquaculture development.

1.4 Application of Remotely Sensed Data and GIS in Coastal Landform and Soil Mapping

It is well established that the use of remotely sensed and GIS is more effective than conducting a detailed terrestrial survey. A large body of research has been conducted on the use of remotely sensed data to map coastal landforms and soils. In Indonesia, remoteness and field-based risks affect access to areas for sampling, which makes conventional mapping methods significantly difficult. This is also a problem throughout the region. Due to the difficulties involved in conventional soil mapping methods, new techniques for soil mapping were developed. Lillesand & Kiefer (1985) identified that the association of soil properties with geology and vegetation can be determined from aerial photographs and satellite data. There have been several methods used in interpreting features in remotely sensed imagery, but the geomorphological unit approach has been the most common (Campbell, 2011; Fitzpatrick, 2012; McKenzie *et al*., 2008; Odgers *et al.*, 2014; Rossiter, 2012). Airborne photography is still routinely used but does not address many of the data acquisition challenges that can now be resolved through advanced satellite-based imagery (Campbell, 2011; Jensen, 2007). Current studies utilize more multispectral and hyperspectral imageries, supported by high technology spectral collection instruments (McKenzie *et al*., 2008; Rossiter, 2012; Shi *et al*., 2014).

Similar to general soil mapping, coastal soil mapping has been utilizing geomorphological units to represent soil landscapes and soil types based, in particular, on coastal landform mapping and also have been explored to assist soil survey at various scales (Fitzpatrick *et al.,* 2008c, 2012; Sullivan, 2012). In NSW and Queensland, Australia, there was very basic ASS mapping using topography (elevation) to indicate the probability of ASS presence with depth; this approach was for rapid mapping of ASS, but not accurate (Naylor *et al.*, 2000; Powel, 2011). Since ASS fieldwork is often conducted in isolated locations, such as tropical coastal lowlands and wetlands, remote sensing provides a significantly faster alternative to conventional methods and allows sample points to be selected from images (Bregt, 1993; O'Brien & Manders, 2010; Rossiter, 2008). The remotely sensed data allows us to recognize the properties which are related to surface features, such as drainage, vegetation, topography, surface colour or wetness (Campbell & Wynne, 2010; Mulder *et al.*, 2011). For instance, infrared band remotely sensed data provides information on surface wetness and temperature that can be analysed to measure soil moisture content, material density and type, and the surface vegetation (Baroni *et al.*, 2013; Matgen *et al.*, 2012; Yang *et al.*, 2013).

In recent times remotely sensed data are being used to understand the landscape features that relate to the soil characteristics of ASS. The drainage pattern, erosion and topography have been intensively studied to distinguish the types of soil or parent material. Digital Elevation Models (DEM) and Shuttle Radar Terrain Mission (SRTM), and Aster DEM (Huang *et al.*, 2014; Shuisen, 2004) can distinguish landscape features to assist soil mapping. In ASS mapping, this method was developed further to identify the relationships between soil characteristics and visible features in the landscape from topographic maps, geological maps and aerial photography (Dent, 1986; Huang *et al.*, 2014; Madsen, 1985, 1988).

Geographic Information Systems facilitate data analyses from information provided by remotely sensed data. The physical processes affecting the soil properties and their distribution, and other multitask analyses can be accommodated by GIS. The combination of DEM and raster GIS can be used to derive, analyse and display information on geomorphology, drainage and channel networks (McDonald, 1996; Mulder *et al.*, 2011).

Recent developments in ASS mapping focussed more on applying high technology satellite data and soil field measurement instruments and mostly were conducted in developed countries such as Australia and Finland (Beucheur *et al*., 2014; Huang *et al*., 2014; Shi *et al*., 2013). However, there is a lack of consideration to exploring coastal and estuarine evolutionary processes as a landscape approach to comprehend the morpho-chronology of ASS development (Dent, 1986; Fitzpatrick, 2012; Roy, 2000). In addition, the utilization of remotely sensed data and GIS has to be strongly supported by good local knowledge, background information on soil properties, and an ability to interpret the results. Thus, a deep understanding of ASS development processes is compulsory when utilizing remotely sensed and GIS in ASS mapping.

In Indonesia, ASS were mapped based on former mapping of soil classes that did not include or provide any morpho-chronological information or understanding of how ASS varies in the landscape (Anda & Subardja, 2013; Mustafa *et al.,* 2014). There is a lack of research that had used GIS and remote sensing as a specific method in ASS mapping for multi-scale, multi-level, and multi-area studies. Those recent studies merely involve simple mapping showing the presence and absence of ASS, instead of providing systematic mapping method that can be applied elsewhere. Therefore, in this thesis, remotely sensed data and GIS analyses underpin the methods to determine the hydro-geomorphic units. The choice of appropriate remotely sensed data that must consider map scale output for the best information for the final product, along with available topographic and geology maps (Blaschke, 2010; McKenzie *et al.,* 2008) are also accommodated in this thesis. Although field survey is the main way to validate the results of remotely sensed data processing, the right approach allows us to effectively assess the ASS occurrence using the processing capacity of the methods that depend on remotely sensed imagery. Therefore, this study aims to develop a systematic approach using multi-scale, multi-temporal and multi-resolution data. The preparation includes data extraction of land-use, landform, and physical features that can be recognised from remotely sensed data. GIS analysis includes overlying all basic and thematic maps to generate a hydro-geomorphic unit. This study also discusses the advantages and disadvantages of all types and levels of RS & GIS for ASS mapping.

1.5 Research Problem and Significance

1.5.1 Problem Statement

The exploitation of coastal areas for aquaculture has occurred without awareness of the impact of ASS on the environment in which aquaculture takes place. Coastal planning policy and regulation for aquaculture in Indonesia has not included ASS as a consideration for or constraint on development. As a result, aquaculture is undertaken in areas of unsuitable soil with the result that it fails after a short initial period of production. Accordingly, there is a need to provide spatial information that is able to show the suitable areas for aquaculture, based on information on the vertical and horizontal distribution of ASS. This information is also required to target remediation efforts for existing, degraded areas. To accurately map this information, the understanding of hydro-geomorphic processes on ASS formation through an estuary classification approach is very important. The currently used mapping methods (Ahmed & Dent, 1997; Beucher *et al*., 2012; Bregt & Gesink, 1992; Husson *et al.*, 2000; Tarunamulia, 2008; ACIAR, 2011) have not included coastal and estuarine evolutionary processes when defining landscape mapping units although some have acknowledged the importance of such information. The robust mapping method proposed in this study will address this limitation and limitation and strengthen the methods used by other approaches.

1.5.2 Significance of the Research Problem

The research problem is significant in three aspects:

1. This study is significant because it will produce a basic classification scheme of estuary types in Central Java; to date, estuaries in Central Java have not been classified adequately. This scheme not only supports this research but also provides a classification that can be useful to other land development, because a lot of management in Indonesia has been undertaken in the absence of an estuary classification scheme.
2. The current local and overseas ASS maps (ACIAR, 2011; Ahmed & Dent, 1997; Beucher *et al*., 2012; Bregt and Gesink, 1992; Fitzpatrick *et al*., 2008a, 2008b, 2008c; Husson *et al*., 2000; Tarunamulia, 2008) only indicate the presence and absence of ASS. Information on the depth of pyrite is urgently needed to avoid this layer being exposed due to rapid coastal lowland development. The vertical and horizontal distribution of ASS can only be estimated when the mapping method involves the understanding of hydro-geomorphic processes that control ASS development. This can be addressed by developing hydro-geomorphic mapping units and methods. These

units will represent hydro-geomorphic processes and their roles in coastal landscape evolution including estuarine processes that influence the ASS development process.

3. This work will identify, for the first time, the association between the formation of ASS and associated landforms in the estuarine environments of Central Java. This knowledge is significant because it will facilitate future mapping of ASS using knowledge about soil (ASS) properties and distribution based on landform units, represented by a hydro-geomorphic unit (HGU). This is significant in the sense that it will reduce the amount of fieldwork and data analysis required to understand where these soils occur, what their characteristics are, such as chemical and physical properties.

1.6 Research Questions

1. What are the major hydro-geomorphic processes that create differences in estuary types in Central Java, Indonesia?
2. What are the key hydro-geomorphic processes that drive the formation of ASS in the landform?
3. How are ASS chemical and physical properties and their distribution related to hydro-geomorphic processes that created the landforms in which they occur?
4. Is variation in the concentration of pyrite in ASS associated with particular landforms in specific estuary classes as a result of differences in the hydro-geomorphic processes that formed those estuaries?
5. Can mapping efficiency be improved using knowledge of association between soils and landforms within different types of estuaries?

1.7 Objectives and Hypotheses

1.7.1 Overall Objective

The overall objective of this study is to develop an understanding of the distribution and formation of ASS based on hydro-geomorphic controls, principally sedimentary processes driven by hydrology, and the subsequent formation of pyrite-bearing coastal landscapes in Central Java, and to incorporate this knowledge into improved mapping.

1.7.2 Specific Objectives

1. To provide a method to derive the multi-level information of hydro-geomorphic processes that control ASS development through the establishment of an estuary classification scheme for Central Java, to underpin mapping of ASS.
2. To define differences in vertical and horizontal variation in the physical and chemical properties of coastal sediments in intertidal and supra-tidal areas;
3. To create a scientifically-robust ASS mapping model that incorporates knowledge on the relationship between soil and landform formation in Central Java estuaries.

1.7.3 Generalised Hypotheses

The main hypotheses below are provided to support this study's specific objectives:

1. Different types of estuaries represent different energy and sedimentary processes from upland to lowlands which influences their landscape formations;
2. The landscape formations, represented by landforms, with their land-use and vegetation types, determines the development, distribution and properties of ASS, both vertical and horizontal;
3. There is a strong relationship between high pyrite concentration and low energy environment in estuaries;
4. Low pyrite concentrations are likely to occur in high energy environments where the supply of organic material is less;
5. Hydro-geomorphic unit is able to represent multi-level environmental elements which influence the pyrite development;
6. Hydro-geomorphic unit establishment is a robust approach to map the vertical and horizontal distribution of ASS.

1.8 Research Approach

In this study, the understanding of coastal ASS formation through the knowledge of estuary development processes will be incorporated into a more robust method to map ASS. For this reason, this thesis is divided into four sections which are (1) Introduction and background, (2) Methods and Preliminary Results and (3) Results and Discussion and (4) Conclusions and Recommendations (Figure 1.3). Section one consists of

Chapter 1 which introduce the background to the research problem, followed by Chapter 2 which provides a literature review on the formation and development of ASS in different landforms, the challenges of mapping ASS in coastal lowlands and the latest methods applied in ASS mapping. Chapter 2 supports Chapter 3 which presents the conceptual framework of this study including a brief outline of the multi stage methods applied in producing multi-level hydro-geomorphic information.

Section two contains Chapters 4, 5 and 6 describing the results of each level in the multi-level mapping methods specified in three hierarchical steps explained in Chapter 3, i.e.: the determination of geo-climatic regions (GcRs), the development of an estuary classification scheme and the determination of hydro-geomorphic units (HGUs). Chapter 4 describes the geographical setting of the study area. This includes a general description of the climate, geology & geomorphology, hydrology, soils, and land-use. This chapter also includes the determination of the GcRs, using remote sensing and GIS approaches, leading to more detailed descriptions of geographic characteristics of 4 regions in Central Java.

Chapter 5 consists of the methods and the results of estuary classification and zonation. Using this knowledge a framework for estuary classification is used to determine estuary types as a corner stone to develop an understanding of the hydro-geomorphic controls on ASS formation. There have been many investigations of how coastal evolution, especially affected by the recent Holocene sea level rise (10,000 years BP), has influenced present-day estuary characteristics (Nordmyr, 2008; Ellison, 2005; Woodroffe, 2000). Fluvial and marine energy, in association with sedimentary properties and the paleo-environments of coastal areas, are major factors that determine the evolution and ultimately the types of estuaries that formed on distinct landform and soils (Roy *et al*., 2001; Hume *et al*., 2007). Chapter 6 describes the methods and results of hydro-geomorphic unit (HGU) determination. This chapter also explains the remote sensing and GIS application to define the HGU which underpins the soil sampling method.

Section three describes the results of laboratory-based soil analysis with a focus on the physical and chemical properties of coastal sediments and soil formation processes. In Chapter 7, the explanation of the field and laboratory results, in relation to the HGU units is provided, complemented with statistical analysis. Chapter 8 demonstrates the linkage between hydro-geomorphic processes represented in HGU with the presence and absence of ASS and their horizontal and vertical distribution and properties. Chapter 9 summarizes the results from this study and provides recommendations for future research.

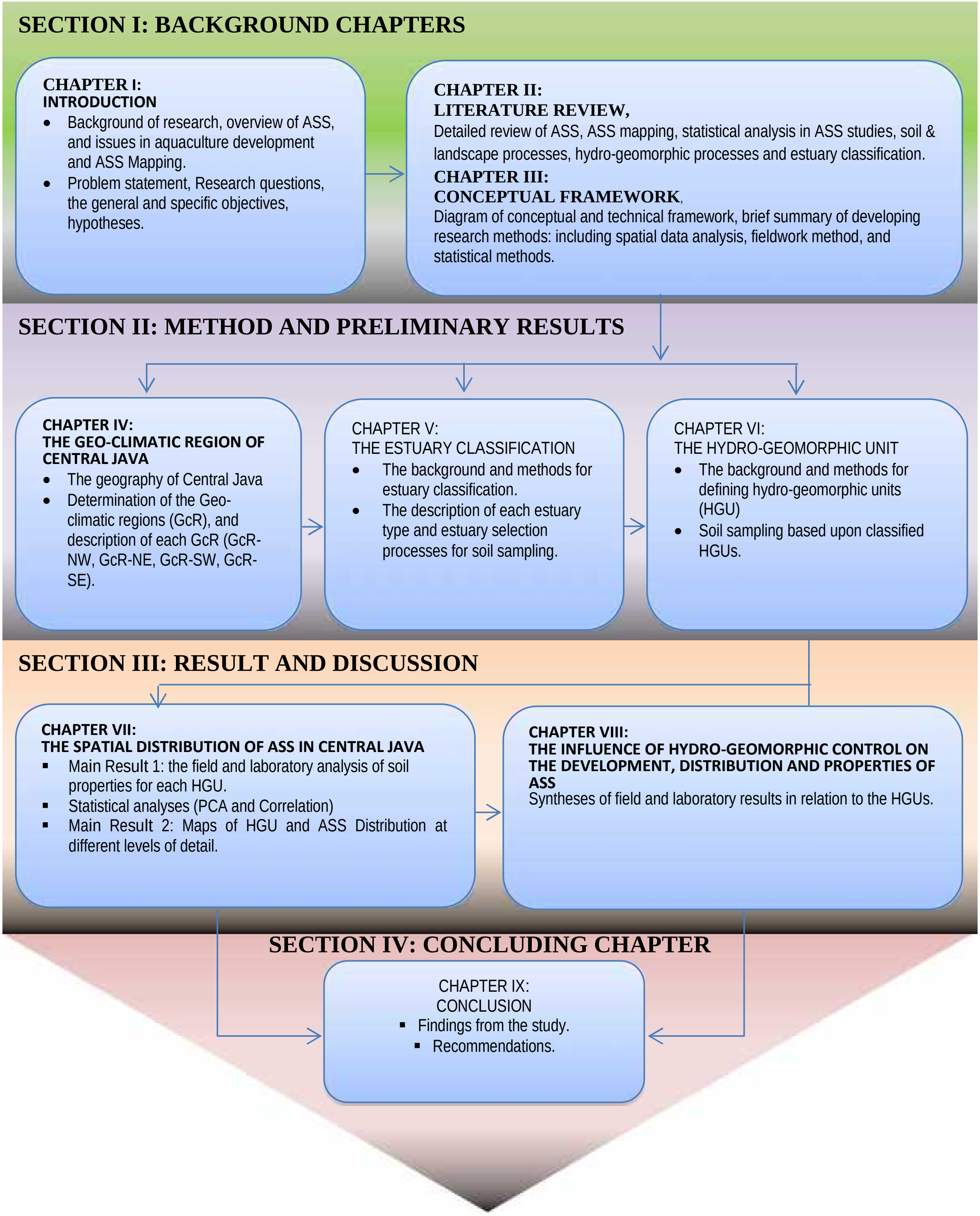

Figure 1.3. Understanding hydro-geomorphic controls on the development and distribution of acid sulfate soil to establish a robust mapping method

CHAPTER TWO

LITERATURE REVIEW AND CONCEPTUAL FRAMEWORK: CHALLENGES OF MAPPING ACID SULFATE SOIL IN COASTAL LOWLANDS

2.1 Introduction

Robust acid sulfate soil (ASS) mapping is required to provide sufficient information on the horizontal and vertical distribution of ASS in soil profiles. This study intends to overcome issues in the understanding of ASS formation processes in coastal lowlands. This knowledge will then contribute to effective aquaculture planning in ASS affected regions, as outlined in Chapter 1.

This literature review underlines the importance and the problems in developing robust mapping methods by reviewing: (1) ASS formation and development; (2) Soil (ASS) and landscape formation processes; (3) hydro-geomorphic characteristics of different type of landscapes related to estuary evolution processes; and (4) previous and current ASS mapping methods. The literature review serves as a foundation to establish a conceptual framework for the methods utilised in this research project.

2.2 Understanding Acid Sulfate Soil Formation and Development

2.2.1 ASS Formation and Forms of ASS

Following a rapid rise in sea-level between 11,650–7000 cal. BP, there were periods of sea level fluctuation and then stability approximately 3,500 BP. Known as the Holocene Stillstand, this period of sea level stability provided ideal conditions for the sulfidic sediment to develop (Perillo, 1995; Smith *et al*., 2006; Verstappen, 2000). The presence of ASS in tidal swamps, mangroves, backswamps and other coastal wetlands is largely the result of the low energy conditions that occurred during the Holocene. The Holocene Stillstand, in particular, created low-energy estuarine conditions that suited the accumulation of sediments and organic matter, which is commonly provided by mangrove leaves (Berdin *et al*., 2003; Golez, 1995; Li *et al*., 2012; Roy, 1994). These root systems trap sediments and organic matter, such as leaves, which create reducing conditions activated by anaerobic bacteria (*Desulvibrio* and *Desulfotomaculum* genera). These bacteria utilise the abundant sulfate supply from sea-water to create disulfide.

The term "acid sulfate soil" (ASS) incorporates "actual acid sulfate soil" (AASS) and "potential acid sulfate soil" (PASS). The PASS layer is usually found beneath actual acid sulfate soils in the same soil profile (Ahern *et al*., 1998a) when partial oxidation occurs. PASS contains iron sulfides or sulfidic material (ASS), which have not been oxidized by exposure to oxygen in the air. While these soils remain in an undisturbed state, the iron sulfides in the soil are stable and the surrounding soil pH is often considered neutral to weakly acid or slightly alkaline. Usually PASS are soft, sticky and saturated with water. Their soil textures are usually gel-like mud, but pyrite can be found in soils with a sandy or gravel texture (Dent, 1986). When PASS are disturbed or exposed to oxygen, they develop into AASS. In the field the very ripe AASS can contain pale yellow mottling representing *jarosite* which is a by-product of the oxidation process. Red and orange mottles, associated with various iron oxides, may also be present.

In other environments, ASS may not exist because conditions were not suitable or due to the high acid buffering capacity of soil. The acid buffering capacity or acid-neutralising capacity of soil is the ability of soil to neutralise the acidity (Ahern *et al*., 1998b). Soils commonly contain neutralising substances such as calcium carbonate deposits (usually from shells), or as the result of the reaction between the organic soil fraction and cation exchange (White *et al.*, 1997). The level of buffering capacity is highly variable due to sediment textures and properties (Bowman, 2012; Indraratna *et al*., 2002). Hence, it is important to consider the presence of carbonates in ASS mapping through catchment characteristics and coastal evolution processes.

In terms of soil taxonomy, initially, soil experts considered ASS only as strongly acid clay located in some depths in soil profiles (van der Kevie, 1972). Together with more advanced research and technology, the most recent soil classification schema classified ASS in a separate great soil group. In FAO Soil Taxonomy (FAO, 1972), ASS was grouped as Fluvisol (Thionic) and Gleysol, whereas the Comprehensive Soil Classification System of USDA (1999) groups them as Sulfaquents and Sulfaquepts. In

Indonesia, based on the Indonesian Soil Classification (ISC) year 1957 (CSR, 1983), ASS is classified independently as ‘acid sulfate soil’ (tanah sulfat masam). This class is in line with Fluvisol (thionic) in classification system of FAO released in 1972; and as sulfaquents in that of USDA Soil Taxonomy in 1971. In the new ISC 1983, the ‘acid sulfate soil’ class is absent and is classified as alluvial soil. However, the existing soil maps mostly still refer to ISC 1957. The placement of ASS and PASS in world soil classification and its correlation to the Indonesian soil map are outlined on Appendix 1.A.

2.2.2 The development of ASS in Different Types of Landforms and Estuaries

Various studies describe different types of landforms, in relation to estuary type setting, and their pyrite concentration and properties (Dent, 1986; Diemont *et al*., 1992; Fanning, 2009; Fitzpatrick *et al.,* 2008b; Lin *et al.,* 1995; Lin & Melville, 1993, 1994; Sylla *et al*., 1996). The accumulation of pyrite depends on the geomorphic processes that are involved in the formation of different landforms (Lin *et al*, 1995). However, only a few studies have specifically looked at the relationship between the formation of ASS under different land forming processes (Kinsela & Melville, 2004). Lin & Melville (1994) stated that “the formation of pyrite has been limited generally by high rates of sedimentation and an insufficient supply of sulfate ions”. This study concluded that high pyrite accumulation occurred in the environments where large amounts of organic matter were able to accumulate under low energy conditions, thereby providing enough time for sulfur compounds to reduce. Sylla *et al.* (1996) identified how hydrology, the potential organic matter and salinity, as a source of sulfate, influenced pyrite formation in Great Scarcies River, Sierra Leone for agricultural purposes. During dry seasons, the seawater is able to penetrate this river, reaching about 100 km upstream. As a result, during rainy seasons, the salinity conditions of up to 80 km upstream is at a medium level (<17 mS/cm), even though fresh water starts to dominate the estuary. These conditions allow pyrite to develop, indicated by (mangrove species) *Rizhophora.* There was no information on the actual pyrite concentration in this study, but it found that the pyrite forming conditions were more favourable upstream but were less likely in the estuary entrance due to high seasonal salinity and low organic matter content.

Soil texture also influences pyrite concentration in ASS (Dent, 1986). Diverse soil textures will respond differently to the soil moisture and temperature changes and will affect the development of the structure and the layer size of ASS (Bloomfield & Coulter, 1973). Medium to high pyrite concentrations (2-4% and >4%) are typically developed in clays and silt or in clay or sandy loam with dense mangrove roots (Dent & Pons, 1995; Brinkman *et al.*, 1993; Burton *et al.*, 2006). By contrast, pyrite concentrations in sandy soils are usually low (<2%) to very low (<1%) (Madsen *et al*., 1985). Sandy soil textures in fluvial, or alluvial in common, soil types limit pyrite development, since the ability of Fe to react is low (Ferreira *et al.,* 2007). However, although it is rare to find ASS in sandy soils, the very low pyrite concentration can result in extreme acidity due to the low acid buffering capacity of sands. When those low pyrite contents are oxidized and leached, the high permeability of sandy soil leads to severe acidity of water, and of associated aquifers (Miller *et al*., 2010; O'Shea *et al*., 2007). In summary, the different concentrations of ASS and their potential impacts on landforms are related to different energy environments controlled by the various conditions of catchments, tides and waves. These energy sources dictate sedimentary processes, the amount of organic matter, soil texture, and subsequently influences soil pyrite development.

In the areas below the minimum low tide mark of river-dominated estuaries, it is common to find floodplains and deltas overlying the pyritic sediment, as in the Mahakam, Pearl and Mekong Delta (Diemont *et al*., 1992; Lin & Melville, 1994; Minh *et al*., 1997). The depths of the pyritic layers vary depending on the sedimentation process and tropical season (number of wet and dry months) and also the exposure of the landscape to waves and the tidal range. However, in an active developed delta, it is rare to find recent pyrite development because the fresh river water dominates the sedimentation process (Lin & Melville, 1994). In most cases this river-dominated delta overlaid the previous pyrite layer in various depths.

Backswamps provide an environment for pyrite to develop in higher concentrations (Andriesse, 1993; Chiem, 1993). Backswamps, which are located behind natural levees, undergo flooding and inundation, with different inundation periods, because of overland flow from the river during rainy seasons. In brackishwater river environments, some of these processes leave a waterlogged depression during dry seasons and allow pyrite to develop because of the accumulation of sulfates and organic material. In some freshwater backswamps, the layer of non-pyritic alluvial sediment overlies the pyritic sediment which is often located less than 1 meter below the surface (Rosicky *et al*., 2004a). This indicates that there was a change in dominant energy from tidal to fluvial, due to seasonal factors, which allowed high rates of sedimentation to bury the existing pyrite layers. Okubo *et al.* (2003), in a coastal lowland agricultural planning study, stated that geomorphological processes typically determine the landform location (geographically), thus its soil profile and properties. In this case, the higher pyrite concentration (5.53 %) in a seaward backswamp compared to landward (0.79 %) led to the conclusion that the younger backswamp was susceptible to acidification. Even though this study also investigated the soil properties of other landforms such as beach ridges and swales, there was no information on the pyrite concentration of these landforms.

Swales, a depression between beach ridges or dunes, are also a common landform where pyrite accumulates (Atkinson *et al.*, 1998; Jakobs & Baker, 2004). Swales were formed with the involvement of the seawater inundation through coastal geomorphic processes. In Indonesia, the beach ridge-swale system is one of the major landforms in coastal lowlands (Verstappen, 2000). As in Southeast Asia, the formation of this system followed the stabilization of sea level during the Holocene (Tjia *et al*., 1977; Woodroffe, 2000). The Holocene Stillstand (Smith *et al.,* 2006; Tjia, 1987; Verstappen, 2000) was possibly the period when the swales developed. The variety of swale development influenced the amount of sulfate supply from seawater and thus the time for pyrite to accumulate (Roslan *et al*., 2010).

Geomorphic processes also determine the conditions for pyrite development in the formation of salt marshes and tidal marshes, additional landforms where ASS can form in coastal lowlands, (Bescansa & Roquero, 1990; Bush *et al*., 2004; Bush & Sullivan, 1999; Diemont *et al*., 1992). Salt marshes develop in supra-tidal and upper inter-tidal zones and have different seawater inundation periods which determine their soil properties (Bird, 2007). Salt marsh sediments are initially deposited by the wave action that washes sediment into the intertidal zone, producing an accreting mudflat. This wave action continually supplies sediment to the mudflats until eventually creating a micro-cliff on the sea margin protecting the environment from wave action and allowing vegetation to establish (Allen & Pye, 1992; Bird, 2007). Some micro-cliffs develop a mudflat seaward and evolve into mangrove-fringed salt marsh terraces (Bird, 2007). Different stages of salt marsh evolution are indicated by the dominant salt marsh species present (Bescansa & Roquero, 1990). Salt marsh vegetation, the main source of organic matter, combined with saline sediment, are an ideal environment for potential acid sulfate clay development. The pyrite concentration, however, will depend upon the composition of seawater and freshwater supplies during the development of the salt marsh (Rosicky *et al*., 2004b).

2.3 Understanding the Relationship between Acid Sulfate Soil and Hydro-Geomorphic Processes

2.3.1 Soil-landscape Approach and Hydro-geomorphic Processes in ASS

The various sedimentary processes that influenced the development ASS are strongly influenced by geomorphological and pedological processes. Research has also demonstrated the strong relationship between pedology and geomorphology, which are important fields in earth science (Gerrard, 1992; Kerry & Oliver, 2011). Some soils are formed by weathering of parent material and the others form due to deposition. The parent material may be derived from underlying bedrock from which its composition and structure form the setting of the landscape (Strahler, 2003). In agriculture, for soil survey purposes, the relationship between landscape evolution and associated soil has been examined by including the terrain elements to understand soil formation. These factors include topography, drainage patterns, local erosion, natural vegetation and human land activities (Avery, 1980).

In the past, slope was the main element that affected soil development and type (Milne, 1935). Slope controls hydrological and sedimentary processes which influence soil formation. Slope can control the effect of rainfall by influencing runoff, and also have a bearing on temperature. This climatic condition is including rainfall and temperature changes which are important in soil formation processes. However, later study has revealed that there were some issues of accuracy when determining soil distribution and genesis using only slope and climate (Butler, 1958). Therefore, it has been suggested that the accuracy of soil distribution maps could be improved by including information based on geomorphic and stratigraphic principles, and acknowledging landscape morpho-cronology in the soil formation identification (Walker, 1989; McKenzie *et al.*, 2008). This approach, later named as soil-landscape processes and evolution approaches, aimed to enhance the understanding of soil and landscape processes and relationships, related to soil distribution (and spatial variability) and soil genesis. Specifically for Australian soils, it includes emphasizing the significance of erosional and depositional processes on soil formation. Walker (1989) also highlighted the importance of understanding the soil-landscape process in managing ASS coastal lowlands including sensitive wetlands which has potential to produce more ASS.

In relation to ASS, it is not enough to only involve soil-landscape processes in understanding pyrite formation. As mentioned in Section 2.1, hydrological elements represented by river energy, natural tidal prism, water table fluctuations, drainage system etc. affect the rate of sedimentation and deposition where pyrite accumulated (Dent & Pons, 1995). Husson *et al*., (2000), Fitzpatrick *et al*., (2008b), Rosicky *et al*., (2004a), conducted studies on ASS distribution using hydrological elements added into geomorphic parameter. Thomas *et al*., (2003b) developed a conceptual model for soil-water-landscapes in coastal environments as a more appropriate approach to describe the distribution of ASS. This current study, then, translates this soil-water-landscapes term into hydro-geomorphic. Scheidegger (1973) synthesised the role of hydrological and geomorphic processes in landscape formation and called it hydro-geomorphology. It combines the spatial view of how landforms are shaped with how water forms the soil. The term water included geographical, geological and hydrological features of a water body, and also those aspects in response to events caused by natural and anthropogenic processes (Babar, 2005). Thus, in term of this present ASS development study, knowledge of hydro-geomorphology is not only needed to identify the characteristics of catchments and their hydrology (climate and river system) in the development of fluvial landforms, but also to recognize the influence of coastal marine hydrology (tide, wave, current) to the characteristics of coastal landforms.

2.3.2 Hydro-geomorphic Processes Identification using Estuary Classification

It was noted in earlier sections that previous ASS study areas were typically located in coastal environments. These coastal lowland environments consist of the material deposited from upper catchment landscapes and coastal processes (Gerrard, 1992; Woodroffe, 2000). Fluvial processes, such as flooding and sedimentation, also shape coastal lowlands. Marine processes influence the coastal environment through present and paleo-coastal energy. Sea level rise caused by local tectonic activity or in the post-glacial era, created sub-aqueous brackish water environments in the coastal areas and also further inland (Dent & Pons, 1995; Pons *et al*., 1982; Verstappen, 2000).

Coastal flood plains show the stratigraphic junction between alluvial sediment and marine/estuarine sediments (Walker, 1989). These interbedded sediments are associated with the fluvial response to the sea level changes between late Quaternary from about 125 m below current sea level between 20,000 B.P. and 6000 B.P. (Brewer and Walker, 1969; Shackelton, 1987). There is consistency between these worldwide late quaternary sea level rises and the general pattern of ASS occurrence (van Breemen & Harmsen, 1975; Lin *et al.*, 1995). The Stillstand period after the Holocene sea level rise (6500 years ago) also contributed to the development of ASS formation environments (Thom & Roy, 1985; Sammut, 1999). This Stillstand created barrier systems that generated intertidal-swamp and mangrove swamp environments (Thom & Roy, 1985; Ward & Larcombe, 1996; Wilson, 2005). Existing sulfurous materials (including pyrite) have been found on several different elevations relative to mean sea level, and related to the Holocene Stillstand (Wilson, 2005). This ASS spatial vertical distribution pattern based upon elevation, makes it possible to understand coastal evolution and sedimentary processes (Lin *et al.*, 1995). Furthermore, pyrite has been used as an indicator of the Stillstand. In Indonesia the Holocene sea-level rise has been recorded at around 6000 – 5000 BP ($\pm$ 5 m from present mean sea level), then decreasing at 3000 BP ($\pm$ 3 m from present mean sea level) and 2000 BP ($\pm$ 1 m from present) (Verstappen, 2000; Tjia, 1987, 1996). This means the Holocene Stillstand affected more than 50,000 km of coastline in Indonesia. Hence, the possibility of the development of pyrite formation environments around its thousands of islands was high, both in numbers and disparity. Yet, there have not been any studies which specifically utilize these Stillstand data for the identification of potential pyrite containing soils and their properties in Indonesia. Recent work in Central Java on sea level rise focused on its potential impacts on aquaculture and the environment (Joseph, 2013). Earlier mentioned Holocene Stillstand information in Indonesia, then, perhaps enable this study to explore the possibility of ASS potential distribution among Indonesian archipelago in general scale.

Estuary-based ASS studies also show a strong relationship between coastal evolution and estuary responses to fluvial, tidal and wave energy (Johnston, 2009a, 2009b). Different estuary processes develop various estuary types, subsequently controlling landform development within estuaries (Dalrymple *et al*., 1992), and spatial variability in pyrite accumulation (Fitzpatrick *et al.*, 2008b; Oenema, 1990; Sylla *et al*., 1996). Estuary type identification can provide the information of the estuarine infilling process, freshwater flooding period, tidal inundation and even groundwater level to investigate soil and water acidification caused by ASS (van Breemen, 1975; Johnston, 2009; Fitzpatrick *et al.*, 2008b). By classifying estuaries, the relationship between landform development and fluvial and marine processes are identified, and the hydro-geomorphic processes can be evaluated. Therefore, it is possible to conduct integrated comparison studies, to explore the ASS-landscape relationship in different types of estuaries and other potential ASS locations.

2.4 Acid Sulfate Soil Mapping: The Importance of a Landscape Unit Approach and Its Challenges

2.4.1 General Soil Mapping: Approaches and Development

For the past 100 years, soil survey and mapping methods have been intensively developed and discussed to produce approaches that are systematic and efficient (McKenzie *et al.*, 2008). Systematic survey and mapping provide clear procedures that are built around the research purposes. An effective method is one that is as simple as possible and depends on a minimum data set for the level of required accuracy and uses minimum resources (McKenzie *et al.*, 2008; McDonald *et al*., 1990).

It is commonly recognized that conventional soil mapping techniques provide a meticulous way of determining sampling sites in order to obtain detailed soil class boundaries (Dent, 1986; McKenzie *et al.*, 2008). Unfortunately, most detailed soil surveys consume a great deal of time and effort. The challenges include logistical issues, such as access to remote areas, and data acquisition, i.e.: unsophisticated mobile instruments, large amount of samplings, and lack of remote sensing data. Even though detailed boundaries which differentiate the soil units can be mapped, maps do not always reveal landscape processes that underlie soil formation (Walker, 2009; Gerrard, 1992).

In line with these soil-mapping challenges, continuous investigation into new methods has allowed mapping practices to develop, from manual to high technology surveys and mapping methods. The purposes of soil mapping are also shifting, not only for pedogenetic and classification criteria, they are also being adjusted for other users and professional groups. Applications include agriculture, mining, environmental protection and more recently, aquaculture development (McKenzie *et al*., 2008; Myar & Hollis, 1998; Rossiter, 2004). Accordingly, several new approaches for soil mapping have been introduced in those fields and have become a part of the soil-mapping standard. A common approach which has been applied in soil mapping involves an understanding of the relationship between soil and landscape processes. It involves a deeper exploration of how landscape processes, which mostly consist of geomorphological and hydrological processes, influence soil development and soil properties (Gerrard, 1992; Pennock & Veldkamp, 2006; Strahler, 2003; Walker, 1968; 2009;).

Lillesand & Kiefer (2004) established that the association between soil properties, key interpretations and radiance spectral data can be determined using aerial photographs. There have been several approaches used to interpret features in remotely sensed imagery, such as: topography, drainage pattern, land-use and vegetation (Campbell & Wynne, 2010; Jensen, 2007). However, the landscape unit approach through identifying terrain characteristics has been the most common (Lillesand & Kiefer, 2000; Campbell, 2011). This approach assists the soil mapping process by recognising the environmental factors that influenced the development of soil, i.e.: climate, topography, vegetation, etc. The more advanced soil-landscape mapping methods increasingly use aerial photographs, remotely sensed imagery and geographic information systems (GIS) to identify landscape processes. This included using statistical and modelling approaches, such as: generalized linear models, classification and regression trees, artificial neural networks, fuzzy systems and geo-statistics (Burrough, 1996; Gessler, *et al*., 1995, 2000; McBratney, 2003; Scull *et al*., 2003). Enhanced digital image processing also enables comprehensive soil survey through spectral radiance identification of soil properties. It consists of GIS spatial modelling for prediction, digital terrain models (DTM), and other spatial statistical calculations. Advanced remote sensing data and modelling are used for producing base maps for field survey guidance, and also to improve the level of detail (minimum object which can be mapped based on map scale) in soil mapping using soil landscape analysis without using large numbers of sample points (Hole & Campbell, 1985). These spatial approaches are generally more accurate and effective in establishing a more valid correlation between soil properties and their origin, and existing environmental characteristics (McBratney *et al*., 2003; Zhai, 2006).

2.4.2 Acid Sulfate Soil Mapping

ASS mapping methods have been keeping pace with trends in soil mapping methods discussed above. Mapping methods applying landscape approaches have been rapidly developed in an effort to solve the problems caused by ASS (Lin *et al.*, 1995; Dent, 1997). Most of these approaches rely on an understanding of geomorphological processes in estuarine areas as well as biological indicators of the estuarine environment. This approach is supported by developments in technology including computer and information technology that underpin improvements in mapping methods and database management (McKenzie *et al*., 2008). Recent ASS mapping studies have used spatial variability approaches to map acid sulfate soil distribution, examining the soil-landscape relationship, landforms, land-use and geology, and sea-scape (Table 2.1).

van der Kevie (1972) used geomorphological information including: sedimentary environment, landform and vegetation pattern to predict ASS occurrence. This paper emphasized the need to understand the ASS development process to determine its relationship to landscape features. van der Kevie (1972) demonstrated that different types of ASS occurred in different climatic zones using the USDA and World Soil Maps. However, due to the complexity of ASS formation, mapping units were not established. By the 1980s, the mapping of ASS relied not only on existing topographic maps but also landscape maps (Madsen *et al*., 1985). While a topographic map shows only the elevation and imaginary landscape through contour lines, the landscape map indicates the existing processes through land units which are developed from topography, land-use and vegetation information (Gerrard, 2000). Madsen *et al.* (1985) used the landscape map to identify wetland and non-wetland areas, instead of using the existing landscape types, as a mapping unit, to guide soil sampling in the field. As a result, because of the large areas of wetland and non-wetland sampled, fieldwork still relied on a large number of soil samples. This method did not generate or incorporate information about landscape characteristics and processes.

Table 2.1 Spatial variability approaches in previous studies of ASS mapping

Author	The elements of spatial analysis	Type of Mapping Unit	Group of elements	Application/Topic
Van Der Kevie (1972)	Sedimentation environment, Vegetation Pattern, Landform	Not defined	Geomorphology	General Agriculture
H.B. Madsen et al. (1985)	Landform & Geology	Land system	Geomorphology	Wetland
C. Lin et al. (1993, 1994, 1995)	sedimentary, geomorphology, vegetation evolution and land-use	Landscape, topographic	Geomorphology	Land development, coastal resources
A.K. Bregt, et al (1992); F. Ahmed and D.L. Dent. (1997)	Spatial statistic (Kriging)	Soil-geomorphic	Geomorphology	Soil Survey
O. Husson et al. (2000)	Soil Characteristics, natural vegetation, groundwater table, micro-elevation	Micro-elevation	Geomorphology and Hydrology	Agriculture Agronomy
Fitzpatrick et al. (2008a, 2008b, 2008c)	Bathymetry, soil and vegetation mapping	Still in progress, but refer to landscape unit.	Hydrology	General - Management
D.S. Fanning et al. (2009)	Soil characteristics	Landscape/Seascape	Hydrology - Geomorphology	General - Soil Mineralogy
Current study	Geomorphology Hydrology data Land-use Vegetation type	Hydro-geomorphic Unit	Hydro-geomorphology	Aquaculture & Coastal Planning

Lin & Melville (1993, 1994) and Lin *et al*. (1995) used the term landscape to describe an environmental unit based on sedimentary properties, geomorphology, vegetation evolution and land-use, which also applied in this current study. The studies investigated three different types of estuary to describe the relationship between ASS properties and landscape units including the anthropogenic activities that influence soil formation. The studies were conducted in Eastern Australia and China which both have significantly different of geomorphic backgrounds. Their sampling locations were based on limited fluvial landform units (only levees and backswamps) near the main river (Lin *et al*., 1995), delta (Lin & Melville, 1994) and drainage systems (Lin, 1998). The investigations in those studies scrutinized the paleo-geomorphology and hydro-geomorphology of the catchment and its estuary however it was only limited landform units identified to see their relationship with ASS distribution possibilities. The uses of paleo-geomorphology and hydro-geomorphology information are supposed to reveal more varied landscapes outside the common ASS related landforms, as proposed in this current study. Nevertheless, the result is significant and led to the conclusion that estuary types indeed determine the pyrite formation processes. The conclusion was that a tide-dominated estuary has greater pyrite accumulation compared to river- and wave-dominated estuaries. This tide-dominated estuary generated more low energy environments which enable the organic matter and sulfate to reduce and to develop the pyrite.

Some researchers have developed spatial variability calculations through statistical methods to investigate the distribution of pyrite and the depth at which occurs or where it is greatest in the soil profile. Bregt & Gesink (1992) applied the Kriging statistical method to assess the depth of pyrite in one type of landform unit, tidal flats. This research involved large numbers of soil samples to give this statistical method improved mapping accuracy. The approach showed clear boundaries of different classes of pyrite depths. However, without including landscape processes in the analysis, this approach was only reliable on the assumption the landscape processes were uniform, whereas every single unit where ASS occurs has its own distinct processes (Dent, 1986). Ahmed & Dent (1997) also applied spatial statistics in a study on ASS using the Kriging statistical method after the soil-geomorphic units were determined from aerial photographs, based upon field work results (Dent & Ahmed, 1995). The application of soil-geomorphic units was considered urgent to avoid bias in the final ASS boundary, especially when the soil sample points were uneven between each mapping unit. These soil-geomorphic units covered three types of landform only: tidal flats, tidal stumps, and estuarine terraces, which had strong indication of the presence of ASS. In contrast, this current study accommodates all possible landforms present in an estuarine environment, regardless of their association with the presence and absence of ASS. However, the seasonal salinity and progress of tidal and river energy, and soil characteristics in Dent & Ahmed (1995) study presented the method which should be applied in seasonal tropical estuarine environment. Dent and Ahmed (1995) also acknowledged the significant role of GIS in selecting large sampling data into a dataset for spatial statistical analysis, which is also essential in this current study. The results showed better mapping unit boundaries compared to those from the Kriging application without including more detailed data on spatial variation obtained from field sampling.

It is known that in a potential ASS environment, water table fluctuations and tidal ranges can enable pyrite to oxidize naturally (Fitzpatrick *et al,* 2008b; Hart *et al*., 1987, 1988; Husson *et al*., 2000; Rosicky *et al*., 2004b). The acid released following oxidation contaminates the surface water, drainage systems, tributaries and rivers, and the soil itself (Minh *et al.,* 1997; Hart, 2004). Some research conducted in Northern Australia, on the transport of contaminants in fluvial systems, found pyrite bound to suspended particulate matter (SPM) and coarse colloidal matter (CCM) (Hart *et al.,* 1987). This pyrite was detected on the samples taken during a flood event, and classified as weathered pyrite. Although there was no explanation in this paper about this pyrite weathering process, it is well known that weathered pyrite starts with pyrite oxidation, and subsequent iron oxidation produces higher acid concentrations and can release heavy metals (Lu *et al*., 2005; Lin, 2012). Although it was conducted in a mining environment, Hart's study (2004) emphasized the impact of water table fluctuation on ASS landforms. This study suggested that there were dry periods that allowed pyrite to oxidize, possibly caused by water table fluctuations or soil exploration for new irrigation systems. During the wet season, a flood event then transported this weathered pyrite to the main river and unfortunately with other toxic material this will potentially lower the river water quality.

Husson *et al*. (2000) focused on river-dominated estuaries, including deltas, and micro-elevation units to identify water table and tidal flushing influence on the depth of sulfidic material layers in the Plain of Reeds, Mekong Delta. Micro-elevation of these mapping units was determined relatively to mean sea level. The ‘high locations’ were the mapping units located higher than 85 cm above mean sea level and ‘low locations’ were located less than 75 cm above mean sea level. The vegetation types of those two units, however, were different and this becomes a factor in soil development. The study showed that during the dry season, with tidal flushing affecting the ‘low location’ mapping units, the ground water table was raised because of tidal movement in the delta drainage system. This tidal movement provided the sulfuric sediment layer with more organic matter compared to the ‘high location’ mapping units. On the other hand, the lowering of the water table, as a result of high evaporation during dry season, also affected the soil development in these two mapping units, which were the oxidation of pyrite. This condition indicated that the micro-elevation and the duration of tidal flooding influenced pyrite development. Because there were significant differences in the pyrite concentration of these two units, it was stated in this paper that the micro-elevation units could be scaled up into the wider study area (smaller scale). However, this up-scaling suggestion ignored the variability of micro-elevations and landform processes in wider area which will mislead the determination of the probability of pyrite concentration. In fact, the multi-scale approached (introduced by Fresco & Kroonenberg, 1992) was applied in this study. Further examination is required to use this micro-elevation unit approach when applying down- or up-scaling the ASS properties to an ASS map’s units at different scales. Therefore, this current study, tries to fill that gap by including all landforms in the study area (covering all type of landform elevation) using multi-scales approaches. This approach will provide multi-scale ASS mapping units to obtain more comprehensive information that can support the ASS occurrence rapid assessment.

Fitzpatrick *et al*. (2007, 2008b) investigated the probability of ASS occurrence level using a landscape approach that differentiated tidal and non-tidal areas to establish new associated ASS landforms as mapping units. This study was based on: previously mentioned, soil-water-landscapes conceptual model in coastal environments (Thomas *et al*., 2003), coastal ASS management guidelines, and inland ASS (Fritsch & Fitzpatrick, 1994). These studies examined the influence of hydrological conditions on the ASS setting (water logging, soil salinity caused by drought). In the Fitzpatrick *et al.* (2007)

study, the mapping units referred to landscape units which were assessed to have a high probability of ASS occurrence. Every mapping unit described soil-landscape development processes in relation to the formation of pyrite layers. This soil-water-landscape approach also supplied the conceptual model on how lowering the watertable affected the establishment of different types of pyrite properties both in coastal and inland environments. The conceptual framework and approach, which utilized mapping units representing soil-water-landscape processes, is worth scrutinizing. This current study adapts this framework as part of a broader hydro-geomorphic approach which not only considers the water table but also other hydrological aspects within the catchment as stated earlier in section 2.2.1.

Fanning *et al*. (2009) developed a conceptual framework to investigate the origin of ASS formation based on their mineral properties (mainly Fe and S). Through the study of chemical processes in the soil, it was found that the landscape and seascape processes determined the environmental setting of pyrite development. This study described possible interactions between upland and wetland areas, and how present and paleo-landscape/seascape sediment (past geology and geomorphological setting) were affected by dynamic changes in brackish or sea water. The interactions between these environmental factors during landscape formation determined the duration of iron oxide burial in soils and the natural control (uplifted sea-based anaerobic soil, Ca biological precipitation, water table fluctuation, tidal prism, etc.) to expose the sulfidic materials to aerobic conditions. The authors explained that in landscapes rich in Fe oxides there is rapid Fe sulfide transformation. A resulting conceptual framework is in line with the understanding ASS hydro-geomorphic process. In this case, pyrite development is related to landscape units influenced by various subaqueous and seawater environments.

In summary, previous studies outline the necessity of establishing landscape units as mapping units that represent landscape formation processes as the foundation of ASS mapping. These landscape units not only represent the landscape formation processes, but also portray other dynamic environmental factors (e.g.: river tides, waves, water table depths, land use changes etc.) included in those processes. The analysis of ASS in each landscape unit will validate and clarify the ASS formation processes, since the development processes of ASS differ (Dent, 1986). Therefore, in addition to analyse the

ASS physical and chemical properties in detail, investigation of spatial variation of ASS across different environmental settings and hydro-geomorphic processes influencing ASS development should be combined to improve ASS mapping.

2.4.3 Estuary Classification Approach for ASS Mapping Purpose

Bird & Ongkosongo (2000) have conducted some studies in some Indonesian coastal environments and estuaries. Their study covered coastal development and evolution during the last 100-200 years which included geomorphology, climate, fluvial sediment, tidal energy and the changing land and sea levels. Their descriptions consider landform and marine factors influencing the development of the coastal area. In 1984, Ongkosongo then developed a modified classification of deltas in Indonesia based upon sediment formation and location of delta development (Ongkosongo, 2010). There are four types of delta in this classification; these are land to sea delta, sea to sea delta, land to land delta, and sea to land delta. This study discussed different delta and estuary definitions but there was not any further classification of estuary systems. Other studies examined the physical processes of estuaries for engineering purposes, the detailed chemical and physical properties, and the individual characteristics of main channels and tributary rivers (Table 2.2). However, there were no comprehensive studies looking at detailed characteristics of the existing estuaries types, leading to a classification system. Therefore, a review of estuary classification systems developed outside Indonesia was undertaken for this current study.

Previous estuary classification schemes have applied various approaches in order to identify and classify estuaries (Table 2.3). The scopes vary from global, regional to local scales. Boyd *et al.* (1992) proposed a new classification system using the different settings of depositional processes in coastal environments. It involved the definition of relative fluvial power, wave versus tidal relative power and evolutionary classification based on sedimentary environments. Even though this classification was applied to all coastal landscapes, specific estuary types were also included; these were wave- and tide-dominated estuaries.

Table 2.2. Previous estuarine studies in Indonesia

References	Location	Research Focus
Verstappen, 2000; Yuanita, et al., 2008	Cimanuk estuaries in West Java	Reconstruction of the delta formation
Engelen, 1980; Goffau & Linden, 1982	Serayu, Garang, Bogowonto estuaries in Central Java	Soil erosion and water resources management
Hoekstra et al., 1988, 1989; Jenerjahn, et al.,2004	Bengawan Solo, Brantas estuaries in East Java	Sedimentation
Carbonel & Moyes, 1987; Storm, et al., 2005; Caratini & Tissot, 1988	Mahakam Delta, East Kalimantan	Palaeo-environment, peleogeographical, paleo-sedimentary
Sanderson & Taylor, 2003	Mendahara and Lagan estuaries, Central Sumatera	Water Quality
Ongkosongo, 2010	Indonesia	Delta Classification

Table 2.3.A Methods and parameters used to classify estuaries in previous studies (Part 1)

References	Location	Parameters/Method used	Type of estuary in the classification system
Hayes, 1975	World	Tidal range based on geomorphology. Correlating depositional sand bodies in estuaries with different coastal environment.	Microtidal, (tidal range <2 m) Mesotidal (tidal range 2-4) Macrotidal (tidal range > 4 m)
Boyd et al., 1992; R. W. Dalrymple et al., 1992	World	Dominant river and marine processes, evolutionary process.	Wave-, tide- and river-dominated estuary.
Pritchard, 1995 in Haslett, 2000	World	Based on the level of salt and fresh water mixing within estuary	Type A: Stratified Type B: Partially mixed Type C: Well-mixed
C.D. Woodroffe, 2000	World	Morphodynamics and evolution of estuaries.	Drowned river valleys Tide-dominated estuaries Wave-dominated estuaries Coastal Lagoon
H.H.G. Savenije, 2005	World	Tide, Wave, River Discharge, lateral sediment Combined estuary classification based on shape, tidal and river influence and geology.	Detailed estuary classification based on shape, tidal and river influence, and geology.

This study also provided a ternary diagram (Figure 2.1) to show how different types of energy combinations control the types of estuaries which develop. This enables non-scientific users to identify relative energy level (in this study, it was called ‘power’) existing in an estuary. However, as the term estuary in this paper was defined as a drowned valley influenced by fluvial and marine processes, and a study by Roy *et al.*, (2001) demonstrates that not all estuaries are drowned valleys, it is important to identify the estuarine processes in more detail before applying this classification approach.

Table 2.3.B Methods and parameters used to classify estuaries in previous studies (Part 2)

References	Location	Parameters/Method used	Type of estuary in the classification system
E. Bird, 2007	World	Morphology and sediments	Descriptive explanation based on channel shape, sediments, shore, tidal delta and lagoon.
V.D Engle,. et al., 2007	US	Physical and hydrological properties of estuaries	Nine classes based on area, volume, river flow, depth, salinity.
Geoscience Australia D.A. Ryan et al, 2003	Australia	Based on geomorphology and sedimentary environments.	Seven classes: Embayment, wave-dominated estuary, tide-dominated estuary, wave-dominated delta, tide dominated delta, coastal lagoon, tidal creek.
P.S. Roy et al., 2001	South-east Australia	Geology, Form of maturity Part of types of coastal water body (different coastal setting and differing rates of sediment infilling)	Tide-dominated estuaries Wave-dominated estuaries Intermittent estuaries
T.M.Hume et al. , 2007	New Zealand	Controlling factors divided into 4 levels that contain information of physical and ecological characteristics of estuaries.	Seven full categories based on 8 hydrodynamic classes, 7 geology categories and 5 landcover category
Z.Z. Ibrahim et al., 1996	Malaysia	The salinity structure of the estuary; biological and chemical characteristics.	Low, moderate and high estuary quality.
This current study	Central Java, Indonesia	Geo-climatic Region Hydro-geomorphic Units	Wave-, tide- , river- dominated estuary and seasonal tropical estuary. Focus on the development landforms in different types of estuaries.

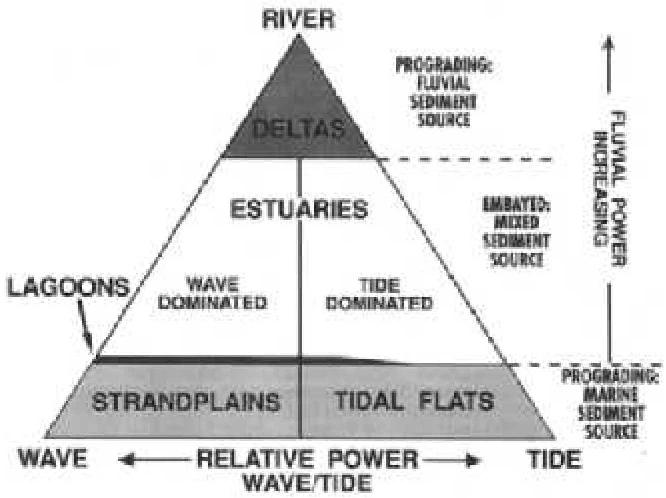

Figure 2.1 The ternary diagram showing different type of coastal landform and estuary type based upon different levels of fluvial, wave/tidal relative power (Boyd et al.1992).

Other estuary classification studies applied salinity level measurements to identify different mixing levels of salt and fresh water in estuaries (Pritchard, 1995 in Haslett, 2000). The estuary types were classified into 3 categories: (1) Type A: Stratified, (2) Type B: Partially mixed and (3) Type C: Well-mixed (Table 2.3). Type A is comparable to river-dominated estuaries, where the fresh water flow is above the highly saline layer of sea water, and develops a salt-wedge. Type B is related to mixed river and tide energy, where between fresh water flow and sea-water flow there is a layer that content both fresh and salt water. This layer generates a zone which has gradual salinity levels and maximum turbidity, because both sediments flow from that fresh- and sea-water trapped in this zone. In this zone, when the average velocity is zero (null point), an estuary bed is commonly developed. The well-mixed estuary (Type C) has a homogeneous salinity level from the water surface to the bottom. This estuary is generally dominated by tides, so there is no clear separation between fresh- and sea-water layers. In brief, this study enables this current research to recognize the relative distribution of salinity levels both vertically and horizontally within an estuary, based on the dominant energy of different estuary types. These types of estuaries, however, were quite board and could not reflect the entrance condition and channel geometry which controls tidal penetration into estuary, thus the estuarine salinity level (Perillo, 1995).

Previous estuary classification by Hayes (1975) used tidal range to represent the physiographic characteristics on estuaries (Table 2.3). It presented three classifications: micro-tidal, meso-tidal and macro-tidal. A micro-tidal estuary, with the tidal range of below 2 m, is commonly related to a river delta with longshore current. A meso-tidal estuary, in contrast, represents seasonal tidal current dominance caused by marine, fluvial and climatic agents (wind or storm). A macro-tidal estuary commonly occurs in an environment where tidal currents are generated by wave action, and have tides greater than 2 m. The unclear definition of geomorphic process involved in each estuary, causes ambiguity in fitting the existing estuaries into this classification. However, the aim of Hayes' classification was to see the correlation between tidal range and the occurrence of sand depositional processes and some of these principles can be applied in this current study.

About a decade later, global estuary classification was developed based on combination of several approaches including salinity, morphology and sedimentary (river and marine) processes and, morpho-dynamics and estuary evolution (Savenije, 2005; Bird, 2007; Woodroffe, 2002). The relationship between coastal evolution and estuary infilling processes were also considered in estuary type identification. Woodroffe (2002), classified bedrock embayments and coastal lagoons as estuaries because of their similar characteristics, together with river-, tide-, and wave-dominated estuaries However, in a later study, bedrock embayment and coastal lagoon were excluded from estuary classification established by Bird (2007). This classification also introduced general estuary zonation based on tidal conditions and salinity. The first zonation was classified as 'seashore', indicating the environment is influenced by marine energy. The second one is the 'tidal shore' zone representing the environment created as a result of tidal activity. The last one is the 'river deposition' zone which is dominated by fresh water flow. The ranges of salinity level from river deposition to the sea shore estuary zone are 0.1 – 35 ppt. This estuary zonation system is consistent with the estuarine salinity structural types developed by Haslett (2000) who established salinity levels based on the shape of an estuary.

At regional and local scales, estuary classification criteria become more detailed and are determined by regional geographical characteristics and classification purposes. For example, in the USA, for coastal resource protection purposes, the criteria for estuary classification utilize physical and hydrologic characteristics of catchments (Engle *et al*., 2007). There were nine classes established based on area, volume, fresh-water flow, depth of estuary and salinity level. However, the application of this classification needs further assessment on how the physical and hydrological characteristics in each class affect water and sediment quality. In New Zealand, estuary classification process utilized abiotic components to classify the estuary types (Hume *et al*., 2007). The component used in this study mainly based on geomorphic or physical point, established by Pritchard (as cited in Haslett, 2000). This classification was divided into four different approaches, area scale and units. Level 1 is at a global scale based on latitude, oceanic and terrestrial process. Level 2 is based on estuary hydrodynamic process (basin morphometry, oceanic forcing and river forcing). Level 3 is based on the catchment features including land-cover and geology. Level 4 focuses on different types of local hydro-dynamic processes (sediment deposition and erosion). This work utilized GIS, including digital elevation models (DEM) and Triangulated Irregular Networks (TIN) to manage and analyze metadata from 443 New Zealand estuaries. Despite the result, there is a need to consider further validation by testing this approach in individual estuaries. The current study adopts the approach of using DEM as basic information of catchment characteristics and validates it in different types of estuary.

Before national estuary classification established recently by Geo-science Australia (2002), several states and regions in Australia utilized different estuary classification schemes because of their differences in environment and coastal conditions. Roy *et al.* (2001) investigated the function and structure of estuaries in south-east Australia. Their method used the relationship between coastal geological properties and morphology, water quality attributes and ecological aspects. This study defined estuary classification and zones. The estuaries are grouped into tide-dominated, wave-dominated and intermittently closed estuaries. The classification is completed with information of development stages referring to details of mature forms from infilling estuarine processes. The zonation was adapted from Bird (2007) and Roy (1984b) and included marine flood-tidal deltas, central mud basins, fluvial deltas and fluvial channels (Figure 2.2). Each zone represents water quality, bio-chemical signature and ecosystems related to sedimentation environments for mapping purposes. These two groups then were further classified into coastal water body groups. Further sediment type and hydrological types are also available in each zonation class. In fluvial channel zones, there are strong reducing environments but these are buried by sediment from fluvial processes. This subaqueous alluvial plain is associated with pyrite development. The information of central mud basin zone occurrence is also important to indicate the development of low-energy environments.

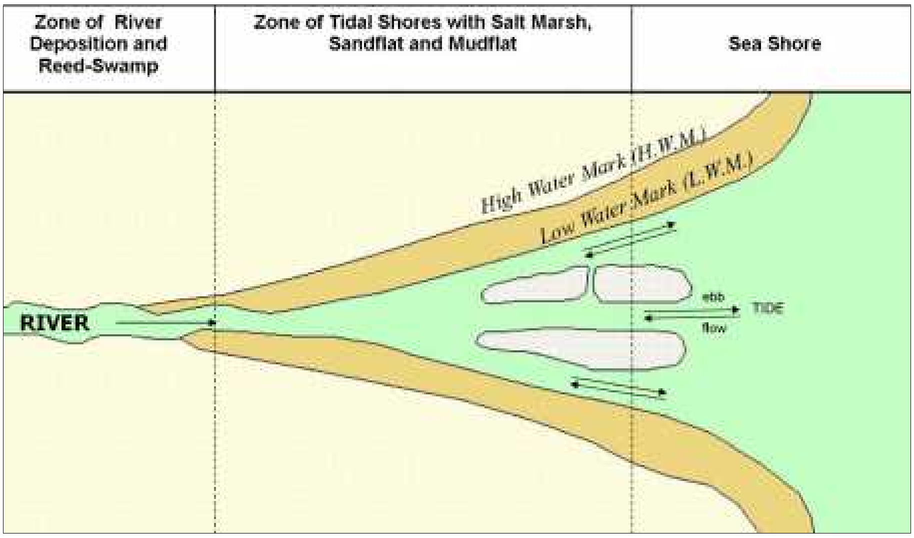

Figure 2.2 Estuary zonation based on tidal condition and level of salinity (Bird, 2000).

Table 2.4 Estuary zonation based on depositional sedimentary environments (Rochford, 1951 in Roy et al., 2001).

Main depositional environments	Sub-environments/habitats	Hydrological zones (Rochford, 1951, cited in Roy et al., 2001) and substrate types
Sea Shore	Rocky shoreline and rock reefs, tidal channels, tidal banks, tidal flats, delta front slope, back barrier sand flat	Marine (Vegetated and unvegetated sand and muddy sand and rocks)
Central mud basin	Rocky shoreline and rock reefs, slope and shoreline zone, basin floor, shell biotherms	Tidal (Unvegetated muds, sandy muds and muddy sands, vegetated rocks)
Fluvial delta	Levees, distributary channels, mid-channel shoals, delta mouth bar, crevasse splays, delta top and delta front, interdistributary bays	Gradient (Vegetated and unvegetated, sandy muds, muddy sands and sands)
Riverine channel and alluvial plain	Riverine channel, point bars, mid-channel bars, eroding banks, levees*, floodplain*, backswamp*	Freshwater (Unvegetated sands, gravelly sands and muddy sands)
*Subaerial depositional environments.		

Ryan *et al.* (2003) developed broader estuary classification for Australia, based on geomorphology and sedimentary processes, including climate, hydrology, water quality, morphology, habitat types and ecology. They used the combination of several estuary classification schemes from other parts of the world. About 974 estuarine environments were identified using remotely sensed data. This national classification scheme established seven estuary classes: embayment, wave-dominated estuary, tide-dominated estuary, wave-dominated delta, tide-dominated delta, coastal lagoon and tidal creek. This study provides detailed characteristics of each estuary class, including hydro-dynamic, sediment dynamic and nutrient dynamic. This conceptual model of estuary classification using biophysical processes is intended to support the assessment of environmental indicators. The climatic conditions of Australia, where rainfall is unpredictable, influences the consistency of the determination of estuary types. Nevertheless, description of the existing estuaries were well defined, providing strong justification in classifying the estuaries.

Malaysia, a country neighbouring Indonesia, also established an estuary classification scheme for development planning (Ibrahim *et al.*, 1996). The approach utilised water quality (salinity, turbidity, dissolve oxygen) and nutrient availability for fish resources. There was three estuary types with detailed ranges of water quality parameter values and salinity structures. There is no clear information about what hydro-geomorphic processes that influence determination of estuary type. However, Ibrahim *et al.* (1996) recommended considering the river discharge and tidal cycle data in future studies.

2.5 Remote Sensing and GIS Application in Acid Sulfate Soil Mapping

The uses of remote sensing and Geographic Information System (GIS), which facilitate more effective mapping techniques than only conducting detailed terrestrial surveys, have been explored further to accommodate the specific needs in ASS mapping (Dent, 1995; Fitzpatrick, 2011). Although ground-truthing is still compulsory for interpreting remotely sensed data, it plays a smaller role than in conventional mapping which does not use remotely sensed imagery to determine the sample location. Because ASS fieldwork is often conducted in isolated locations, such as tropical coastal lowlands and wetlands, remotely sensed data provide an alternative to conventional methods allowing sampling points to be selected from imagery with consideration of accessibility and mapping unit coverage (Bregt & Gesink, 1992). Fitzpatrick (2011) and McKenzie *et al.* (2008), improved mapping ASS and other soil types to reduce the need for detailed terrestrial surveys. These methods included soil-landscape and landform unit approaches. However, they have had a different focus and were not intended to detail soil and landscape relationships, as is the focus of the present study. The main focus of this study is on mapping ASS, particularly for aquaculture development and to improve coastal management. Other studies have focussed on soil mineralogy, moisture, carbon, organic, land evaluation or agriculture purposes (Belfon *et al.*,2014; Baroni *et al.*, 2013; Ladd, *et al.*, 2013*;* Yang *et al.*, 2013; Matgen *et al.*, 2012).

Besides simplifying the soil sampling method by reducing the need for sampling, another use of remote sensing in ASS mapping is to classify the landforms and land-cover/land-use, especially vegetation associated with ASS, such as mangroves (Dent, 1993; Muttitanon, 2005). The landform information is still effectively derived from visual interpretation rather than digital multispectral classification (Dent, 1986; Grealish *et al.*, 2013; Rossiter, 2014). The visual interpretation for landform identification also needs higher skill and more data support (soil, geology, topography) due the complexity of landscape process producing landforms (Campbell, 2011) rather than developing key interpretation for land-cover/land-use.

Hengl & Rossiter (2003) applied supervised landform classification in semi-detail soil survey to reduce the number of manual photo-interpretations, using digital elevation model (DEM). Due to the lower resolution of DEM, the result of this study was only able to identify hilly land, total area, plains and then other more detail landform at a semi-detailed scale, deducted from those three main classifications. Consequently the approach could not accommodate the more complex nature of landforms such as: point bar complexes, levees, active channel banks, and ASS related landforms, such as: backswamps, swamps and abandoned channels. Some of the parameters derived from DEM in this study, such as groundwater depth, slope, wetness index, and the distance from the nearest watercourse, however, can assist this current study to determine the landscapes which possibly enable pyrite to develop, in semi-detail scale.

Drainage patterns, erosional features and topography have been intensively studied to distinguish types of soil or parent materials using Digital Elevation Models (DEMs) such as from NASA's Shuttle Radar Topography Mission (SRTM), and Aster DEMs. These 3-dimensional data contributed positively in decreasing the complexity in determining the landscape units. However, similar to earlier discussed research (Hengl & Rossiter, 2003), the spatial resolution of the DEM data has to be monitored to avoid the inaccuracy that can affect analysis of the soil-landscape processes (Mulder *et al*., 2011).

The identification of landscape units, which represent the physical setting for a group of landforms (volcanic, fluvial, structural, marine etc.), has been developed further using remote sensing data to identify visible features in the landscape associated to the ASS formation environment. ASS mapping methods can utilize remote sensing data to recognize the ASS properties related to surface features, such as drainage, vegetation, topography and surface colour (Dent, 1986; Dwivedi, 2001). These landscape features can be related to the development of ASS (Madsen, 1985, 1988; Dent, 1986; Lin, 1995; Fitzpatrick *et al.*, 2008a, 2008c).

GIS provides a spatial analytical method to facilitate the processing and analysis of remotely sensed data to gain information for decision-making processes (Boettinger *et al.*, 2010; Bohner *et al.*, 2014; DeMers, 2000; Pradhan, 2013). This system-based tool is able to help the user to process a small or large amount of data using aggregation and clasification, analyses and iterative processes, and from a single set to a myriad of spatial data. The application of GIS to soil mapping has been utilized for modelling soil loss (USLE and RUSLE) and landslides (Moore *et al.*, 1992, 1993; Dosmet & Govers, 1996; Longley *et al*., 2001; Chang, 2002; Lee & Choi, 2004; Chen *at al.*, 2011). GIS has been also used to improve the accuracy of Kriging, multi-fractal and other spatial statistical interpolation method for spatial prediction of soil variables (Cruz-Cardenas *et al.*, 2014; Hengl & Rossiter, 2003; Webster & Oliver, 2001; Yuan, *et al.*, 2012; Zhang *et al.*, 2013;). The latest advances in GIS technology for soil mapping modeling has involved artificial neural networks, fuzzy logic (Beucheur *et al*., 2014), GIS expert systems and spatial data mining (McBratney *et al.*, 1991, 2003; Moran & Bui, 2002; Behrens *et al.*, 2005; Anda & Subardja, 2013; Shi *et al*., 2013; Huang *et al*., 2014;).

However, basic understanding of soil-landscape processes remains crucial in underpinning advanced mapping methods (McKenzie *et al.*, 2008).

Zhu *et al.* (2001) developed a GIS model for soil mapping as an “expert knowledge-based fuzzy soil inference scheme” that applied the soil-landscape concept as the foundation approach. The landscape information was derived from the similarity representation model, using GIS techniques with fuzzy logic. This method systematically synthesizes soil types and properties with local soil scientific knowledge to mine the similar soil properties within the units. The approach of developing landscape models in digital soil mapping for deriving new landscape units is relevant for this study. In ASS mapping, where this landscape unit approach has been commonly applied, GIS is able to accommodate the multi-scale, multi-temporal and multi-layer data with multitasking analysis to aggregate the data systematically to determine ASS mapping units (Chang, 2002). Current GIS applications relating soils and landscapes use a combination of DEM and raster GIS to derive information about geomorphology, drainage and channel networks (McDonald, 1996). But still, for the best result, utilization of remotely sensed data and GIS has to be strongly supported by good local knowledge and good basic knowledge of soil mapping, and an ability to interpret the results.

2.6 Statistical Applications in ASS Mapping

Statistical analysis of soil mapping accuracy (including ASS mapping) had not been rigorously applied until 10-20 years ago (Andriesse, 1993; Hewitt, 1993). Before then, most soil studies were based on field survey descriptions or laboratory analysis. Highly complex soil data require statistical analysis to validate the field and laboratory soil analysis (Webster, 2001). There were challenges in selecting suitable statistical methods to analyse soil data sets. These were due to the variety of soil data dimensions covering spatial, temporal and vertical profiles of soil properties. Soil researchers needed enough statistical understanding to select appropriate statistical methods in analysis soil field or laboratory analysis result.

Previous soil classifications used linear regression or correlation coefficients to test the relationships between sampling points and their soil properties (McBratney & Gruijter, 1992; Moore & Wilson, 1992). More recently multivariate analysis (e.g. analysis of variance (ANOVA) and principle component analysis (PCA), were also applied in soil science (Facchinelli *et al.*, 2001) supported by geostatistics, such as kriging (Sylla *et al*., 1996; Ahmed & Dent, 1997). New developments in soil digital mapping include more advanced statistical applications through spatial modelling and advanced geostatistics (McBratney *et al., 2003).* The most recent remote sensing and GIS studies applied statistical approaches to analyse correlations between field soil spectral measurements (mostly using spectrometry), remotely sensed data spectral values and soil properties (field & laboratory) (Oldak *et al., 2002;* Velasco *et al.,* 2005). However, few studies developed an approach to combine the soil data layers and synthesize them into one value to represent one mapping unit (Mallants, *et al*., 1996; Storm *et al.*, 1995). Commonly, if the sample profiles have multiple layers, analyses then focus on an individual layer or develop some group of layers based on existing knowledge of horizon depths. Previous analysis (McKenzie *et al.*, 2008; Webster & Oliver, 2001) calculated mean or median functions of samples taken at many depths in the soil profile to determine the soil properties of multi-layer samples, obtaining a single average value to represent one sample point or mapping unit. This data analysis could cause bias, therefore the decision to select or to waive a statistical analysis requires a cautious approach. In some cases, statistical analysis was not possible because the dataset was insufficient for the analysis because the data variability is too low or too large (Webster, 2001).

In terms of ASS mapping, the ASS layers in coastal area consists of diverse horizon layers because of different environmental conditions during sedimentation processes (Dent, 1986, Diemont *et al.*, 1992). Due to these different pyrite development, some ASS soil profiles, such as in fluvial plains, show very obvious soil horizons. However, many ASS horizons in tidal marsh, swamp, and mangrove forest show undefined layers. Therefore, soil datasets with fixed depth increments sampling is required to see the variation in soil properties at each sample point (Dent, 1986). Some studies in ASS suggest applying ANOVA to analyse data sets with several layers and to measure the relationship between the mapping unit and their soil properties (Burgess & Webster, 1980). Their analyses were usually based on the data set developed from soil sampling, and will then examine the results to identify the appropriate method for ASS mapping validation. However, beside the correlation between mapping unit and soil properties, this current study needed to identify the process on how each ASS development factors interact to influence the pyrite accumulation. Soil properties analysis through principles component analysis (PCA) seems to be appropriate to fulfil this current study need. Several studies applied spatial variability among factors using PCA showed better results in identifying the dominant factors that influenced the dependant variables, compared to other statistical analysis (Bullock *et al*., 2000; Bulluck III *et al.*, 2002; Fox *et al*., 2005). Therefore this current study utilized this PCA analysis to identify the factors that influence the development and distribution of pyrite in different landforms.

2.7 Concluding Remarks

In conclusion, understanding of the relationships between soil, water and landscape processes will facilitate the understanding of how landscape processes and influencing the development of ASS. These soil-water-landscape processes control the coastal evolution, sedimentation and land formation. The result of this hydro-geomorphic process determines pyrite concentration and distribution. Thus, further research is needed to understand hydro-geomorphic and estuary evolution processes, which can be used in classifying the estuary. The most suitable estuary classification approach to meet the purpose of this study will evaluate the energy levels involved, and how they affect sediment processes and landform development. The combination of classification approaches used by Boyd *et al.* (1992), Bird (2007) and Haslett (2000), will facilitate the identification of salinity structure, estuary sedimentary process and dominant energy environment through estuary classification. The estuary evolution and development stage and sedimentary process information based on estuary zone (Roy *et al.*, 2001; Woodroffe, 2005) will enable identification of the sedimentary process (infilling and maturity stages) to identify possible formation and distribution of pyrite. However, because of differences in climate (especially rainfall and temperature) and coastal geomorphology settings between Australia and Indonesia, further methodological adjustments will need to be applied in this study.

CHAPTER THREE

CONCEPTUAL FRAMEWORK AND METHODS

3.1 Introduction

This chapter describes the conceptual framework that connects the literature review and the methods applied in this study. This framework consists of some main points of the research background and literature review to select appropriate material and methods in addressing the research problems. The conceptual framework is intended to provide a scaffold for the research chapters of the thesis and to provide a more effective approach to integrating the background material, research outputs and the interpretation of the results and its relevance of effective mapping of ASS in Central Java. At the end, this chapter provides concise descriptions of the multi-level mapping method used in this study. It also explains the importance of the result from each method level in establishing a robust ASS mapping method.

3.2 Understanding the Development of ASS from a Spatial Perspective

Based on the literature review, the current study utilises the formation of ASS in coastal lowlands and the problems of ASS in aquaculture to underpin the development of the method (Figure 3.1). It has also explored the environmental factors that influenced ASS development from a soil-landscape relationship perspective (Hole & Campbell, 1985; McKenzie *et al.*, 2008; Walker, 1989). It was concluded that the term hydro-geomorphic processes can represent those ASS environment factors, because the role of hydrological elements in the development of ASS (see Chapter 2, Section 2.2.1). In Section 2.3.2, it was also explained that this study will identify the hydro-geomorphic processes using estuary classification. Therefore, at this point, this current section will explain how to incorporate hydro-geomorphic processes (knowledge on ASS development processes) into a technical framework to develop a robust mapping method. This explanation included the justification to generate a method to gain information of hydro-geomorphic characteristics from different scales, considering that ASS development were influenced by many environmental factors on a regional scale as explained in Chapter 2. The description of the technical framework is summarised in Figure 3.2 and in detail in several sections below.

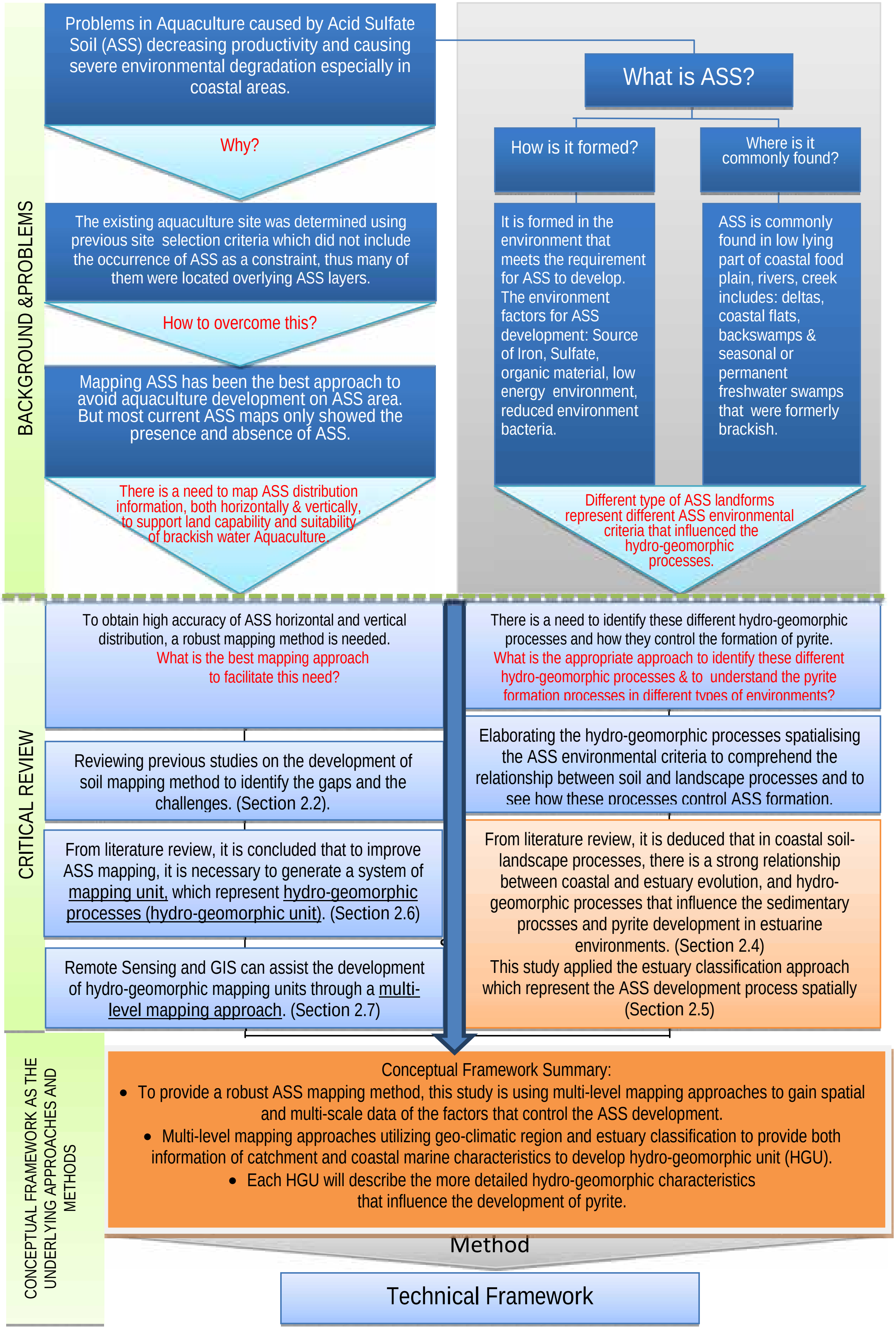

Figure 3.1 The conceptual framework of this study, concluding the foundation for multi-level mapping method

3.2.1 Spatialising ASS Formation Processes Using Estuary Classification

The estuary classification process, as explain in Section 2.3.2, needs comprehensive information that covers energy levels of rivers, tides and waves. The energy level information could not be derived only from the estuary scale, but also from larger environmental scale including climate, catchment characteristics, estuary evolution, inshore marine environment and land-use changes. This hydro-geomorphic characteristics information from regional to catchment and estuarine level enable this study to identify whether the environmental factors that develop ASS are available in a particular region (Figure 3.2, Part A: criteria). Once the estuary classification is established, this study can identify more detailed hydro-geomorphic processes at the estuarine level. To obtain these different levels of hydro-geomorphic characteristics information, there is a need to establish multi-level mapping methods so this study can collect this information from different scale of mapping.

In order to achieve the hydro-geomorphic information from the multi-level mapping approach, it is important to spatialise the ASS formation environmental factors as a key to identify the possibility of ASS occurrences in an environment. From five environmental factors for ASS to develop, the iron-containing sediment is the only factor that occurs in most soils and sediment. So, the existing soil maps can be used for the spatial data that represent this iron-containing sediment factor.

The second environmental factor of ASS development: source of sulfate, is related to the seawater and brackish water environment (Chapter 2, Section 2.2.2). The existing base maps and remotely sensed data that provide the information on marine and estuarine location can represent this factor to identify current sufficiency of sulfate supply in an environment. These data, however, are not sufficient to identify the past tide ranges, areas where seawater intruded, or the extent of sea level rise; these factors would have influenced past ASS formation. Hence, this study considered coastal and estuary evolution at the study sites to identify areas where ASS could have potentially formed. Geology, hydrogeology, geomorphology and paleo-geomorphology maps, and salinity and sea level rise data from previous studies were used to complement information on present-day tidal influence. Coastal landform identification is used as an approach to identify the hydro-geomorphic process that occurred in relation to the intensity of marine interference to the land. Therefore, a multi-level mapping approach is applied to identify the different types of landform in different scales.

The presence and absence of organic material (the third environmental factor of ASS development) in brackish water environments is identifiable from the presence of brackish water vegetation (mangroves, including *Nypa fruticans*). However, the changes of coastal and estuarine environments affect the occurrence of these brackish water environments. There are some areas, which used to have vegetation cover, are currently bare, due to mangrove clearance. Some of these areas, however, still contain organic matter in their sediment. Therefore, this study includes the multi-temporal spatial and remotely sensed data in the multi-level mapping methods, to detect land-cover and landform changes, specifically which is related to the mangrove area changes.

The forth environmental factor for ASS to develop is low energy. Low energy environments were identified in this study based on several criteria. As explained in Section 1.1 and 2.1, a low energy environment is defined as an environment which is not influenced by high marine and/or river energy. This environment allows colonizing vegetation to grow, therefore generating sediment with high organic content, which supports pyrite formation. In this study, this type of environment was identified by landforms including land-cover or land-use, and the existence of colonizing vegetation, such as mangrove and *Nypa fruticans*. Data of land-cover/land-use changes from existing maps and multi-temporal remotely sensed data were also analysed to identify the absence of colonizing vegetation in low energy environment landforms. In this low energy environment, Fe and S reducing bacteria normally decompose the organic matter and produce a reducing environment (Pons *et al*., 1991). Therefore, the presence of these bacteria, the fifth factor in ASS formation, is not specifically addressed in this data spatialisation process.

All spatial data that represent the environmental factors of ASS were scrutinized to achieve the hydro-geomorphic characteristics information in different levels, depending on their mapping scales. Further explanation of this development of method is provided in Section 3.2.2.

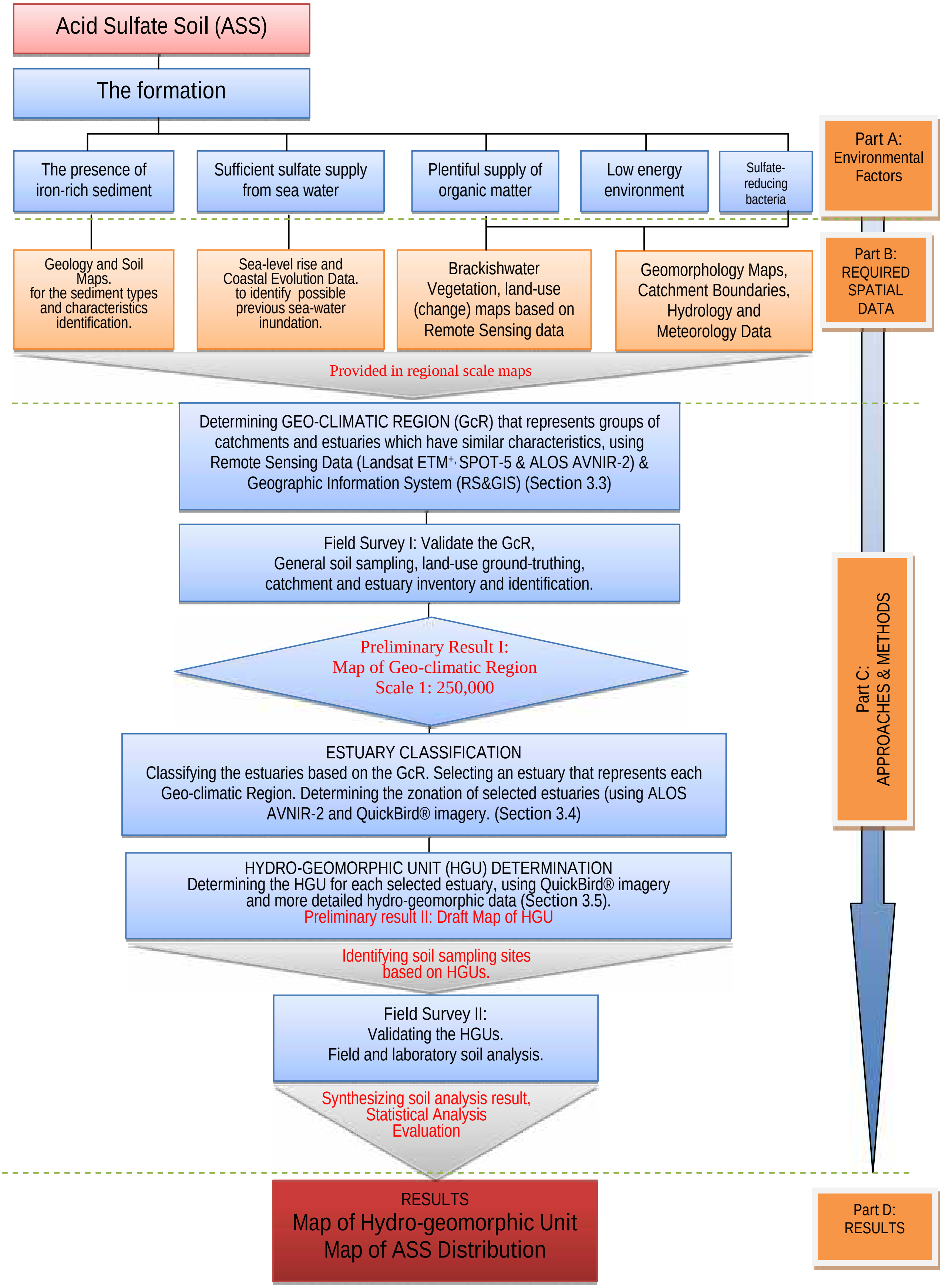

Figure 3.2 Technical Framework of the Research

3.2.2 Multi-level Mapping Approach to Derive the Spatial Hydro-geomorphic Data

As explained in section 3.2.1, pyrite development, despite being an *in situ* process, is indirectly influenced by hydro-geomorphic processes at different scales. These scales included the regional scale (1:500,000 – 1:250,000) represented by geography and biophysical characteristics of the study area, such as climate, geology and geomorphology; and fine scale (1:100,000; 1:50,000 to 1 1: 10,000) represented by land-cover, vegetation types, and coastal landforms. These different scales of hydro-geomorphic information were obtained from applying multi-level mapping approach (Figure 3.2, Part B: Material and Method). To simplify these different scales of hydro-geomorphic processes, the following multi-level methods were applied:

a. Regional level

The regional rainfall pattern, geological parent material of the catchment, sedimentary processes and characteristics of the coastal marine environment were identified. The regional boundaries were established to group the catchments and in-shore marine areas, which have similar hydro-geomorphic characteristics. These boundaries utilized data aggregation of remotely sensed data and GIS analysis (Chang, 2002). The regions created from this analysis are named Geo-Climatic regions (GcR), because they combine catchment physical characteristics and climatic conditions. It was also supplying information on the characteristics of in-shore marine, such as: tide and wave energy level, and how these energy levels influenced the development of coastal lowlands. This regional hydro-geomorphic information is summarised in a Map of Geo-climatic Regions generated in Chapter 4.

b. Catchment level

As explained in Section 2.2.3 and portrayed in Figure 3.1, the essential environmental criteria for pyrite to develop are associated with certain types of estuaries (Lin *et al*., 1995; Roy *et al*., 2001). Therefore, this study utilized estuary classification. The approach to classify the estuary applied the identification of river, tide and wave energy level. In addition to regional geo-climatic information, more detailed catchment data were synthesized to describe the existing energy levels influencing the estuary environment. This estuary classification scheme is the second preliminary result in this study. Some of the identified estuaries in this level were selected to represent the GcR(s) of Central Java for detailed analysis described in Chapter 5.

c. Hydro-geomorphic unit level

The hydro-geomorphic level mapping provided more detailed information of hydro-geomorphic processes at the estuary scale through establishment of mapping units called hydro-geomorphic units (HGU). The HGU determination process was applied to selected estuaries identified from the estuary classification. These HGUs were generated by combining information about landforms, land-uses, vegetation type and distance from the sea and brackish tidal watercourses. While doing landform identification, this study also established estuary zones based on tidal characteristics to recognize the transition zone of fluvial and seawater flow. Subsequently, field survey utilized these HGUs as a basic map for soil sampling. Detailed parameters observed in field survey and laboratory analysis are explained briefly in the following section. The results of this third level mapping, which are list of HGUs and its description, and Maps of Hydro-geomorphic Unit and ASS Distribution, are provided in Chapter 6.

3.3 Soil Sampling Method and Analysis

3.3.1 Field Sampling Method

This study applied multistage stratified random sampling to locate soil-sampling sites to represent each mapping unit, which is in this study named as HGU (Gruijter *et al*., 2006; McKenzie *et al*., 2008). The first stage included allocating one soil sample in each HGU and observing its physical characteristics. The second stage used the size of smallest area of HGU to determine additional sampling sites in a wider HGU. The numbers of samples taken from a map unit varied, but they were distributed as evenly as possible across the mapping unit. Several (at least 4) drillings were made before deciding on a soil profile that represented a mapping unit. This ensured the soil profile sampled for further field and laboratory analysis was the most representative. Further detail on the method to determine the sample sites and the number required are provided in Chapter 6.

3.3.2 Field and Laboratory Soil Analysis

The field and laboratory analysis followed methods from the Acid Sulfate Soils Laboratory Methods Guidelines 1998 (Ahern *et al*., 1998a, 1998b; Ahern *et al.*, 2004). The soil sampling utilized two different types of bore soil-sampling equipment to accommodate the different soil characteristics. A standard Jarret bucket auger was used to collect dry and moist soil, and a tapered gouge auger was used to collect the soft mud (Ahern *et al*., 1998b). For ASS and aquaculture purposes, the depth of the soil sample is normally to 2 meters minimum or the estimated drop in watertable heights (Ahern *et al.*, 1998b; FAO, 1998). The soil profiles were analysed at increments of 10 cm for both field and laboratory measurements. Soil samples were collected every increment of 10-20 cm and weighed 0.5 kg.

All soil samples were packed in sealed airtight plastic bags and immediately put into an icebox to maintain the temperature before being frozen (at a nearby facility) and sent to the laboratory. Meanwhile, field soil analyses were conducted without delay. The parameters included field pH (pH_F), pH after oxidation (pH_{FOX}), Redox (Eh), soil colour and texture. Eh and pH were measured using Ionode IJ44 and IJ64, before and after oxidation using H_2O_2 (peroxide). Soil texture was analysed using the feel method (Tien, 1979) and soil colour using a Munsell soil colour chart (Munsell, 2000).

The soil variables measured in the laboratory were KCl extractable Sulfur (S_{KCL} %), peroxide oxidation sulfur (sulfate) content ($S_{P\ \%}$), peroxide oxidisable sulfur ($S_{POS\ \%}$), Total Potential Acidity (TPA), Total Actual Acidity (TAA), Total Sulfidic Acidity (TSA), Pyrite (TOS method %), Organic material and Organic Carbon, Iron (Fe), Aluminum (Al), PO_4, P_2O_5, and N total (Table 6.7). Soil laboratory preparation and analysis procedures were done according to the Acid Sulfate Soils Laboratory Methods Guidelines (Ahern *et al.*, 1998a; Ahern *et al.*, 2004).

Table 3.1 List of measured soil properties in the fields and laboratory

Field Measured Variables (Ahern et al., 1989.b, 2004)	Laboratory Measured Variables	References for laboratory procedures
Field pH	Sulfur (S_{KCL}), Sulfur (sulfate) content (S_P),	Ahern et al, 1998.b
pH after oxidation	Total Potential Acidity (TPA) Total Actual Acidity (TAA) Total Sulfidic Acidity (TSA)	Method 21F ASSMAC, Ahern et al, 2004
Redox before and after oxidation	Pyrite	Ahern et al, 2004
Soil Texture	Electric Conductivity (EC)	Method 3A1 Rayment & Higginson, 1992
Soil Colour	Organic material and Organic Carbon	Dumas combustion – Method 6B3 Rayment & Higginson,1992
	Iron (Fe)	Ahern et al, 2004
	Aluminum (Al)	
	PO_4, P_2O_5	
	N total	

3.3.3 Statistical Analysis

This study presented descriptive data analyses which included minimum and maximum values, means, and standard errors, for hydro-geomorphic unit soil parameters. Principles Component Analysis (PCA) was applied to analyse the dominant factor which control pyrite development. Pre-treatment data processes involved variable individual ranking and normalizing the different scale data. R 2.13.0 (GNU Project) and Primer 6 (Primer-e Ltd., UK) statistical software were used to perform all statistical analyses.

3.4 Summary

The conceptual framework and method provided in this chapter respectively underpin and explain the order of stages of methods applied in this study. The establishment of GcR, estuary classification and HGU is an integrated multi-level approach for ASS mapping which produced hierarchal reliant data. The method review leads to the more specific multi-level mapping methods which are explained in detail in Chapter 4, 5 and 6, together with results.

2

METHOD AND PRELIMINARY RESULT

CHAPTER FOUR

THE GEO-CLIMATIC REGIONS OF CENTRAL JAVA

4.1 Introduction

This chapter provides broad information on the geography of Central Java and regional biophysical characteristics that are represented by Geo-climatic Regions (GcR). GcRs are regional groups of catchments with similar hydro-geomorphic characteristics (geology, geomorphology) and climatic regimes. They were established in this study to obtain regional-scale information of hydro-geomorphology characteristics, as the first level of the multi-level mapping approach of this study (Chapter 3, Figure 3.1). This chapter also outlines how each GcR was established using remotely sensed data and existing regional hydrology and geomorphic data sets. The GcR will assist the estuary classification process (the second stage of methods in this study).

4.2 The Geography of Central Java: General Review

Central Java province (Figure 4.1) is located in Java which is one of the five main islands in Indonesia. In comparison to all other islands in Indonesia, Java has experienced the most rapid development of infrastructure and population growth since the country urbanized. Java has an area of 132,187 km^2 and 60% of the Indonesian population resides on the island (IBS, 2010). The largest economic activities (trading, port, central market, etc.) in this area mostly occur along the northern coastline where the main national road connects three of the biggest cities in Java: Jakarta, Semarang and Surabaya. As Jakarta is the Indonesian capital city, and with fertile land and abundant water resources in the rest of Java, people from outside the island migrate to Java. This results in high population density that causes many environmental and resource management issues, such as forest clearing, soil loss and pollution of water, soil and air (Repetto, 1986; Verburg *et al.*, 1999). The development of land required to meet these socio-needs has led to the conversion of forests and mangroves to built-up areas. The advantages of more level landscapes compared to hilly and rugged areas inland, and ready access to the sea, means economic related investors and the general population prefer the coastal zone for development.

Central Java has experienced the development of coastal areas in both the north and the south. It is the third most populous province in Indonesia with a population of about 32.18 million people (14 % of national population) in 3.25 million hectares, after West Java (1st) and East Java (2nd) Provinces (SI, 2010). The most populated areas in Central Java are in the northern coastal cities, such as Tegal, Pekalongan and Semarang. In these coastal areas, about 51,000 ha (1.6 %) is used for brackishwater aquaculture (Hutabarat, 2008).

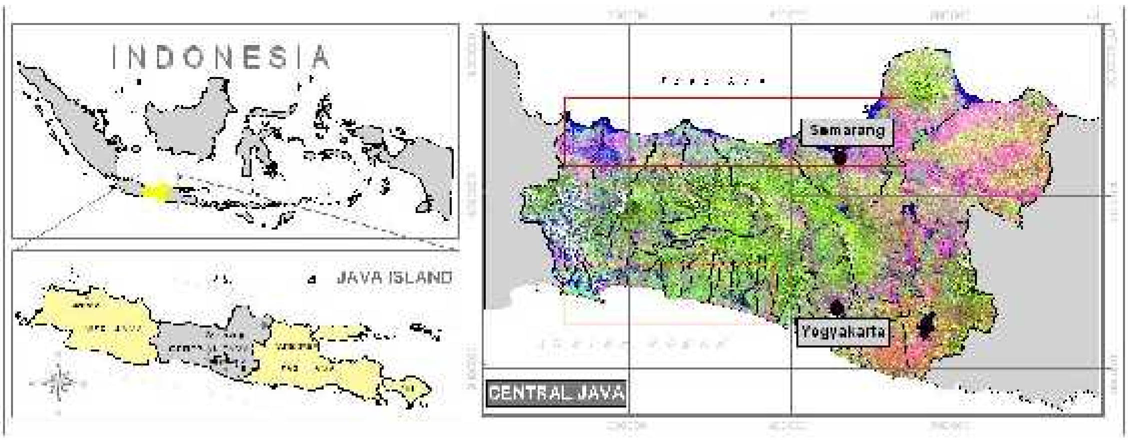

Figure 4.1. The study areas are located along the north and the south coast of Central Java as outlined by the two red rectangles.

4.2.1 Climate

Central Java is in the humid tropics, with a climate governed by the Southeast Asian Monsoonal wind system, and influenced by the Inter-tropical Convergence Zone (ITCZ) (Verstappen, 2000). This monsoonal belt is broader compared to other places in the world, generated by the vast Asian continent in the north and the Indian Ocean to the south. The location of Central Java at the south of the equator, along with the ITCZ dynamic, creates a specific climate and local weather. The annual mean temperatures are about 24^oC to 28.5^oC and relative humidity is around 73% - 86%. The temperature and relative humidity in the coastal areas are higher than the mean values for Central Java.

The average annual rainfall is 3000 mm on the coast and 3200 mm in the uplands areas (Figure 4.2). Rainfall in Central Java is mostly orographic rainfall (Puri, 1985). This heavy orographic rain in the bare uplands areas causes erosion and delivers a large amount of clastic and organic material to the coastal lowlands. Therefore, the level of sedimentation in Central Java is considered high with some catchments reaching more than 1000 t/km^2/year (Gupta, 2007; van Dijk *et al.*, 2004). In the dry season, the humidity becomes lower as the dry wind from the Australian region blows northwest to Indonesia. As a result the average annual rainfall is lower in the east compared to the western side of the island (Sukanto, 1969; Hamada *et al*., 2002; Aldrian & Susanto, 2003), and generates some drier agro-climatic zones in the eastern region of Central Java (Figure 4.3).

Figure 4.2. Map of the average annual rainfall in Central Java. This image shows lower average annual rainfall (below 2000 mm/year), occurs in the northeast, northwest and southwest Central Java lowlands, whereas high and very high rainfall occurs in the uplands (more than 4500 mm/year) - (MCGA, 2005)

Figure 4.3. Agro-climate map of Central Java shows climatic zones for agricultural purposes (MCGA, 2005).

4.2.2 Geology and Geomorphology

The geology of Indonesia, including Java, is mostly influenced by the active process of the continental Sunda Plate south edge, overriding the oceanic Australia-Indian plate, resulting in a subduction-induced volcanic-plutonic arc (Figure 4.4). Consequently, Java is located in an active volcano ring. Generally, geologists divide Java into West Java and East Java, with Semarang and Karimun Java as the dividing area on the meridian line. However, Central Java is usually described independently, as it has specific geological features and processes (Bemmelen, 1949). Based on geological maps, the structural units of Central Java comprise the south coast plain with the Karangbolong Mountains, the South Serayu and West Progo Mountains, the Serayu depression, the North Serayu Range, and the north coast plain (Figure 4.5).

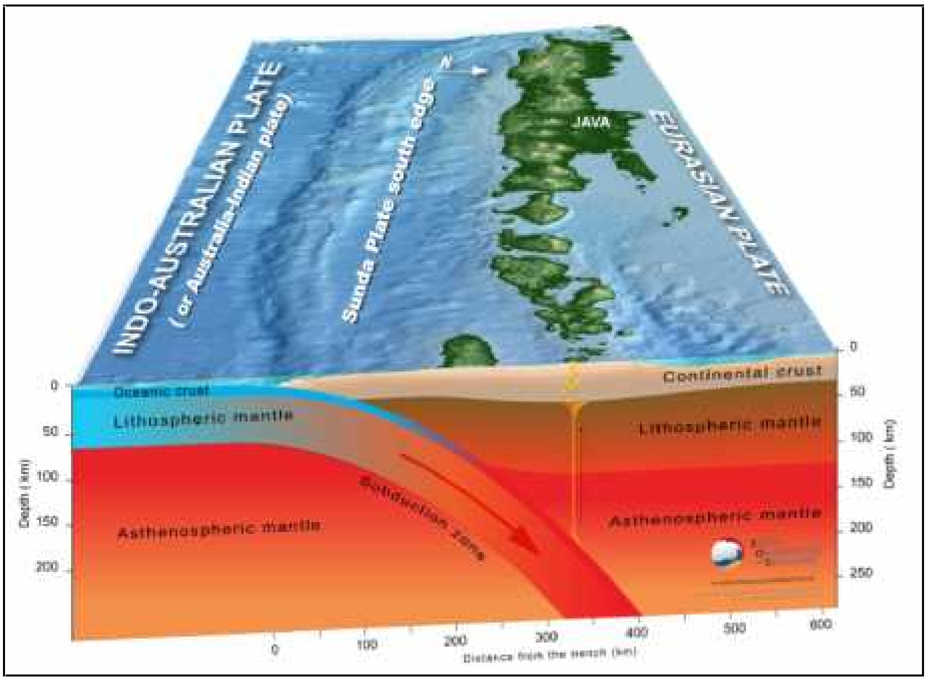

Figure 4.4 Schematic of the Java subduction zone cross section showing the continental Sunda Plate's south edge overriding the oceanic Australia-Indian plate, resulting in a subduction-induced volcanic-plutonic arc (adopted from Earth Observatory of Singapore, NTU, 2013).

The subduction process of the Indian Ocean plate and the Southeast Asian plate also influences the geomorphology of Java. Based on this process, Verstappen (2000) has divided Java into 3 parts, which are:

(1) The North Folded Zone, consisting of low hilly areas overlying Tertiary strata, and the Quaternary coastal lowlands bordering the Java Sea;

(2) The Central Depression filled with Quaternary volcanic landforms with the majority of great volcanic cones lying within this structural zone; and

(3) The Southern Tilted Zone which comprises uplifted and tilted plateaus of Tertiary strata, complemented by narrow coastal lowlands.

In the North Folded Zone (northern part of Java), landform development between the volcanic arc and the South Asian Plate has created a synclinal landform called the geo-syncline northern limb. In the middle, there is a central depression, which is the backbone of Java and comprises of relatively young active volcanoes, with average height of 3000 m. In the southern zone, southward-tilted plateau fringes comprise some interrupted limestone and are located further along the southern part of Java. Some of the limestone are covered by an old volcanic plain (Pannekoek, 1949).

The Central Java geomorphology map (Figure 4.6) shows the more detailed geomorphic features which divided the earlier mentioned Java geomorphic zone into more specific landforms. The alluvial plain covers most of the coastal lowlands on both the northern and southern coast of Central Java. However, the existence of the piedmont intra-montana hills on the north and dissected tilted block mountain on the south differentiate two coastal lowlands. The volcanics existed in a central depression and the northern east is divided into a volcanic cone, middle slope, lower slope, and strongly eroded zone.

The coasts in Indonesia are influenced by geologically recent sea-level changes and (neo) tectonics (Verstappen, 2000). However, it is difficult to separate those processes to classify most of the coasts; the common coasts present in Indonesia cover coastal lowlands rocky coasts, and coral reefs and islands. In Central Java, the coasts are classified mostly into coastal lowlands which have been developed under humid tropical conditions (Bird & Ongkosongo, 2000; Verstapen, 2000). High river flows have deposited clays and formed extensive mudflats. These mudflats were populated by mangroves which contributed to the low energy conditions that formed the landscape. Coastal lowlands with low energy environments, where small tidal current and range occurred, favoured estuary and delta development in the northern coast. On the other hand, the southern coastal lowlands are dominated by waves and currents generated by onshore winds which developed sandy shores or sand barriers.

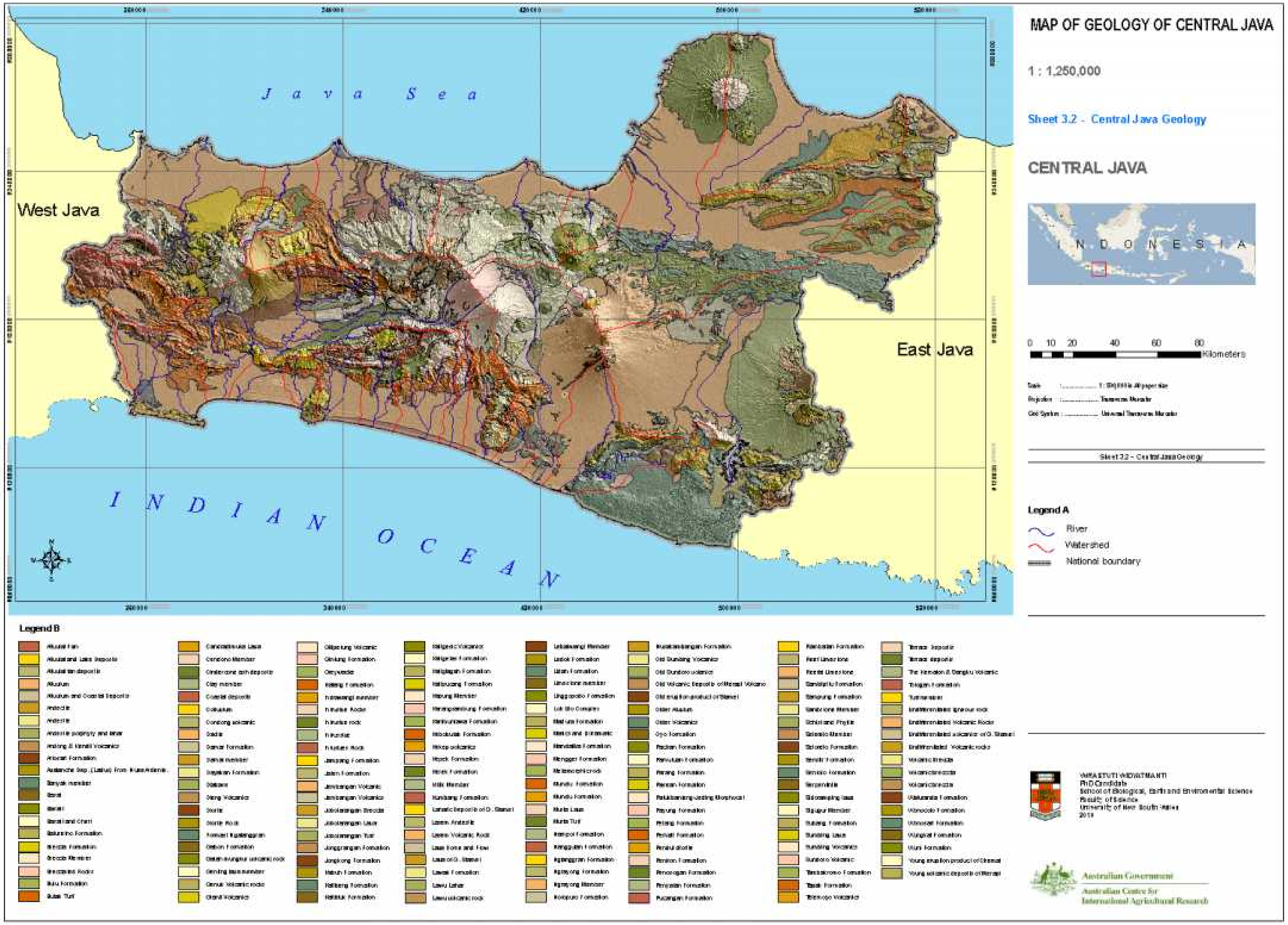

Figure 4.5 The geology of Central Java showing the dominant alluvial deposits in the lowlands of Central Java.

Figure 4.6 Map of the geomorphology of Central Java clearly showing volcanic landforms in the central zone, alongside alluvial landforms in the lowlands. Some dissected tilted blocked mountains are found in the southern part of Central Java which differentiate the southern zone from northern zone.

4.2.3 Soil

Soil classification studies in Indonesia commonly utilize the Indonesian Soil Classification 1957 and 1983 (Notohadiprawiro, 1989), FAO 1985 and USDA 1971 (CSR, 1983). Current Central Java Soil Maps, at a Scale of 1:250,000 (CSR, 2000), are using the Indonesian Soil Classification (1957) and geomorphic features approach to divide soil types into three groups (Figure 4.7). The soils in the northern and southern coast are mostly influenced by marine and alluvial processes but with different intensity, whereas volcanic processes formed the soils in the uplands. Figure 4.7 shows that the lowlands of the northern coast are dominated by alluvial-dark grey soil. Alluvial-grey, greyish brown soils occur in the west whilst grumusol-dark grey-clay sediment is common in the east. However, both the western and eastern coastal lowlands are dominated by grey regosol-lowlands and alluvial hydromorphs. Conversely, the lowlands of the southern coast consist of various soil types, from complex Lathosol, Lithosol, Podsolic, Regosol, which originated from old volcanic material from the uplands, to common clay/loam Alluvial soil with different type of colours, such as: Alluvial Hydromoph, Alluvial - yellowish grey and Alluvial - grey and greyish brown. The coastal lowlands, however, are dominated by sandy Grey Regosol-lowlands, which were influenced by marine and Aeolian processes.

4.2.4 Hydrology

The hydrological characteristics of Java are strongly influenced by the high average annual rainfall, seasonal river discharges, and the biophysical characteristics of the river basins (Verstappen, 2000). These hydrological conditions are different to other regions such as: Thailand, Vietnam, Malaysia and the northern part of Australia, despite being typical tropical countries. Low temperature fluctuation, wind and rainfall during the rainy and dry seasons generate distinct weathering processes that influence landscape formation, especially in coastal lowlands where sedimentation largely occurs (Dosmet & Govers, 1996). The high rainfall intensity, depending on the landscape's resistance level, results in various topographic conditions through different types of erosion producing large range of topographic features (slope, elevation, profile etc.) (Scheidegger, 1973). The specific hydrological and topographic condition can exhibit a variety of soils that related to pyrite development oxidation.

Based on provincial administration areas, Java island can be divided into 14 major catchments including seven in West Java (Ciujung - Ciliman, Ciliwung - Cisadane, Cisadea -Cikuningan, Citarum, Cimanuk, Ciwulan, Citanduy), four in Central Java (Pemali Comal, Serayu, Jratun Seluna, Progo-Opak-Oyo, Bengawan Solo) and two in East Java (K. Brantas, and Pekalen Sampean) (BPDASPS, 2007). The river discharge in Java ranges from about 15 $m^3/100\ km^2$ to 80 $m^3/100\ km^2$, with about 60 % under 30 $m^3/100km^2$ (BPDASPS, 2007). The main function of catchments in Central Java, besides conservation, is to supply water for agriculture, industries, electricity generation and domestic uses. However, the very high population in Central Java demands more land for residential uses than are currently available. This also means the need to access water resources is increasing. As a result, water catchment management is not sustainable, and sooner or later water resources will decrease rapidly (Mawardi, 2010), resulting in the present water resources being lower than in previous decades.

In Central Java, the major rivers, such as the Serayu, Luk Ulo, Opak and Progo Rivers, discharge to the Indian Ocean, whereas the Garang, Pemali, Comal and Bodri Rivers drain into the Java Sea (BPDASPS, 2007). These rivers present a strong seasonal ratio of maximum and minimum discharge (coefficient of river regime = 3:1), with the discharge during rainy season on average being more than 3-4 times compared to the dry season (Verstappen, 2000; DGWR, 2013). This means that the rivers are influenced mostly by the intensity and volume of rainfall and hence, their estuaries that are characterised by intensive sedimentation. These data are consistent with world percentages indicating that about 75% of total annual suspended matter delivered by fluvial processes on Earth is from tropical rivers (Milliman & Meade, 1993; Milliman & Farnsworth, 2011).

Meanwhile, population pressure and forest clearance creates an unnatural imbalance in the hydrological cycle (Drummond & Loveland, 2010). The large amount of precipitation that should infiltrate into the ground is converted to run off due to deforestation. The increase in runoff in turn increases the delivery of eroded sediment to estuaries. Correspondingly, decreased rainfall infiltration in the uplands lowers the groundwater table and creates drier uplands soils. It means that during the dry season there is possibility of water table fluctuation that affected the occurrence of ASS.

Figure 4.7. Soil map of Central Java showing the complexity of soil types. Soil development is influenced by alluvial and volcanic material, such as: alluvial, and grumusol, regosol, lithosol and lathosol soil classes.

On the other hand, groundwater flows follow topographic and geological features, coming from the mountains where recharge is initiated (Krampe, 1982). Groundwater is mainly used for domestic purposes, irrigation, and industry. These continuous demands, followed by the increases in forest clearance, reduce the groundwater volume. Nevertheless, most catchments are still able to provide sufficient water resources periodically because of the high annual rain average over most areas (Verburg *et al*., 1999). However, in some coastal lowlands, the lack of water supply in groundwater results in significant lowering of the water table (Koolsterman, 1989). When this depletion cannot be recharged rapidly (controlled by precipitation, surface runoff or temperature that controls the evapotranspiration), this freshwater aquifer system produces a zone of depression, which allows the intrusion of seawater at the interface.

Since coastal land-uses have been expanding, brackish groundwater is occurring further inland, and the north coast of Central Java has this issue more than in the south coast (Krampe, 1982; Matsumoto *et al*., 1974). Research has attempted to solve these seawater intrusion problems in terms of hydrology and engineering, by applying injection wells, supplying water from resources other than coastal groundwater, or mangrove forest rehabilitations (Noordwijk *et al*., 2002; Simoen, 2000). However, uncontrolled coastal development prevents a solution being applied effectively.

4.2.5 Vegetation

Java is the most fertile island in Indonesia as it has a ring of volcanoes which supply sedimentary material with a high natural nutrient content to the soil through eruption (Verstappen, 2000). This area has a high diversity of vegetation from the uplands to lowlands. However, the rapid increases of development and population have triggered intensive land (vegetation) clearing, without any consideration of potential environmental impacts.

Since this research focuses on ASS distribution and development, which is commonly related to the presence of estuarine wetland vegetation (Dent, 1986), this section discusses vegetation that indicates the likely presence of ASS (brackishwater vegetation) to underpin the spatial data analyses and to better understand biological indicators of ASS. The colonized brackishwater vegetation is able to guide the prediction of the presence and concentration of sulfides because their different species are related to the types of sediment and salinity (van der Kevie, 1972). Mangroves, *Nypa fruticans* and other wetland/lowlands species dominate the ASS-related vegetation communities. The mangrove genera found in Central Java are *Rhizophora, Avicennia,* and *Bruguiera.* The mangrove-palm species, *Nypa fruticans,* is also scattered along the estuaries (Hinrichs *et al.,* 2009). In the areas where mangroves have been disturbed repeatedly, the near water zone is mainly occupied by the *Acanthus* family (mostly *Acanthus ilicifolius*), spiky-leaved vegetation that is commonly found in salt marsh or brackishwater environments (Chong *et al*., 1990).

The intense anthropogenic activities in coastal Central Java have included both clearing natural vegetation cover from the landscape and re-utilising, more intensively, already cleared land. Land-use conversion has occurred in mangrove forests despite their conservation value and the risk of ASS-related problems (MMAF, 2011). Settlements located on former mangrove areas are often considered slums because most are located in estuaries where domestic waste has accumulated and the population exceeds the carrying capacity of the environment. On the northern coast of Central Java, medium to severe damage to mangrove forest occurred, as the main cities are located along this northern shore. Those cities include Semarang, Batang, Demak and Pati where the industrial districts are located. In these areas, the destruction of mangrove forest is estimated to reach 90% of the total 95,000 ha that once existed (MoF, 2007). From this figure, 61,000 ha of mangrove forest area have experienced severe damage and about 31,000 ha are classified as having a medium level of damage (Table 4.1). The criteria for levels of damage established under the Indonesian Ministry of Environment Act (2004) were determined from the remaining percentage cover and density of mangroves in an area (Table 4.2).

The pressure to develop new aquaculture ponds, settlements, tourism facilities and industry triggered land conversion in these areas. This environmental damage leads to vulnerable ecosystems in estuaries, and such areas are also affected by increased wave attack, shoreline changes, pollution and destruction of important habitat (Marfai & Lorenz, 2008; Sanderson & Taylor, 2003). Fortunately in 2005, as part of a government coastal rehabilitation program, Central Java planned to establish 77,000 ha for the development of new mangrove forest with a sustainable management system (MoF, 2007). However, the program achieved less than 40 % of the target by 2010 due to the severe damage caused by clearing in most potential areas and to the conflicts among the owner of the current land-use (MoF, 2011).

Table 4.1 Mangrove area and the level of damage

Regency	Mangrove Condition and Area (ha)		
	Good	Medium Damage	Severe Damage
North Coast			
Brebes	21,000	205,0000	9000
Tegal	770,500	4,215,000	3280
Pemalang	54,900	41,487,500	12,000
Pekalongan	n/a	n/a	n/a
Batang	-	20,000	1200
Kendal	2,900	668,600	124,080
Semarang	n/a	n/a	n/a
Demak	145,500	7700	37,000
Jepara	8500	-	-
Pati	5000	6450	4505
Rembang	491,250	33750	103,715
South Coast			
Cilacap	-	2,154,500	176,250
Kebumen	n/a	n/a	n/a
Purworejo	n/a	n/a	n/a

Source: Regional Environmental Management Agency of Central Java, 2002

Table 4.2 The criteria to clasify mangrove damage level

Criteria	Remaining Coverage (%)	Density (trees/ha)
Good	>70	>1500
Medium	50-70	1000-1500
Severe	<50	<1000

Source: Indonesian Ministry of Environment Act, No. 201, 2004

4.2.6 Land-use types in coastal areas

In Central Java, land-use along the coast is predominantly brackishwater aquaculture, followed by ricefields further inland. The brackishwater aquaculture areas are mostly located on previous mangrove forest (Table 4.3), in low lying coastal areas, specifically along the delta margin (Bird & Ongkosongo, 2000). Large number of ponds which formerly belonged to intensive shrimp pond companies, as in Pemalang, have been abandoned because of the declining productivity (MMAF, 2008). Large traditional ponds still operate in Tegal, Brebes and Pemalang, but seasonally in Demak. However, they often experience problems with their production system, such as disease outbreaks and poor water quality (Personal observation, 2009). To overcome this problem, some farmers cultivate milkfish and shrimp during the dry and rainy seasons respectively, or focus mainly on rice cultivation during the rainy season.

Table 4.3. Area of mangrove converted to ponds in Central Java

Regency	Pond Area (ha)	
North Coast	1999	2000
Brebes	7416	7688
Tegal	743	746
Pemalang	1578	1578
Pekalongan	136	101
Batang	131	132
Kendal	2427	2832
Semarang	1999	1792
Demak	5117	5485
Jepara	1228	1228
Pati	8118	9436
Rembang	1119	1271
South Coast		
Cilacap	100	65
Kebumen	9	18
Purworejo	32	32

Source: Central Java Department of Forestry, 2009

On the south coast, land-use changes occur along the beaches or estuaries. In the eastern part of estuary, the land-use changes from bare land to tourism-related built-up areas whereas in the western part, such as Cilacap, it changes to industrial areas. Ricefields are usually located further inland as the sandy soils of the marine-influenced landscapes are not suitable for this type of land-use. Settlements are mostly located on old beach ridges and levees which are more stable and have more fertile soil (Personal observation, 2009; Verstappen, 2000). On the other hand, settlement and industrial areas on the north coast occupy most of the coastal area. Settlements are associated with ricefields and ponds and are located between the main cities (Figure 4.8.A&B). The majority of industrial areas are located near the main city adjacent to the main river. Over the last decade, coastal environmental issues (i.e.: air, water, soil pollution), have been exacerbated, as there are no formal environmental management plans developed by either government or industry. Indeed complaints and feedback concerning pollution of rivers and pond abandonment were raised by the communities living on the estuary and by farmers, but the solution remains elusive (personal communication with local people/farmer, 2009, 2010).

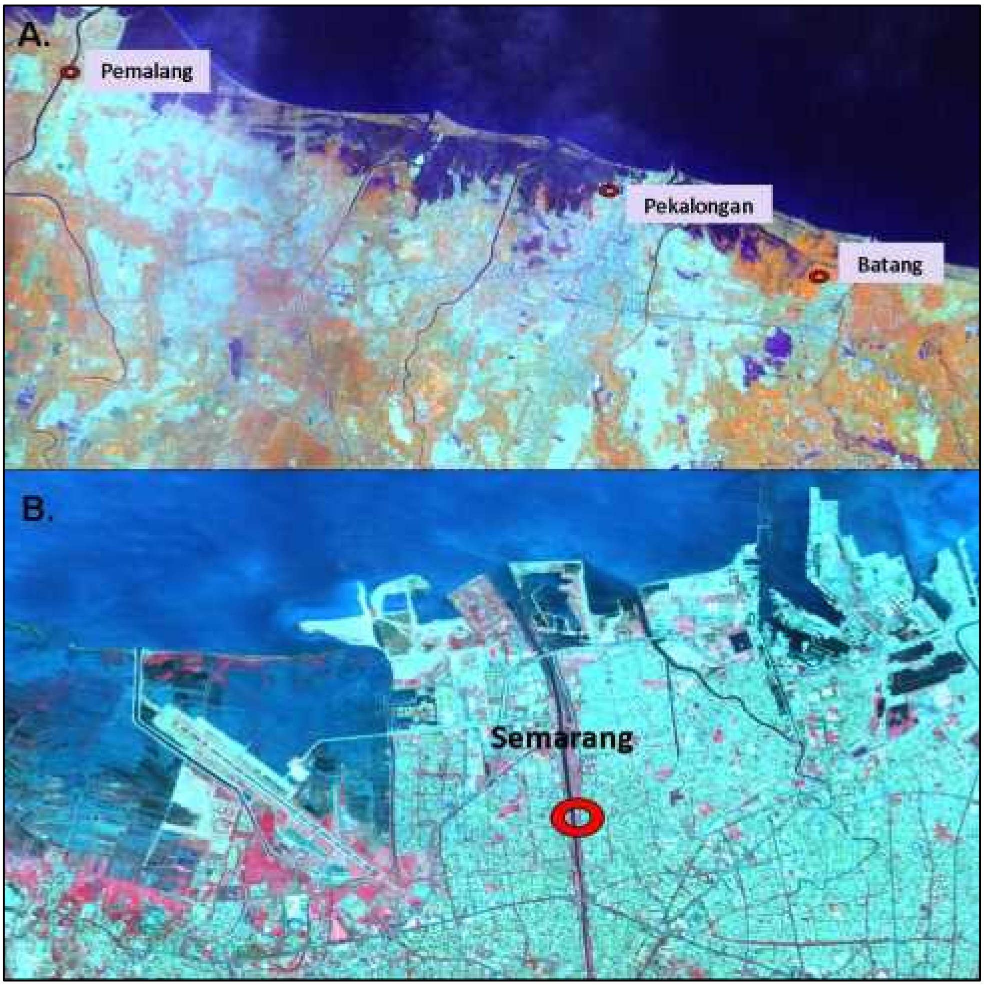

Figure 4.8. (A) Landsat ETM+ imagery recorded on 30 July 2009 showing brackishwater aquaculture (dark blue tone behind the coastline) located between the cities of Pemalang, Pekalongan and Batang (light blue tone, rough texture). (B) The same source of satellite imagery showing high density urban areas in Semarang Municipality (light blue tone, rough texture), the biggest industrial city in Central Java, which is located on the north coast of Central Java.

To date, discussion on land-use changes and the implications for the development of ASS in Central Java has not intensively occurred amongst managers and researchers. The knowledge that ASS influences the quality of water and soil in aquaculture was recently recognized by farmers and government agency through ACIAR Projects FIS/97/22 and FIS/2002/076. Adoption of recommended outputs from these projects could halt further degradation and improve management of already degraded areas.

4.3. Determination of Geo-Climatic Regions (GcR)

This study divided Central Java province into Geo-climatic Regions (GcRs) to identify the hydro-geomorphic characteristics at regional levels. The catchments with similar hydro-geomorphic and climatic characteristics were chosen to collect the information of hydro-geomorphic characteristics, because they represented the dynamic hydro-geomorphic processes which occur in uplands and lowlands and influenced the characteristics of their estuary (see Chapter 2). The following sections explain the materials and methods used to identify and describe each GcR present in Central Java.

4.3.1 Materials and Methods to Delineate the GcRs

The GcR classification was applied across Central Java, using Landsat ETM$^+$ year 2002, Shuttle Radar Terrain Mode (SRTM), and regional scale (1:250,000 – 1:100,000) geomorphology and hydrology related data (maps and tables). The Landsat ETM$^+$ and SRTM were used to validate the catchment boundaries (watersheds) from existing watershed maps, and to recognise the features of the terrain that differentiate the lowlands and uplands, within existing regional land-cover/land-use and the latest coastal boundary. The catchments selected for this study were limited to the catchments located in Central Java and connected to the open sea on the north and the south coast of Central Java. This watershed map was used as a base map to synthesize the hydrology and geomorphology data, and then to group the catchments with similar hydro-geomorphic process into one regional class (Figure 4.9).

The data synthesis included the grouping of the existing secondary data into geomorphology and hydrology data (Table 4.4). The geomorphology data group included maps of geology, geomorphology and soil. The hydrology group covered maps of regional coastal environment and climate, agro-climate, and rainfall. These two data groups then were examined using multi-stage analysis to obtain the GcR. The GcR development process consists of 3 stages based on different scales of data (Figure 4.10). These multi-scale data were categorized into 3 levels of detail to generate hierarchical structural data to anticipate the bias when using different scales of thematic data, such as data generalization or invalid mapping unit boundaries (Walsh *et al.*, 1998).

This study used ArcGIS™ 9 to facilitate the multi-stage analysis. As shown in Figure 4.10, this analysis involved a hierarchical overlay where each thematic dataset was overlaid based on the order in each stage. The next step was collecting similar data attributes from the vector maps result of the overlay based on the watershed units. This method is known as spatial data aggregation: "the process of collecting a set of similar, usually adjacent, polygons (with their associated attributes) to form a single, larger entity" (Chang, 2002), and is commonly applied in multi-level GIS analysis for environmental applications (Burrough & McDonnell, 1998). The first stage of GcR determination aimed to create the synoptic view of hydro-geomorphic information in Central Java. In this stage, the first stage of data in each group of geomorphology and hydrology were overlaid and aggregated to establish geomorphology and catchment zones.

Table 4.4 Data input for each stage and scale based on hierarchical aggregation of data

Geomorphology Group		**Hydrology Group**	
Source	**Stage Level/ Map scale**	**Source**	**Stage Level/ Scale**
Map of Central Java Watershed, Ministry of Forestry, 2009	I 1:500,000	Map of Watershed, Ministry of Forestry, 2009	I 1:250,000
Map of Geomorphology, Verstappen 2001	I 1:500,000	Map of Indonesian Coastal Environment, 1997 Marine Climatic Atlas, US Navy 1977	I 1:250,000 1:500,000 -
Map of Geology of Central Java, Geological Research and Development Center, 1996	II 1:250,000	Map of Agro-climate, Soil Research and Development Center, 2003	II 1:250,000
Map of Soil of Central Java, Soil Research and Development Center, 2000	II 1:250,000 1:100,000	Map of Rainfall (Annual average rainfall data, BMG 1971-2000)	II 1:250,000
		Map of Hydrogeology, Directorate of Environmental Geology, 1996	III 1:100,000

Figure 4.9. The final watershed map after validation using Landsat ETM+ year 2002, Shuttle Radar Terrain Mode (SRTM) satellite data.

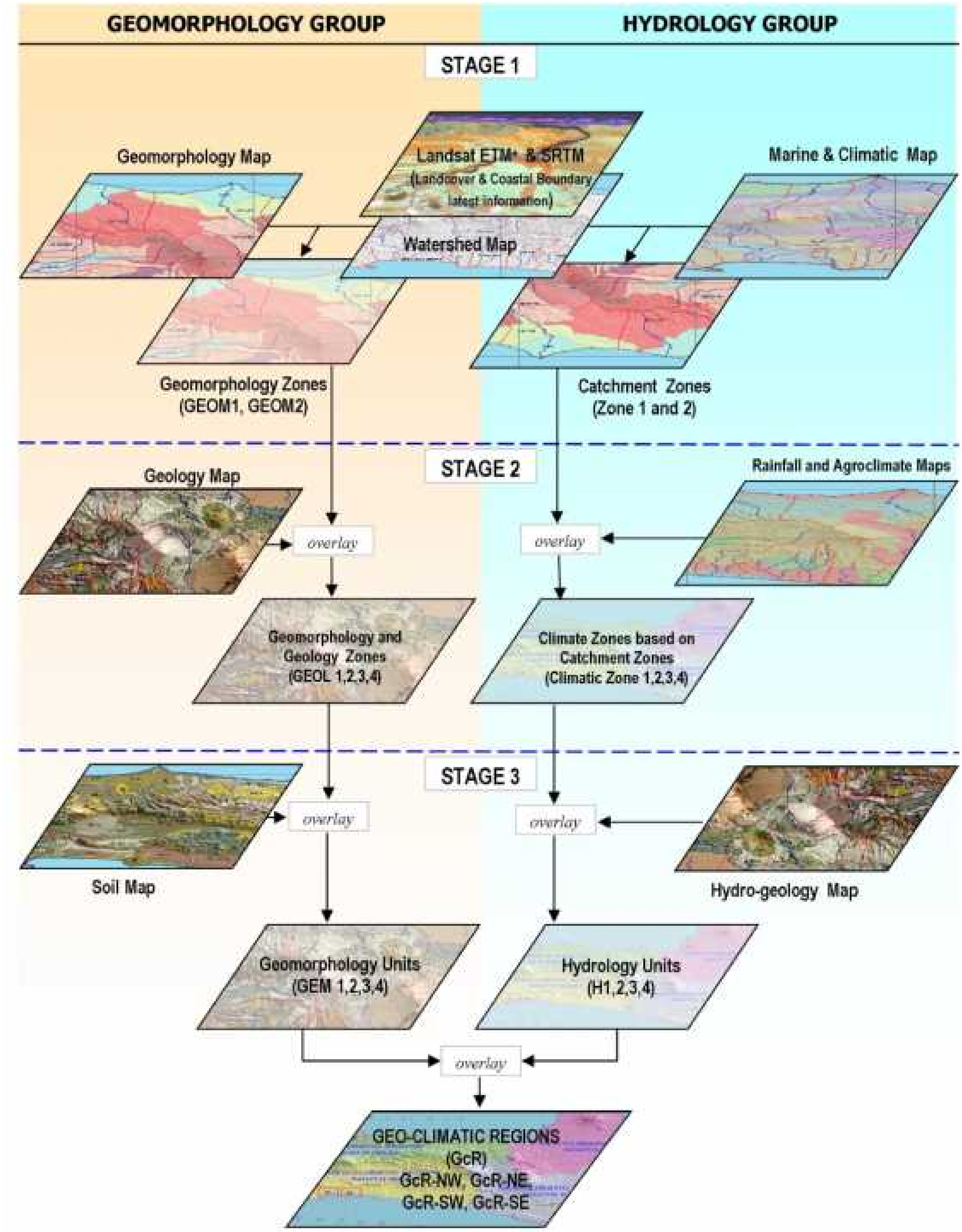

Figure 4.10 Flowchart representing the multi-stage (Stage 1,2 and 3) methods used to determine the Geo-climatic Regions.

4.3.1.1 Multi-stage Method in the Geomorphology Data Group

This study utilized the geomorphology map established by Verstappen (2000) that divides Central Java into 3 zones (see section 4.2.2), to generate geomorphology zones. However, when it was overlaid with the watershed map, the spatial aggregation process split the central zone (The Central Depression filled with Quaternary volcanic landforms), into 2 parts. The north part merged with the catchments located in the North Folded Zone. The south part merged with catchments located in the South Tilted Zone. These two catchment groups were delineated as GEOM 1 and GEOM 2 zones, representing catchment group located north and south accordingly (Table 4.5, Column 3).

In the second stage, the geomorphology zone map was overlaid with the geology maps. The geology map grouped catchments in Central Java into four zones. These geology zones together with geomorphology zones produced 4 new geology zones, called GEOL 1 and 2, located in the north, and GEOL 3 and 4 in the south (Table 4.5, Column 4, and Table 4.6). The soil map was then used to complete the third stage, by providing information of soil types in the uplands, midland and lowland areas in each geology zone. Subsequently, these four GEOL zones, complete with their soil attributes, were renamed as Geomorphology Units: GEM1, GEM 2, GEM 3 and GEM4 (Table 4.5). This Geomorphology Unit Map was the summary map from the geomorphology group multi-stage analysis (Figure 4.6).

Table 4.5 The Gemorphology Units of Central Java, based on geomorphology, geology and soil maps.

Geomorphology Unit (1)	Catchment Location (2)	Geomorphology Setting (3)	Geological Setting* (4)	Geomorphology Feature		Soil		Landuse (mangrove)
				Uplands	Lowlands	Upper Land	Lowland	
GEM1	a. Pemali - Pekalongan b. Bodri - Garang	GEOM1 Lowlands: North Folded Zone Uplands: Central Depression filled with Quaternary volcanic landforms	GEOL 1	a. Structural Landform: Dissected Calcareous and Tuffaceous Montain b. Depositional Landform: Piedmont, intramontane basinfills and Plesitocene Terraces	Depositional Landforms: Alluvial Plain	Grumusol, Latosol Gleysol, regosol,	Fluvisol. Gleisol, regosol	Mostly recent
GEM2	Serang - Juana	GEOM1	GEOL2	Volcanic landform: Older, strongly eroded volcanic terrain (locally sedimentary); Highly dissected calcareous and sedimentary rocks hills	Depositional Landform: Alluvial Plain	Grumusol, Latosol Gleysol, regosol,	Grumusol Vertisol Mediteran, Luvisol	Some parts are mature age, but mostly recent on the west coast.
GEM3	Serayu – Bogowonto	GEOM2 Lowlands: South Tilted Zone Uplands: Central Depression filled with Quaternary volcanic landforms	GEOL 3	Volcanic Landform: Older, strongly eroded volcanic terrain (locally sedimentary); Tuffaceous Rock Mountain	Depositional Landform: Alluvial Plain	Red Yellow Podsol, Latosol	Regosol, Gleisol	Recent
GEM4	Serang - Oyo	GEOM2	GEOL4	Volcanic Landform: Volcanic Cone and related relief,Volcanic Plain Structural Landform: Dissected block mountain.	Depositional Landform: Alluvial Plain	Grumusol, Regosol	Regosol	Recent

See table 4.5 for detailed information of geology setting

Table 4.6. Description of the geological settings.

Geology Unit	Catchment Location	Geology Feature		
		Uplands	**Middle (between uplands and lowlands)**	**Lowlands**
Geol1	Pemali - Garang	Mostly Neogene sediment combined with Pleiosen Sediment: Shale, marl, calcareous sandstone. Thickness: 300 m.	Mostly tuffaceous claystone, tuffaceous sandstone, conglomerate and breccia from Pleistocene sediment. Middle lower part: Plio-pleistocene sediment, locally from lahar deposit. Interbedded volcanic breccia, coarse tuff, conglomerate, fine tuff and tuffaceous claystone.	Sediment consists of pebbles, sand, silt, and clay from river, beach, swamp deposit, from Holocene sediment. Thickness : up to 150 m.
Geol2	Serang - Juana	(AL): Lava of basalt or andesit, leusit and syenite from Holocene and Plesitocene activities. (K): Miocene Flysch Sedimentary rocks in lower part, and marls intercalating with calcareous-tuffaceous sandstone with very abundant of volcano-clastic material. (R): Miocene sediment with interbedded claystone, calcareous sandstone and limestone in the lower part; and claystone in the upper part; and contain large forma and benthic forams of Meddle Miocene age.	(AL): Pleistocene sediments contain tuff, lava, volcanic breccia, lahar and sandy tuff. (K): Neogene Sediment with massive marls on upper part., intercalacting limestone moduls in lower part (R): Miocene Carbonate contains marl with calcareous sandstone intercalation of platy limestone, sandy and clayey limestone. Abundant forams indicate a late Miocene age.	
Geol3	Serayu- Bogowonto	Pliocene sediment with greenish coarse grained sandstone and conglomerate in lower part, gradually grading upward into fine-grained sandstone and sandy marl.	Neogen turbidit sediment on late Miocene- early Pliocene with interbedded matls, calcarenite, lithic sandstone and conglomerta. Well-developed sediment such as graded bedding, parallel lamination, and flute cast occurred.	From Holocene sediment: Sediment consists of swamp and beach deposits from mud, sand, gravel; commonly loose. Loose sand, locally bedded and contains magnetic material up to 45%, ilmenite 25%, as well as shell and limestone fragments.
Geol4	Serang - Oyo	Holocene Lava Flows and flow breccia on Opak and Oya upperland. Miocene Intrusive and Miocene turbidit sediment on Serang upper catchment. This unit was presumably deposited in the shallow to deep marine environments. Thickness more than 1500 m.	Holocene Volcanic consists of various rocks as an eruption product of some strato volcanoes. Generally it is composed of andesit to basalt of eruption products.	From Holocene sediment: Sediment consists of swamp and beach deposits from mud, sand, gravel; commonly loose. Sand dunes mostly contain magnetic concentrates averaging nearly 55% Fe and 12.5% TiO_2.

4.3.1.2 Multi-stage Method in the Hydrology group

In the hydrology group (Table 4.7), the first stage of the process involved combining the regional base map (watersheds map) and marine environment maps that provided general tide and wave characteristics information. The spatial aggregation process divided Central Java into the northern catchment zone 1 which has low marine energy, and southern catchment zone 2 with high marine energy (Table 4.7, Column 7). The level of marine energy was determined by identifying the general coastal landscape found in each catchment and classifying them based on the Dalrymple marine energy classification, which includes wave and tidal energy (Dalrymple *et al.,* 1992, Figure 2.1; Chapter 2).

The second stage involved overlaying the rainfall map and agro-climatic map onto the catchment zones. This process divided Central Java into four zones named as climate zone 1, 2, 3 and 4 (Table 4.7, Column 2 & 4). The third stage then added the hydrogeology map to these four climate zones to obtain information on water quality, seawater intrusion, and groundwater depth. These final four zones were assigned as Hydrology units (H1, 2, 3 and 4; Table 4.7, Column 1).

In the last step of stage 3 the maps for the Hydrological Units and Geomorphology Units were overlaid to define catchment units (GeoClimatic Regions or GcRs). These GcRs encompass the characteristics of geography and climate that influence the hydro-geomorphic processes within the catchments. This superimposed process generated four main GcRs which included the GcR of Northwest (GcR-Northwest), Northeast (GcR-Northeast), Southwest (GcR-Southwest) and Southeast (GcR-Southeast). The North and South areas are partitioned by a pseudo middle-line of a volcanic/mountainous ring in the central part of Central Java (Figure 4.11). The GcR-Northwest and GcR-Northeast cover areas in the northern part of Central Java from Brebes to Kendal, and Semarang to Rembang respectively. In the southern part of Central Java there are GcR- Southwest, which is located in Cilacap to Kulonprogo regencies, and the GcR- Southeast which is in Bantul and Wonosari regencies. The description of each GcR is provided in the following sections. However, because this thesis only focuses on Central Java Province, the study areas only covered the GcR- Northwest, the GcR-Northeast and the GcR-Southwest. The map of GcRs is presented in Figure 4.11.

Table 4.7 The hydrological units of Central Java, based on maps and data attributes of coastal environments, agro-climate, rainfall and hydro-geology

Hydrological Unit (1)	Catchment Location (2)	Catchment Zone (3)	Marine Characteristics (4)					Climate Zone (5)	Agroclimate Zone (6)	Rainfall (mm/year) Per Season (7)		Wind (season) (8)	Groundwater Characteristics (9)	
			Avarage Tide (meter)	Average Wave Height (meter)	Near Coastal Surface Current W	Near Coastal Surface Current D	Surface Suspension Distribution (gr/l)			Wet (W)	Dry (D)	Wet & Dry	Depth (m)	Seawater Intrusion (km)
H1	Pemali - Garang	1	0.4	<1	E	W	0.022-0.03	1	Uplands; Dryland: wet climate	1500-3500	-	N/NW S/SW	1-2.5	1-3
H2	Serang - Juana	1	0.4	<1	E	W	0.026-0.03	2	Dryland: dry climate	1000-2500	-	W/NW E/SE	0.5-1.5	1-5
H3	Serayu – Bogowonto	2	1.5	1-1.5	W	W	0.03 – 0.047	3	Uplands; Dryland: wet climate	3000-3500	-	W E/SE	1-6	1-2
H4	Serang - Oyo	2	1.5	1-1.5	W	W	0.03 – 0.045	4	Uplands; Dryland: wet climate	2000-2500	-	W E/SE	1-6	1-2

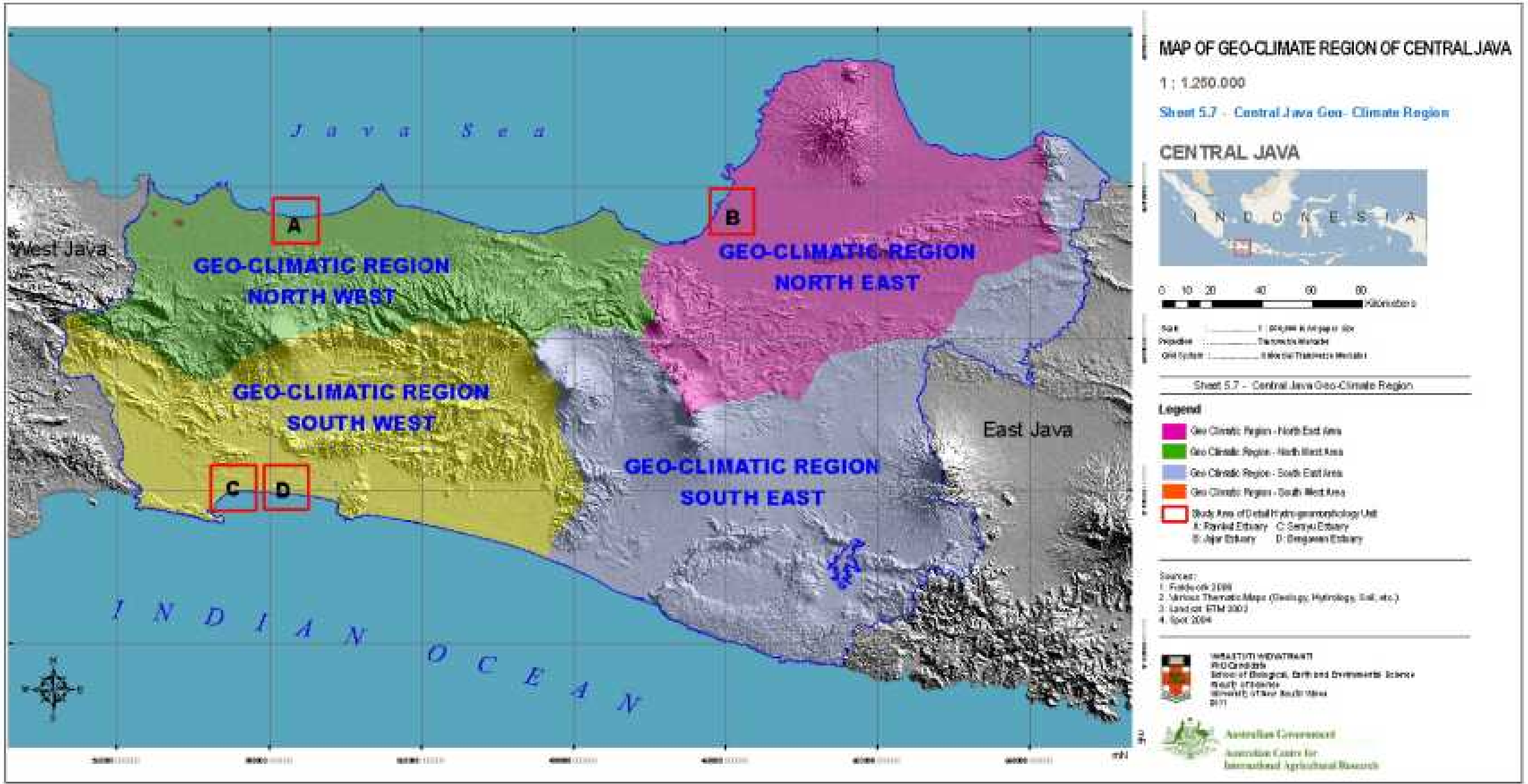

Figure 4.11 Map of the geo-climatic regions of Central Java.

4.4 Detailed Descriptions of the Geo-Climate Regions

4.4.1 Geo-climatic Region of Northwest (GcR-Northwest)

The GcR-NW is bordered by Cisanggarung river in the west and Miocene limestone hills, between Pekalongan and Bodri catchment, in the east (Figure 4.10). Based on the description of geomorphology and hydrology units, GcR- Northwest has structural landforms in the uplands which are part of an old volcanic system. The high annual rainfall (3000-3500 mm/year), and extensive weathering processes deliver a large amount of sediment (> 2500 t/km^2/y) to the lowlands (Koolsterman, 1989; van Dijk *et al.,* 2004). This depositional process has formed the alluvial plain along the coast of GcR-Northwest. The size of catchments in this GcR varies from small to large, generating distinct rivers and estuaries. The wave and tidal heights are below 1 m and below 0.4 m accordingly, forming a low-energy coastal area (Table 4.6). The land-use here is mostly high density settlement and the built-up areas are surrounded by ricefields in the lowlands, whereas the middle- and uplands areas are dominated by rural settlements, dry cultivated land and scattered forest clusters. Some of the coastal areas are fringed by mangroves and some mangrove forest clusters. However, many brackishwater ponds are found behind or in the middle of the mangrove areas (Personal observation, 2009, 2010). Most of the shrimp ponds exist in the Brebes to Pekalongan coastal areas.

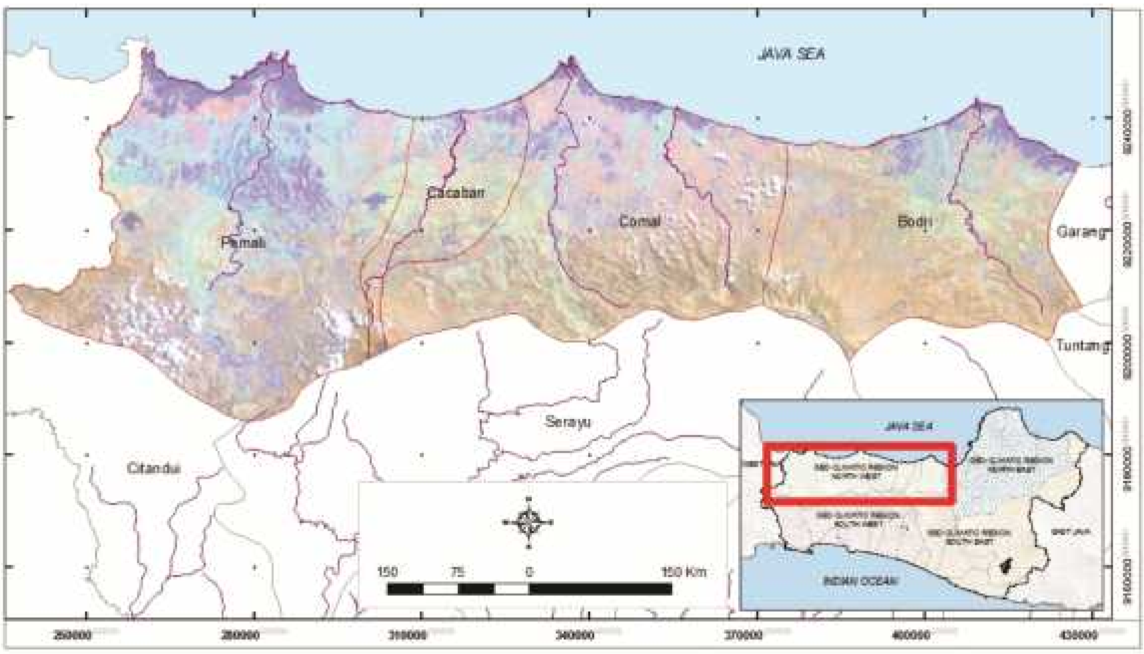

Figure 4.12 The GcR-Northwest shown by the Landsat ETM+ 453 composite imagery. The red boundaries show the watersheds of the Pemali, Cacaban, Comal and Bodri.

4.4.2 GcR- Northeast

The GcR- Northeast is bordered by Miocene limestone hills on the western side and by the Wulan river on the eastern side (Figure 4.11). The geomorphic setting of this GcR is a marginal geosyncline which was described in Section 4.2.2, as part of the north folded zone that emerged in the central depression that experiences intensive weathering and erosion (Verstappen, 2000). As stated in the Hydrology Unit section (Section 4.3.1, Table 4.6), GcR- Northeast has lower general annual rainfall than the GcR-Northwest. Based on more detailed rainfall maps (BMG,2000), the lower range of annual rainfall (<1000 mm/year) occurs in the upper and middle catchment areas, and the catchment in the eastern part of GcR- Northeast. The upper catchment of Bodri, Garang (Ungaran) and the coastal area of Serang have an average 2500 mm/year which is considered as high compared to the rest of GcR- Northeast, which is around 1500 mm/year. The narrow mangrove fringes exist along the coastline, together with brackishwater ponds, which are mostly used for milkfish cultivation.

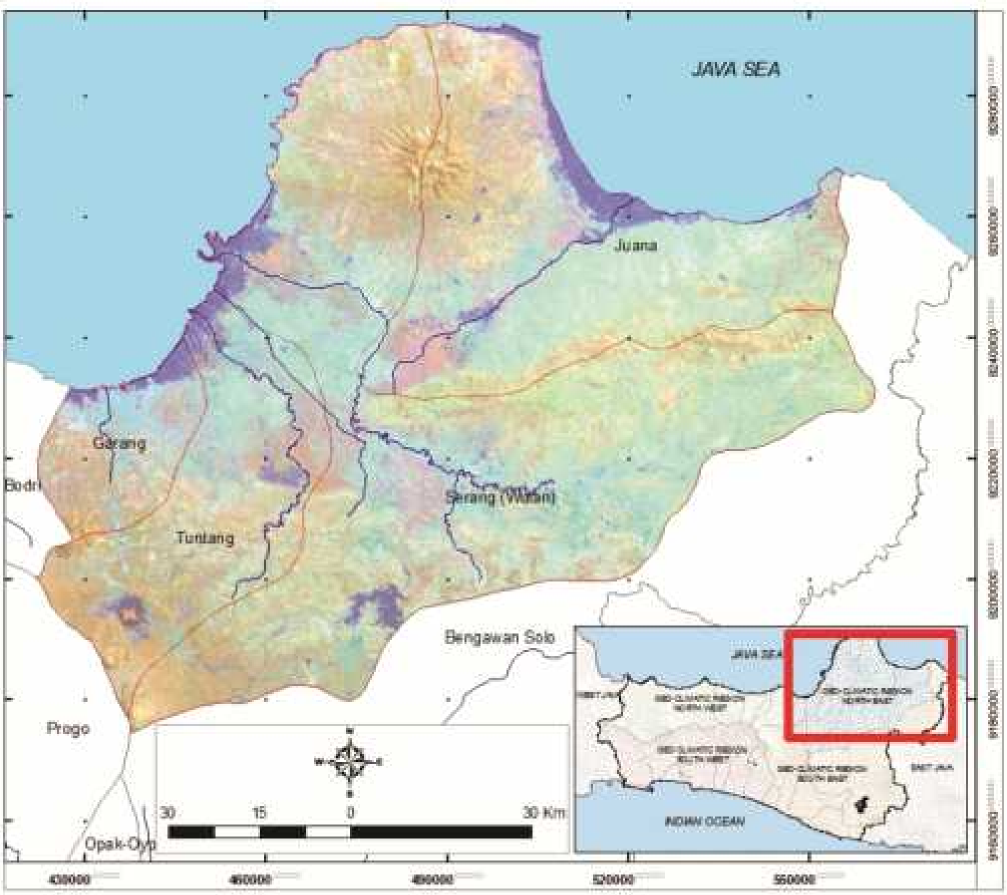

Figure 4.13 The GcR-Northeast, presented by Landsat ETM+ 453 composite imagery, shows a large alluvial plain in light to dark blue tone. This region consists of the Garang, Tuntang, Serang and Juana catchments.

4.4.3 GcR- Southwest

The GcR- Southwest is situated in the southern part of Central Java, ranging from the Serayu to Bogowonto catchments (Figure 4.12). This unit is bounded by the Donan River in the west, Serayu mountain range in the north and the Kulon Progo Menoreh mountainous range in the east. Its regional geological and geomorphic setting is part of the Sunda volcanic arc with the central volcanic zone in the uplands. This highly weathered structure is influenced by a high annual rainfall (3000-3500 mm/year), which has undergirded the development of alluvial plain (Koolstermen, 1989; Verstappen, 2000). This alluvial plain originated from the Southern Java Mountain Zone which collapsed in the Late Miocene and Early Pliocene, leaving only some limestone outcrops in the western, middle and eastern part of this south west part of Central Java (Bemmelen, 1949; Goffau & van den Linden, 1982). Despite similar annual rainfall and weathering levels, a variety of catchment characteristics has resulted in a variety of river lengths, drainage networks and types (Schum, 1981) within this GcR. This was shown by existing rivers which have intensive meandering like Serayu river and rivers with straight channels like the Wawar river. Wave height averages 1-1.5 m and wave energy dominates the coastal development process in this unit (HODIN, 2008). Land-use is dominated by ricefields and rural settlements. Built-up areas such as industrial areas are concentrated around Cilacap in the western part of the region. Mangroves and *Nypa frutican* forest are found scattered near a few estuaries. There are not many brackishwater ponds found in this region.

4.4.4 GcR- Southeast

The GCR- Southeast is located in the Yogyakarta region, in the southeast part of Central Java (Figure 4.13). Even though this area is not part of the area of this research, the description is still provided to show the complete hydro-geomorphology processes that influence Central Java. Generally, the regional geological and geomorphic setting and the hydrological features of GcR- Southeast are almost equal to GcR-Southwest. They have volcanic zones, which are part of the Sunda Arc Zone in the uplands, and alluvial plains in the lowlands. The differences between them are: in the GcR- Southeast the annual rainfall is lower (2000-2500 mm/year) compared to GcR- Soutwest; and the volcanic landforms are mostly younger (Holocene), contrasted to those of GCR- Southwest (Pliocene). Volcanic activity provides sediment to the Progo, Opak and Oya catchments on the central part of Yogyakarta largely through eruption.

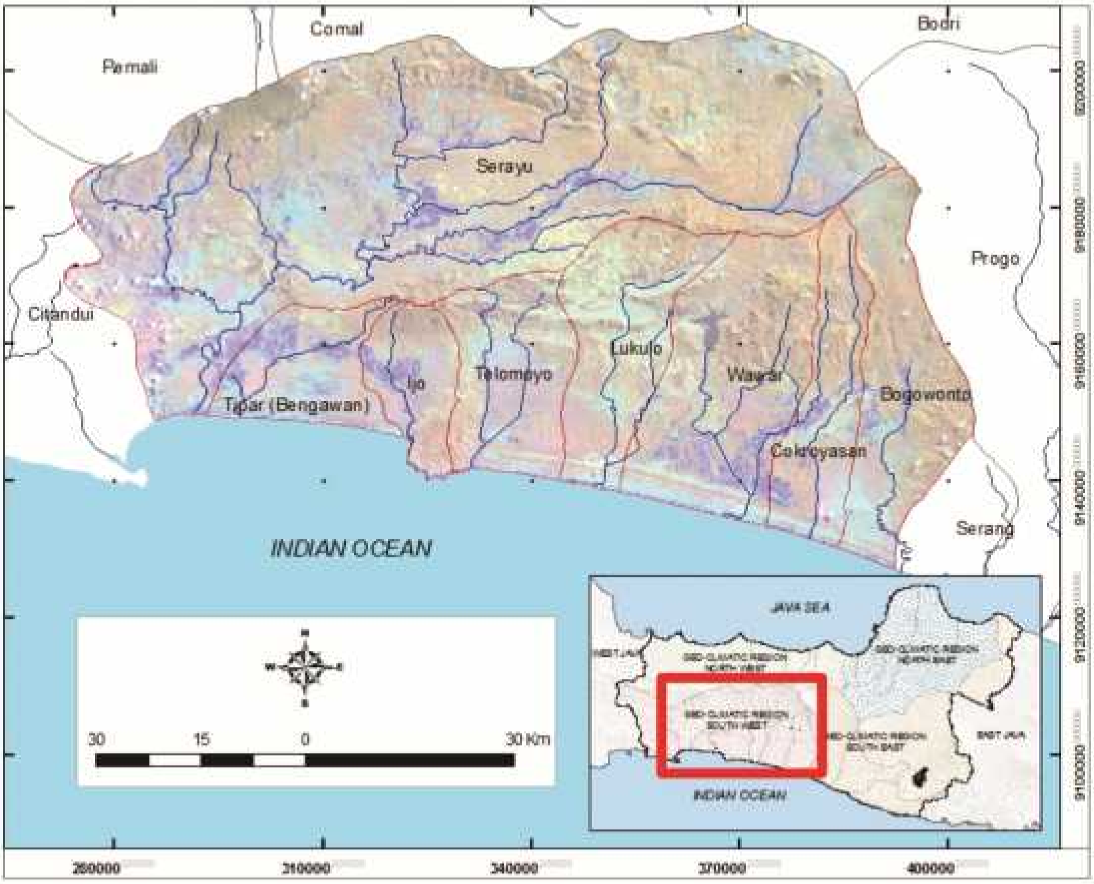

Figure 4.14. The Geo-climatic Region of Southwest (GcR-Southwest) consists of the Serayu, Tipar (Bengawan), Ijo, Telomoyo, Lukulo, Wawar, Cokroyasan, and Bogowonto catchments.

The Menoreh mountainous ranges, located west of Yogyakarta, however, have the same sediment as the central volcanic zone in GcR- Southwest and influence the river sediment of Serang. The coastal development process in GcR- Southeast is also similar to GcR- Southwest, which is dominated by wave energy, but is distinguished by more aeolian processes in the eastern part of the Yogyakarta coast. Thus, coastal dunes are well developed here (Verstappen, 2000).

The land-use of this region is mostly rural settlement with ricefields. In the centre of the catchment lies the biggest city of southern Central Java, Yogyakarta. This city has grown significantly in the last 10 years, especially on the volcanic plain of Merapi volcano (IBS, 2010). In terms of mangrove forests, based on Landsat ETM+ interpretation, there is no large area of mangrove or *Nypa* forest remaining. In the field, mangroves were only found as individuals or in small groups of less then 5-10 plants (Survey, 2009).

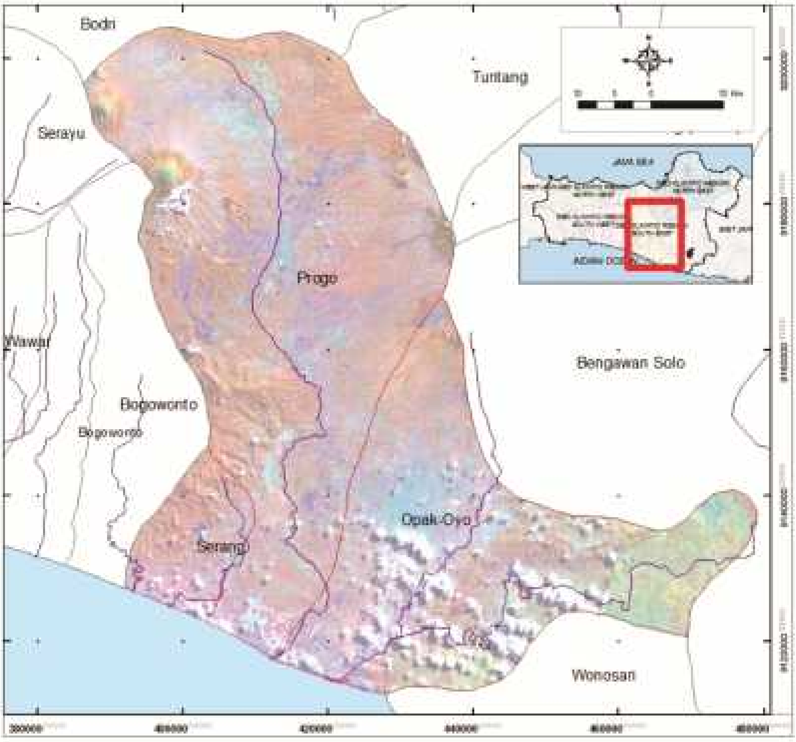

Figure 4.15 The Geo-climatic Region of Southeast (GcR-Southeast) consists of the Serang, Progo, Opak-Oyo catchments.

4.5 Utilizing GcR to Classify the Estuaries

The GcRs facilitates the estuary classification processes by providing information on the hydro-geomorphic processes of each catchment. It was concluded in Chapter 2 that to classify estuaries this study requires information on energy level of rivers, tides and waves as the main criteria to determine the estuary types. Hence, the GcR classes provide the parameters needed to determine the existing energy level of each estuary, such as: the origin of sediment from the uplands, the transport processes, volume and intensity of the sedimentation, and its influence on the development of estuary, and broad information of wave and tidal characteristics that form the estuarine landscape. The results and discussion of estuary identification and classification processes are further outlined on Chapter 5.

CHAPTER FIVE

ESTUARY CLASSIFICATION: ESTUARY DEVELOPMENT PROCESSES IN CENTRAL JAVA

5.1 Introduction

This chapter outlines the estuary classification processes in Central Java to understand the control of hydro-geomorphic processes on ASS development. This chapter addresses the second stage of the methodology outlined in Chapter 3. It also provides a platform for an in-depth discussion of ASS formation through an understanding of the estuary development processes. The classification process utilizes the Geo-climatic Regions (GcR) (described in Chapter 4) as a framework to describe the hydro-geomorphic characteristics of catchments and of the coastal environment. This study establishes criteria to classify estuary types, based upon landform features and the energy driving estuary development processes.

5.2 Estuary Classification Criteria

The main hydrological criteria used to determine each estuary type were the energy level of rivers, and tide and wave characteristics, because these are the main environmental drivers that influence coastal landforms including the estuarine environment (Boyd *et al.*, 1992; Haslett, 2000; and Bird, 2007). This study used quantitative and qualitative approaches to identify the dominant form of energy involved in estuary development. The approach involved categorization of the river morphometry, landscape features and marine energy parameters (wave and tide).

5.2.1. Criteria for River Energy Level

In ASS development, rivers deliver sediment to estuaries. This sediment is often the dominant source of fine materials and organic matter which are then trapped around mangrove roots (Dent, 1986). On the other hand, marine sediments are generally coarse and restricted to the marine-tide deltas and other seaward areas of the estuary where energy conditions are higher (Roy, 1984a, 1984b). Hence, to identify the extent of river energy and the material it deposits, this study utilized parameters of catchment morphometry (size and drainage density), the average discharge and sediment yield (Table 5.1). Catchment morphometry represents the characteristics of present drainage density, channel geometry, slope, catchment soils, geology, rainfall, infiltration rates, channel roughness within the catchment that influence the river energy level. The catchments were divided into low, medium and high energy classes following criteria used by Gupta (2007) and Knighton (1998). The drainage density classes followed the system established by Rompaey *et al.* (2001) and Soewarno (1999). The average discharge and sediment yield were classified based on previous classifications from Hasslet (2000) and the Water Resources Study Centre (2008).

Table 5.1 Levels of river energy in Central Java, based on several catchment parameters.

Parameter	Low Energy Level	Medium Energy Level	High Energy Level
Catchment size[1] (km^2)	<100 (small)	100-500 (medium)	500-1000 (large) 1000< (very large)
Drainage density[5] (km^{-1})	<0.55 (low)	0.55-10 (medium)	10-25 (high), 25< (very high)
Average Discharge[3] (m^3/s)	<40 (low)	40-70 (medium)	70 < (high)
Sediment Yield[4] ($t/km^2/y$)	<500 (low)	500-2500 (medium)	2500 < (high)

Source: [1, 2] Gupta (2007), [3]Knighton (1998); [4]Public Works Dep., 2008; Water Resources Study Centre, 2008;[5] Van et al, 2001 & Soewarno, 1991 with mod.

The qualitative approach assisted this study to determine the dominant energy in an estuary, by identifying the physical characteristics of the river and estuary themselves. The river energy was determined based on the diagram of channel shape by Knighton (1998) (Figure 5.1) and by assessing the catchments and the estuarine areas from aerial photographs, remote sensing data and topographic maps (Bakosurtanal, 1998; Landsat 7 ETM$^+$, 2002 updated with Landsat 7 ETM$^+$ 2010; ALOS AVNIR-2, 2010). Using the diagram of channel shape, the observed rivers were identified to obtain channel type information based on visual interpretation of their shape, and the occurrences of the lateral and mid-channel bars. The channel type will assist the qualitative assessment of the characteristics of sediment size, sediment load, total bed ratio and relative stability. Using these parameters, the dominant energy in an estuary was possible to identify (Table 5.2). The levels of river energy from both quantitative and qualitative approaches were used as basic information to finalize the level of river energy in an observed estuary.

Table 5.2. Levels of river energy based on the channel shape diagram of Knighton (1998).

Parameter	Low Energy Level	Medium Energy Level	High Energy Level
Relative Stability	high	Medium	low
Bed load/Total bed ratio	low	Medium	high
Sediment load	low	Medium	high
Sediment size	small	Medium	large

Source: Knighton (1998); with modification

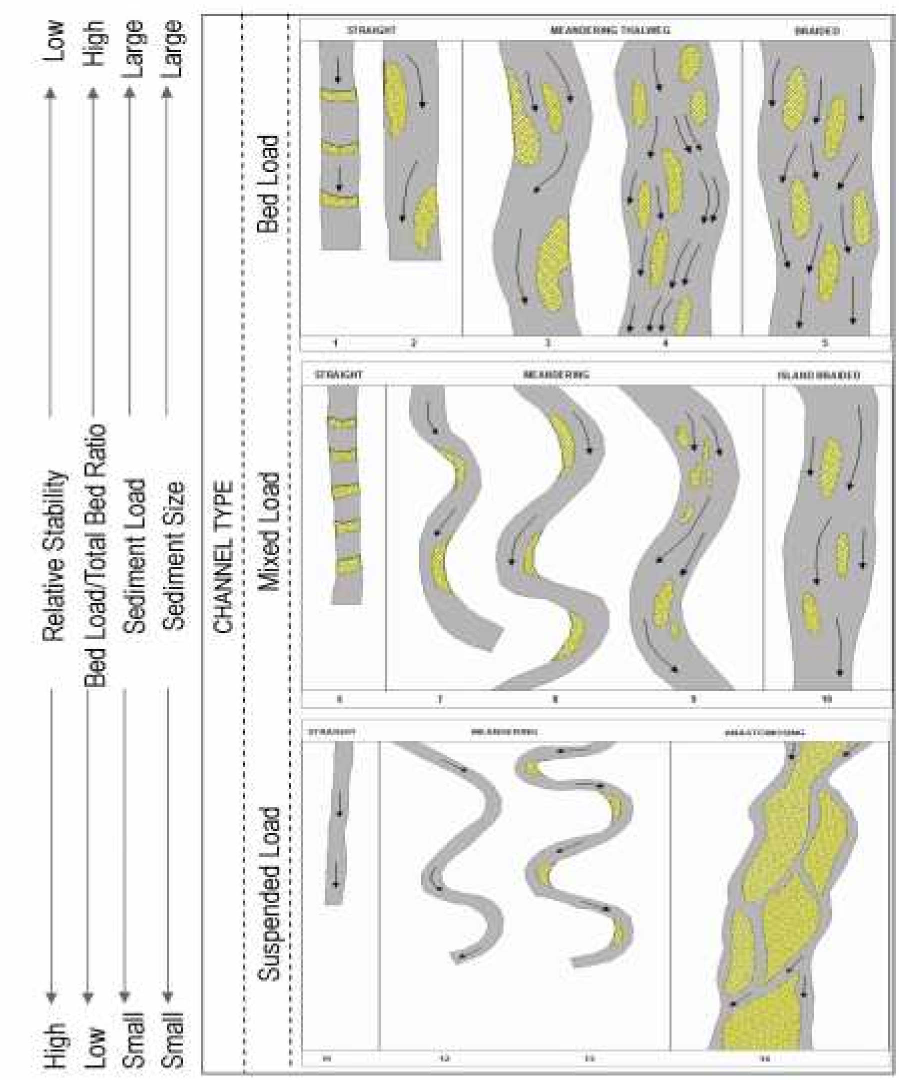

Figure 5.1. Channel shape diagram in relation to sediments characteristics from Knighton, (1998). This diagram is used to determine the river energy level based on the river's physical characteristics identified from the channel shape and channel bar in the coastal lowlands. These characteristics indicate the quantitative level of river relative stability, total bed ratio, sediment load and sediment size.

5.2.2. Criteria for Marine Energy Level

Marine sediments also play a role in landform evolution in estuaries and thus ASS formation. In some sandy beaches in Indonesia and Australia, wave, wind and long-shore current are also major factors in beach development and the type of materials that accumulate in this zone (Ongkosongo, 2010; Bird, 2007; Carter & Woodroofe, 1994). The quantitative approach applied in the classification of marine energy levels in this study, involved the determination of wave and tidal energy and their influences on the development of an estuary, as also suggested by Davies (1964, 1980), Hayes (1975), Jackson *et al.* (2002) and Engle *et al*. (2007). The secondary data provided from the wave and tidal energy criteria are presented in Table 5.3.

Table 5.3 Classification of wave and tide energy level.

Energy Type	Low Energy Level	Medium Energy Level	High Energy Level
Wave energy (WE)	Low WE<0.6 m	Medium 0.6m<WE<1.5m	High WE>1.5m
Tidal Energy (TE)	Micro-tidal TE<2,	Meso-tidal 2m<TE<4m	Macro-tidal TE>4m

Source: Davis , 1964; Hayes, 1979; Ongkosongo, 1982; Bird, 2000; Roy, et al., 2001; Jackson et al., 2002

In the qualitative approach, the identification of wave and tidal energy were based on the ternary process-based coastal classification diagram from Dalrymple *et al*. (1992) (Figure 2.1). The dominant energy occured in the coast and estuary is also possible by applying the estuary entrance shape identification (using geomorphic approach), observed from remotely sensed data and basic maps (Bird, 2000; Roy *et al*., 2001; Ryan *et al*., 2003; Ongkosongo, 2010). The conceptual model of estuary and coastal waterway by Geoscience Australia (2003), which referred to Boyd *et al.* and Dalrymple *et al.* (1992), Woodroffe *et al*. (1989,1999), Roy *et al*. (2001), explains the existing hydrodynamics, sediment and nutrient dynamics of each type of estuary (see Chapter 2, Section 2.3.2). Knowledge on the hydrodynamics and sediment dynamics is important for ASS identification, because it provides information on water movement, salinity variability, grain size and the depositional processes that can be used to identify conditions where pyrite may form. Even though this conceptual model has been applied only for Australia, the use of estuary entrance conditions to identify the type of estuary can be used in Indonesia, where its catchment characteristics are different to Australia (climate, geology, geomorphology, morphometry), because wave, tidal and river energy still are the main identification factors used in this model.

This study identified the estuary types in Central Java, using a modified Australian conceptual framework, and also considering Ongkosongo's coastal and estuary types (Ongkosongo, 1979, 2010), which also utilised estuary entrance/delta, and wave and tidal, river energy conditions to classify estuaries in Indonesia. The combination of the Geoscience Australia and Ongkosongo approaches covered the estuary entrance types which exist in Central Java. Figure 5.2 shows the different types of estuaries based on the shape of the estuary entrance.

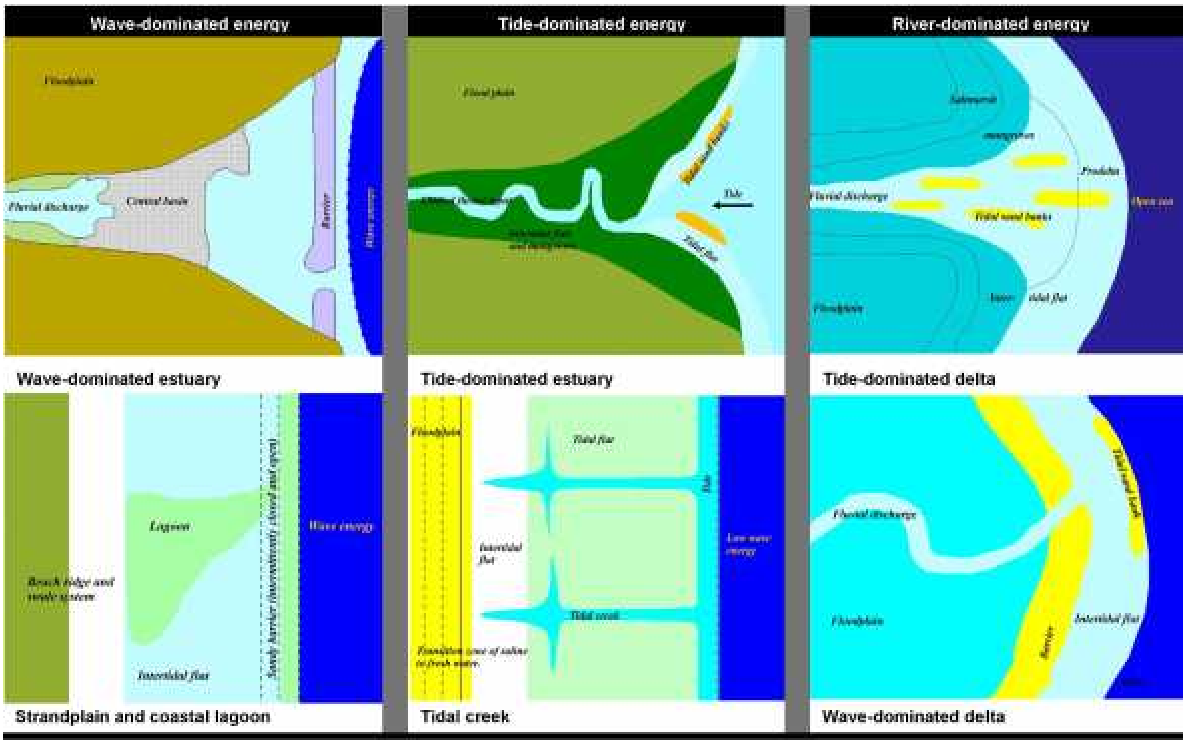

Figure 5.2 Different types of estuaries based on the geomorphology and the estuary entrance conditions (Geoscience Australia, Ryan et al. 2003).

5.3 Estuary Identification and Classification

This study gathered detailed hydrological and geomorphological data from remotely sensed images, basic and thematic maps, and detailed secondary catchment and marine information data, in addition to data from the regional hydro-geomorphic characteristics for each GcR. The more detailed data concerning catchments, estuarine and inshore-marine environments included: catchment size, volume, depth, river flow and sediment load and type, salinity, estuary entrance shape, tide, current and wave. These data were grouped based upon the parameters identified in the estuary classification criteria (Table 5.1, 5.2, 5.3 and Figure 5.2).

The catchment and river data were obtained from North and South Regional Catchment Profile in Central Java (BPDASPS, 2007) and Central Java's Department of Forestry (DoF, 2007), and field measurements. Wave height data were obtained from the Indonesian Hydrology and Oceanography Agency (HODIN, 2008) and from previous studies of coastal geomorphology in Central Java (Ongkosongo, 1982; Hoekstra, 1988; Ray *et al.* 2005; Marfai & King, 2008; Koropitan *et al.*, 2008). The tide data were derived from the monthly average tidal data from the last 10 years (HODIN, 2008) and from previous studies (Ongkosongo, 1982; Ray *et al.*, 2005; Koropitan *et al.*, 2008).

The results show that based upon on a quantitative approach (Table 5.5; Column 3), each estuary contains diverse combinations of river, tidal and wave energy levels. Some of the estuaries had more than one dominant energy type, such as: high river-energy and high wave-energy level or high river-energy and high tidal-energy level. This would have created difficulty in deciding the type of estuary if this study did not incorporate shape identification of the estuary entrances. Therefore, the channel diagram (Figure 5.1) and estuary entrance types (Figure 5.2) used in the qualitative approach, significantly contributed knowledge to classify the dominant energy that influenced the estuarine landform processes (Table 5.5; Column 4).

From all estuaries identified based on several topographic map scale 1: 25,000, remotely sensed data (Table 5.4 and 5.5), and field survey (2009), only 12 estuaries with the most complete data sets were selected for further classification (Section 5.4).

The result shows that on the north coast of Central Java, the GcR-Northwest coastline is characterised by river-dominated estuaries, whereas the GcR-Northeast has tide-dominated estuaries (Figure 5.3). Conversely, the south coast of Central Java is characterised by wave-dominated estuaries for both GcR-Southwest and GcR-Southeast. A new estuary type, wave-dominated estuary with pre-existing barrier is identified in GcR-Southwest. All further descriptions and figures related to these identified estuary types are provided in section 5.4.

Table 5.4 List of estuaries in Central Java and their administrative location.

No.	Catchment Name	Main River Name	Other Rivers within Catchment (sub-catchment)	Regency (estuary location)
North Coast of Central Java				
1.	Pemali	Pemali	Cigunung, Pemali, Keruh, Glagah, Kumisik, Rambatan, Pemali Hilir, Gung	Brebes
2.	Cacaban	Cacaban	Wadas, Gung, Konang Jimat, Rambut, Wuluh, Waluh	Tegal
3.	Comal	Comal	Comal Hilir, Sragi, Sengkang	Pemalang
4.	Bodri	Bodri	Blukar, Blorong	Kendal
5.	Garang	Garang	Kripik, Garang Hilir,Babon Hilir	Semarang
6.	Tuntang	Tuntang	Tuntang Hilir, Jajar Hilir	Demak
7.	Serang (Wulan)	Serang	Bakalan Pacangan	Demak
South Coast of Central Java				
1.	Serayu	Serayu	n/a	Cilacap
2.	Tipar (Bengawan)	Tipar	n/a	Cilacap
3.	Ijo	Ijo	n/a	Cilacap
4.	Telomoyo	Telomojo	n/a	Kebumen
5.	Lukulo	Jatinegara	n/a	Kebumen
6.	Wawar	Wawar	n/a	Purworejo
7.	Cokroyasan	Badgolan	n/a	Kebumen
8.	Bogowonto	Bogowonto	n/a	Purworejo
Special Region of Yogyakarta				
9.	Serang	Serang	n/a	Kulon Progo
10.	Progo	Progo	n/a	Yogyakarta
11.	Opak	Opak	Winongo, Code, Gadjah Uwong, Tambakbayan, Kuring, Tepus, Wareng, Gendol	Yogyakarta
12.	Oyo	Oyo	n/a	Yogyakarta

Source: Survey, 2009; BPDASSO, 2009.

Table 5.5 List of the name and types of estuaries based on Geo-climatic Regions.

Geo-climatic Region (GcR) (1)	Estuary name (2)	Energy level based on quantitative criteria (3)			Type of energy influencing the estuary based on Geo-science, Knighton and Dalrymple diagram (4)	Final classification of the estuary type (5)
		River	Tide	Wave		
GCR-NW	Pemali Comal Bodri	High	Medium	Medium	River-dominated	River-dominated Estuary Sub-classification: Wave -dominated Delta Tide-dominated Delta
	Cacaban Rambut Sragi Sengkarang	Low	High	Medium	Tide-dominated	Tide-Dominated Estuary
GCR-NE	Jajar	Low	High	Low	Tide-dominated	Tide-dominated Estuary
	Tuntang	Medium	High	Low	Tide-dominated	
	Serang (Wulan)	High	High	Low	River-dominated	Tide-dominated Delta (River dominated)
GCR-SW	Serayu Lukulo Wawar Cokroyasan Bogowonto	High	Medium	High	Wave-dominated	Wave-dominated Estuary and Strandplain/Sand Barrier
	Bengawan Ijo Telomoyo	Medium	Medium	High	Wave-dominated	Wave-dominated Estuary with pre-existing Barrier
GCR-SE	Serang Progo Opak Oya	High	Medium	High	Wave-dominated	Wave-dominated Estuary

Source: Analysis and field survey, 2010/2011

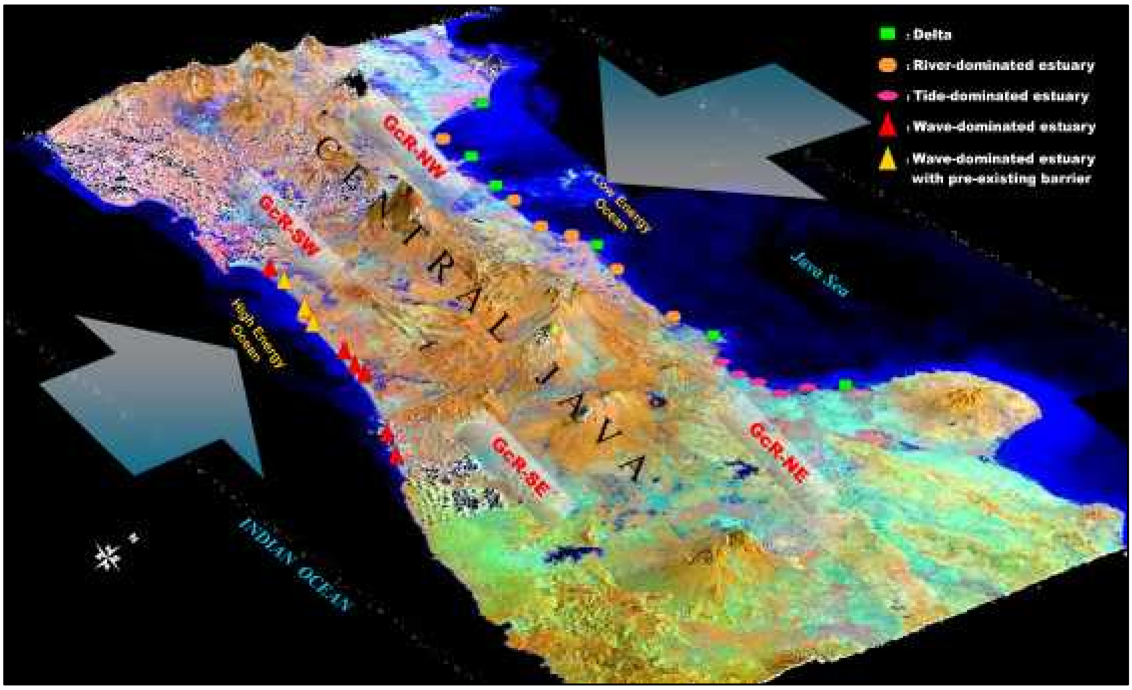

Figure 5.3. The distribution of estuary types in Central Java using Landsat ETM+ and DEM from SRTM as the background. Even though the delta type of rivers is not part of this current research, deltas are shown for reference.

5.4 Estuary Types in each Geo-Climatic Region

The following sections describe the type of estuaries observed in each GcR, including detailed characteristics of estuaries representing each region.

5.4.1 Estuary Types in GcR- Northwest

The catchments in GcR-Northwest experience low to high river energy levels (see Table 4.5). Hence, the estuaries in this GcR are commonly river-dominated estuaries, as tidal and wave energy do not strongly dominate the estuarine environments. The micro- and meso-tides in this region range between 0.4 – 0.8 meters (HOA, 1995-2005). However, the rivers of small catchments has more tidal influence on their estuary development, because of their low river discharges (below 50 m^3/s, Table 5.3), even during the rainy season (BPDASPS, 2007; Water Resources Study Centre, 2008). These previously prograded deltas were swampy coastal plains before the 1900s (Ongkosongo, 1979). Due to population pressures, their catchments experienced extensive deforestation for farming purposes which contributed a large amount of sediment (more than 2000 ton/km^2/year), covering the river systems (BPDASPS, 2007; Koolsterman, 1989; Repetto, 1986). This process has occurred rapidly over approximately 100 years with an average of 1-4 km shoreline progradation along the Central Java northern coast which continues today (Verstappen, 2000). These coasts were then formed and shaped by wave action generated by local winds.

Table 5.6 Hydro-geomorphic characteristics of selected estuaries in GcR-Northwest for estuary classification purpose.

No	Variable	Sragi	Sengkarang	Rambut	Comal	Bodri
1.	Catchment Area (km^2)	287	238	127	1642	682
2.	River length (km)	64	26	47	109	80
3.	Annual Average Q (dry/wet month) - (m^3/s)	27/46	25/40	9/20	70/130	9/54
4.	Drainage Density (km/km^2)	0.3	0.11	0.37	0.08	0.12
5.	Sediment yield (ton/km^2/year)	178-250	164-256	80-124	750-2000	400-800
6.	Type of estuary (based on quantitative and qualitative approaches)	Tide-dominated (small catchment)	Tide-dominated (small catchment)	Tide-dominated (small catchment)	River/Tide - dominated (very large catchment)	River/Tide - dominated (medium catchment)

(Source: Ministry of Public Work, 2010; Ministry of Forestry, 2007)

There are two groups of estuary types in GcR-Northwest. The first group includes the Pemali, Comal and Bodri Estuaries which have large catchment areas. These estuaries were categorized as river-dominated estuaries but have been evolving into deltas. Medium to high level rainfall and weathering in the uplands delivered a large amount of sediment (up to 2000 ton/km^2/year), which produced a large floodplain and shaped the estuary entrance (Public Work, 2008). During the rainy season, this large amount of sediment together with high river energy was able to exceed the ability of waves and currents to erode the estuary entrance (Bird *et al*., 2000). However, because waves and currents were able to shape the deltas during the dry season, they were sub-classified into wave-dominated deltas. Traditional and semi-intensive aquaculture ponds mostly occupied these estuaries, with mangroves fringing the riverbanks, canals, and along the shorelines of some estuary entrances. Figure 5.4 shows one example of the estuary from this group: Comal River, which has a large catchment size (896 km^2) and experiences medium rainfall intensity and high weathering of material in the upper catchment. This produces a large amount of sediment which is transported to the lowlands and creates a delta plain. The younger delta plain has mangrove fringes around the outlet just before the area of the sub-marine deposit delta front. On the coastline near the estuary mouth the medium wave energy has created some lagoons behind the sandy shore face. The present land-uses are mostly settlements, ricefields and ponds situated behind the coastline. Mangrove fringe development is relatively recent following sedimentation of the low energy environment and reforestation by local communities and/or initiated by government programs (DoF, 2006).

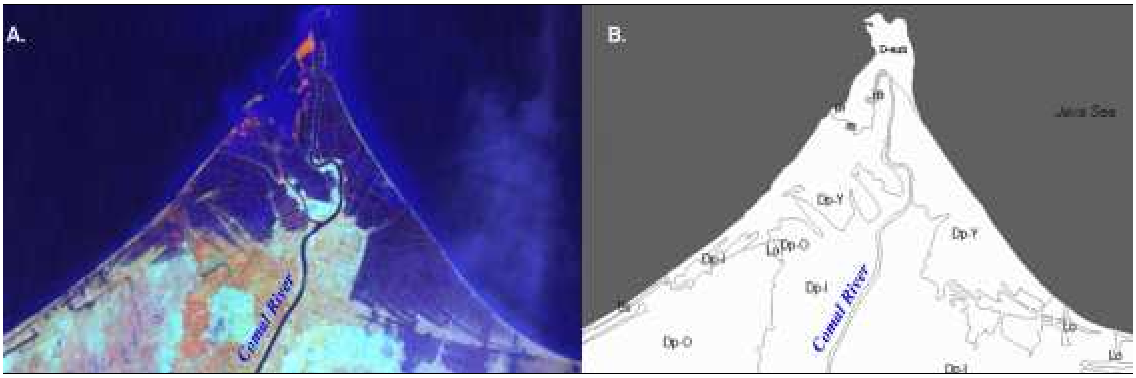

Figure 5.4 (A) The Comal River; a wave-dominated delta in GcR-Northwest. (B) Some landscape features include: Dp: Delta front with sub-marine deposit (o: older; in: inland, y: younger), m = mangrove, Lo = lagoon and Ss= sandy shore face.

In the second group, the estuaries have a small to medium catchment, with an average of a 200 km^2 catchment area (Table 5.6). Some small catchments were located between large catchments. There rivers included Wadas, Gung, and Rambut in Cacaban catchment, and Sragi Baru, Sekarang and Kupang in Comal catchment (Figure 5.5.A). In the rainy season, even though these rivers had lower discharges and sediment loads compared to the rivers in the previous group, they were able to dominate the estuary environment, but did not develop a delta (Personal observation, 2009, 2010). However, during the dry season, the estuary entrances were more influenced by tides and longshore currents that enabled low-tidal energy to penetrate upstream. Therefore, these groups of estuaries were classified as tide-dominated estuaries. The coastal landforms occurred in this type of estuary cover: sandy shore face, dune ridges or low beach ridges, intertidal flat and floodplain (Figure 5.5.B).

The seawater intrusion, however, does not affect the groundwater and agriculture drainage system as strongly as observed in tide or wave dominated deltas (Ongkosongo, 1979). The low-tidal energy and fresh water discharge during the wet season provided enough recharge of the groundwater to, prevent seawater intrusion (Kloosterman, 1989). The coastal environment in this group also has more stable landforms with more coherent sediment and soil texture of floodplain and intertidal flat, compared to tidal flats on the delta (Bird, 2007). Therefore, freshwater wells were found behind the tidal flat in about 50-100 m from the coastline (field observation, 2009).

In medium-sized catchments such as Cacaban and Rambut rivers, long-shore currents generated from medium wave energy developed seaward chenier ridges at the front of the inter-tidal flats. In the Sragi and Sengkarang estuaries the development of chenier ridges were more intense. Therefore, jetties were developed to prevent the closure of the estuary entrances (BPDASPS, 2007). These jetties are important to prevent flooding (overbank flow) during the rainy season. These ridges were relatively small compared to those of the Pemali and Comal deltas or numerous chenier ridges along the north Australian coast (Short, 1989). However, their existence, despite their different sizes, explains that the similar marine and tide energy could drive similar geomorphological processes and landforms at various scales of coastal environments.

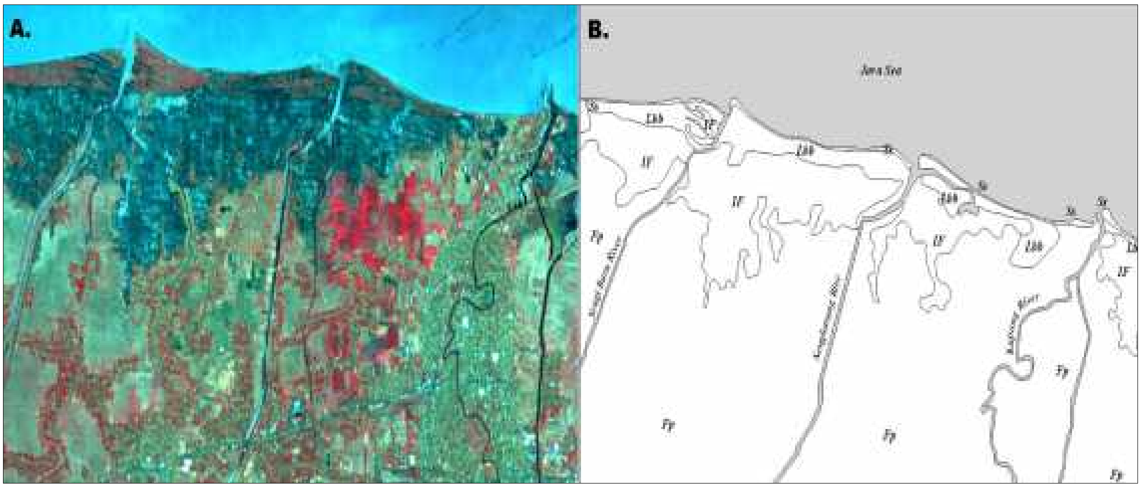

Figure 5.5 (A) ASTER imagery of the Sragi, Sengkarang and Kupang rivers represent the tide-dominated estuary type in GcR-Northwest. (B) Schematic of general landforms present in these tide-dominated estuaries: sandy shore face (Ss), low beach ridge/foredune (Lbb), intertidal flats (IF) and flood plain (Fp).

5.4.2 Estuary Types in GcR-Northeast

Estuary classification showed that the estuarine processes in GcR-Northeast were dominated by tidal energy. The existing catchment sizes varied from small to large, but all had low drainage density and a very small gradient (Table 5.7). The large catchments observed in this GcR were Tuntang and Wulan, whereas the medium was Jajar. The existing landforms in the lowlands of these rivers were flood plains (Fp) and intertidal flats (IF), with mangrove fringes along the open coastline. However, there were diverse river energy levels that influenced the estuarine processes and environment, especially based on the average discharge during the rainy season. First, as shown in Table 5.7, the Jajar River represented the estuaries with seasonal low-energy rivers with high tide- and low wave-energy. These estuaries were located within the Tuntang and Serang catchments, and were closely spaced (5-10 km). During the dry season, due to a large alluvial plain along the coast (Figure 5.6.A), and to a very low discharge (Table 5.7), the river energy was low allowing tidal waters to penetrate 10 km upstream. During the rainy seasons, however, the river discharge was higher (Table 5.7) and caused severe flooding. There have been many canals built to control this natural hazard. However, when flooding coincides with the occurrence of springtides, the canals cannot store the volume of water, resulting in severe overbank flow (brackish water) into the ricefields, affecting about 160 ha (BPDASSO, 2010). For this reason, ricefields have been gradually replaced by brackish aquaculture along the river up to about 15 km inland (Verstappen, 2000).

Table 5.7 Hydro-geomorphic characteristics of selected estuaries in GcR-Northeast for estuary classification.

No.	Variable	Tuntang	Jajar	Wulan
1.	Catchment Area (km^2)	2600	312	3660
2.	River length (km)	258	64	208.5
3.	Average Normal Discharge (dry/wet months) - (m^3/s)	27/500	12/31	60/123
4.	Drainage density	0.09	0.21	0.6
5.	Sediment yield ($ton/km^2/year$)	800-2300	200-650	2,500-3,500
6.	Type of estuary (based on quantitative and qualitative approaches)	Tide-dominated (large catchment)	Tide-dominated (medium catchment)	River-dominated (large catchment)
				Ministry of Public Work, 2010; Ministry of Forestry, 2007

The Tuntang and Wulan Rivers represented the second type of estuarine environment that being the river with a very large catchment (Table 5.7; Figure 5.6). During the rainy season, the river energy level was higher than the previous described estuary (Jajar River), demonstrated by an increase in monthly discharge from 27 m^3/s, during the dry season, to 500 m^3/s during the rainy season. This allows the river to transport enough sediment to develop a levee or thin pro-delta at the estuary entrance (Ongkosongo, 2010). The dominant energy that shaped this estuary was mostly tidal with minor longshore current especially during the dry season. The springtide was still able to dominate the estuary entrance during the rainy season (Bird & Ongkosongo, 2000); this estuary was still categorised as tide-dominated estuary. On the other hand, the Wulan River has high river energy, shown by high sediment loads and discharge (Table 5.7). The low tidal and wave energy in this area allows fluvial processes to develop a levee on both sides of a deep incised channel, and a large delta (Ongkosongo, 2010; Bird, 2007; Haslett, 2000). The Wulan Delta was classified as an elongate or a bird's foot delta which is dominated by tidal energy (Figure 5.7; Ongkosongo, 2010). Aquaculture ponds cover about 25 km^2 or 90 % of the delta plain (Sunarto, 2004; ALOS Imagery, 2010). Mangrove forest is well established along the shoreline of the estuary entrance and along the riverbanks. Mangrove fringes developed both naturally and as a result of planting along the rivers and edge of the ponds (BPDASPS, 2007).

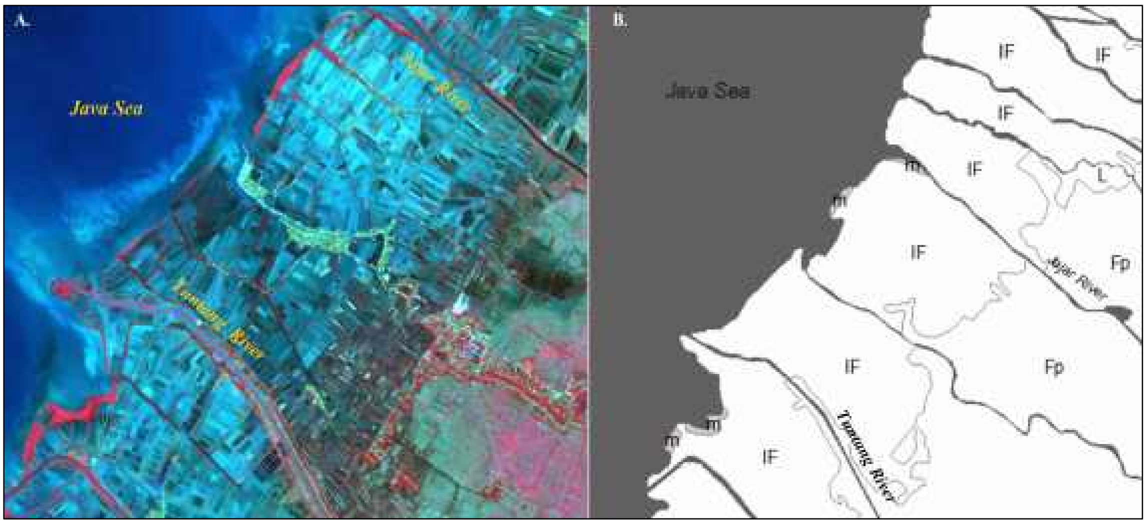

Figure 5.6. (A) ALOS AVNIR-2 imagery of Tuntang and Jajar Rivers, showing mangrove fringes (red feature along the coast) located along the coast and estuary entrances. (B) Landform units of the Tuntang and Jajar rivers, the tide-dominated estuaries: floodplain (Fp), inter-tidal flat (IF).

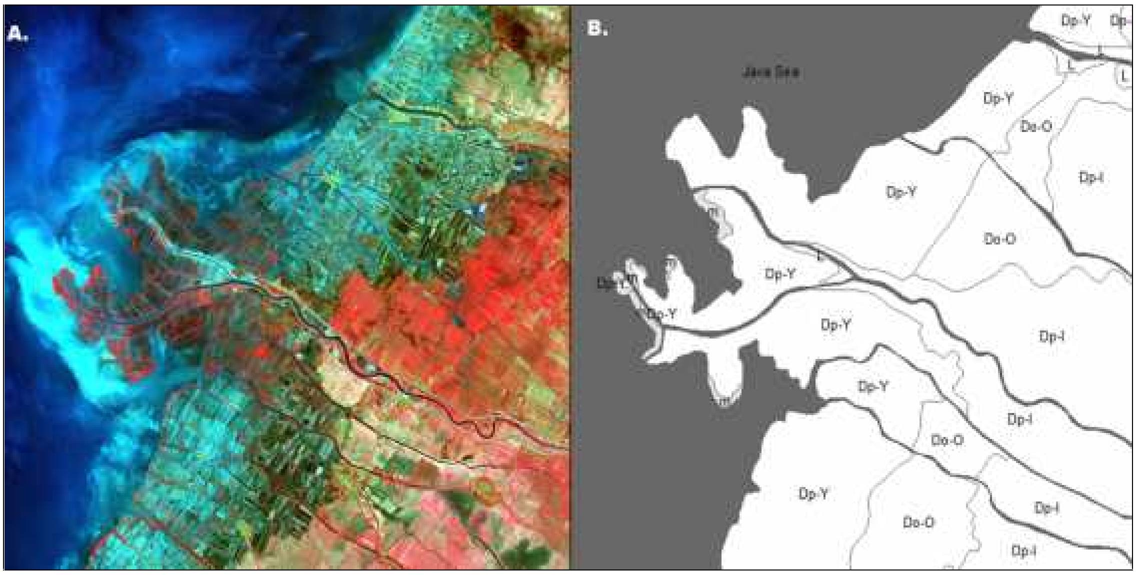

Figure 5.7. (A) The ALOS AVNIR-2 imagery showing different land-uses present in Wulan Delta; (B) Landforms of the Wulan Delta: delta plain (DP), with different geological age (o = older; in= inland, y= younger); and lagoon (L). New mangrove fringes (m) are found scattered along the coastline.

5.4.3 Estuary Type in Geo-climatic Region Southwest and Southeast

The coasts in GcR-Southwest and GcR-Southeast (south coast of Central Java) have similar marine energy levels, characterized by high wave energy. This higher wave energy was generated by the southeast trade winds, with the wave height range 1-3 meters, but occasionally more than 3 meters, and tidal range of about 1-1.5 meters (HODIN, 2008; US Navy, 1977). The southeast winds also caused littoral drift which transports material from the GcR-Southeast coast to the coast along GcR-Southwest (Verstappen, 2000; Ongkosongo, 2010). Therefore, the sandy material in GcR-Southwest, despite containing iron deposits from the old Andesit formation from upper Serayu Catchment (Bemmelen, 1949), was also influenced by Merapi volcanic material deposited along the coast in GcR-Southeast. The river energy level in this area varies due to the size of the catchment and high annual discharge (Table 5.8). However, most estuary entrances were influence by the wind and longshore current explained earlier. Hence, the estuaries in this GcR were classified as wave-dominated estuaries.

Table 5.8 Hydro-geomorphic characteristics of selected estuaries in GcR-Northeast and GcR-Northwest for estuary classification.

No	Variable	Serayu	Lukulo	Ijo	Serang
1.	Catchment area (km^2)	3720	652	303	210
2.	River length (km)	151	40	29	28
3.	Average normal discharge (dry/wet months) - (m^3/s)	300/1750	760/1498	150/297	3/63
4.	Drainage density	0.04	0.61	0.96	0.13
5.	Sediment yield ($ton/km^2/year$)	3,500-4,500	750-1500	500-1500	250-750
6.	Estuary type (based on quantitative and qualitative approaches)	Wave-dominated (large catchment)	Wave-dominated (medium catchment)	Wave-dominated (medium catchment)	Wave-dominated (small catchment)
Ministry of Public Work, 2010; Ministry of Forestry, 2007					

In GcR-Southwest, the wave-dominated energy in the estuaries created sand barriers at their estuary entrances. The length of the sand barriers of the medium-sized catchments, such as Bogowonto (590 km^2), Wawar (780km^2) and Luk-ulo (652 km^2) range from 500 m to 3 km. The length of the sand barrier was influenced by longshore current, sediment supply and wind action (Bird, 2007; Ongkosongo, 2010). Some of the estuaries become intermittently closed lagoons because there is insufficient water flow to incise a channel through the entrance. Figure 5.8 shows the closed lagoon on the western side of the Luk-ulo estuary. During dry seasons, the very low discharge (almost 0 m^3/s – Triatmodjo, 2010) allows marine energy (wave and southeast wind) to drive littoral drift which causes the closure of the estuary entrance because of sand sedimentation along the coast (Triatmodjo, 2000). Others landforms such as river banks, wash over and sand bars are more visible during this season. However, during the rainy season, these landforms were mostly submerged and high discharge flow through the sand barrier is able to open the new estuary outlet (Triatmodjo, 2000). The beach ridge and swale system were present behind the lagoon and were occupied by ricefields all year round.

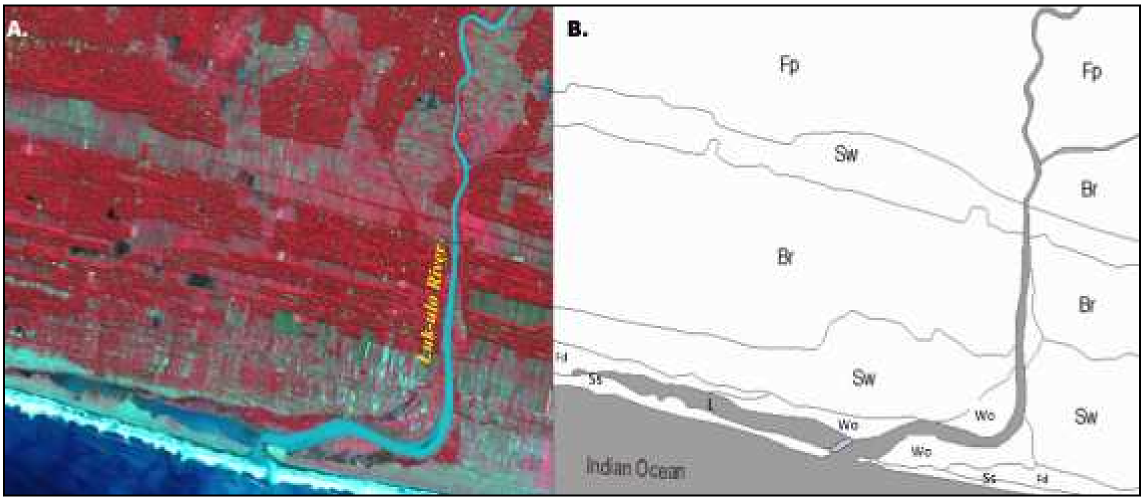

Figure 5.8. (A) ALOS AVNIR-2 satellite imagery, recorded in June 2009, showing the Luk-ulo estuary in GcR-Northwest. (B) The landforms in this wave-dominated estuary (medium catchment size) include: sandy shore faces (Ss), sand barriers (Sb), lagoons (L), washovers (Wo), swales (Sw), beach ridges (Br), floodplains (Fp), low beach ridges (Lb) and fore dunes (Fd) in front of the low beach ridge and lagoon.

Figure 5.9. (A). The sand barrier (red dash rectangles) in the Luk-ulo estuary is an example of landform in a wave-dominated estuary with medium energy rivers. (B). Ricefields cultivated by the local people in the swales (red dash rectangles) occur between beach ridges.

The other large catchment in GcR-Southwest was that of the Serayu River. Despite the dominant influence of wave energy, the estuary entrance of this catchment was very dynamic due to annual flooding caused by high annual discharge (1750 m^3/s) and sediment load (3,500-4,500 ton/km^2/year) during the rainy season. Field observations during 2008-2010, covering both rainy and dry seasons, recorded changing landscape features at the estuary entrance of Serayu River. Quickbird and ALOS AVNIR imageries showed different Serayu River estuary entrance conditions during years 2002 (Figure

5.10.A) and 2010 (Figure 5.10.B). In 2008, the low beach ridge and sand barrier at the Serayu River estuary entrance was about 2-3 m high and 500 m in length (Figure 5.11.A & C). However, in 2010 both of the low beach ridge and sand barrier disappeared (Figure 5.10.B & D). Local residents reported, during the interviews, that a flood in January 2010 removed half of the existing barrier (Figure 5.11.B). This flood also triggered overbank flow (BPDASSO, 2010), which caused the removal of some part of the low beach ridge thus the damage to the ricefields behind it.

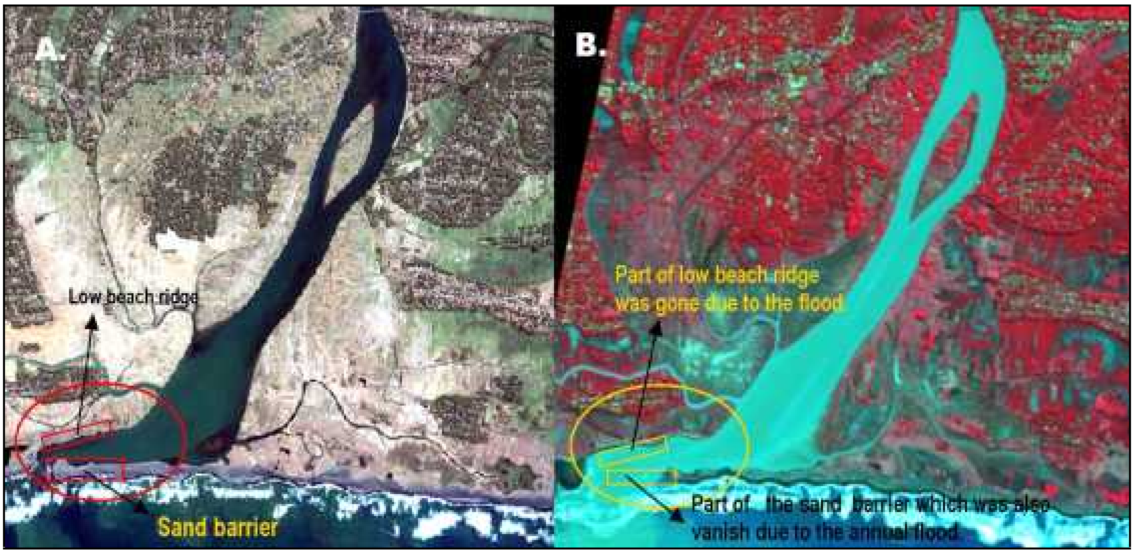

Figure 5.10 The changes in the Serayu's estuary entrance conditions due to periodic floods, shown by (A) Quickbird imagery recorded in June 2002 and (B) ALOS AVNIR image recorded in June 2010.

The other type of estuary in GcR-Southwest was the wave-dominated estuary with pre-existing barriers. This type of estuary covered Bengawan/Tipar, Ijo (Figure 4.10) and Telomoyo estuaries. The term pre-existing barrier referred to a landscape feature which blocked or slowed the river outflows before it discharged to the sea. In this study, these barriers were characterized by calcareous hills which were part of a stranded isolated remnant outcrop of the south mountain zone (Goffau & Linden, 1982). They were located in Nusakambangan, Selok Hill and the Karang Bolong Mountains. These hills affected the sedimentation process by slowing down the river flow. Consequently, the environment behind these barriers was gradually altered to a lower river energy environment, leading to sediment accumulation (Figure 5.12.A).

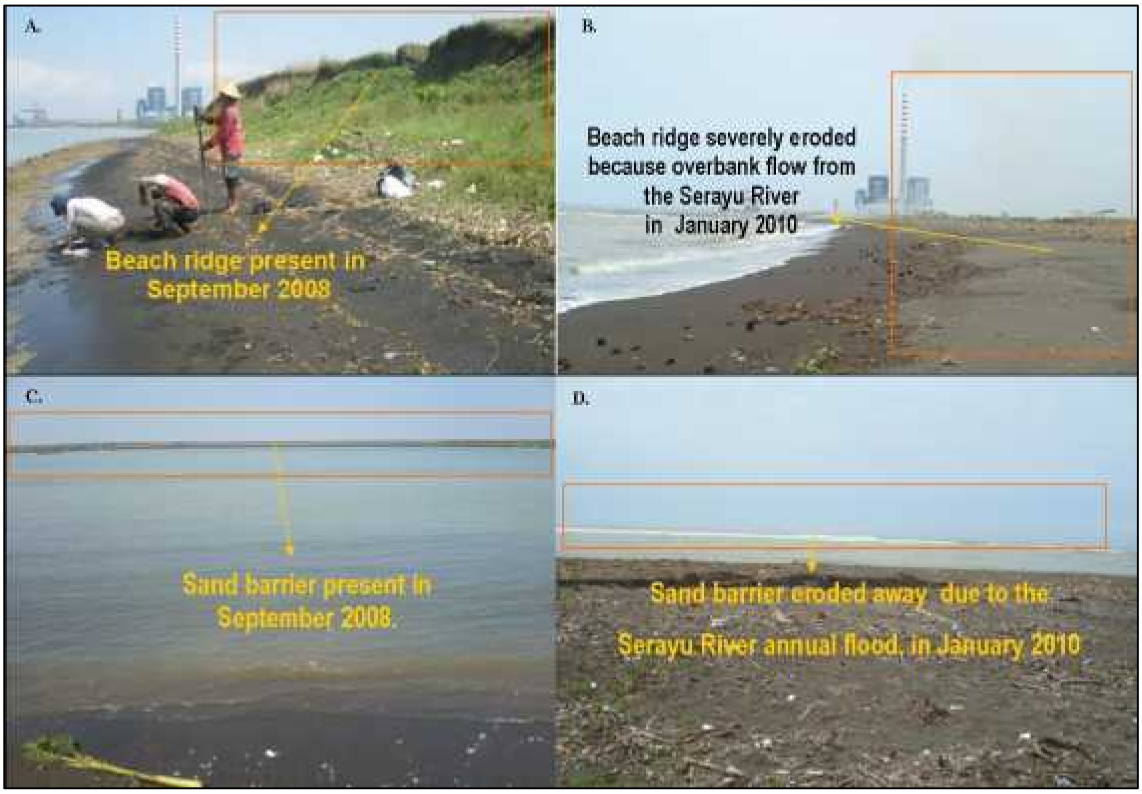

Figure 5.11. (A & C) A beach ridge and sand barrier were present in September 2008. (B & D) However, the Serayu River annual flood occurred in January 2010 and eroded sections of both the beach ridge and the sand barrier.

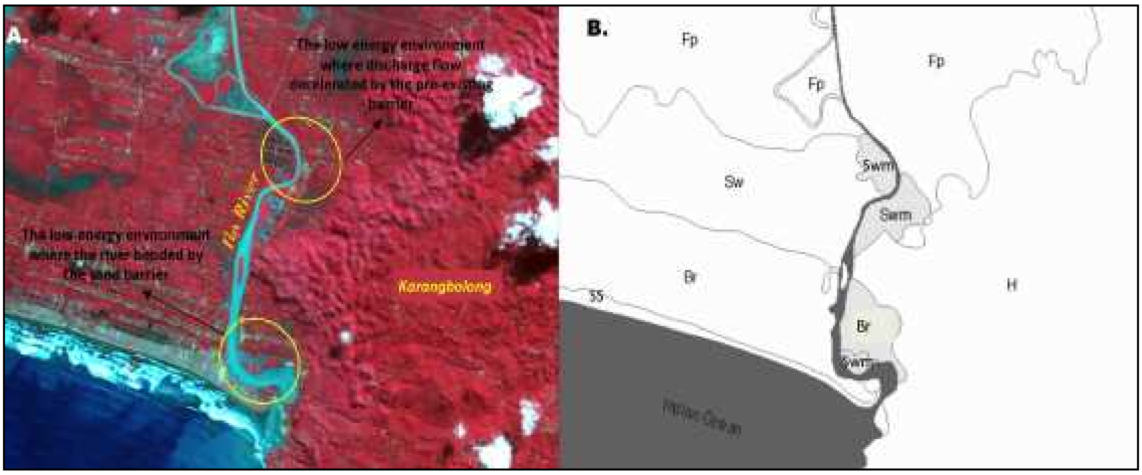

Figure 5.12. (A). The Ijo River representing the wave-dominated estuary with pre-existing barrier. Consequently, a backswamp/swamp (Swm) with mangrove and Nypa fruticans formed. (B). The other landforms found in this type of estuary include: sandy shore face (Ss); beach ridges (Br), swales (Sw), floodplain (Fp) and hill (H).

The salinity of the river water on the north of the low energy environment where discharge flows decelerated by the barrier, had values of <1%. Conversely, the one after (on the northwest side of the barrier) had salinity level of 3-5 % (field observation, 2009). There was another swamp located near the entrance where the river was refracted by the sand barrier (Figure 5.12). This swamp was a low-energy environment indicated by the presence of mangrove and *Nypa fruticans*. Commonly in the south coast of Central Java, this vegetation is rarely found in the areas close to estuary entrances because of high wave-dominated energy conditions. The sediment textures on the environment near the sea (the south of the barrier) were coarse due to the high energy from waves (Personal field observation, 2009-2010). Conversely, the sediment which accumulated in the surrounding (western and northern side) Karang Bolong hills had fine soil textures, representing low-energy environments influenced by both the tides and river (brackishwater environment).

The sediment accumulation caused by southeast–west longshore current during the dry season commonly caused the closure of the estuary entrances (Triatmodjo, 1998). However, this closure never happened in the Ijo River, because the pre-existing barrier of Karang Bolong hampered the southeast–west longshore current to enter the estuarine environment. During the rainy season, the estuary entrance remains open, because the Ijo River energy (annual discharge: 600-1000 m^3/s) is sufficient to dominate the entrance against the southwest–east longshore current. Despite this continuously open estuary entrance, the annual floods still inundate about 2000-4000 ha in the upstream area, triggered by the very heavy rainfall and overbank flow (Triatmodjo, 2000).

Based upon the distinct environmental conditions, this study proposes this 'wave-dominated estuary with pre-existing barrier' become a new type of estuary for Central Java. This new type of estuary will contribute significantly in ASS development research, considering the existence of several low-energy environments in brackishwater areas. The various landforms in this estuary are also able to represent the influence of the diverse energy levels on ASS development.

Figure 5.13. (A) Mangroves and Nypa fruticans in Ijo estuaries, developing in a swampy environment as result of the river being blocked by the eastern side of Karang Bolong Mountain. (B). The Nypa fruticans forest is found up to 5-10 km upstream of the Bengawan/Tipar Estuary entrance, the wave-dominated estuary with pre-existing barrier.

As for the GcR-Southwest, high wave-energy also dominated the estuaries in GcR-Southeast. However, in terms of their parent material, the rivers in this region: Serang, Progo and Opak, were different to those in GcR-Southwest. The catchment size of the Serang River was classed as medium, with Sermo dam impounding water in the upper catchment on the West Progo mountains (Figure 5.14). The dam development resulted in low discharge from the Serang River (Triatmodjo, 2010). However, a short sand barrier has developed westward due to the longshore current, refracting this river (which were extended north to south), to the west in the estuarine area (field observation, 2009). During the dry season, the environment before the river being refracted has been developed for tourism with water sport activities (BPDASSO, 2010).

Table 5.9 Hydro-geomorphic characteristics of selected estuaries in GcR-Southeast for estuary classification

No.	Variable	Serang	Progo	Opak
1.	Catchment area (km^2)	210	2380	740
2.	River length (km)	28	138	65
3.	Average normal discharge (dry/wet months) - (m^3/s)	0.3/61	12/330	2/85
4.	Drainage density	0.14	0.06	0.09
5.	Type of estuary	Wave-dominated (small catchment)	Wave-dominated (large catchment)	Wave-dominated (large catchment)
				Ministry of Public Work, 2010; Ministry of Forestry, 2007

The Progo and Opak rivers were located in large catchments with high and medium rainfall environment respectively (Table 5.9). As for the GcR-Southwest, wave energy dominated these estuaries. However, Progo and Opak materials were influenced more by young volcanic material from the active Merapi Volcano compared to Serayu which was by old volcanics (Verstappen, 2000). During the rainy seasons, the Progo River's large discharge (around 590 m^3/s) delivered a large load of sediment from the upper catchment to the lower catchment (Regional Agency of Public Work, 2010). Some severe mudslides occurred after the volcano erupted. Mid channel bars in the downstream were continuously formed towards the end of rainy season. Therefore, during dry seasons, when the discharges were low (9-80 m^3/s), the sandy riverbeds provided an economic resource for local communities and small-scale sand mining companies (BPDASSO, 2010).

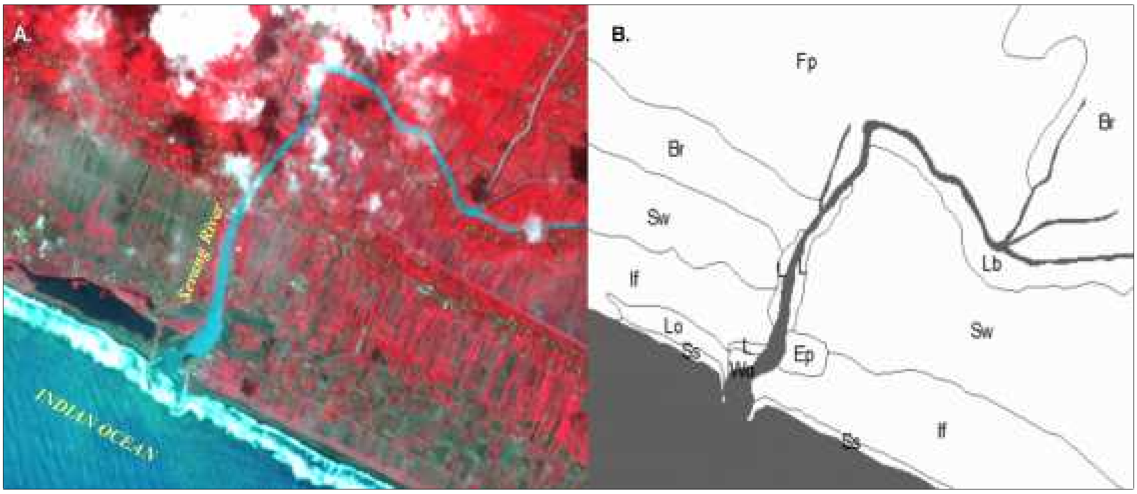

Figure 5.14 (A) ALOS AVNIR imagery of Serang estuary which is a wave-dominated estuary with a medium catchment size in GcR-Southeast. (B) The landform types in the Serang estuary include: floodplains (Fp), beach ridges (Br), lower beach ridges (lb), levee (L), inter-tidal flats (If); ephemeral channels (Ep), wash over deposits (Wo), lagoons (Lo), and sandy shore faces (Ss).

Figure 5.15 Map of the estuary types present in each Geo-climatic Region in Central Java.

5.5 Estuary Selection to determine the Hydro-Geomorphic Units (HGUs)

The completion of the estuary classification enabled this study to move forward to the next stage which was to identify the landform differences within different estuary types using Hydro-geomorphic units (HGUs) (Chapter 3, Section 3.2.2). Several estuaries were selected to represent dominant types of estuaries in each GcR. The selection process considered several prerequisites, especially the availability of secondary data and the accessibility to the study site, particularly the estuary entrance location, for further detailed field surveys. Estuaries for further study were also chosen to represent the variation in catchment size among the estuary types. Subsequently, four estuaries were chosen for detailed study. The first estuary was Rambut Estuary which represented river-dominated estuaries with small to medium sized catchments in GcR-Northwest. The second was Jajar Estuary which represented tide-dominated estuaries with medium to large catchments in GcR-Northeast. The third and fourth were Serayu and Bengawan Estuaries, representing wave-dominated estuaries with large to very large catchments and wave-dominated estuaries with pre-existing barriers with small to medium size catchments, respectively.

5.5 Summary

The descriptions of estuary characteristics for the GcRs of the north and south coast of Central Java assisted this study to develop a general estuary classification scheme for Central Java. While the estuary characteristics are variable, the dominant estuary types are consistent with the properties of each GcR. This consistency demonstrates that the GcR is able to facilitate the identification and classification of estuary types based upon characteristics of catchment and coastal (and in shore marine) environments. The levels of energy from the ocean were identified as the controlling factor in estuary development in Central Java. However, the different combinations of river, tide and wave energies produced complex estuary landforms. It means that one estuary may have similar landforms to others, but involve different levels of energy that affect landform processes. This new estuary classification scheme will be correlated with the distribution and development of ASS at a general and detailed level through the development of the HGU. The complete methods for deriving detailed hydrological and geomorphic processes of the HGU in estuaries are provided in Chapter 6.

CHAPTER SIX

DETERMINATION OF HYDRO-GEOMORPHIC UNITS

6.1 Introduction

This chapter outlines the determination of Hydro-geomorphic Units (HGUs). The HGU is used for the detailed mapping of units within selected estuaries, and is classified based upon landforms, hydrology and geomorphic processes, land-use and vegetation types related to tidal characteristics. These HGUs provide a method to derive the detailed scale information of hydro-geomorphic process control on ASS development, as part of the aims of this study. At this level of mapping, the approach utilized the estuaries selected from the estuary classification outlined in Chapter 5. These HGUs were set up to represent the development processes of ASS (AASS, PASS), and their different physical and chemical properties (Chapter 2, Section 2.2).

There were five stages in the process of determining the HGUs (Figure 6.1). These were: Stage 1: establishing estuary zones (estuary zonation) by dividing the estuarine environment based on river and tidal characteristics; Stage 2: identifying geomorphic units in each estuary zone, using landform identification approach; Stage 3: detailing the geomorphic unit (from Stage 2) to define the land-unit based upon land-use and vegetation types; Stage 4: adding hydrological data and distance of the landform from the sea or the river, into land-units (obtained at Stage 3); and, Stage 5: data validation. These HGUs were validated by conducting field surveys (including soil sampling) as part of Stage 5. The final detailed land-units obtained at Stage 4 were classified as HGUs.

These four stages of HGU determination utilized multi-resolution satellite imageries: Landsat 7 ETM^{+}, ALOS AVNIR2, and QuickBird to obtain different levels of landscape and landform details. All mapping units generated from visual interpretation of satellite imageries in Stage 1-4 were digitised into a digital map. This digital map included a GIS attributes database system that contained all details of the HGU information obtained from Stage 1 to 4.

Soil sampling was conducted to validate the identified HGUs' and to recognise their ASS characteristics through field and laboratory soil analysis. Therefore, this chapter also presents the methods for soil sampling and the sampling sites in each selected estuary. These five stages of HGU determination, including detailed field survey and soil sampling determination for each estuary, are explained in the following sections.

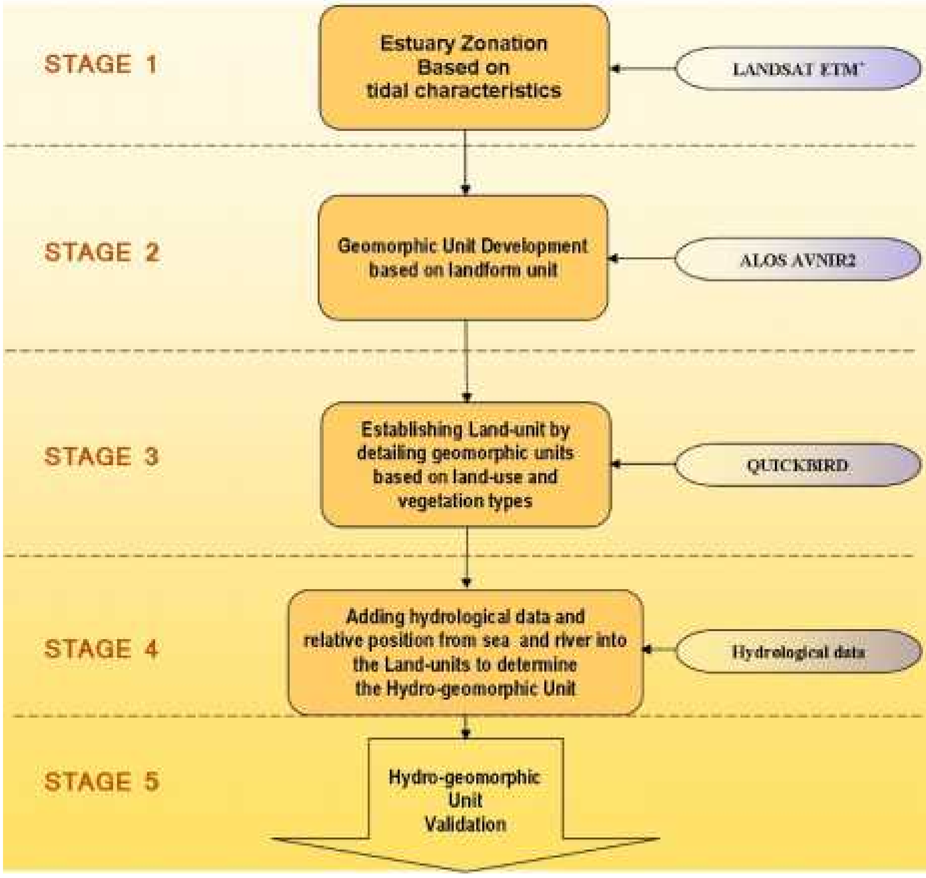

Figure 6.1 The schematic representation of the HGU determination process.

6.2 Stage One: Estuary Zonation

The estuary zones represent different tidal conditions, which influence sedimentary processes and the development of estuarine landforms (Bird, 2007). Hydrological conditions, tides and sedimentary environments are commonly used to define estuarine zones (Bird, 2007; Dalrymple *et al.*, 1992; Roy *et al.*, 2001). In this study, estuary zones were established based on salinity measurement, and tidal processes and landform identification (representing sedimentation processes). Salinity measurements aim to show the distribution of salinity levels in an estuary and to provide information about tidal influence (sea water intrusion) in the estuary. The water salinity was measured by collecting water using a water sample bottle (grab sampling), in the centreline of the estuary from an average depth of 50 cm, to represent surface water salinity level only. This study does not focus on water column salinity influence to the soil. Therefore, it has not accounted for salt wedges which can occur in estuaries, where dense saline water occurs and it flows beneath a layer of fresh water. The measurement was conducted using an ATAGO hand refractometer and digital pocket salinity refractometer (ATAGO PAL-065), during high- and ebb tide to determine the extent of seawater penetration into the estuaries. This measurement utilised QuickBird ® imagery to plot the sample points and Global Positioning System (GPS) to determine the approximate location of samples in the field. The samples was taken from the estuary entrance and continued at intervals of 100 meters upstream to the transition zone. This zone represents the transition of water salinity from brackish to freshwater and has salinity levels down 1 ppt in the upper part of the transect (Savenije, 2005). More detailed measurements were conducted between initial sample points, when the salinity difference between two measured points was considered large (more than 0.5 ppt). This measurement revealed three salinity zones: (i) marine environment with salinity level >35 ppt, (ii) tidal environment (0.1-35 ppt), including the transition zone (<1 ppt), and (iii) river environment (<0.1 ppt). The results of the measurement are provided in Appendix 6.1.

Sedimentary environment types were recognized by identifying landform types, which indicated whether they were formed by marine, tidal or fluvial processes. Different types of landforms indicated different geomorphic processes, including sedimentary processes (see Chapter 2.2.1). These landform types were identified from interpreting Landsat ETM^+ imagery. Using these types of landforms, together with river salinity information, the approximate boundaries between estuary zones were possible to define. Initially, these approximate boundaries were irregular, following the shape of landforms in within each boundary but for this study purpose, they were adjusted into straight lines (Figure 6.2), representing the average fluctuation of the salinity zone from field measurements.

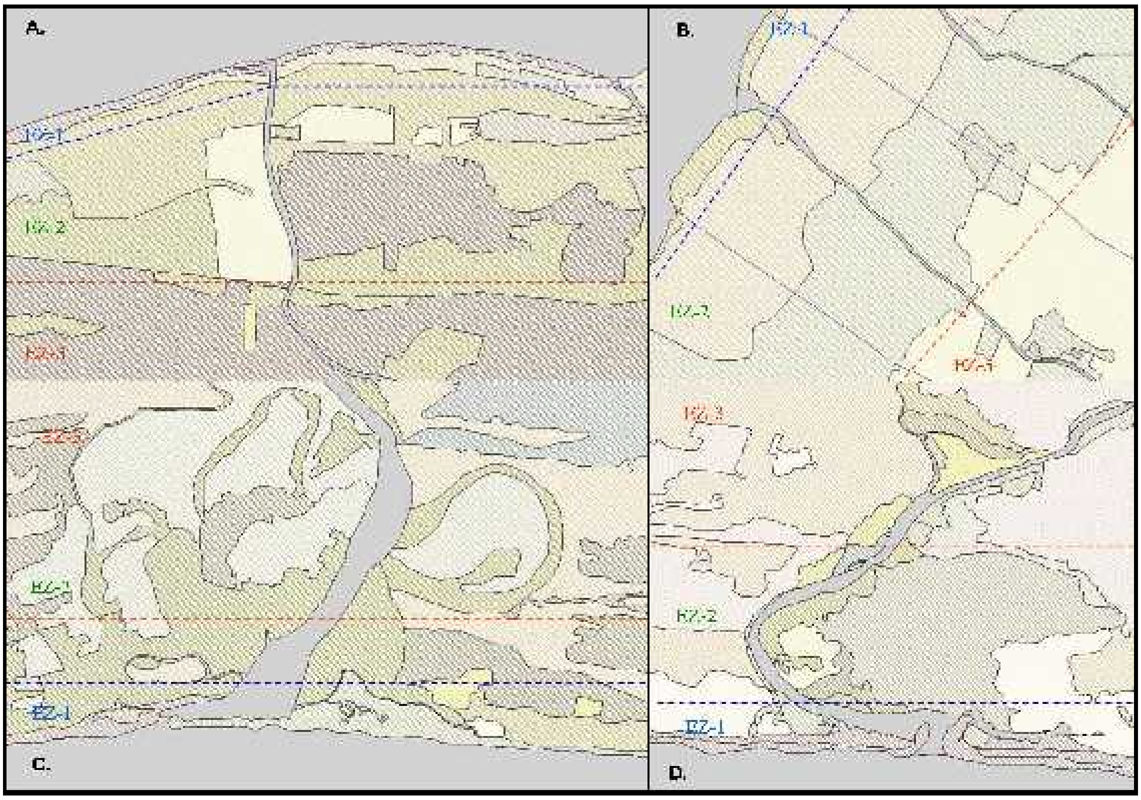

Figure 6.2 Estuary zones in Rambut Estuary (A); Jajar Estuary (B); Serayu Estuary (C) and Bengawan Estuary (D). The Estuary Zone 1, 2 and 3 (EZ-1, EZ-2, and EZ-3) represent include seashore, tidal shore, and the area where fluvial deposition occurs respectively.

Table 6.1 Characteristics of three estuary zones in this study

Estuary Zone	Tidal influence based on salinity	Sedimentary environment type based on general existing landforms	Hydrological zones and vegetation type
EZ-1: Seashore	Marine environment with salinity level around 35 ppt or more	Seashore environment Dominated by marine sediments	Marine (Brackish water and non-brackish water vegetation on sand or muddy sand)
EZ-2: Tidal Shore	Tidal environment with salinity level between 0.1 ppt to the transition of 35 ppt Including transition zone (0.1 - 1 ppt)	Intertidal flat environment Dominated by estuarine sediments	Tidal (Brackish water and non-brackish water vegetation on sandy muds and muddy sands, vegetated rocks)
EZ-3: River Deposition	River (upstream) environment with salinity level below 0.1 ppt	Fluvial environment Dominated by fluvial sediments	Gradational (Brackish water and non-brackish water vegetation on fluvial plain with sandy muds, muddy sands and sands)

Modified Estuary Zonation from Rochford, 1959, Bird, 2007 and Roy et al, 2001

6.3 Stage Two: Determining Geomorphic Units

Two similar geomorphic units can have different soils simply because of the local geology. However, because this study was dealing with sedimentary processes and there is a greater reliance on the geological parent material, geomorphic units are utilised as the boundaries (areas) for representative soil types (Hole & Campbell, 1985). In this study, a geomorphic mapping unit is generated not only to represent a soil type but also the related geomorphic processes, especially the ones that are related to the development of ASS. The geomorphic unit determination utilized ALOS AVNIR-2 (and Landsat ETM$^+$ for synoptic view) to identify more detailed landforms present in each estuary zone which was generated at stage one. The landform classification uses the classification systems and nomenclatures applied in Indonesia, including: Bird (2007), Ongkosongo (1982, 2010), Verstappen (2000) and Zuidam (1986).

The determination of geomorphic units commenced with landform identification in each estuary zone (EZ-1, EZ-2 and EZ-3) and continued by predicting the ASS probability of occurrence based on previous studies (Chapter 2, Section 2.1.2) and field observation (2009). In Rambut and Jajar estuaries (Figure x), the river- and tide-dominated estuaries respectively, the sandy shore faces was the only landform in EZ-1. There were also limited landforms in EZ-2 and EZ-3, including intertidal flat, levee and floodplain. In contrast, there were two types of landforms in the Serayu and Bengawan Estuaries' EZ-1: sand barrier and sandy shore face. These wave-dominated estuaries also had more landform types in EZ-2 and EZ-3 compared to Rambut and Jajar Estuaries. In EZ-2, washover existed in addition to intertidal flats, levees and floodplains. The EZ-3 had more complex landforms than EZ-2, e.g.: floodplains, beach ridges, swales, abandoned channel (including oxbow lakes), ephemeral channels, mud/salt flats and backswamps. These more detailed landforms were called geomorphic units. Using these geomorphic units the probability of ASS presence could be identified based on knowledge of ASS forming factors and associated geomorphic processes. The ASS presence probabilities presented in Table 6.2 show different levels of occurrence in each geomorphic unit.

Table 6.2 The geomorphic units present in each estuary zone and the probability of ASS presence

Selected observed estuaries (type of estuary)	Estuary Zone	Geomorphic unit	The probability of ASS presence	Landform Code for mapping purpose
Rambut (River-dominated estuary)	Estuary Zone -R1	Sandy Shore Face	Low to none	Ss
	Estuary Zone -R2	Intertidal Flat Levee	Medium to high Low to high	If L
	Estuary Zone - R3	Floodplain Levee	Low to high Low to high	Fp L
Jajar (Tide-dominated estuary)	Estuary Zone –J1 Estuary Zone –J2 Estuary Zone –J3	Sandy Shore face Intertidal Flat Floodplain Levee	Low to none Low to high None to high Low to high	Ss If Fp L
Serayu (Wave-dominated estuary)	Estuary Zone -S1	Sandy Shore Face, Sand barrier	Low to none	Ss
	Estuary Zone -S2	Intertidal Flat Floodplain Levee	Low to high None to high Low to high	If Fp L
	Estuary Zone -S3	Beachridge Swale* Backswamp* Mid-channel bar Abandon Channel Ephemeral Channel Floodplain	Low to none Medium to high Medium to high None Low to high Low to high None to high	Br Sw Bs McB Ac Ec Fp
Bengawan (wave-dominated estuary with pre-existing barrier)	Estuary Zone -B1	Sandy Shore Face, Sand barrier	Low to none	Ss, Sb
	Estuary Zone -B2	Washover Intertidal Flat Floodplain Levee*	Low to none Low to high Low to high Low to high	Wo If Fp L
	Estuary Zone -B3	Beachridge Swale Backswamp* Mid-channel bar Abandon Channel Ephemeral Channel Salt Flat/Mud Flat Floodplain* Point bars	Low to none Low to high Low to high None Low to high Low to high Low to high None to high None to high	Br Sw Bs McB Ac Ec Sf Fp

(*) Commonly as sub-aerial depositional environments.
All definitions of the existing landforms in these selected estuaries are provided in glossary.

6.4 Stage Three: Detailing Geomorphic Units Based on Land-Use and Vegetation Types to Establish Land-Units

The third stage of the HGU determination was to establish ‘land-units’ by utilizing high spatial resolution satellite imagery (QuickBird®) to identify land-use and vegetation types in each geomorphic unit, observed in stage two. Land-use types support prediction of pyrite concentration (high, medium or low) in an environment (Chapter 2, Section

2.3.2). This study utilizes multi-temporal satellite imageries recorded during dry and rainy season to see the consistency of land-use types. Land-use incorporated both the use of land (Danoedoro, 2006; Lesslie *et al.*, 2014) and land-cover (Barson & Lesslie, 2004). This term describes the function of both human and natural features of the geomorphic unit. This study also observed other estuaries to identify whether there were any land-uses which could not be found in the selected estuary.

The land-uses observed in those estuaries covered: water, aquaculture ponds, dryfield, rice field, unused-land and settlements (Table 6.3). 'Dryfield classification' refers to the land which is used for crop production not requiring inundation with water (Danoedoro, 2006). In Australia, it is called dry-land farming (Lesslie *et al.*, 2014). Dryfield is a common agricultural type in Indonesia, with typical crops such as: peanuts, corn, cassava, sweet potatoes and watermelon, both grown in rainy and dry seasons.

Unused-lands and bare-lands are any lands which do not currently not developed or actively used, which in this study include: levees, mid channel bars, coast/beaches, hills, wash over or other new form of sedimentation (tidal bank or lateral bar). These geomorphic units with unused-lands contained low to high probability of ASS presence, as provided in earlier Table 6.2.

Water bodies were divided into rivers, tributaries and abandoned channels, using 'spatial dimension classification' described by Danoedoro (2006). Aquaculture ponds were further categorised as active, semi-active or abandoned (see Chapter 1). The status of pond usage was determined from field observations and interviews with the local community. Settlement and built-up area were specified as rural with homestead gardens representing settlement in rural areas and urban settlement in urban areas, and non-settlement.

ASS is commonly associated with brackish water vegetation, such as: mangroves and *Nypa fruticans* (Dent, 1986; van der Kevie, 1976; See Chapter 2). Therefore, to determine if ASS is likely to be present in a land-unit, the vegetation was classified into two groups: brackish water and non-brackish water vegetation with the former indicating a greater likelihood of ASS. This classification was based upon the presence of a dominant vegetation community or colony within a geomorphic unit (Table 6.3, Column 5), including areas with: (i) freshwater vegetation (e.g. trees, agriculture, plantations), (ii) brackish water vegetation (mangroves and *Nypa fruticans*), and (iii) no vegetation. The type of mangrove species were identified and recorded for further analysis (different study on the relationship between ASS and mangrove type distribution), but were not included as land-units data attributes, because this study focuses on ASS characteristics instead of the relationship between mangrove species and soil properties. Further information on the probability of the presence of ASS in this stage was provided in Stage Four method (Section 6.5) after adding the hydrological data attributes into 'land-units'.

Table 6.3 Classification of present land-uses and vegetation for land-unit Attribute

Attribute Code	Land-use	Sub-Attribute Code	Detailed land-use	Vegetation Type
200	Water	201 202 203 204	- Sea - River - Tributary - Oxbow Lake	None
22	Aquaculture Ponds	220 223 225	- Active - Semi-active - Abandoned	None
33	Rice field	33	-	Non-Brackish water vegetation (NBWV)
44	Mangrove/Nypa forest	441 442 400	-	Mangrove (Any types) *Nypa fruticans* None
55	Settlement and Built-up area	551 552 553	Rural With Homestead Garden Urban Settlement Built-up area	Non-Brackish water vegetation
66	Dryfield	66	-	Non-Brackish water vegetation
88	Unused land/ bare land	77	-	Some areas have Non-Brackish water vegetation, there rest have none.

Source: Danoedoro, 2006; Field survey, 2009-2011

6.5 Stage Four: Hydro-Geomorphic Units (HGU) Determination

The various pyrite concentrations are associated with the hydrological conditions including how the sources of sulfate influencing land formation (Section 2.1.2: Sundström *et al.,* 2002; van Breemen, 1982). Hydrological conditions included river, tidal, and wave characteristics, seawater intrusion, climate etc., which had already been covered at the Geo-climatic Region level (Chapter 4, Table 4.6). In this stage, hydrological information only included groundwater depth from the surface. Distance of the land-units from the river and the sea were also added to the land-units to create HGUs.

Groundwater depth and the distance of landforms from the source of sulfate were used as attributes in the geomorphic unit GIS database system. Ground water depth data were obtained from ground water table maps and secondary data (BPDASPS, 2007; BPDASSO, 2010), and were measured in the field utilizing wells in estuarine areas to validate the present maps and to identify fluctuations in the water table depth. As mentioned in Chapter 2, that water table fluctuations can enable pyrite to oxidize naturally in a potential ASS environment (Fitzpatrick *et al.,* 2008b; Hart *et al*., 1882; Husson *et al*., 2000; Rosicky *et al*., 2004). The distance of land-units from the source of sulfate was determined first by measuring ground water salinity from existing wells, to differentiate the land-units which have brackish and fresh groundwater (Appendix 6.2). Secondly, these land-units and measured wells were plotted using GPS and uploaded on the digital map to obtain their distance from the river and the sea. Flood occurrences were also considered in this study by observing inundated areas during the dry and rainy season in the field and wetness tone level from visual interpretation of satellite imagery and secondary data (Triatmojo, 2010). This information was also available from the interviews with local residents. The greatest magnitude flood for a year on the rainy season caused some areas inundated with brackish water (Field observation, 2010; Triatmojo, 2010). The occurrence of backswamps with ponds was one example of this annual flood impact. These areas were identified to have high probability of the presence of ASS (Dent, 1986).

The digital land-unit map with its attributes, which contained water table depth and distance to the sulfate resource information, were named as the draft of HGUs map.

This draft required validation to know whether the difference in water table depth and distance to sulfate resources indeed influence the presence of ASS in each HGU.

6.6 Stage Five: HGU Validation

The draft HGUs map generated from stage one to four contained mapping units with detailed geomorphic (landforms) information, land-use and vegetation, and hydrological related data. As, these HGUs were considered as a draft, they required a field-based validation, and soil field and laboratory analysis to finalise the HGUs. The purposes of this validation are to identify the soil physical and chemical characteristics of each HGU, to check whether the identified HGUs accurately represent distinct hydro-geomorphic characteristics in the field, and to assist the analysis of the relationship between the HGUs and the distribution of ASS.

6.6.1 Determination of the Soil Sampling Area

The sampling areas of this current study were restricted to estuarine environments including their past estuarine environment, as these are the areas where ASS occur. They were bounded by the catchment boundaries which extended landward from the coastline to the river salinity transition zone (Figure 6.3; Section 6.2.4).

6.6.2 The Selection of Soil Sampling Sites

Representative and multistage stratified random samplings, as outlined in Section 3.3.1, were used to capture data on the characteristics of HGUs across the selected estuaries. These sampling methods were commonly used in the study area, which were subdivided into representative (mapping) units (Gruijter *et al*., 2006; Hewitt, 1993; McKenzie, *et al.*, 2008; McDonald and Isbell, 2009; Webster & Oliver, 2001). The representative sampling method is based on selecting and plotting at least one sample point in each block or unit. One sample point represented one HGU which is the smallest in an estuary. Because the sizes of the HGUs varied, multistage stratified random sampling determined the number of samples in each HGU. The larger the size of the HGU, the more samples it had. However, at least one sample site per HGU was collected.

The number of samples defined in the representative sampling method was used to recognize the ideal sample number in a HGU. However, the number of samples could be adjusted according to field condition. Webster & Oliver (2001) called this approach 'unequal sampling', when a mapping unit was observed to have variation in the field, and the need to take more samples within this particular unit is reasonable. Therefore, the larger HGUs will have more than one sample point to cover greater various of soil characteristics, but do not always require more samples when the features were considered uniform. In this particular case, the smaller HGUs which were observed to vary could also have more than one sampling point. These sample points then had to be sorted based on accessibility and disturbance level explained in the following sections.

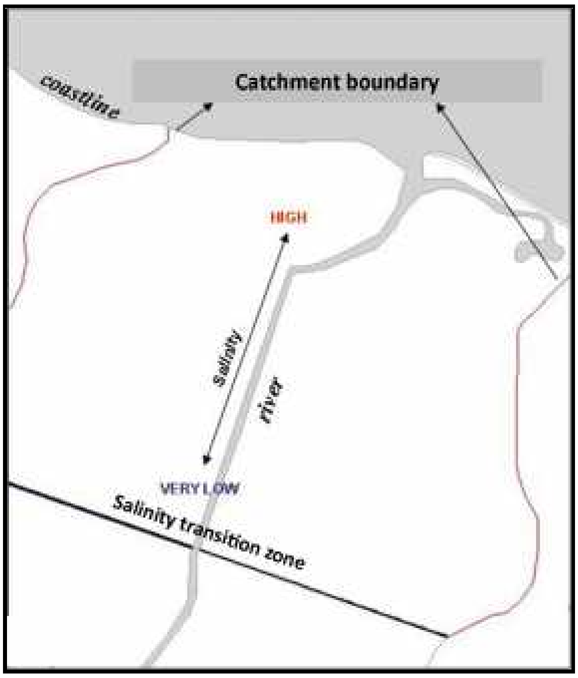

Figure 6.3 Illustration of sampling area bounded by the coastline, catchment boundary and salinity transition zone (Figure not to scale).

Soil pit sampling was also conducted in this study to describe a more detailed soil profile, based on transects that capture as many HGUs as possible. The depth of the pit was a minimum of 2 m, but it depended upon soil depth because some HGU located in coastal areas or close to the river had were less than 1 m in depth. To accurately map the transect profiles, terrestrial measurements were conducted using a Total Station, NIKON DTM352. These profiles were then merged with the other soil samples as elevation/altitude references.

6.6.3 Level of accessibilities and disturbances in Soil Sampling Sites

The soil sampling process in the field did not always go according to the plan. Many selected sample sites were not easy to access. Selected sites represented ideal areas for sampling. Conversely, the more accessible areas corresponded to medium to high disturbance. To overcome this obstacle, sampling sites in the field were selected based on level of accessibility and soil profile disturbance. These low to undisturbed land surfaces were commonly located in a near pristine environment or had not been intensively exploited by recent anthropogenic activities (20-50 years). Therefore, some samples, which were not accessible, and will be replaced with other accessible points in the same HGU. Samples in land used as rice fields, homestead gardens, aquaculture ponds and/or dryfields, sample sites had to be chosen carefully to avoid misleading interpretation of findings because most of them have high levels of disturbance. The information on disturbance level was then classified to provide information of the sample site condition in each HGU to support the soil sample analysis result and synthesis.

Based on visual satellite imageries (Landsat ETM$^+$, QuickBird®) interpretation, topographic maps and general field survey, the disturbance levels were classified into 4 levels (Table 6.4). The first category is ‘none’ or ‘pristine’, which is defined as an area without or with minimum human intervention or anthropogenic activity. Examples of pristine areas included pristine mangrove, swamp, and recently formed landform units e.g. mid-channel bars and lateral bars. The second disturbance category is ‘low’, where the topsoil has not been disturbed intensively, including areas subject to land clearing or grass clearing that is showing little or no sign of disturbance of the topsoil, for no more than 10 cm depth. The third category is ‘medium’ where disturbance occurs from 10 to 50 cm deep in the soil profile, and the boundary between disturbed and undisturbed layers were obvious, because of the seasonal uses of the upper layer for waste/garbage dumping, domestic ponds, and/or agriculture purposes. The fourth category is ‘high’ where the soil profile has been disturbed deeper than 50 cm and the boundary between soil horizons was hardly visible, because of continuing uses for rice field or ponds. The units where the disturbance level was classified as high (category 4), needed to be removed or replaced by other sample point in order to obtain the most representative soil profiles sample of HGU.

Table 6.4 The categories for disturbance and accessibility levels

	Disturbance Level	
No.	Category	Description
1.	None/Pristine	No sign of soil used
2.	Low	Slight used of soil surface
3.	Medium	Intensive used on the 0-50 cm depth of soil surface
4.	High	Soil layer of >50cm depth has been used intensively

Source: Field survey, 2009, 2010; Remote Sensing Data Analysis

6.6.4 Soil Sampling Sites of Each Estuary

This section describes the numbers and distribution of sampling sites in each estuary. In the Rambut Estuary, which consists of 11 HGUs, only 15 samples were taken from the sample plan of 30. The level of disturbance of soil profile in rice fields and settlement areas was very high and the topsoil had been mixed up with deeper soil layers meaning the boundaries between layers were not clear. Similarly with the 12 HGUs of the Jajar Estuary, only 15 out of 30 planned sample sites were surveyed. The Jajar Estuary also had many rice fields and ponds in mangroves, and dryland areas with highly disturbed soil profiles to a depth going below 50 cm because of ploughing or excavation. For similar reasons, in GcR-Southwest, only 13 and 22 sample sites were surveyed in the Serayu and Bengawan estuaries, respectively. The final locations of the sample sites for the four estuaries are presented in Figure 6.5, with detail geographical coordinates provided in Appendix 6.3.

The comparison between the HGUs identified before and after field survey validation showed the difference in numbers and boundaries. There were more HGUs identified based on soil analysis, which could not be identified from the four stages of HGU determination. This new identified HGU occurred because the soil analysis results showed different characteristics within some HGUs (explained in detail in Chapter 7). Consequently, some HGUs have new boundaries that divided them into two or three new HGUs. This comparison shows the importance of field and laboratory analysis in the HGU determination process. The following sections explain the characteristics of the identified HGUs before field survey of each estuary, including the prediction of the

ASS presence and absence based on field soil analysis taken from several samples in each HGU (pH_F, pH_{FOX}, Redox). The final HGU classification after validation is provided in Chapter 7, completed by laboratory analysis result.

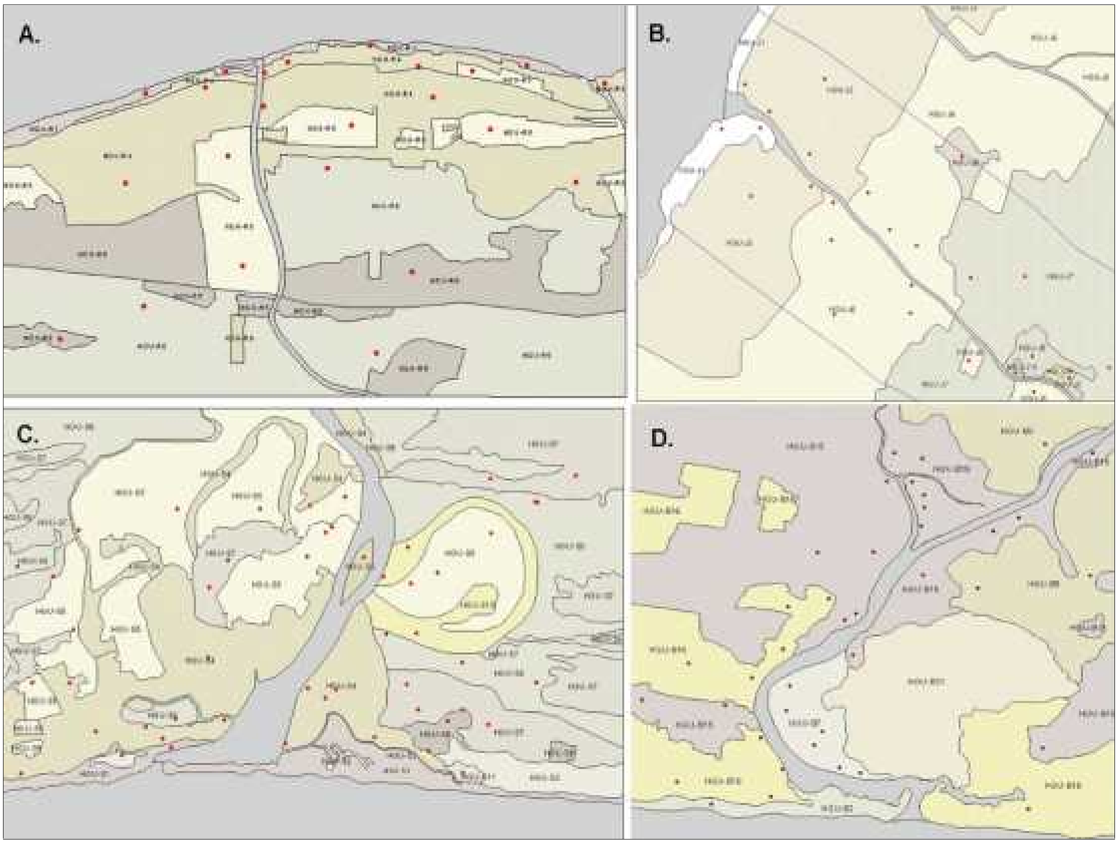

Figure 6.4 Sampling sites (represented by the red dots) for the HGUs in (A). Rambut Estuary; (B). Jajar Estuary; (C). Serayu Estuary and (D). Bengawan Estuary.

6.7 Description of the HGUs for each Estuary

6.7.1 HGUs of the Rambut Estuary

In the Rambut Estuary (GcR-Northwest), 11 HGUs were identified from 3 estuary zones (See Chapter and were denoted as HGU-R(n) (Table 6.5). The Estuary Zone 1: seashore (EZ-R1) was mostly unused land and consisted of two types of detailed geomorphic units i.e.: sandy shore face and foredune (HGU-R1 and HGU-R2). The HGUs in the EZ-R1 had similar water table depth and distance from the sea but their distance from the river varied widely. However, because these units were dominated by wave action and less river energy, the distance from the river was not considered a significant factor of landform development in this zone. These two types of HGU in EZ-R1 were not predicted to have pyrite due to the high-energy environment (see Section

2.2.1). The validation of this prediction is described in Chapter 7. The detail information of these HGUs is provided in Table 6.5.

Table 6.5. The HGUs in the Rambut Estuary based upon estuary zone, land-use and vegetation type. The attribute mapping codes representing the HGU types in an estuary zone are shown.

HGU	EZ	Land-form	Land-use	Vegetation	The probability of ASS presence	Attribute code
HGU-R1	EZ-R1	Sandy Shore Face	Unused land	NBWV	None	1011
HGU-R2		Foredune	Dryfield	NBWV	None	1012
HGU-R3	EZ-R2	Levees	Unused	Mangrove	Low-medium	1023
HGU-R4		Intertidal Flat	Ponds (Abandoned/ semi-active)	NBWV/None	None	1024
HGU-R5			Dryfield	NBWV	None	1025
HGU-R6	EZ-R3	Flood Plain	Rice field	NBWV	None	1036
HGU-R7			Dryfield	NBWV	None	1037
HGU-R8			Settlement	NBWV	None	1038
HGU-R9			Built-up area	NBWV	None	1039
HGU-R10			Swamp	NBWV/None	None	10310
HGu-R11		Levees	Unused	NBWV	None	10311

*Source: RS&GIS Analysis, Field Survey 2008-2010, * = Soil Field Analysis, 2009*

The Estuary Zone 2: tidal shore (EZ-R2) was mostly occupied by abandoned ponds, some of which had been converted back into rice fields. Some units on the eastern side of the estuary, especially the areas near the entrance, included some semi-active ponds, which is only active during dry season due to the availability of brackish water (in the river) through seawater intrusion (Fieldwork and personal communication with local farmer, 2010). Other land-uses in this unit were unused land and dryfield. Dryfields were commonly planted with cash crops such as corn, sugar cane, peanuts, sweet potato, cassava, etc., and vegetables, such as: chilli, eggplant and cabbage. This tidal shore environment also consisted of mangrove. Some of them colonized in the landward side of the estuary entrance, while others were individually scattered on the pond dykes. For this study, only the mangroves and *Nypa fruticans* that existed as clumps in the estuary entrance were classified as brackishwater vegetation types. The final land-units in Estuary Zone 2 were named HGU-R3, HGU-R4 and HGU-R5 (Table 6.5) and were predicted to have very low to no detectable pyrite concentration.

The river deposition zone (Estuary Zone 3: EZ-R3) was mostly influenced by low river energy. It is located about 0.8-1.6 km from the seashore, and has more built-up areas compared to the tidal shore. The built-up areas included the settlements, which were located mostly near main roads and infrastructure or a business centre. The unused lands were commonly present on levees which were adjacent to rice fields upstream, and mangroves downstream. Several freshwater swamps formed because of the annual floods were also found in this estuary zone. Other vegetation was mostly different type of fruit trees and shade trees which were categorized as non-brackish water vegetation. The ground water depths were around 1-2.5 meters, observed on the existing wells with various distances from the river (Table 6.6). This estuary zone comprised six HGUs, named as HGU-R6 to HGU-R11, which were also predicted to have very low to none of pyrite concentration.

Table 6.6. The hydrological attributes of the Rambut Estuary.

No.	HGU	No. of units	Ground water depth (m)	Distance from		Level of Energy		
				Main river (km)	Sea (km)	River	Tide	Wave
1.	HGU-R1	2	0-0.5	0	0.5	L	M	M
2.	HGU-R2	3	0.5	0.02-0.8	0.6	L-M	L-M	L
3.	HGU-R3	4	2.5	0.1-0.6	0.07-0.4	L	L-M	N
4.	HGU-R4	3	1	0.4-0.9	0.5	L	L	N
5.	HGU-R5	1	1	1.3	0.3	L	L	L
6.	HGU-R6	2	1	0.4	0.4	L	L	N
7.	HGU-R7	3	2.5	0.7-1.3	0.8-1.6	N	N	N
8.	HGU-R8	7	1-2.5	0.5-1.2	0.7-1.6	L	L	N
9.	HGU-R9	1	1	0.25	0.5	L	L	N
10.	HGU-R10	1	1.2	0.5	0.15	L	L	N
11.	HGU-R11	1	0.5	0.2	0.8	L	L	N

Low (L), medium (M), high (H), none (N) *Source: RS&GIS Analysis, Field Survey 2008-2010*

6.7.2 HGUs of the Jajar Estuary

In the Jajar Estuary (GcR-Northeast), 11 HGUs were identified and were denoted as HGU-J(n) (Table 6.7). In the Estuary Zone 1 (EZ-J1), the sandy shore face with unused land (HGU-J1) was relatively narrow (less than 2 meters) as humans have developed aquaculture ponds up to the edge of the coast line or at least to the foredune. Therefore, this landform was mostly occupied with semi-active ponds (HGU-J2), which were only actively productive during rainy season when the river salinity is suitable (15-25 ppt) for cultivate shrimp or milkfish (Personal communications with local farmer, 2010).

Even though the ponds were mostly semi-active, this land-use has been expanding following the prograding shoreline because of the high annual sedimentation (see Chapter 5, Table 5.7). The mangrove expansion also follows this changing shoreline gradually. The evidence that mangroves felled for pond development was very obvious, as their roots remained in the ponds and its wood was used to strengthen the dykes. Except in the estuary entrance, most of the remaining mangroves were growing on riverbanks along the river, reaching to the Estuary Zone 2: the tidal shore. They were established relatively recently, shown by their size of trunk and leaves.

The land-use types in Estuary Zone 2 (EZ-J2) consisted of active ponds in intertidal flats (HGU-J3), and unused land and dryfield on levees (HGU-J4 and HGU-J5). Most intertidal flats in this zone have undergone low (10-30 cm depth) to severe (50 cm – 1 m depth) flooding during rainy seasons, due to overbank flow (Personal communication with local resident, 2010). This flooding occurs when high tides entering the estuary coincide with high river flow from the upper catchment, despite relatively high levees along the river (up to 2 m). The unused land on levees was associated with the mangrove fringe along the river side (HGU-J4). This mangrove was a continuation of the mangrove fringe identified in Estuary Zone 1.

Active milkfish ponds (HGU-J6) and rice fields (HGU-J7) were identified in the floodplain zone (Estuary Zone 3: EZ-J3). However, the rice fields located close to the intertidal flat were abandoned during the dry season due to seawater intrusion. This intrusion caused the river water (as a source of irrigation water) to have a very high salinity level (more than 30 ppt) (Personal communication to local farmer and field measurement, 2010). Some of the floodplain located further inland were occupied more by settlements (HGU-J8) compared to other floodplain nearby the intertidal flats (HGU-J7). This area also has lowered the risk of flooding and better soil stability (Chapter 5, section 5.4.2). The depth of the groundwater, distance from sea and river, and the energy levels for each HGU in this Estuary Zone are shown in Table 6.8.

Table 6.7. HGUs identified for The Jajar Estuary based upon the estuary zone, land-use and vegetation type. The attribute codes representing the HGU types in an estuary zone are for mapping attribute purpose.

HGU	EZ	Landform	Land-use	Vegetation	The probability of ASS presence	Attribute code
HGU-J1	EZ-J1	Sandy Shore Face	Unused land	NBWV	None	2011
HGU-J2			Ponds – semi active	NBWV	None	2012
HGU-J3	EZ-J2	Intertidal Flat	Ponds – active	NBWV	Low-high	2023
HGU-J4		Levees	Unused land	Mangrove	Medium to high	2024
HGU-J5			Dryland	NBWV	Low to none	2025
HGU-J6	EZ-J3	Flood Plain	Ponds - active	NBWV	Low to medium	2036
HGU-J7			Rice field	NBWV	None	2037
HGU-J8			Settlement	NBWV	None	2038
HGU-J9			Dryland	NBWV	None	2039
HGU-J10			Unused Land	NBWV	None	20310
HGU-J11			Abandoned Ponds	NBWV	None	20311

*Source: RS&GIS Analysis, Field Survey 2008-2010, * = Soil Field Analysis, 2009*

Table 6.8. Hydrological attributes of the HGUs in the Jajar Estuary

No.	HGU	No. of units	Depth to ground water depth (m)	Distance from		Energy level		
				Main river (km)	Sea (km)	River	Tide	Wave
1.	HGU-J1	1	0.5	0	0	high (h)	medium	medium
2.	HGU-J2	6	1.2	0-3.4	0.6-5	l-h	medium	none
3.	HGU-J3	3	0.5	0.4-2	1.2-2.3	low	medium	none
4.	HGU-J4	1	2	0.2	5	high (h)	medium	none
5.	HGU-J5	2	1	0.8	0.2-0.3	medium	medium	none
6.	HGU-J6	3	1-2.5	0-1.6	4	medium	medium	none
7.	HGU-J7	1	1	0.4-0.7	3-5	medium	medium	none
8.	HGU-J8	1	1.5	0.4	3	medium	medium	none
9.	HGU-J9	1	2.5	0.3	5	medium	low	none
10.	HGU-J10	1	1	0.25	4.8	medium	low	none
11.	HGU-J11	2	1	0.2	5	medium	low	none

Low (L), medium (M), none (N)

6.7.3 HGUs of the Serayu Estuary

The Serayu Estuary has 11 identified HGUs, denoted as HGU-S(n) (Table 6.9). The land-use types in the Estuary Zone 1 (EZ-S1) had less variation than ones in the two previously described estuaries in the northern coast. In this EZ-S1, sandy shore faces, including sand barriers, were commonly classified as unused land (HGU-S1). The other land-uses were power generator and sand mining located on a former lagoon and foredune. However, these land-uses were excluded from this study for two reasons. Firstly, these areas were not open to the public so there was no access to examine the land-unit boundaries and to conduct soil sampling. Secondly, the available QuickBird® satellite imagery was recorded before these areas were developed, thus land-use maps derived from this imagery did not include this area. This area exclusion will avoid confusion in the final map.

Table 6.9 The HGUs in the Serayu estuary based upon the Estuary Zone land-use and vegetation types. The attribute mapping codes representing the HGU types in an estuary zone are shown.

HGU	EZ	Land-form	Land-use	Vegetation	The probability of ASS presence	Attribute code
HGU-S1	EZ-S1	Sandy shore face	Unused land	NBWV	None	3011
HGU-S2	EZ-S2	Ephemeral channel	Water body	NBWV	None	3022
HGU-S3		Intertidal flat	Dryfield /Rice field mixed	NBWV	Low to none	3023
HGU-S4	EZ-S3	Flood plain	Rice field	NBWV	Low to none	3034
HGU-S5			Settlement	NBWV	None	3035
HGU-S6		Beach ridge	Settlement	NBWV	None	3036
HGU-S7		Backswamp/swale	Rice field	*Nypa fruticans*	Low to high	3037
HGU-S8			Settlement	NBWV	Low to high	3038
HGU-S9		Mid-channel bar	Dryfield	NBWV	None	3039
HGU-S10		Abandon channel	Rice field	NBWV	Low to medium	30310
HGU-S11			Swamp	*Nypa fruticans*	Low to medium	30311

*Source: RS&GIS Analysis, Field Survey 2008-2010, * = Soil Field Analysis, 2009*

Other land-uses found in the Serayu Estuary were dryfields, rice fields and settlements. Dryfields (HGU-S2) in Estuary Zone 2 (EZ-S2) were mostly located within 10-20 meters from the coast line, whereas rice fields (HGU-S3,S5,S7) were situated further inland where freshwater irrigation was available. Since the local community uses the river as a resource for irrigation, the boundary of land-use between dryfields and rice fields were subjected to the different river salinity zone during the dry and rainy season

(Field work, 2010). During the rainy season, when the river was dominated by fresh water (hence the requirement of fresh water were fulfilled), some of the intertidal flats with dryfield land-uses were temporarily converted to rice fields. During the dry season, the rice field's land-uses were returned back to dryfields. However, some rice field with brackish water (<4 %) occurred during dry season, but with a rice plant variety which can tolerate low salinity level (personal communication and field survey, 2010). This land-use shifting was important for the analysis of pyrite development in this area, because the ASS occurrences and impacts were influenced by water circulation, especially due to agriculture and aquaculture activities (Hanhart and van Ni, 1993; White *et al*., 1995).

Rural settlement (HGU-S6) was the main land-use in Estuary Zone 3 (EZ-S3), the river deposition zone, which mostly occupied beach ridges and the flood plain. The unique hydrology and soil conditions (high stability), and slightly higher topography of beach ridges, made this unit favourable for rural settlement (Verstappen, 2000), extending back to pre-historic times (Schurman, 1930; Wastl, 1939 in Verstappen 2000). The swales, which were situated between the beach ridges, were predominantly used for rice fields (HGU-S7). However, on some swales, scattered clusters of *Nypa fruticans* surrounded by swampy grass areas were found. These *Nypa fruticans* clusters were initial land-cover of this swale environment before being cultivated for rice field (Personal communication to local resident, 2009, 2010). These clusters have not been used for rice fields as the farmer could not easily access these swampy areas due to its depth of more than 2 m. The *Nypa fruticans* were also observed in the oxbow lake (abandoned channel) of Serayu River (HGU-S11). These both HGU with *Nypa fruticans* have probability of ASS presence.

Other landforms such as mid-channel bars and lateral bars, which were relatively new and unstable were categorised as unused land (HGU-S9 and S10 respectively). The majority of mid-channel bars were inundated during the rainy season. However, in the dry season, when the river discharge was low, some relatively stable mid-channel bars were utilized for dryfields with corn and vegetables crops. Thus, the probability of ASS presence was predicted to be low here. The hydrological attributes of all HGUs described above in the Serayu Estuary are provided in Table 6.10.

Table 6.10. Hydrological attributes of the HGUs in the Serayu Estuary

No.	HGU	No. of units	Depth to ground water depth (m)	Distance from		Energy Level		
				Main river (km)	Sea (km)	River	Tide	Wave
1.	HGU-S1	2	0.3	0.5-3.5	0-0.7	m-h	medium	high
2.	HGU-S2	1	0.3	1.3	0	low	high	high
3.	HGU-S3	2	0.2	0.3	0.5	high	high	low
4.	HGU-S4	1	0.5	0.8	0.4	high	high	medium
5.	HGU-S5	1	1	0.3	2	high	medium	none
6.	HGU-S6	8	1.5	1.5-4	2-3.5	high	low	none
7.	HGU-S7	6	1.5	0.1-2.7	0.5-1.5	m-h	m-h	low
8.	HGU-S8	1	0.5	1.5	1.5	medium	low	none
9.	HGU-S9	1	0.5	2.2	0.4	medium	medium	low
10.	HGU-S10	1	1	2.5	0.8	medium	medium	low
11.	HGU-S11	9	1.2	2-2.5	0.7-4	l-h	l-m	none

high (h), low (l), medium (m), none (n)

6.7.4 HGUs of the Bengawan Estuary

The Bengawan Estuary, the wave-dominated estuary with a pre-existing barrier, has 22 identified HGUs, denoted as HGU-B(n) (Table 6.11). The common land-use and vegetation types found in this estuary were similar to those in the Serayu Estuary. In the Estuary Zone 1 (EZ-B1: the seashore), there was more than 500 m length of sand barrier connected to sandy shore face with unused-land (HGU-B1). A recreation (tourism) area occupied the eastern part of the sandy shore face, near the outlet of underground river from the calcareous hill (Selok Hill). In the tidal shore environment (Estuary Zone 2: EZ-B2), dryfields and unused land dominated the intertidal flat, mudflats and washover (HGU-B2 to HGU-B7). Some HGUs on mudflats closer to the river have vegetation cover of mangroves and *Nypa fruticans* (Figure 6.6). Other *Nypa fruticans* existed along the main river, from 5 to 10 km upstream (see Chapter 5, Section 5.4.3). These HGUs based on soil field analysis showed different probability level of the presence of ASS.

Further inland, floodplains with rice fields and settlements dominated Estuary Zone 3 (HGU-B8 to HGU-B11). As mentioned in Chapter 5 (Section 5.4.3), relatively dense *Nypa fruticans* fringes (3-5 meter wide) were found on the junction of the Bengawan River and its tributary river (Figure 5.13). In this area, the river energy slows down because of the pre-existing barrier (Selok Hill), and its brackish water provides an ideal environment for the expansion of *Nypa fruticans*. This species also occupied other landforms located in this environment, such as levees, lateral bars, backswamps and abandoned channels (HGU-B11 to HGU-B13, HGU-B19 and HGU-B20). These HGUs was predicted to have high probability of ASS presence because the existing *Nypa fruticans* indicated the consistent availability of sulfate (through brackishwater) and a low-energy environment (see Chapter 2, Section 2.1). The six HGUs with *Nypa fruticans* have various landforms and land-use (Table 6.11). From these diverse hydro-geomorphic characteristics, different processes and pyrite contents of each HGU were possible to observe. These HGU environments also have a very low disturbance level, thus they have the most soil sampling sites compared to the rest.

Table 6.11 HGUs in the Bengawan Estuary based upon the estuary zone, land-use and vegetation types. The attribute mapping codes representing the HGU types in an estuary zone are shown.

HGU	EZ	Land-form	Land-use	Vegetation	The probability of ASS presence	Attribute code
HGU-B1	EZ-B1	Sandy Shore Face	Unused land/Beach	NBWV	None	4011
HGU-B2	EZ-B2	Intertidal Flat	Dryfield/Beach	NBWV	None	4022
HGU-B3		Ephemeral Channel	Water	NBWV	None	4023
HGU-B4		Washover – West	Unused Land	NBWV	Low to none	4024
HGU-B5		Washover – East	Unused Land	NBWV	Low to none	4025
HGU-B6		Salt Flat/Mud Flat	Dryfield	NBWV	Medium to high	4026
HGU-B7		Salt Flat/Mud Flat	Unused Land	NBWV	Medium to high	4027
HGU-B8	EZ-B3	Flood plain	Ponds – abandoned	NBWV	Low to medium	4038
HGU-B9		Flood plain	Rice field	NBWV	Low to medium	4039
HGU-B10		Flood plain	Settlement	NBWV	Low to none	40310
HGU-B11		Flood plain	Unused Land	*Nypa fruticans*	Medium to high	40311
HGU-B12		Levees	Ponds	*Nypa fruticans*	Medium to high	40312
HGU-B13		Levees	Unused Land	*Nypa fruticans*	Medium to high	40313
HGU-B14		Levees	Unused Land	NBWV	Low to none	40314
HGU-B15		Beach ridge	Settlement	NBWV	None	40315
HGU-B16		Backswamp/swale	Rice field	NBWV	Low to medium	40316
HGU-B17		Mid-channel bar	Unused Land	NBWV	None	40317
HGU-B18		Lateral bar	Unused Land	Mangrove	Medium to high	40318
HGU-B19		Lateral bar	Ponds – semi active	*Nypa fruticans*	Medium to high	40319
HGU-B20		Abandon Channel	Unused Land	*Nypa fruticans*	High to very high	40320
HGU-B21		Hill	Unused Land	NBWV	None	40321

NBWV: Non-brackish water vegetation *Source: RS&GIS Analysis, Field Survey 2008-2010, * = Soil Field Analysis, 2009*

The remaining HGUs were unused-land on levees and mid-channel bars (HGU-B14 and HGU-B17), settlements mainly on beach ridges (HGU-B15), and rice fields on backswamps and swales (HGU-B16) (See Table 6.11). The rice field in the backswamp and swales but might have lower probability of ASS present compared to the ones in *Nypa fruticans* environment, because of its highly intensive use. The last unit in the Bengawan Estuary comprised of unused land on the pre-existing barrier (HGU-B21). This hill influenced the estuarine processes because it determined different energy level of Bengawan river (see Chapter 5, Section 5.5). Most areas were unused-land with very small-scale buildings on its southern part. The western part of the hills used for spiritual visits or pilgrimage. This landscape and its denudation processes through weathering and high rainfall intensity were also important in contributing sediment to the surrounding area. The probability of ASS presence was predicted very low to none in this HGU. Detailed hydrological attributes of all HGUs that influence the presence of ASS in the Bengawan Estuary are described in Table 6.12.

Table 6.12 . Hydrological attributes of the hydro-geomorphic units (HGU) in The Bengawan Estuary

No.	HGU	No. of units	Depth to ground water depth (m)	Distance from		Energy Level		
				Main river (km)	Sea (km)	River	Tide	Wave
1.	HGU-B1	3	0.5-1	0.1-0.4	0.2	low	high	high
2.	HGU-B2	2	0.5-1	0-1	0-2	low	high	high
3.	HGU-B3	3	0.5	0-1	0.3-0.6	medium	medium	none
4.	HGU-B4	3	3	0.06-0.4	2.2-3	m-h	low	none
5.	HGU-B5	1	3	0.2	2.3	medium	low	none
6.	HGU-B6	4	3	0.5-1.6	2.3-2.7	l-m	low	none
7.	HGU-B7	6	1.5-2	0.4-2.60	0.4-3.3	l-m	l-m	none
8.	HGU-B8	2	2	0-0.15	0.5-1	m-h	l-m	none
9.	HGU-B9	1	4	0.8	3.3	medium	low	none
10.	HGU-B10	2	2-2.5	0.1	0.2	medium	high	Low
11.	HGU-B11	1	2.5	0.05	3.3	high	low	none
12.	HGU-B12	2	1-2	0.1-0.3	0.8-2.6	medium	l-m	none
13.	HGU-B13	2	1-2	0.2-0.6	1-3	medium	low	none
14.	HGU-B14	2	2-2.5	0.5	1-2	medium	low	none
15.	HGU-B15	1	1	1.1	1.75	low	low	none
16.	HGU-B16	1	2.5	0.7	3.4	medium	low	none
17.	HGU-B17	1	1	0.4	1.1	high	low	none
18.	HGU-B18	1	1	0	0.3	high	medium	medium
19.	HGU-B19	1	N/A	N/A	N/A	N/A	N/A	N/A
20.	HGU-B20	3	0.5-1.5	0.2-1.2	0.6-0.35	high	medium	none
21.	HGU-B21	1	0.5	0.3	0.7	high	medium	Low

Low (L), medium (M), none (N)

Sources: RS/GIS Analysis and Field Survey 2008-2010

6.8 Summary

The multi-stage approach to determine the HGUs was systematic and provided more detailed information on the factors that influence ASS formation. This approach is important because units established in every stage influence the accuracy of ASS occurrence assessment. Different characteristics in each HGU determined a dominant type of land-use that was present in a HGU, but not vice versa. The used of multi-resolution satellite imageries through visual interpretation also provided more accurate information of landforms and land-uses because the synoptic view of study area was available.

The landform and salinity data based on estuary zonation, land uses, vegetation, and hydrology related data presented in each HGU, facilitate the assessment of pyrite concentration level in an environment. The establishment of estuary zonation was able to assist the identification of the on-going ASS development processes of each HGU and the prediction of the ASS presence probability. These HGUs became the effective reference for soil sampling to validate those predictions. In summary, the HGUs determination provided an effective way to summarise hydrologic and geomorphic processes in an estuary, especially to identify HGUs where ASS are likely to occur. The verification of initial prediction of the presence of ASS in HGU draft map from soil field and laboratory analysis is provided in detail in Chapter 7.

3

RESULT AND DISCUSSION

CHAPTER SEVEN

THE SPATIO-TEMPORAL DISTRIBUTION AND PROPERTIES OF ACID SULFATE SOILS IN CENTRAL JAVA

7.1 Introduction

This chapter presents the results of field and laboratory analyses for soil samples collected from four estuaries representing the dominant estuary types of Central Java: Rambut (river–dominated estuary), Jajar (tide-dominated estuary), Serayu (wave-dominated estuary and Bengawan (wave-dominated estuary with pre-existing barrier). Soil properties are analysed to determine presence or absence of ASS in each HGU and to validate the HGU boundaries. A representative soil profile from each HGU is selected and described in this chapter.

Soil properties are described with particular reference to the horizontal and vertical distribution of ASS and the presence or absence of ASS was determined from these data. This information will facilitate the understanding of the relationship between HGU and ASS presence or absence presented in Chapter 8, and to support the assessment of land suitability for aquaculture and coastal planning.

7.2 Distribution and Properties of ASS in each Type of Estuary

7.2.1 Soil Properties of each HGU in A River-dominated Estuary

There were 11 HGUs identified across Rambut Estuary (denoted as HGU-Rs) which represented river-dominated estuaries. Soil sampling was possible for 8 HGUs with a total of 28 sampling sites. The selected soil profiles then were grouped into Group A and B. The complete soil profiles and soil results of the HGUs in Group A (no ASS detected) are included in Appendix E; whereas the ones in Group B (containing ASS) are given below. The summary map of HGUs in Rambut estuary confirmed by field survey is shown in Figure 7.1.

Figure 7.1 Map of the Hydrogeomorphic Units of Rambut Estuary (HGU-Rs)

Ten out of eleven HGUs in Rambut estuary did not have any pyrite detected in their soil profiles (Group A). In this estuary, there were ten samples collected from soil profiles with the depth 10 cm increments from 50 -100 cm from the ground surface. The map of the HGU and soil profile graphs (Figure 7.1 and Appendix E.2) show different colours and textures in different estuary zones. The HGU Group A were located in all estuary zones including soil textures from sandy material in a narrow strip along the beach, gradually changing to sandy loam, loam and then from sandy clay to silty clay further inland (Table 7.1). The pH_F values of the soil profile layers were around 6.89-7.28, or from neutral to mildly alkaline (Appendix E.2). Lower values of pH_{FOX} occurred in the coastal and intertidal areas (6.89 to 7.08), whereas the HGUs in the floodplain generally had pH_{FOX} values above 7.00.

Table 7.1. Summary of soil colours and textures based on estuary zones and common landforms

Type of HGU	Estuary Zone	HGU (type of landforms)	Dominant soil colour	Dominant Soil texture
Group A	foreshore, intertidal flat	HGU-R1, R2 (sandy shore, foredune) HGU-R4, R5 (intertidal flat)	GLEY1 5/10Y (greenish grey) 5Y 5/2 (olive grey)	sand, sandy loam, loam silty clay
	supratidal, floodplain	HGU-R6, R7 (floodplain) HGU-R11 (levee)	2.5Y 4/2 (dark greyish brown) 2.5Y 5/3 (light olive brown)	clay loam silty clay
Group B	supratidal	HGU-R3 (L levee with mangrove)	0-50 cm depth: 5Y 3/1 (very dark grey) to 5Y 3/2 (dark olive grey); below 50 cm depth: GLEY1 3/10Y - 5/10Y (dark to very dark greenish grey)	sandy loam silty clay loam
Complete results for profiles from Rambut Estuary are provided in Appendix E.2				

The only HGU which showed the presence of ASS was HGU-R3, which consisted of mangrove fringes along the estuary entrances about 0 -1 m from the edge of the river and 0 - 500 m upstream of the estuary entrance, and in several ephemeral channels (Figure 7.1, Grid B-2). Most of these mangroves established recently and were distributed in a regular pattern along the river (Figure 7.2). This very regular pattern indicated human intervention in mangrove cultivation, supported by an interview with the local residents whom stated that there was a local government program that facilitated the mangrove forest rehabilitation between 2000 and 2005. The soil colour and textures of HGU-R3 were mostly sandy loam in the top 35 cm followed by silty clay loam (Figure 7.3, Graph a). The sandy soil textures with GLEY1 colour in this HGU were found in the mangrove areas that were closer to the shore, but not exposed to the sea.

Other indications of ASS presence in HGU-R3 soil profiles were high TPA and pyrite values (Appendix E.3). The difference between pH before and after oxidation (pH_F – pH_{Fox}) is on average 2-3 with pH_{Fox} about 3 to 4, which is considered very strongly acidic (Table 7.2). The vertical distribution of pyrite concentration and pH_F – pH_{Fox} is fairly consistent with profile depth (Figure 7.3, Graph b). Hydrogen peroxide reactions were moderate to strong but were poorly related to pH values and the TPA ranged from 76 to 126 mol H^+/ton, at an average soil profile depth of 90 cm (Appendix E.3). The maximum pyrite values are located between 70 and 90 cm from the ground surface and are associated with the lowest average pH_{Fox} soil layer.

Table 7.2. Summary of average soil chemical properties of HGU where ASS was present

Depth of soil profile (cm)	pH_F	pH_{FOX}	Redox (mV)	Conductivity (mS)	SPOS (%)	Pyrite (%)
0-50	6.73	4.75	-93.60	75.11	5.42	0.58
Below 50	6.65	4.38	-120.33	77.32	5.72	0.59
Standard deviation (SD)	0.08	0.15	29.77	2.89	3.68	0.06
Complete result for profiles from Rambut Estuary are provided in Appendix E.2						

Figure 7.2 Mangrove fringe along the river of Rambut estuary.

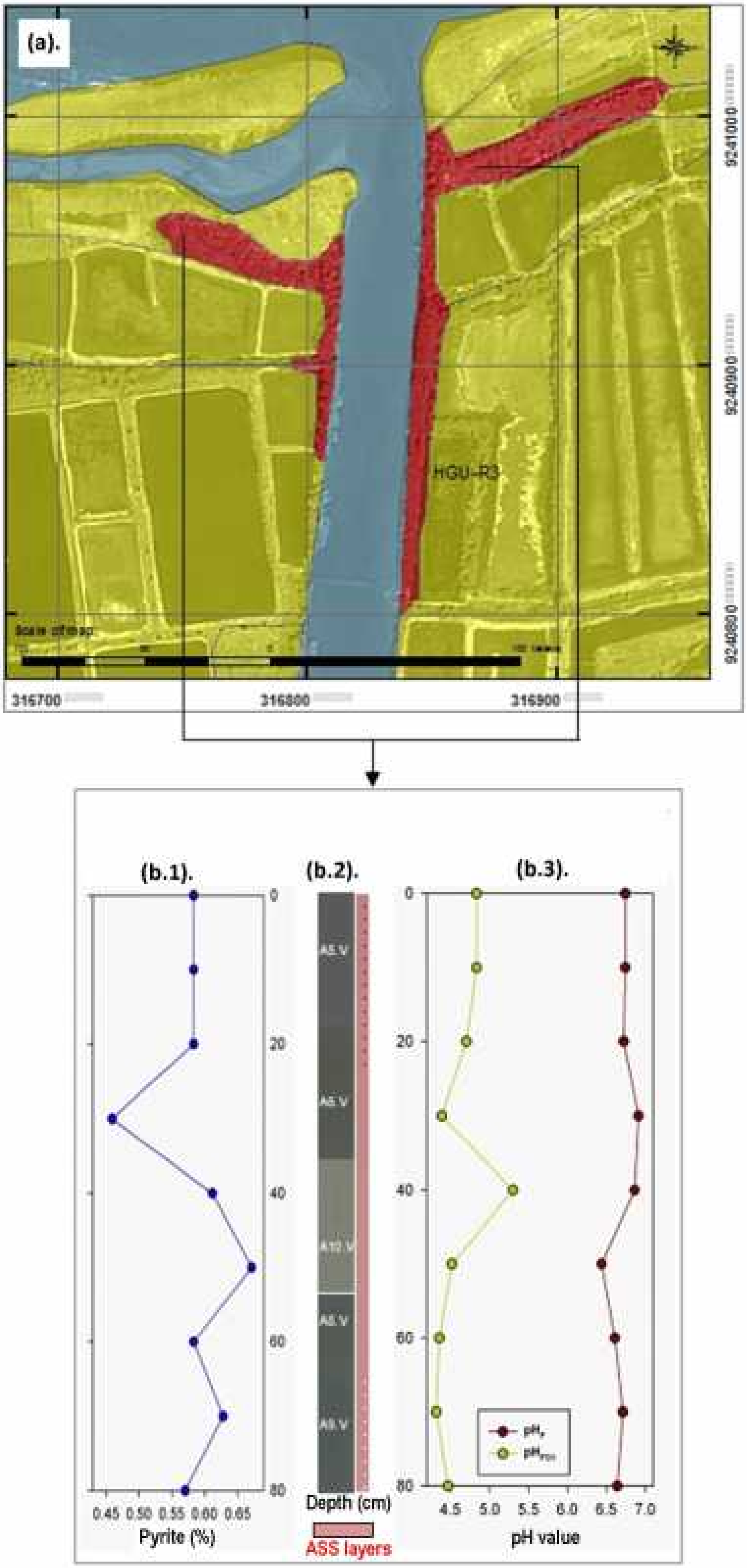

Figure 7.3 (a) Map of Rambut Estuary showing mangrove fringes (shaded red) where ASS were present. Graphs show vertical distribution of pyrite (b1), and pH before (pH_F) and after (pH_{FOX}) hydrogen peroxide treatment (b3) in average. Soil profile (b2) showing soil colours and textures with depth, the red shade indicates presence of ASS.

7.2.2 Soil Properties of HGUs in a Tide-dominated Estuary

The tide-dominated estuary in GcR-Northeast is represented by the Jajar Estuary which has 11 HGUs (denoted as HGU-Js) with 23 soil sample sites. The study area extended about 5 km upstream from the estuary entrance (measured along the river), and 3 km from each side of the river banks (Chapter 6). The water table depths in this estuary were about 1-2.5 m. The complete soil profiles and analytical results are provided in Appendix F. The summary map of HGUs (Figure 7.4) in Jajar estuary was validated by field survey.

Similar to Rambut Estuary, there were marked soil colour differences with depth in the soil profiles (Appendix F.2, Group A) in the HGUs where ASS was not detected. The soil colour and texture varied from dark greyish brown to olive grey with loamy sand, sandy loam and silty clay on the top 20 cm (Table 7.3). Most of these layers overlaid the dark to very dark greenish grey soil colours at depths of 20 to 110 cm. The majority of soil textures at these depths were silty clay, with minor silty clay loam. For HGU-J9 to J10 (Figure 7.4, Grid E4&5), where the land-use types were dryland and unused land, clay sediments developed a very firm soil structure.

Table 7.3. Summary of soil colour and texture based on estuary zone and common landforms

Type of HGU	Estuary Zone	HGU Common landforms	Dominant soil colour	Dominant Soil texture
Group A	foreshore, intertidal flat lower part of floodplain	HGU-J1, J2, (sandy shoreface) HGU-J3 (intertidal flat) HGU-J5 (levee)	2.5Y 4/4 (olive brown) 2.5y 4/2 (dark greyish brown) 5Y 5/2 (olive grey)	loamy sand, sandy loam and silty clay
	middle part of floodplain	HGU-J7, J8, J11 (floodplain)	2.5Y 4/2 (dark greyish brown) to 5Y 5/2 (olive grey)	silt, silty clay loam and small amount of silty clay.
	middle part of floodplain	HGU-J9-J10 (floodplain)	2.5Y 3/2 (very dark greyish brown) 5Y 5/2 (olive grey)	clay, silty clay
Group B	supratidal	HGU-J4 (levee with new growth mangrove)	0-50 cm depth: 5Y 3/1 (very dark grey) to 5Y 3/2 (dark olive) grey); below 50 cm depth: GLEY1 3/10Y (dark greenish grey) to GLEY1 5/10Y (very dark greenish grey)	silty clay loam

Complete result s for profiles from Jajar Estuary are provided in Appendix F.2.

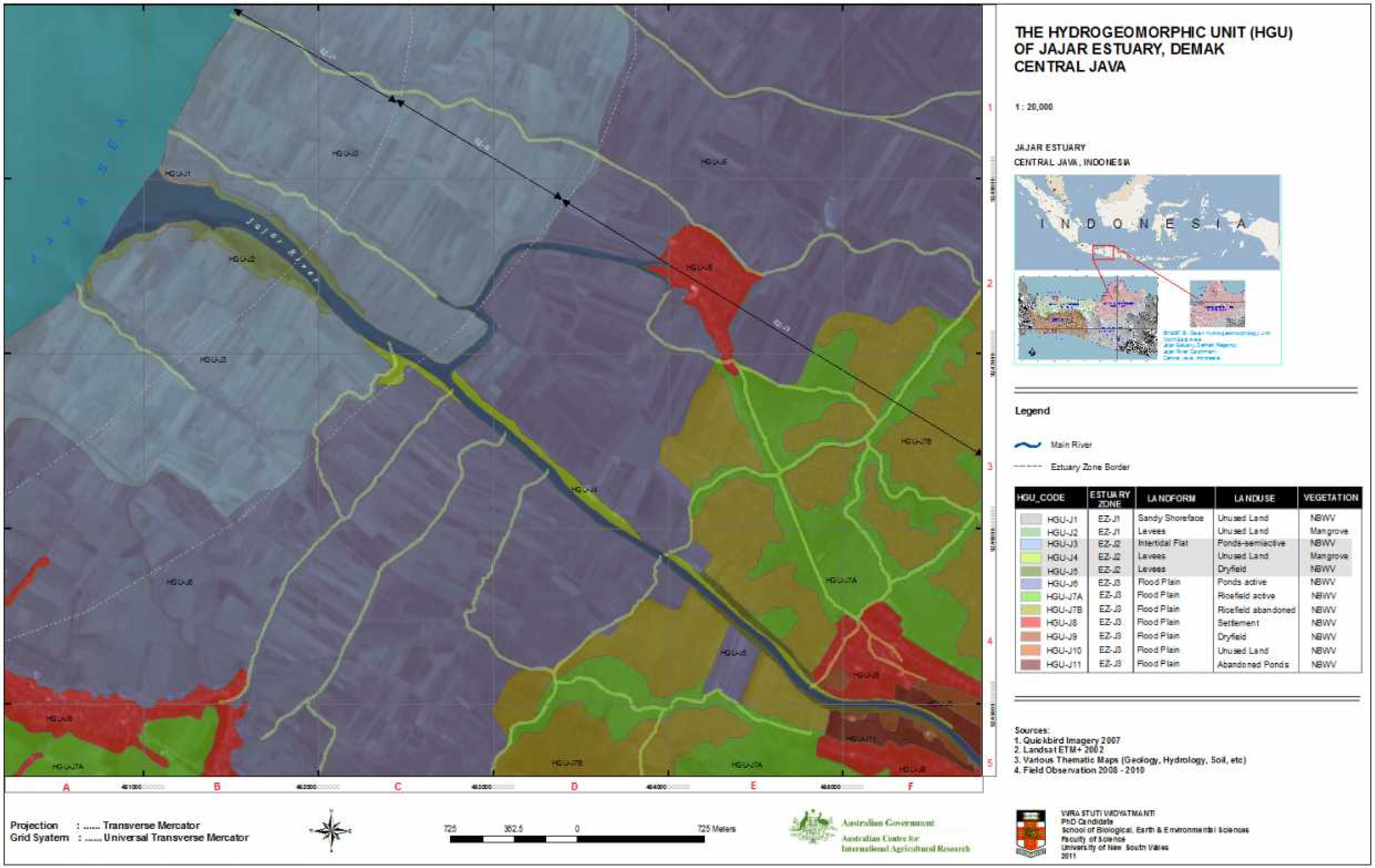

Figure 7.4. Map of the Hydrogeomorphic Unit (HGU) of Jajar Estuary

The pH_F values were mostly neutral in the HGUs where ASS layers were not detected (Appendix F.3). After treatment with hydrogen peroxide, no apparent acidity was produced, shown neutral to slightly alkaline pH_{Fox} values. Tides and floods coincide periodically, inundating some ricefields and ponds along the riverbank. This inundation was exacerbated by the existing black clayey textured soils and lack of continuous water circulation. In this riverbank, the pH_F values were neutral and slightly alkaline after hydrogen peroxide treatment (Appendix F.3). However, the hydrogen peroxide test showed a strong reaction, which was possibly triggered by the organic content in the soil, shown by high organic matter content in soil (above 3 %). The other possibility was that another oxidisable mineral reacted and/or shell material buffered the acidity. Further discussion on this hydrogen peroxide strong reaction is provided in Chapter 8.

One interesting feature found in Jajar Estuary is the presence of shell grit on the soil surface at the estuary entrance, and the presence of fully-shaped shells visible at 50 cm soil depth (Figure 7.5-A). The shells were indentified as *Terebralia sulcata, Turitella terebra* and *Anadara granosa* (Figure 7.6 - Yogyakarta Archeology Research Centre in Sunarto, 2004). These shells are commonly found in tidal flats or mangrove swamps or marine sediment (Wells, 1983; Sunarto, 2004). In the layer underneath this mixture of fully shaped shell and mud, orange brownish mottles were found in some soil bores and pits (Figure 7.5-B). In some areas further inland (3 - 5 km of the entrance), the fully-shaped shell material was found very deep in the soil profile, up to 250 cm below the surface (with the height of levees being on average 1 m), while according to local Public Work Agency secondary data (2009), the average depth of the river in this area is about 4 meter.

Only one HGU containing ASS, i.e. HGU-J4 was present in the Jajar Estuary. This HGU is situated on the levees with mangrove fringes (Figure 7.4, Grid C3 and D3). These mangrove fringes were found along the riverside up to about 2 km upstream of the estuary entrance, and were relatively young compared to the ones near the estuary entrance, shown by the shorter and smaller size of mangroves (Figure 7.7 A and B). The textures in the ASS of this mangrove environment ranged from silty to silty clay (Table 7.3, Figure 7.8.b). Very low pH_{FOX} was found at 50 cm to 100 cm soil depth, reaching the value of two, which is strongly acidic and suggests a mineral source of acid. The soil texture of these layers with lowest pH levels was silty clay. The strong hydrogen peroxide reactions and low pHF-pH_{FOX} (Figure 7.8, Graph b) indicate the presence of PASS. The laboratory results showed TPA value ranged from 20 - 146 mol H^+/ton with pyrite concentration between 0.10 – 0.80 % (Appendix F.3), which is considered low compared to other mangrove sediments (more than 2 % in pyrite concentration in Lin & Melville, 1994; Soekardjo, 2000). The factors influencing this low pyrite concentration in this low part of the levee are discussed in Chapter 8.

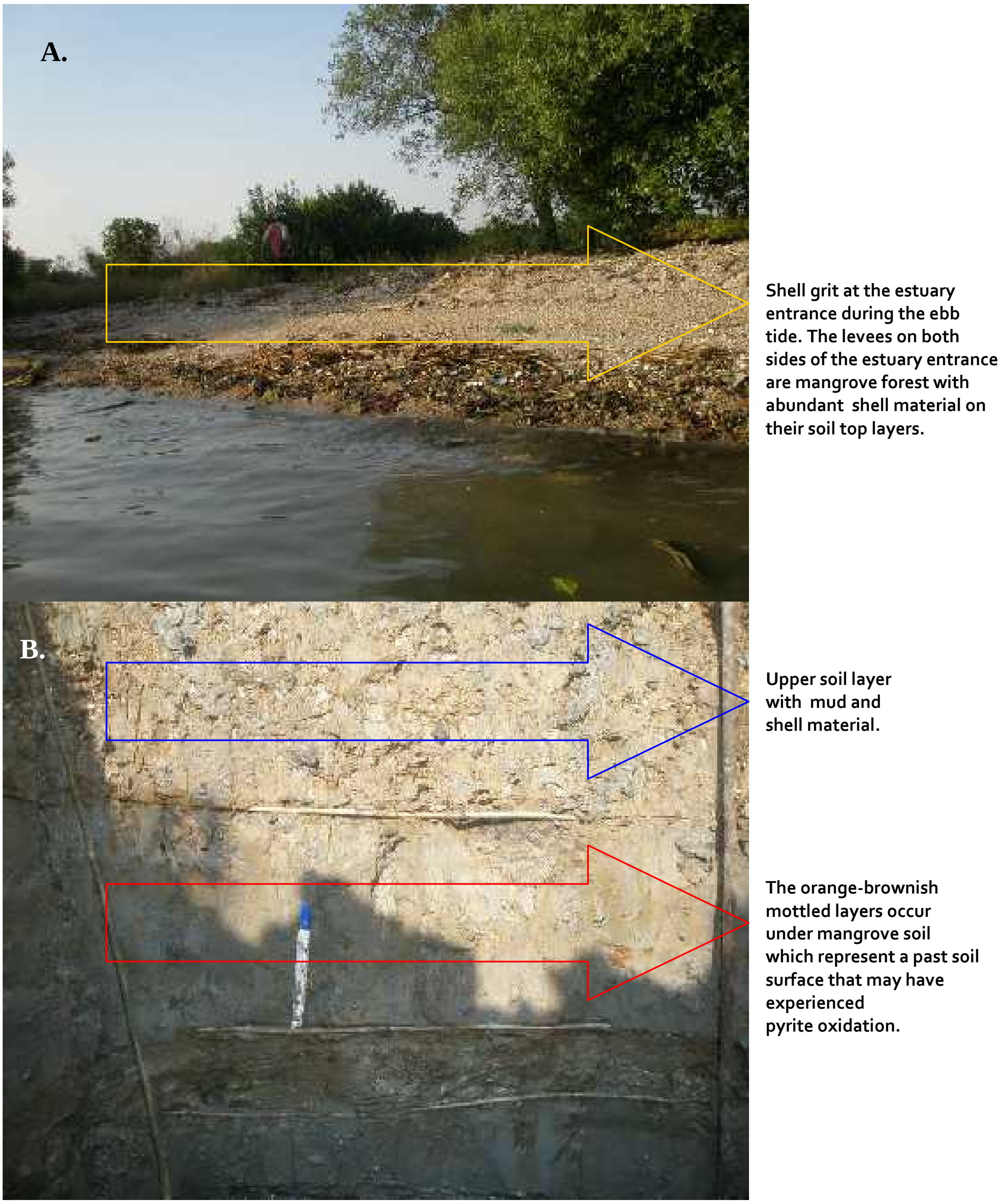

Figure 7.5 (A) Mangroves near the estuary entrance with shell grit on the surface. (B) Soil profiles showing the interbedded layers of shell material and grit, iron and organic material, brownish mud, and greyish colour mud. There is no ASS in these layers.

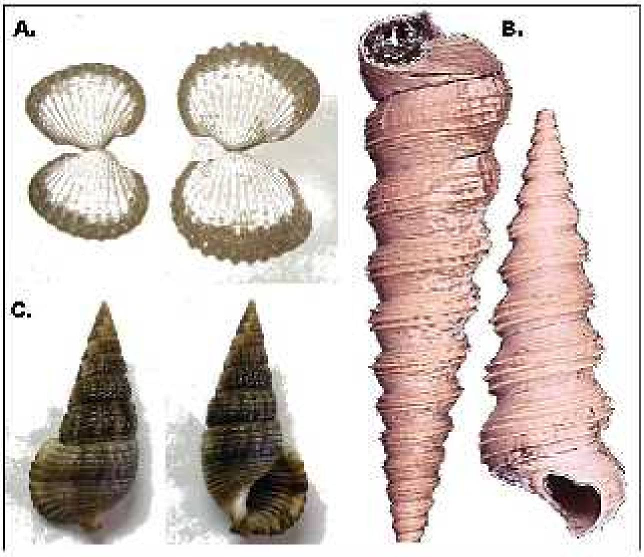

Figure 7.6. Type of shells found in Jajar estuary: (A) Andara granosa; (B) Turritella terebra; (C) Terabralia sulcata (Field survey, 2010; Shell Collection, 2010).

Figure 7.7 (A) The relatively recent mangrove development located about 2 km from the Jajar estuary entrance. (B) Low pyrite concentrations were identified in the soil of these mangrove and Nypa fruticans fringes (HGU-J4).

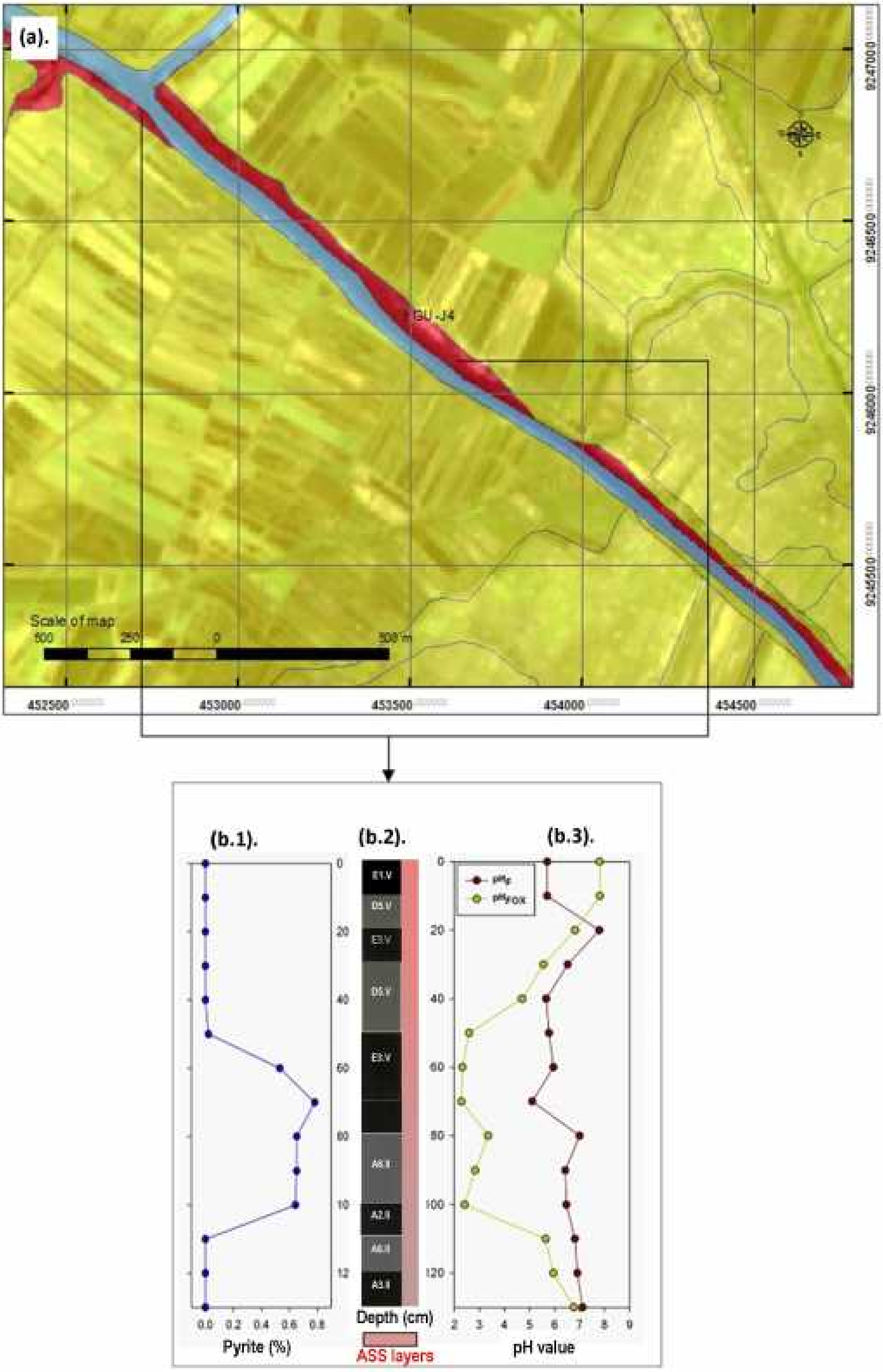

Figure 7.8 (a) Map of Jajar Estuary showing mangrove fringes (shaded red) where ASS were present (HGU-J4). Graphs show vertical distribution of pyrite (b1) and pH before (pH_F) and after (pH_{FOX}) hydrogen peroxide treatment (b3) in average. Soil profile b2 showing soil colours and texture with depth; the red shading indicates presence of ASS.

.

Table 7.4. Summary of average soil chemical properties of HGU where ASS was present

Depth of soil profile (cm)	pH_F	pH_{FOX}	Redox (mV)	Electrical Conductivity (mS)	SPOS (%)	Pyrite (%)
0-50	6.42	6.22	36.75	7.08	0.85	0.00
Below 50	6.47	3.94	10.50	11.44	2.44	0.41
Standard deviation (SD)	0.74	2.00	84.30	4.9	3.93	0.33

Complete results for profiles from Jajar Estuary are provided in Appendix F.3

The upper sediment layer containing shell were found in almost every HGU located within 10 meters of the riverbanks, reaching 1-2 km upstream of the estuary entrance. Similar conditions were also found on some of the upper layers of the levees that were 3-7 km inland. By contrast, in Tuntang Estuary (west side of Jajar), there were no shell fragments that could be found in the upper layer of levees and riverbanks after about 1 km inland from the estuary entrance (Figure 7.9). The only shell grit found approximately 20 m away from the levee was only in one spot and originally from the pond excavation. The heights of most levees in Jajar were also higher (more than one meter) compared to the ones in Tuntang. Thus, there was the possibility that the levee located 3-5 km upstream of the Jajar Estuary entrance was constructed. This was supported by the presence of a newly constructed levee containing shell grit (Figure 7.10).

Figure 7.9. The natural levees eroded by alluvial flow presented in (A) Tuntang River and (B) Jajar Estuary, showing no presence of shell grits.

Figure 7.10. The levee with shell grit content in Jajar Estuary, built as part of a dredging project (1996) to control annual flood (large to high magnitude). (B) The new levee constructed by excavator in year 2010.

An interviewed farmer confirmed that the river was dredged several years ago. Data provided by Central Java Public Work Agency (2004) also confirmed that some dredging projects had been conducted in Demak Regency, including in the Jajar River, since 1996 to control the annual flood. This project started together with the development of the Jajar inflatable dam which is located 7 km inland from the entrance (Figure 7.11). Consequently, during the sampling process, the riverbank and levees between 3-5 km inland, were firstly observed to determine whether they were natural or artificial (Figure 7.9 and 7.10). For instance, most natural levees inland did not contain or only had little shell content in the upper soil layer, as fluvial process developed them naturally. This natural levee was the appropriate area to be sampled. Conversely, when coarse seashell fragments were visible on the surface soil layer of a levee, it indicated that it was potentially constructed by people. Accordingly, this area was not suitable for sampling.

Further discussion on how dredging material influences the presence and absence of ASS in Jajar estuary is provided in Chapter 8.

Figure 7.11 Kali Jajar inflatable dam built to prevent sea water penetrating further inland during the dry season.

7.2.3 Distribution of ASS and Its Properties in Wave-dominated Estuary

The preliminary HGU determination (Chapter 6) indicated that there were 11 HGUs identified in a wave-dominated estuary, represented by Serayu Estuary (denoted as HGU-S). However, the soil analysis results showed that there were some distinct soil profiles present within each HGU. As a consequence, the HGUs (HGU-S4; HGU-S6, and HGU-S7) for this estuary were divided into more detailed sub-units, resulting in 6 new sub-HGU-Ss. Interestingly, there was another different characteristic in the soil profiles in A sub-HGU. As a result, this sub-HGU needed to be reclassified into two further detailed sub-units named co-sub-HGU-Ss (Table 7.5). The following descriptive sections are the summary of soil properties based upon the presence and absence of ASS. The detailed soil profiles and laboratory and field results are provided in Appendix G. The summary map of HGUs in Serayu Estuary, validated by field survey is shown in Figure 7.12.

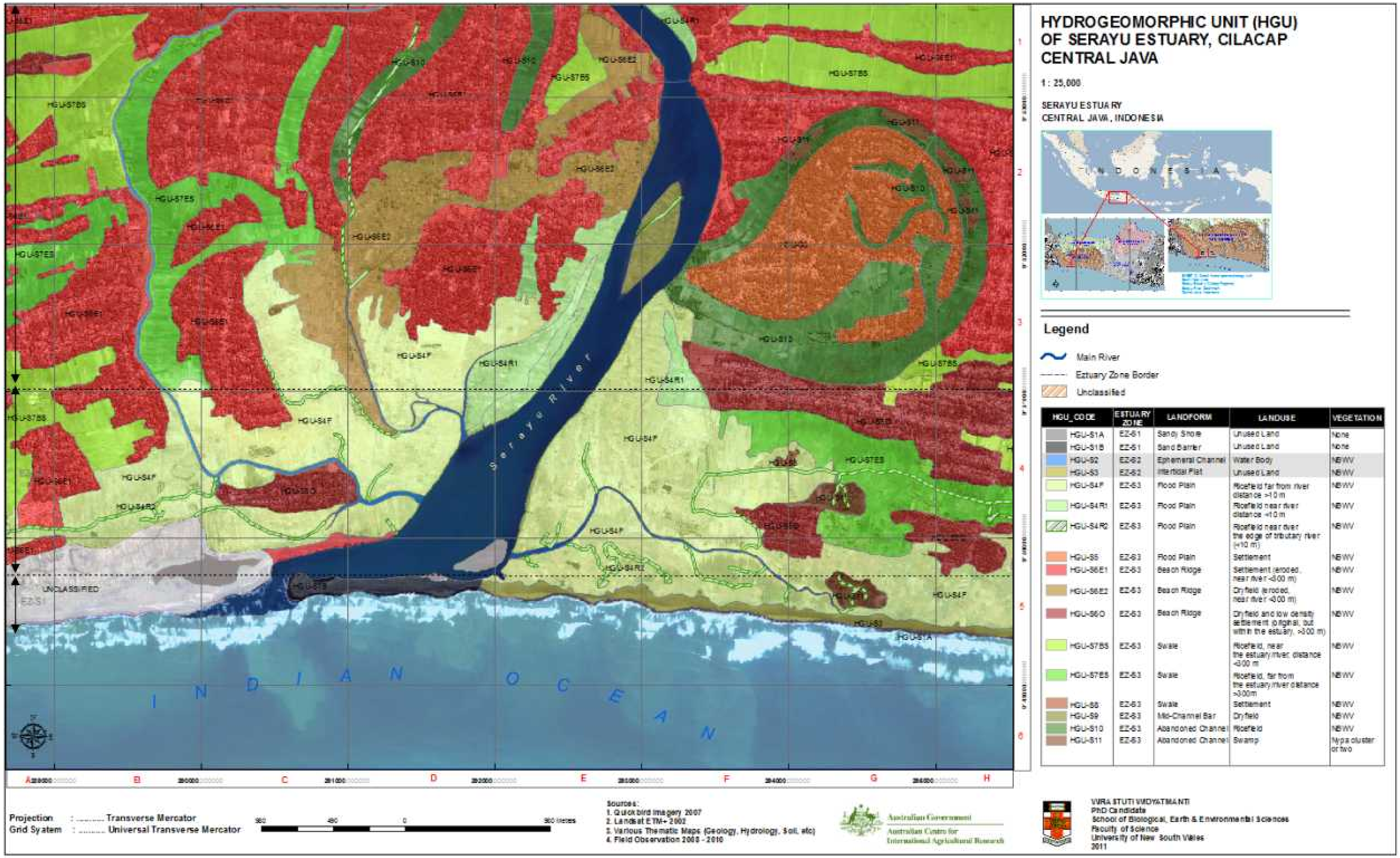

Figure 7.12 Map showing the Hydrogeomorphic Units (HGU) identified in Serayu Estuary

Table 7.5 List of HGU and sub-HGU based on the presence and absence of ASS in Serayu Estuary

GROUP A: HGUs with NO ASS			GROUP B: HGUs with ASS		
Main Unit	Sub-unit	Co- Sub-unit	Main Unit	Sub-unit	Co-Sub-unit
HGU-S1	-	-	HGU-S4	HGU-S4R	HGU-S4/R1
HGU-S3	-	-			HGU-S4/R2
HGU-S4	HGU-S4/F	-			
HGU-S5	-	-	HGU-S7	HGU-S7/ES	-
HGU-S6	HGU-S6/O	-		HGU-S7/BS	-
	HGU-S6/E	-			
HGU-S9	-	-	HGU-S8	-	-
HGU-S10	-	-	HGU-S11	-	-

7.2.3.1 The Soil Properties of HGU-Ss where are ASS Absent (Group A)

Thirty two samples sites represented eight HGU-Ss with no ASS (Group A). The soil profiles ranged from 40 to 200 cm in depth and were distributed evenly across the estuary (Appendix G.2). HGU-S6 and HGU-S4 showed diverse soil properties (Table 7.6 and Appendix G.4). The HGU-S6, beach-ridges with settlements, was divided into two more detailed units which are: sub-HGU-S6/O (no disturbance) and sub-HGU-S6/E (eroded). The sub-HGU-S6/O was situated in the upper part of beach ridge which did not have any disturbance from the Serayu River annual flood which affected the lower part (sub-HGU-S6/E).

The differences in elevation between these two beach ridge units were around 1-3 m. For HGU-S6/O, soil samples were situated higher than HGU-S6/E, and were taken from the beach ridge which had not experienced high disturbance except on its surface (settlement and its homestead garden). In contrast, in HGU-S6/E soil profiles, which were moderate to highly eroded beach-ridges due to the seasonal floods, the soil samples were mostly collected on the edge (lower part) of the beach ridge along the Serayu River (see Figure 7.10, Grid E2/D2, and Table 7.6). The samples taken on the upper part of beach ridge have different soil textures in each layer, but were dominated by sandy clay, whereas those in the lower part had loamy sand, sandy clay and silty clay in their profiles (Table 7.6 and Appendix G.2). This clayish soil texture on the highly eroded beach ridge was located in the lower part of the soil profiles, which commonly contained alluvial material, as a foundation for beach ridge development generated mostly by wave action (Houghton, 1985; Verstappen, 2000).

Table 7.6. Summary of soil colours and textures of soils in the HGU-Ss where ASS was absent (Group A).

Type of HGU	Estuary Zone	HGU Common landforms	Dominant soil colour	Dominant Soil texture
Group A	Seashore environment	HGU-S1 (sandy shore face/unused land)	5Y 2.5/2 (black)	sandy loam
	Tidal shore : Intertidal flat environment	HGU-S3 (intertidal flat/unused land)	5Y 4/3 (olive) to 5Y 4/1 (dark grey)	sandy clay to silty clay
		HGU-S9 (mid-channel bar/dryfield)	10YR 2/2 (very dark brown) to dark olive brown (2.5Y 3/3)	sandy clay to clay loam
		HGU-S10 (abandoned channel/ricefields)	5Y 2.5/2 (black) to 5Y 4/1 (dark grey)	sandy clay to silty clay
	River deposition: Fluvial environment	HGU-S4/F & HGU-S5 (floodplain/ricefields & settlement)	10YR 3/3 (very dark grey) to 2.5Y 5/4 (light olive brown)	silty clay loam to sandy clay loam
		HGU-S6/O & HGU-S6/E (Beachridge/settlement & unused land)	10YR 2/1 (black) to 2.5Y 3/3(dark olive brown)	sandy clay to loamy sand

Complete results for profiles from Serayu Estuary are provided in Appendix G.2.

The HGU-S/4, floodplain with ricefields, was differentiated into sub-HGU-S4/F and sub-HGU-S4/R, because in the field it was found that they were located in two different environments, and soil analysis also showed different characteristics (Figure 7.12, Grid B4, D4, D3 and F3). The HGU-S4/F locations were scattered from about 100 m to 3 km from the Serayu River, thus the influence of brackish water was not significant. On the other hand, based on soil analysis, the HGU-S4/R units, which were located closer to the river (<50 m) were classified as a HGU with ASS layers (Group B). Hence, the description for this unit will be provided in Section 7.2.3.2 (soil properties in HGU-Ss where ASS was present). These soil analyses also show that the different distance of HGU from brackish water resources provide different soil characteristics and development processes. How this distance factor affects ASS development will be discussed further in Chapter 8. Complete soil profiles and properties of HGUs of this group are provided in Appendices G.2 and G4.

7.2.3.2 The Soil Properties of the HGU-Ss where the ASS are Present (Group B)

The HGU-Ss soil profiles where ASS was present (Group B) in Serayu Estuary were mostly situated on the floodplain. They included the sub-units from HGU-S7 (S7/ES and S7/BS), the swale with ricefields; the sub-unit HGU-S4/R from the HGU-S4 (see Section 7.2.3.A), the floodplain with ricefields; and HGU-S8, the swale with settlement (Table 7.6). The soil profiles analysis for HGU-S7 showed the samples from the swale with ricefields that were near the Serayu River (< 100 m) had different soil characteristics compared to samples taken further from river farther (> 100 m) (Table 7.6). Therefore, this HGU was sub-divided into a more detailed HGU: sub-HGU-S7/ES and S7/BS, based upon distance from the Serayu River.

Another subdivision was also applied for sub-HGU-S4/R, the floodplain with ricefields, because it had two group of soil profiles with different soil properties (Table 7.6). This sub-HGU was divided into co-sub-HGU-S4/R1, situated within 100 m of the large tributary (>10 m width), and co-sub-HGU-S4/R2 situated near tributary (<10 m width) with *Nypa fruticans* forest. These more detailed sub-HGUs could represent different levels of supply of brackish water based on the size of the tributary, and how that supply influences the pyrite development (see Chapter 8, Section 8.3.1 for further explanation).

The soil colour and texture of HGU-Ss Group B ranged from, black (5Y 2.5/1), very dark greenish grey (5Y 3/1) and olive (5Y-5/3 to 5Y – 4/3) in floodplain landforms; and from olive brown (2.5Y 4/3) to yellowish brown (10R 5/4) in swales (Table 7.7). The soil texture ranged from sandy clay, sandy clay loam, loamy sand to silty clay (Appendix G.5). The vertical distribution of ASS properties in Group B, shows that the pH_F values were mostly neutral (Table 7.7). The pH_{FOX} decreased significantly, but did not reach the value of lower than 4 (Figure 7.13, 7.14, 7.15, Graph (b)). The pyrite and TPA/TPS values varied from surface to the deepest soil layers ranging from 1- 9% and 100 – 500 mol H^+/ton respectively (Table 7.7 and Appendix G.4).

The darker (dark grey to black) soil colours were related to *Nypa fruticans* and were found in the ricefields located near the smaller tributary (co-sub-HGU-S4/R2). These soil samples contained high pyrite concentration reaching 9%, with TPA value of 1120-4087 mol H^+/ton (Figure 7.13). The soil texture in this unit was mostly sandy clay loam.

Conversely, the lighter soil colours with silty clay textures (5- 40% estimated clay concentration) were mostly located in the ricefields both on floodplains and swales (see Appendix G.3). The pyrite concentration varied, but was lower on average (2%) compared to the ricefields near to the tributary (Figure 7.13). Slightly higher pyrite concentrations were found in swales with settlements (HGU-S8), reaching 2.5% (Figure 7.16).

Figure 7.13 HGU-S4/R2 showing a floodplain with a Nypa fruticans cluster along the tributary bank. The pyrite concentration is considerably high in this HGU, reaching 8-10 %.

Figure 7.14. HGU-S11 showing swamps and Nypa fruticans clusters in a Serayu oxbow lake. The occurrences of Nypa fruticans indicates an environment where ASS could potentially develop or is already present. No soil samples taken in this HGU but the ones the surrounding area showed the presence of ASS.

Table 7.7. Summary of soil colour and texture based on estuary zone and common landforms in HGU-Ss where ASS are present (Group B) in Serayu Estuary.

Type of HGU	Estuary Zone	HGU Common landforms	Dominant soil colour	Dominant soil texture
Group B	Fluvial Deposition (downstream) (EZ-2)	HGU-S4/R1 (floodplain/ricefields)	5Y-5/3 to 5Y – 4/3 (olive) 5Y 2.5/1 to 5Y 3/1 (black to very dark grey) (0-20 cm soil depth)	sandy clay to sandy clay loam
		HGU-S4/R2 (floodplain/ricefields)	GLEY1 2.5/N to GLEY1 3/10Y (black to very dark greenish grey) (>20 cm soil depth)	sandy clays silty clay and silty clay loam
	Fluvial Deposition (upstream) (EZ-3)	HGU-S7/ES (swale/ricefields/bare land)	2.5Y 4/3 (olive brown) to 2.5Y 5/3 (light olive brown)	loamy sand to silty clay
		HGU-S7/BS (swale/ricefields)	10YR 4/4 (dark yellowish brown) to 2.5y 5/4 (light olive brown)	silty clay to clay loam
		HGU-S8 (swale/settlement)	10YR 4/4 (dark yellowish brown) to 10R 5/4 (yellowish brown)	sandy clay
Complete results for profiles from Serayu Estuary are provided in Appendix G.3				

Table 7.8. Summary of average soil chemical properties of HGU-Ss with ASS present

The HGU	Depth of soil profile (cm)	pH_F	pH_{FOX}	Redox (mV)	Electrical Conductivity (mS)	SPOS (%)	Pyrite (%)
HGU-S4/R1	0-50 cm	4.83	4.35	-79	0.15	0.31	0.36
	Below 50 cm	6.36	4.15	-128	0.11	0.46	0.40
	SD	0.68	0.14	39	0.18	0.12	0.10
HGU-S4/R2	0-50 cm	5.96	4.05	-62	1.45	9.17	3.37
	Below 50 cm	7.70	3.35	-103	1.12	10.36	9.30
	SD	1.10	0.51	56	1.18	9.52	3.36
HGU-S7/ES	0-50 cm	6.74	5.60	280	0.45	0.29	0.20
	Below 50 cm	7.27	5.91	39	0.64	0.19	0.11
	SD	0.46	0.44	119	0.28	0.12	0.07
HGU-S7/BS	0-50 cm	5.61	4.70	203	0.54	0.24	0.01
	Below 50 cm	6.66	4.19	-75	0.58	0.37	0.04
	SD	0.51	0.64	233	0.35	0.14	0.01
HGU-S8	0-50 cm	5.80	2.90	-50	0.33	3.70	1.60
	Below 50 cm	7.83	4.00	-3	0.57	11.6	2.75
	SD	1.03	0.63	22.9	0.12	2.87	0.58

SD : Standard Deviation
Complete soil properties of HGUs in Serayu Estuary are provided in Appendix G.5

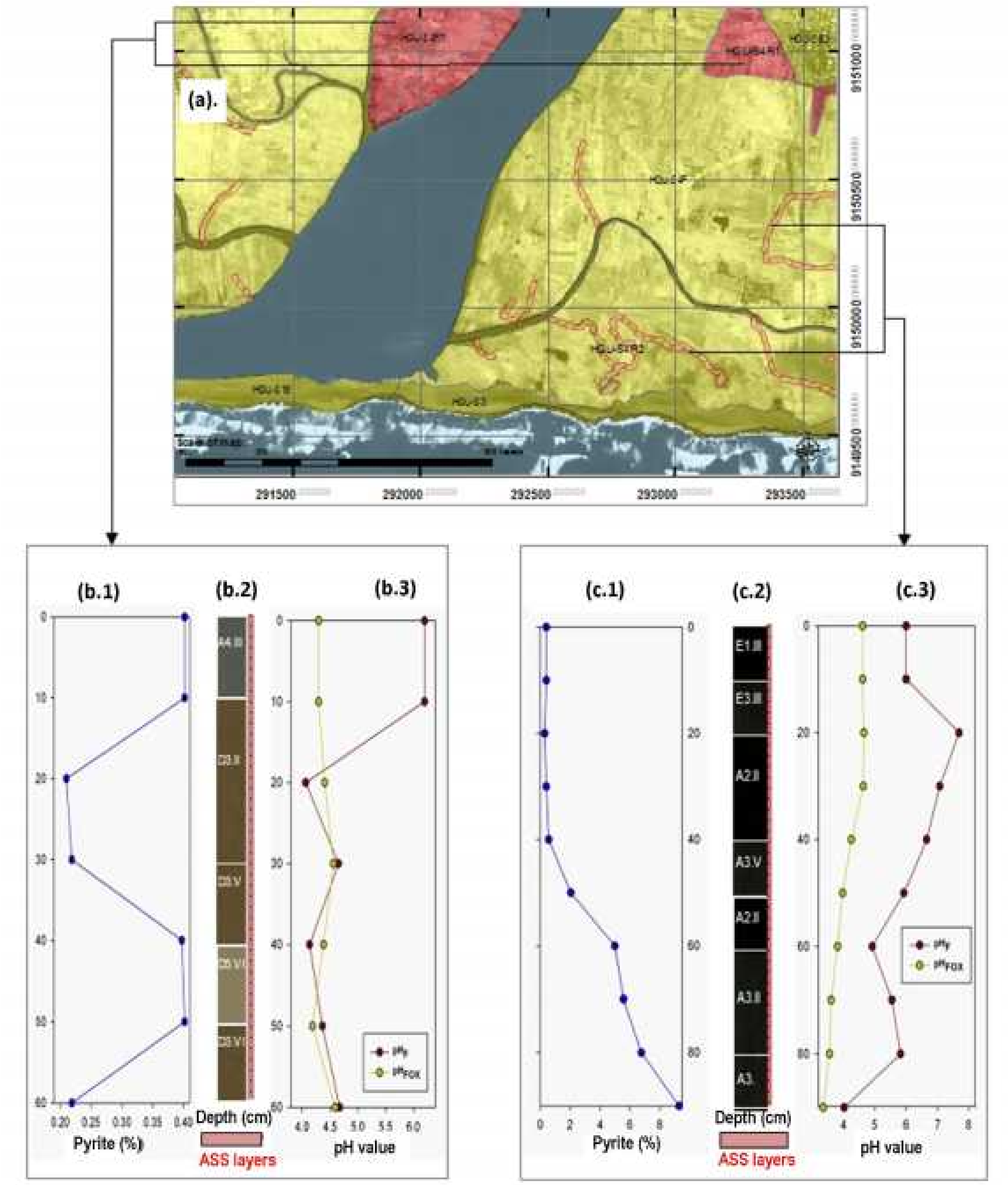

Figure 7.15. (a) Map of Serayu Estuary showing HGU-S4/R1 (shaded red) and HGU-S4/R2 (shaded red lines) where ASS were present. Graphs show vertical distribution of pyrite (b1, c1), and pH before (pHF) and after (pHFOX) hydrogen peroxide treatment (b3,c3) in average. The soil profiles (b2,c2) show soil colour and texture with depth, the red shading indicates the presence of ASS.

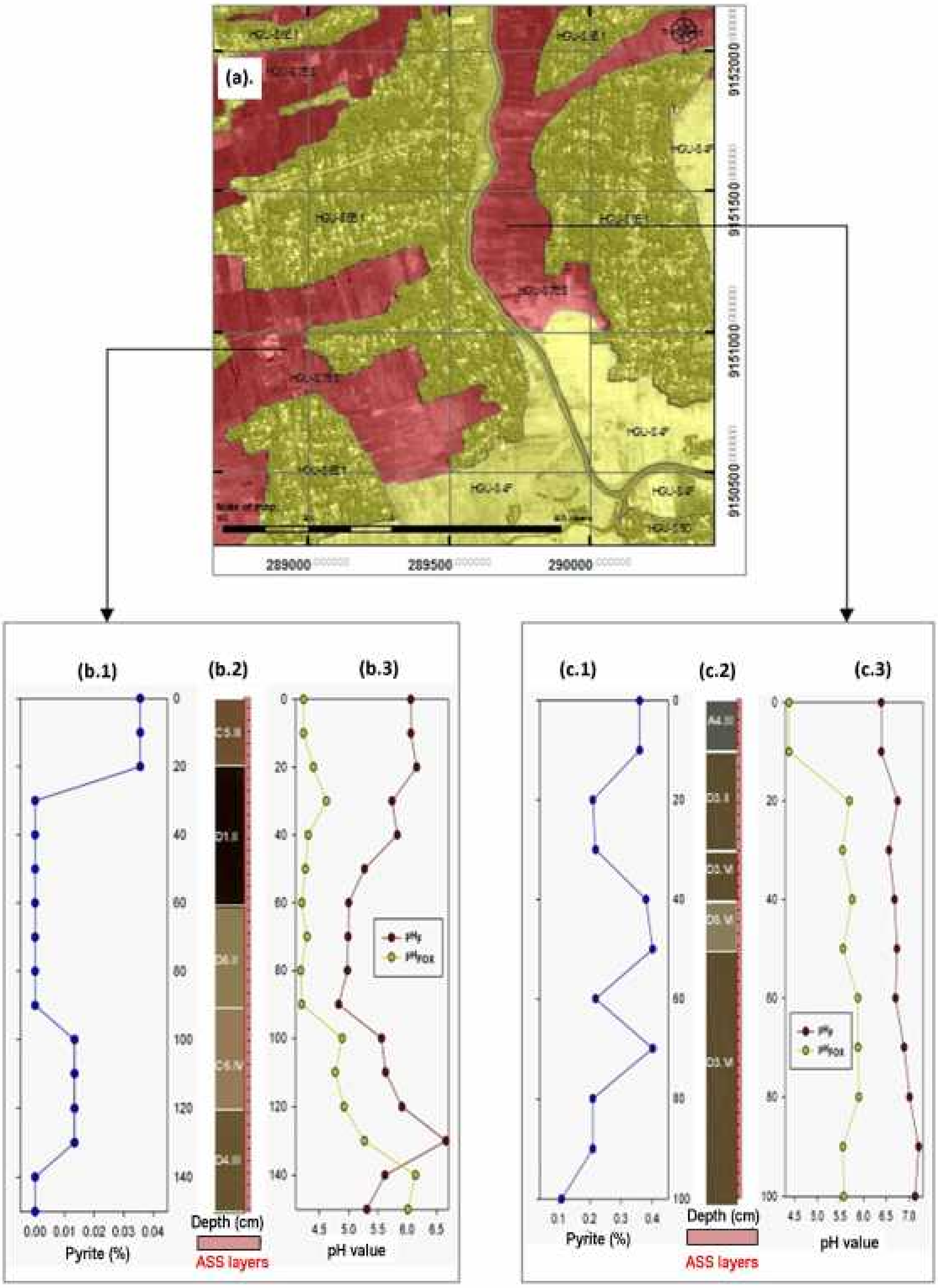

Figure 7.16 (a) Map of Serayu Estuary showing HGU-S7/BS and HGU-S7/ES (shaded red) where ASS was present. The graphs show vertical distribution of pyrite (b1, c1), and pH before (pHF) and after (pHFOX) hydrogen peroxide treatment (b3,c3) in average. The soil profiles (b2,c2) show soil colour and texture with depth; the red shading indicates the presence of ASS.

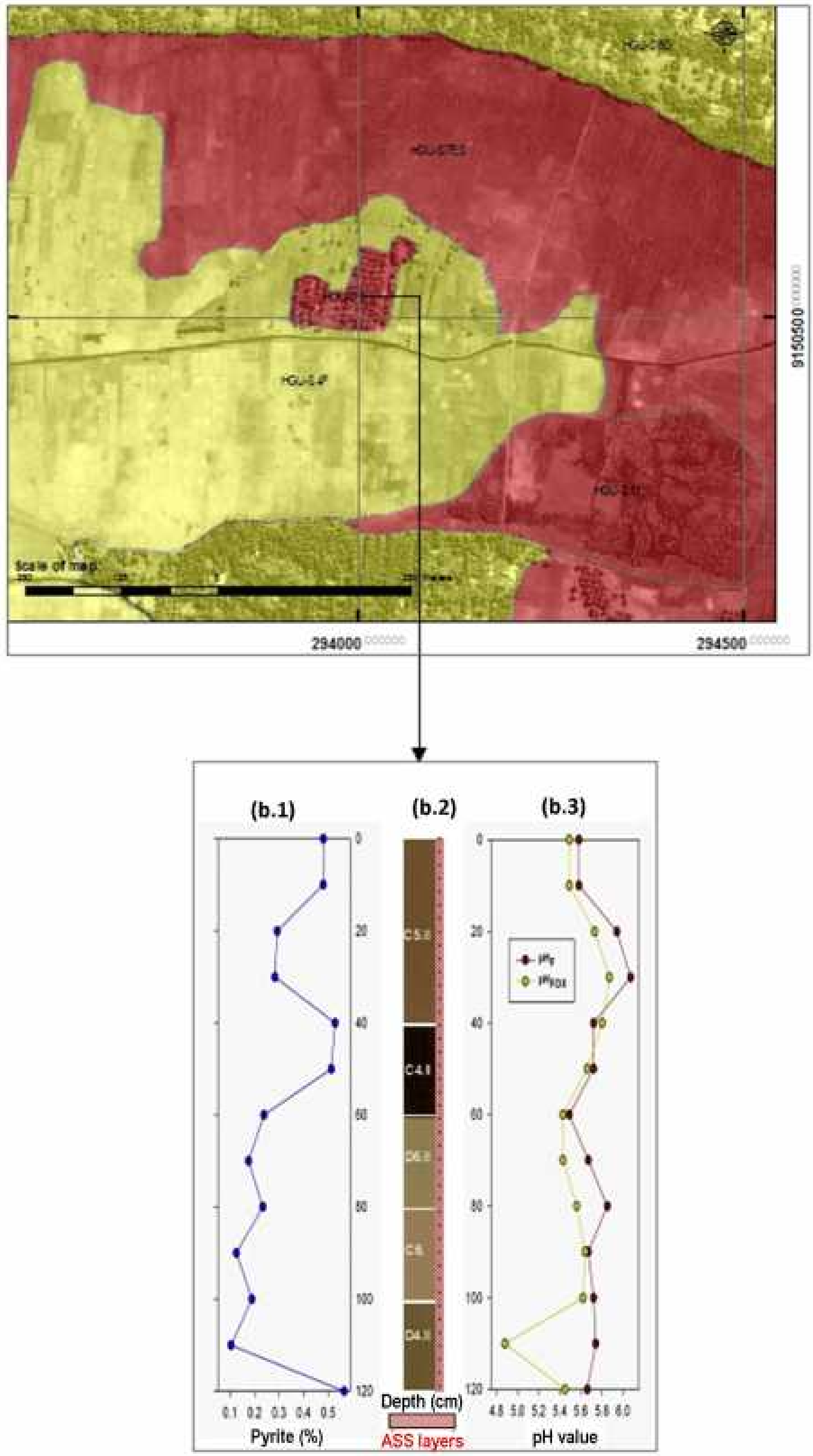

Figure 7.17 Map of Serayu Estuary showing HGU-S8 area (small shaded red) where ASS were present. Graphs show vertical distribution of pyrite (b1), and pH before (pH_F) and after (pH_{FOX}) hydrogen peroxide treatment (b3) in average. The soil profiles (b2) show soil colour and texture depth, with the red shading column indicates the presence of ASS.

7.2.4 The Complexity of ASS Properties in a Wave-dominated Estuary with Pre-existing Barrier

The wave-dominated estuary with pre-existing barrier, which is represented by Bengawan estuary, had more HGUs than Serayu Estuary despite its similar wave energy. Not all units had suitable sites for soil profile sample collection. This was usually due to high levels of disturbance after development of ricefields and settlements, and the presence of water bodies. The descriptions are divided into Group A (no ASS detected) and Group B (ASS detected) (Table 7.8). Complete results of soil profile analysis are provided in Appendix H. The summary map confirmed by field survey is presented in Figure 7.16

Table 7.9 Hydrogromorphic units for Bengawan Estuary where ASS is present (Group A) and absent (Group B)

GROUP A: HGUs with NO ASS		GROUP B: HGUs with ASS	
Main Unit	**Sub-unit**	**Main Unit**	**Sub-unit/CoSub-unit**
HGU-B1	-	**HGU-B4**	-
HGU-B2	-	**HGU-B6**	-
HGU-B5	-	**HGU-B7**	-
HGU-B9	HGU-B9/F	**HGU-B8**	-
HGU-B10	-	**HGU-B9**	HGU-B9/R
HGU-B14	-	**HGU-B11**	-
HGU-B15	-	**HGU-B12**	-
HGU-B17	-	**HGU-B13**	-
		HGU-B16	HGU-B16/ES HGU-B16/BS
		HGU-B18	-
		HGU-B19	-
		HGU-B20	-

7.2.4.1 The HGUs where ASS is Absent in the Bengawan Estuary (Group A)

There were eight HGU-Bs in Group A (Table 7.8). The soil colours in HGU-B1(sandy shore face/unused land), HGU-B2 (intertidal flat/dry-field), HGU-B5 (washover/unused land), B14(levee/unused land) and B17 (mid-channel bar/unused land) (Figure 7.14, Grid B4, C4, D4 and B3) were mostly black (5Y 2.5/1 or 2.5/2) (Table 7.9). These HGU-Bs sites adjoined the sea or the river and were dominated by sandy soil textures (Appendix H.5). In contrast, the HGU-B9/F (floodplain/ricefields), HGU-B10 (floodplain/ settlement) and HGU-B15 (beach ridge/settlement), have brownish to olive soil colours (10YR 2/2 to 2.5Y 5/3). Their soil textures ranged from sandy clay, silty clay to sandy loam (Table 7.9). Detailed soil profiles and properties are outlined in Appendix H.

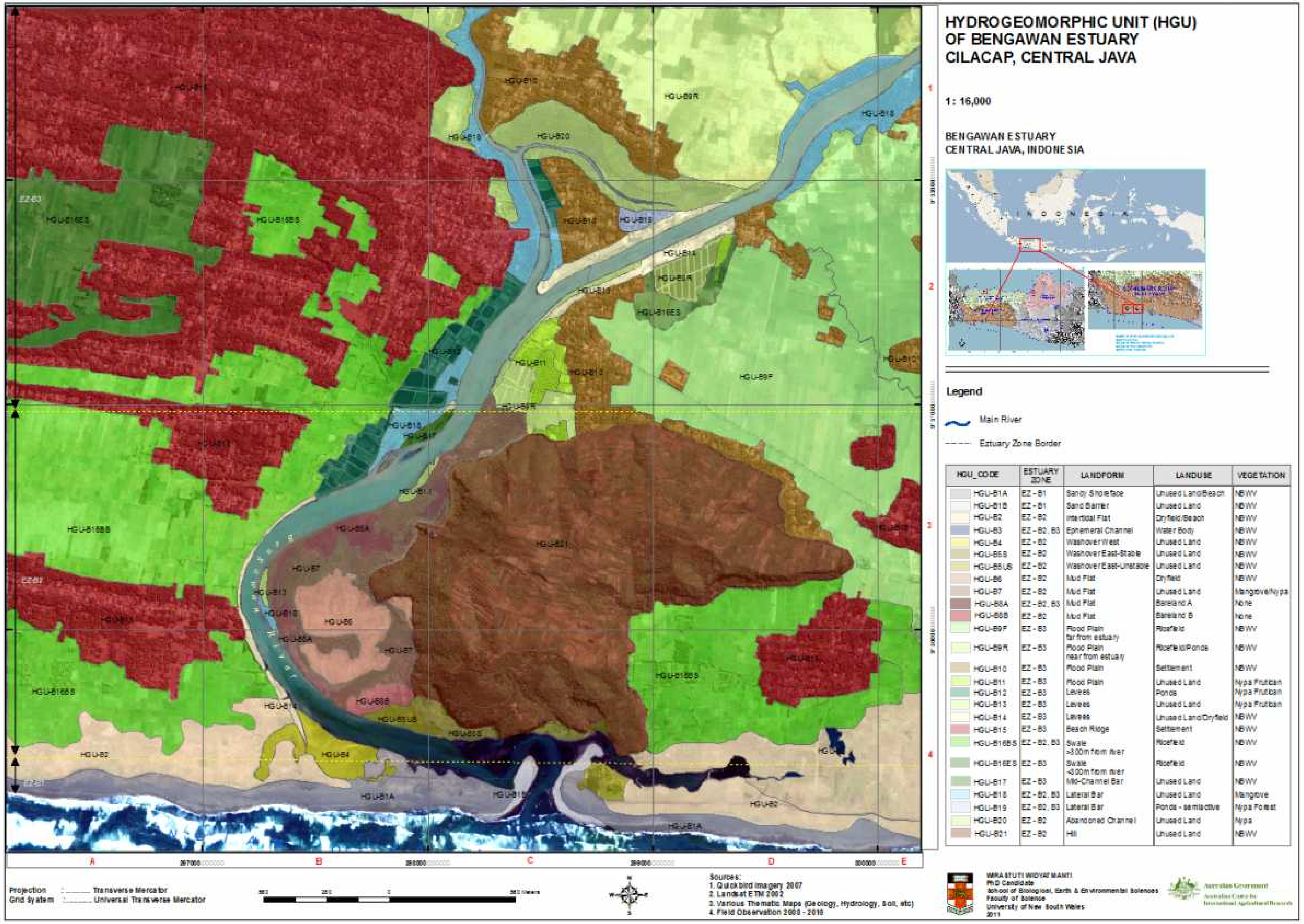

Figure 7.18 Map of the Hydrogeomorphic Units (HGU) of Bengawan Estuary

7.2.4.2 The HGU where ASS is Present in the Bengawan Estuary (Group B)

There were 13 HGU-Bs in Bengawan Estuary with ASS (Table 7.8). Because of this large number of HGU-Bs in Group B, their soil profiles, pH graphs, and soil properties are shown in two parts, based on their location in the estuary zones (Table 7.9 and 7.10). The first group, the HGU-Bs located in estuary zone 2 (intertidal/tidal flat zone), mostly have black to very dark greenish grey soil colour, dominated by sandy clay texture (Table 7.8 and Appendix H.3.1). They were generally situated in landforms which bordered the river including washover, levees, mid-channel bars, abandoned channels and floodplains adjoining rivers (Figure 7.16, Grid B4 and C4). For the second group, the HGU-Bs in estuary zone 3 (fluvial deposition/floodplain), soil colours ranged from very dark brown to light olive brown (Table 7.8). The soil texture of soil profiles sampled close to the river in this group ranged from sandy loam to sandy clay. Landforms included floodplains, swales, and mudflats (Table 7.8 and Appendix H.3.2).

Table 7.10. Summary of soil colour and texture in HGU-Ss based on estuary zones and common landforms where ASS are present (Group B) in Bengawan Estuary

Type of HGU	Estuary Zone	HGU (Common landforms)	Dominant soil colour	Dominant soil texture
Group B	Intertidal/tidal flat zone (EZ-2)	HGU-B4 (washover)	GLEY 2.5/N – 3/10Y (black to very dark greenish grey)	sandy clays
		HGU-B6 (mudflat) HGU-B7 (mudflat) HGU-B8, HGU-B9, (lower part of floodplain)	10YR 2/2 to 2.5Y 5/3 (very dark brown to light olive brown).	sandy loam to sandy cla
	Fluvial deposition zone/Flood plain (EZ-3)	HGU-B11, (floodplain)	GLEY1 2/5N (black)	sandy clay
		HGU-B12, HGU-B13 (levee) HGU-B16/ES, HGU-B16/BS (swale)	10YR 2/2 to 2.5Y 5/3 (very dark brown to light olive brown)	sandy loam to sandy clay
		HGU-B18 (midchannel bar) HGU-B19 (lateral bar)	5Y 2.5/1 – 5Y 3/1 (black to very dark grey)	sandy clay silty clay
		HGU-B20 (abandoned channel)	GLEY1 2.5/10Y (very dark greenish grey and greenish black soils)	sandy clay loam and silty clay
Complete result for profiles from Bengawan Estuary are provided in Appendices H.2, H3.				

Soil analysis showed different soil characteristics in soil profiles of HGU-B9, floodplain with ricefields; and HGU-B16, swale with ricefields. This led to the reclassification of HGU-B9 into sub-HGU-B9/F and sub-HGU-B9/R; and of HGU-B16 into sub-HGU-B16/ES and sub-HGU-B16/BS. The sub-HGU-B9/R were located within 10 m from Bengawan tributary and the sub-HGU-B9/F were located >10 m from the estuary and identified as HGU with no ASS present (mentioned earlier in Group A). Sub-HGU-B16/ES was situated within 100 m from the Bengawan River, whereas sub-HGU-B16/BS was situated at distances of between 100 m to 2 km from the river.

Chemical analysis also shows diverse soil characteristics among the HGUs. Figure 7.15 to 7.18 present the relationships between pyrite concentration, pH_F and pH_{FOX}. Generally, there is an inverse relationship between pyrite concentration, and pH_F and pH_{FOX}. The pH_F of soil profiles in Bengawan estuary ranged from slightly acidic to slightly alkaline. The HGU-Bs with neutral pH_F was commonly located in estuary zones 2 (HGU-B6, B7, B8, B9/R, B11, B13, B16/ES and B20). However, after peroxide reaction, soils from these HGU-Bs became strongly acidic and reached pH_{FOX} less than 3. The difference between pH_F and pH_{FOX} was from 2 to 5 units. This indicates the presence of PASS, which was confirmed by high TPA (10- 400 $molH^+$/ton) and large range of pyrite values (0.05 – 2.5 %). The lowest pyrite value was related to the sandy soil texture located in the estuary zone 2 (Appendix H.3). The highest pyrite value was identified in the estuary zone 3 (HGU-B6), in the mudflat with dry-field and sandy clay loam soil texture.

Very acidic pH_{FOX} levels were also measured in the HGU-Bs where the pH_F levels were slightly acidic and slightly alkaline. Both HGU-B12 and B13, levee with ponds and unused land respectively, have pH_F values between 7.4-7.8 before hydrogen peroxide treatment but then decreased 2-4 pH units after hydrogen peroxide treatment (Figure 7.16B). Meanwhile the slight to very strong acidity pH_F (6.5 – 4.5) that occurred in HGU-16/BS and HGU-B/19 decreased less than one pH unit from pH_F to pH_{FOX}. TPA values of these soil profiles ranged from 3 to 346 $molH^+$/ton, and the pyrite values were 0.01-1.54 % (7.10).

Interestingly, not all soil profiles show that pyrite is present in all layers. For example in HGU-B4 and HGU-8/A, the layers, where ASS was detected, were located in the lowest and the uppermost layers respectively (Figure 7.19 and Appendix H.4), whereas in HGU-

B16/BS, ASS was detected on both the uppermost and lowest layers of its soil profile (Figure 7.19). Pyrite development processes controlling the distribution of soil pyrite in these HGUs will be further discussed in Chapter 8. More details for the chemical soil properties associated with pyrite, pH_F and pH_{FOX} of HGU-Bs in Group B are presented in Appendices H6 and H7.

Table 7.11. Summary of average soil chemical properties of HGU-Bs where ASS was present

The HGU	Depth of soil profile (cm)	pH_F	pH_{FOX}	Redox (mV)	Electrical Conductivity (mS)	SPOS (%)	Pyrite (%)
HGU-B4	0-50 cm	7.41	6.83	-164.11	0.74	1.49	0.09
	Below 50 cm	7.31	4.86	-250	0.20	0.26	0.27
	SD	0.08	0.79	37.55	0.75	3.17	0.09
HGU-B6	0-50 cm	6.70	3.39	-32.00	0.88	6.93	2.20
	Below 50 cm	6.30	1.43	-68.00	0.14	0.31	0.89
	SD	0.24	1.56	30.54	0.87	4.03	0.75
HGU-B7	0-50 cm	7.01	4.00	-135.4	0.97	0.53	1.54
	Below 50 cm	6.88	2.35	-289	0.11	0.91	1.83
	SD	0.17	0.56	16.99	0.45	0.14	0.37
HGU-B8	0-50 cm	7.07	2.86	-142.3	0.86	0.42	1.04
	Below 50 cm	6.45	4.79	-72	0.15	7.93	1.79
	SD	0.09	0.73	86.99	0.90	0.15	0.49
HGU-B9/R	0-50 cm	5.48	4.95	387.26	0.53	0.24	0.10
	Below 50 cm	4.99	4.20	341	0.35	0.33	0.25
	SD	0.37	0.93	19	0.34	0.14	0.02
HGU-B11	0-50 cm	7.30	2.84	-120.00	0.91	8.51	0.02
	Below 50 cm	6.99	2.32	-267	0.21	0.66	0.05
	SD	0.20	0.74	69	0.94	2.86	0.91
HGU-B12	0-50 cm	7.11	2.95	-43	0.65	3.22	1.35
	Below 50 cm	5.58	1.98	-112	0.02	16.00	2.21
	SD	0.75	0.71	55	0.58	4.74	0.22
HGU-B13	0-50 cm	7.74	2.60	-119	0.51	13.38	1.18
	Below 50 cm	7.07	2.35	-156	1.84	13.38	1.79
	SD	0.17	0.92	44	0.45	2.63	1.13
HGU-B16/ES	0-50 cm	5.47	4.95	387.26	0.53	0.24	0.01
	Below 50 cm	5.56	4.20	341	0.60	0.08	0.01
	SD	0.61	0.55	20.28	0.22	0.12	0.24
HGU-B16/BS	0-50 cm	5.86	5.47	-43.83	0.38	0.30	0.39
	Below 50 cm	5.11	4.38	-33.00	0.70	0.46	0.75
	SD	0.37	0.63	19	0.34	0.14	0.012
HGU-B18	0-50 cm	6.76	3.12	-50.22	0.62	4.79	0.28
	Below 50 cm	6.04	4.19	-108	2..65	10.38	0.75
	Sd	0.48	0.79	47.87	0.80	4.24	0.28
HGU-B19	0-50 cm	6.54	4.56	-53.05	0.21	60.75	0.26
	Below 50 cm	8.52	5.03	39	0.47	126	0.56
	SD	1.42	0.23	41.89	0.11	32.66	2.98
HGU-B20	0-50 cm	7.29	2.67	-121	0.56	8.06	1.18
	Below 50 cm	7.02	2.25	-267	2.72	12.55	1.54
	SD	0.17	0.53	68	0.64	2.63	0.37

Sd = Standard deviation.
Complete result for profile from Serayu Estuary are provided in Appendices G.2 & G3.

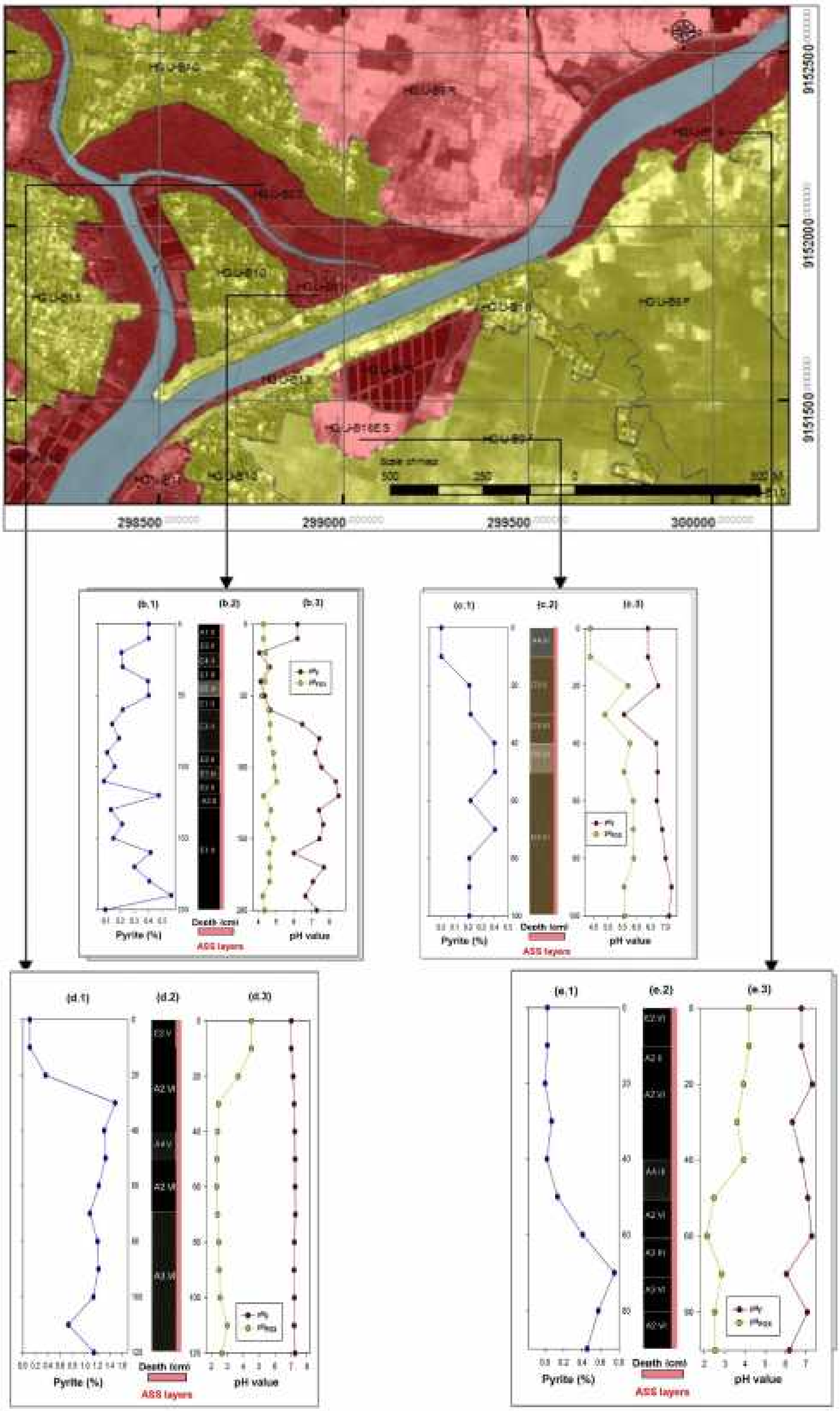

Figure 7.19. (a) Map of Serayu Estuary showing HGU-B20, HGU-B19, HGU-B16/ES and HGU-B18 where ASS were present. Graphs show vertical distribution of pyrite (b1, c1, d1, e1), and pH before (pH_F) and after (pH_{FOX}) hydrogen peroxide treatment (b3, c3, d3, e3) in average. The soil profile (b2,c2,d2,e2) showing soil colour and texture depth; the red shading column indicates the presence of ASS.

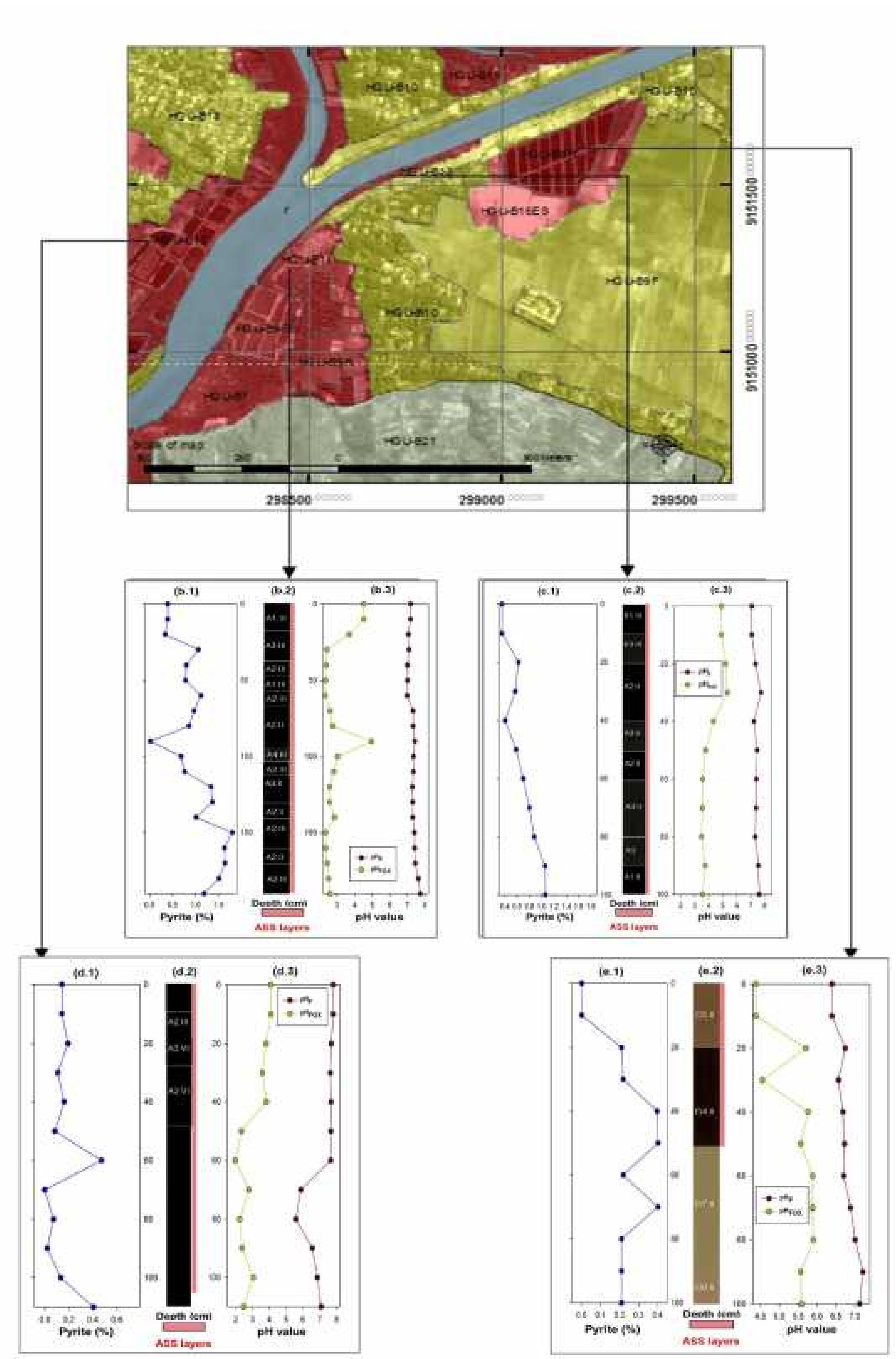

Figure 7.20. (a) Map of Serayu Estuary showing HGU-B12, HGU-B11, HGU-B13 and HGU-B9/R where ASS were present. Graphs represent vertical distribution of pyrites (b1, c1, d1, e1), and pH before (pH_F) and after (pH_{FOX}) hydrogen peroxide treatmen (b3, c3, d3, e3) in average. The soil profiles (b2,c2,d2,e2) show soil colour and texture depth; the red shading column indicates the presence of ASS.

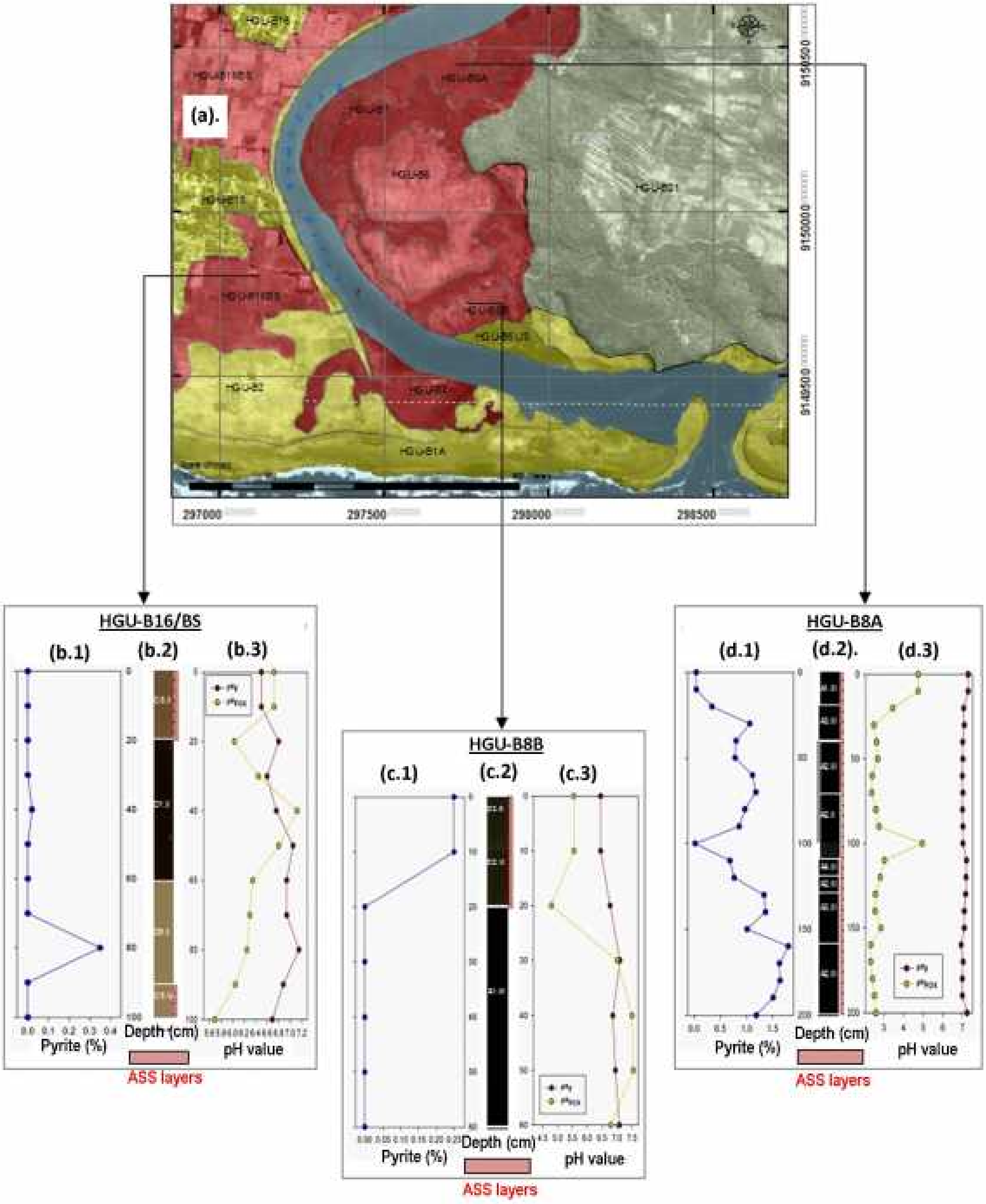

Figure 7.21 (a) Map of Serayu Estuary showing HGU-B16/BS, HGU-B8/A and HGU-B8/B where ASS was present (red shaded). Graphs show vertical distribution of pyrite (b1, c1, d1, e1), and pH before (pH_F) and after (pH_{FOX}) hydrogen peroxide treatment (b3, c3, d3, e3) in average. The soil profiles (b2,c2,d2,e2) show soil colour and texture depth; the red shading column indicates the presence of ASS.

7.3 Dominant Factors that Influence the Distribution of ASS in Central Java Estuary

Principle Component Analysis (PCA) was applied to examine the environmental factors that influence the distribution and characteristics of ASS. The result of this statistical analysis, given in Tables 7.12, 7.13 and Figure 7.22, show the variables controlling ASS occurrence and the distribution of HGUs in Serayu and Bengawan estuaries. Table 7.12 demonstrates that PC1 and PC 2 together explain nearly 60% of the variation within samples from Serayu Estuary, and nearly 50% of the variation in soil samples from the Bengawan Estuary.

Table 7.12 Total variance of PCA for the factors controlling the ASS distribution in the Serayu and Bengawan Estuaries.

Estuary	PC	Eigen values	%Variation	Cum.% Variation
Serayu	1	4.55	32.5	32.5
	2	3.47	24.8	**57.3**
	3	2.11	15.1	72.4
	4	1.13	8.1	80.5
	5	0.88	6.3	86.7
Bengawan	1	4.57	32.7	32.7
	2	2.31	16.5	**49.2**
	3	1.74	12.5	61.7
	4	1.59	11.4	73.0
	5	1.29	9.2	82.2

The Serayu and Bengawan estuaries PCA loading plots show clear HGU distributions (Figure 7.22, Graph A1 and B1). This HGU distribution can be divided into two groups, Group A (blue triangles) contains the HGU where no ASS was detected, and Group B (red circles) shows the HGU where ASS is present. For the Serayu loading plot (Figure 7.22, Graph A2 and B2), most of the HGUs in Group B, are located in the second quadrant or PCA2 positive area. The HGU with ASS was mostly located in the second quadrant area and tend to follow the trend line that divided the group.

Conversely, for the Bengawan loading plot, most of the HGUs in Group B are located in the third quadrant or PCA2 negative area (Figure 7.22, Graph B1). Besides the control elements that dominated Serayu Estuary, electrical conductivity also significantly influences the distribution of HGU with ASS in Bengawan Estuary. There are some HGUs in Group A and B located close to the centre of the graph (the origin), despite the line that separates those groups. The soil properties loading plot show that a similar pH value before oxidation, perhaps brought these HGUs closer to the origin. The SPOS, water table and distance from the river elements pulled some HGUs in Group B leftward. Conversely, N_{total} and Phosphorus concentration draw out some of the HGUs in Group A (Figure 7.22; Graph B.1 and B.2).

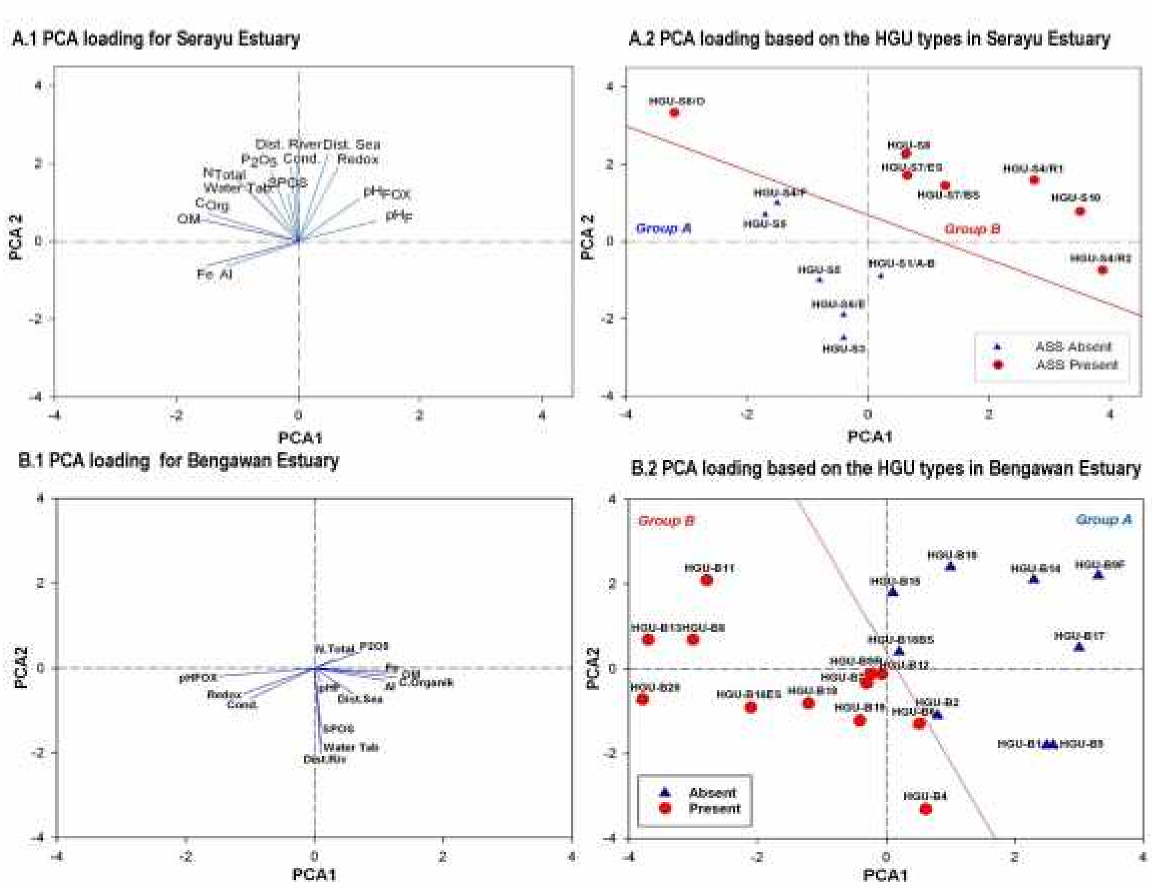

Figure7.22. PCA loading graphs based on the ASS properties (A1 and B1) and the HGU types (A2 and B2) for the Serayu and Bengawan Estuaries' data.

The distributions of HGU with ASS in Bengawan Estuary are spread more evenly compared to the ones in Serayu Estuary. In Serayu Estuary, the HGU distribution more closely follows the trend of the group dividing line. In Bengawan Estuary, about half of HGU plots are located at 2 unit distance from the origin. When comparing the HGUs plot distribution with their pyrite concentration, it reveals that there is a relationship between them. The HGU-B8, HGU-B11, HGU-B13 and HGU-B20, located far from the origin and in the negative area, had a pyrite value more than 1 %. This suggests that in the

Bengawan Estuary PCA loading plot, in the horizontal negative quadrant, the further the distance of Group B (HGU-B8, HGU-B11, HGU-B13 and HGU-B20) from the origin (negative quadrant), the higher the average pyrite concentration is. Further discussion on how this PCA analysis assisting the understanding of hydro-geomorphic control on ASS distribution is provided in Chapter 8, Section 8.5.

7.4 The Hydro-Geomorphic Characteristic of the HGUs where ASS are Present

The PCA score data (Table 7.13), provided information of other environmental factors that characterised the HGUs through a PCA factor plot (Figure 7.23 and 7.24). These factors include estuary zone, river energy, tidal energy and wave energy. The estuary zone is expanded in detail into Estuary Zone 1: Sea shore, Estuary Zone 2: Tidal shore, and Estuary Zone 3: River Deposition; river energy into low, medium and high; tide energy into high, medium and low; and wave energy into high, medium, low and none.

Table 7.13 The component matrixes of the control factors on ASS distribution

Variable	Component matrix - Eigenvectors		Variable	Component matrix - Eigenvectors	
Serayu Estuary	PC1	PC2	**Bengawan Estuary**	PC1	PC2
pHF	**-0.293**	-0.228	pHF	0.034	-0.101
pHFOX	-0.210	**-0.329**	pHFOX	**-0.433**	-0.061
Redox (mV)	-0.070	**-0.393**	Redox (mV)	**-0.314**	-0.186
Electrical Conductivity (mS)	0.108	-0.211	Electrical Conductivity (mS)	-0.285	-0.220
SPOS (%)	0.243	**-0.327**	SPOS (%)	0.026	**-0.415**
Carbon Organic (%)	**0.418**	-0.152	Carbon Organic (%)	**0.399**	-0.058
Organic matter (%)	**0.420**	-0.128	Organic matter (%)	**0.397**	-0.048
Fe (ppm)	0.380	0.249	Fe (ppm)	**0.327**	-0.029
Al (ppm)	0.378	0.255	Al (ppm)	**0.333**	-0.097
P_2O_5 (ppm)	0.111	-0.216	P_2O_5 (ppm)	**0.220**	0.120
N Total (%)	0.292	-0.334	N Total (%)	0.093	0.044
Distance to the river (m)	0.038	**-0.601**	Distance to the river (m)	**0.131**	0.006
Distance to the sea (m)	0.188	-0.181	Distance to the sea (m)	-0.099	-0.101
Water Table (m)	0.042	**-0.551**	Water Table (m)	-0.003	**-0.311**

In the Serayu and Bengawan Estuaries, which were wave and river energy dominated respectively, the more complex energy combination occurred in the HGUs where ASS are present (Group B). This energy combination is seen in the river and tidal energies loading plot of Serayu Estuary (Figure 7.22). Other Serayu Estuary PCA factors plots (Figure 7.23, Graph A2, A3 and A4) show that the energy combination that influences the development of ASS (HGUs in Group B) are low to medium river energy, combined with low to high tidal energy but zero wave energy. These HGUs are mostly located in estuary zone C which is the farthest distance of salinity penetration in the estuarine reaches of the river. Estuary zone C, as explained in Chapter 6, is a gradient or transitional zone with the lowest salinity level in an estuary. It indicates that river energy is gradually dominated by tidal energy. The Bengawan Estuary PCA factors plot (Figure 7.24, Graph B.1), shows that the HGU with ASS (Group B) are located in estuary zone B and C. The HGU with ASS is formed as a result of an energy combination of low to high river energy, low to medium tide energy and low to no wave energy (Figure 7.24, Graph B2, B3 and B4).

7.5 Final HGU Classification Scheme and Associations Between Landform and Pyrite

Soil profile analysis in this chapter demonstrates that HGU characteristics identified in each estuary contribute to the presence and absence of detected ASS. The classifications of estuary type based upon geo-climatic regions were related to the level of ASS development and soil pyrite concentration. Rambut and Jajar Estuaries, despite having low energy environments, only contained one HGU each where ASS was detected in the soil profile. In contrast, Serayu and Bengawan Estuaries, which were located in high energy environments, had more HGUs where ASS was present.

Table 7.14 shows the summary of the more detailed HGUs derived from soil laboratory analysis and higher resolution remotely sensed data. From this table, it can be concluded that finer subdivisions of HGUs: Sub-HGUs and Co-Sub-HGUs were required only in the Geo-climatic Region (GcR) Southwest. The HGUs in this region cover large areas with a variety of landforms and hydrological features such as distance from the fresh-, brackish- and sea-water resources which influence their soil properties. This was in contrast with GcR-Northwest and Northeast where the hydrological and geomorphological features were more uniform.

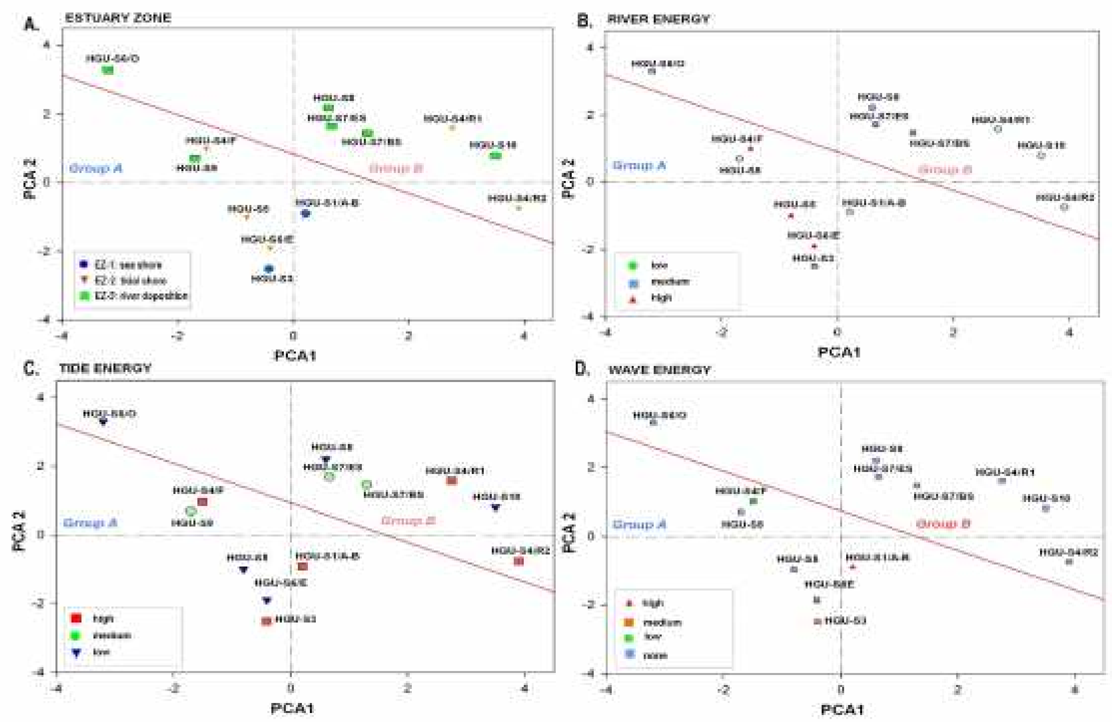

Figure 7.23 PCA factors plots presenting the HGU in Group A (HGU where ASS are absent) and B (HGUs where ASS are present), characterised by the types of estuary zone (Graph A), river energy (Graph B), tide energy (Graph C) and wave energy (Graph D).

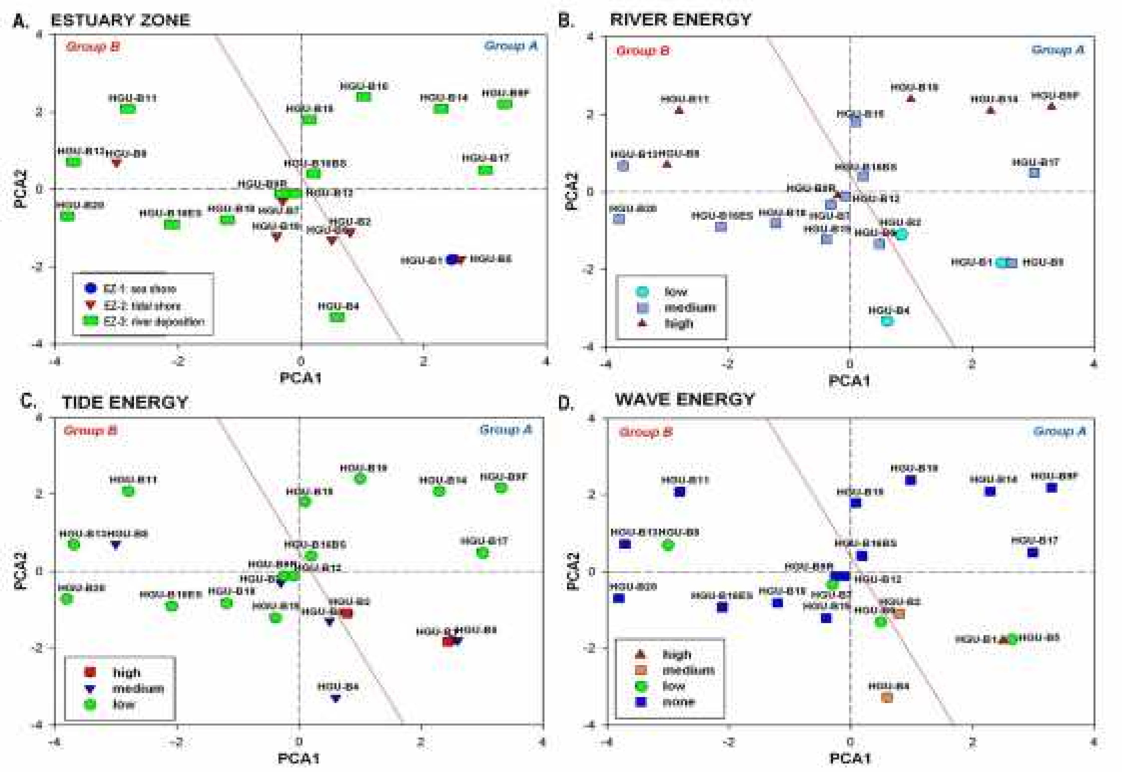

Figure 7.24 PCA factors plots presenting Group A (HGU where ASS are absent) and B (HGUs where ASS are present), characterised the types of estuary zone (Graph A), river energy (Graph B), tide energy (Graph C) and wave energy (Graph D).

The association between landform and pyrite concentration for further application are provided in Table 7.15, 7.16 and 7.17. These tables provide ranges of soil pyrite concentration based upon the types of landforms, together with their HGU and land-use information. The pyrite concentration information covers the pyrite occurrence in each HGU, and the range values of pyrite present in every 50 cm increment of soil depth, in the HGUs where ASS is present.

Table 7.14. Summary of the more detailed HGUs derived from soil laboratory analysis and higher resolution satellite imagery

Geo-climatic Region (GcR) The representative estuary Type of estuary	HGU	Sub-HGU	Co-Sub-HGU
GcR Northwest Rambut Estuary River dominated estuary	HGU-R1 to HGU-R11	-	-
GcR Northeast Jajar Estuary Tide dominated estuary	HGU-J1 to HGU-J12	-	-
GcR Southwest Serayu Estuary Wave dominated estuary	HGU-S1	HGU-S1/A; HGU-S1/B	-
	HGU-S2	-	-
	HGU-S3	-	-
	HGU-S4	HGU-S4/F; HGU-S4/R	HGU-S4/R1; HGU-S4/R2
	HGU-S5	-	-
	HGU-S6	HGU-S7/E; HGU-S7/O	
	HGU-S7	HGU-S8/ES; HGU-S8/BS	-
	HGU-S8 to HGU-S14	-	-
GcR Southwest Bengawan Estuary Wave dominated estuary with pre-existing barrier	HGU-B1 to HGU-B4	-	-
	HGU-B5	HGU-B5/S; HGU-B5/US	
	HGU-B6 to HGU-B8	-	-
	HGU-B9	HGU-B9/F; HGU-B9/R	
	HGU-B10 to HGU-B15	-	-
	HGU-B16	HGU-B16/S; HGU-B16/US	-
	HGU-B17 to HGU-B19	-	-
	HGU-B20 to HGU-B22	-	-

Source: Various Satellite Imageries, Field survey, and Soil Laboratory Analysis

Table 7.15. The association between HGU and pyrite concentration, in alphabetical order (Part 1: A to I)

Type of estuary	The pyrite concentration level:	Note:
(A) River-dominated estuary	1. Very high	*: average distance from the river.
(B) Tide-dominated estuary	2. High	**: the average distance from the tributary river.
(C) Wave-dominated estuary	3. Medium	
(D) Wave-dominated estuary with pre-existing barrier	4. Low	

The types of landform	Type of estuary	HGU	Landuse	Pyrite Occurrence	Range of pyrite concentration (%)			
					0-50 cm depth	50-100 cm depth	100-150 cm depth	150-200< cm depth
Abandon channel	(C)	HGU-S10	Ricefields	Absent	0	0	0	0
	(D)	HGU-B20	Unused land & *Nypa*	Present	0.1-1.3	1.1-1.3	0.7-1.4	N/A
Beach ridge	(C)	HGU-S6	Settlement	Absent	0	0	0	0
	(D)	HGU-B15	Settlement	Absent	0	0	N/A	N/A
Backswamp	(D)	HGU-B12	Ponds	Present	0.08-0.2	0.02-0.5	0.4-0.7	N/A
		HGU-B18	Mangrove	Present	0.01-0.07	0.1-0.75	N/A	N/A
Floodplain	(A)	HGU-R6	Dryfield,	Absent	0	0	0	0
		HGU-R7	Ricefields	Absent	0	0	0	N/A
	(B)	HGU-J6 to J11	Unused land , ponds, dry field, ricefields	Absent	0	0	0	N/A
	(C)	HGU-S4/F	Ricefields, >100m*	Absent	0	0	0	N/A
		HGU-S4/R1	Ricefields, 10-100 m*	Present	0.2-0.4	0.2-0.4	N/A	N/A
		HGU-S4/R2	Ricefields, <10**	Present	0.3-0.6	3-9	N/A	N/A
		HGU-S5	Settlement	Absent	0	0	N/A	N/A
	(D)	HGU-B8	Abandoned pond	Present	0.04-1	0.02-1.2	0.7-1.4	1.2-1.8
		HGU-B9/R	Ricefields	Present	0.02-0.05	0	0	N/A
		HGU-B10	Settlement	Absent	0	0	N/A	N/A
		HGU-B11	Unused land	Present	0.3-1	0.02-1	0.6-1.3	1-1.8

Table 7.16 The association between HGU and pyrite concentration, in alphabetical order (Part 2: I to M)

The types of landform	Type of estuary	HGU	Landuse	Pyrite Occurrence	Range of pyrite concentration (%)			
					0-50 cm depth	50-100 m depth	100-150 cm depth	150-200< cm depth
Intertidal flat	(A)	HGU-R4 HGU-R5	Abandoned Pond Dryfield	Absent Absent	0 0	0 0	0 0	0 0
	(B)	HGU-J3	Pond	Absent	0	0	0	0
	(C)	HGU-S3	Unused Land	Absent	0	0	N/A	N/A
	(D)	HGU-B2	Dryfield	Absent	0	0	N/A	N/A
Lateral bar	(D)	HGU-B18 HGU-B19	Unused land & *Nypa* Unused land & *Nypa*	**Present** **Present**	0.02-0.08 0.2-0.4	0.1-0.8 0.1-0.2	N/A 0.1-0.4	N/A 1.8-2.8
Levee	(A)	HGU-R3 HGU-R11	Mangrove Unused land	Present Absent	0.4-0.5 0	0.5-0.6 0	N/A N/A	N/A N/A
	(B)	HGU-J4 HGU-J5	New growth mangrove Dryfield	Present Absent	0.02-0.05 0	0.5-0.6 0	0.6-0.8 0	N/A N/A
	(D)	HGU-B13 HGU-B14	Unused land Unused land NBWV	Present Absent	0.3-0.6 0	0.5-1.1 N/A	0.9-1.3 N/A	1 -1.7 N/A
Mid-channel bar	(C)	HGU-S9	Dryfield	Absent	0.3	0.5	N/A	N/A
	(D)	HGU-B17	Unused Land	Absent	0	N/A	N/A	N/A
Mud flat/Salt flat	(D)	HGU-B6 HGU-B7	Dryfield Unused land	**Present** **Present**	0.03 – 0.07 0.25	0.1-2.4 0	N/A N/A	N/A N/A

Table 7.17 The association between HGU and pyrite concentration, in alphabetical order (Part 3: S to W)

The types of landform	Type of estuary	HGU	Landuse	Pyrite Occurrence	Range of pyrite concentration (%)			
					0-50 cm depth	50-100 m depth	100-150 cm depth	150-200< cm depth
Sandy shoreface	(A)	HGU-R1	Unused land	Absent	0	0	N/A	N/A
		HGU-R2	Dryfield	Absent	0	0	N/A	N/A
	(B)	HGU-J1	Unused land	Absent	0	0	N/A	N/A
		HGU-J2	Ponds	Absent	0	0	N/A	N/A
	(C)	HGU-S1	Unused Land	Absent	0	N/A	N/A	N/A
	(D)	HGU-B1	Unused Land	Absent	0	N/A	N/A	N/A
Swale	(C)	HGU-S8	Settlement	Present	0.2-0.5	0.1-0.6	N/A	N/A
		HGU-S7/ES	Ricefields, <100 m*	Present	0.2-0.3	0.2-0.4	N/A	N/A
		HGU-S7/BS	Ricefields, >100 m*	Present	0.4	0.1	N/A	N/A
	(D)	HGU-B16/ES	Ricefields, <100 m*	Present	0.2-0.3	0.2-0.4	N/A	N/A
		HGU-B16/BS	Ricefields, >100 m*	Present	0.4	0.1	N/A	N/A
Washover	(D)	HGU-B4	Unused land (west)	Present	0	0.27	N/A	N/A
		HGU-B5	Unused land (east)	Absent	0	N/A	N/A	N/A

Several landforms, which had ASS present in all soil samples collected across all HGUs, include backswamps, swales and mudflats/salt flats with various land-uses. Additional HGUs where ASS was detected sometimes included floodplains, levees, abandoned channels, lateral bars and washover. On the other hand, analysis of soil profiles from the sandy shoreface, beachridge and mid-channel bar landforms did not detect any ASS.

In summary, utilising hydrological and geomorphological information to identify HGUs, and subsequently the occurrence of ASS, captured detailed soil properties within these units. The spatial distribution of ASS indicated that there was no hydro-geomorphological process which was exactly the same for all estuaries. Further discussion of the distribution of ASS in each estuary and the influence of landform types, represented by HGUs, to the vertical and horizontal distribution of ASS are provided in Chapter 8.

CHAPTER EIGHT

HYDRO-GEOMORPHIC CONTROLS ON THE DEVELOPMENT AND DISTRIBUTION OF ACID SULFATE SOILS

8.1 Introduction

This chapter synthesizes the results of the soil analysis for each estuary (as described in Chapter 7) and the evaluation of the multi-stage mapping methods used to formulate a robust ASS mapping procedure (as outlined in Chapters 4, 5 and 6). The first section describes anthropogenic and natural controls on the presence and absence of ASS. The second section analyses the presence and absence of pyrite in relation to the level of hydrological energy in the systems under investigation. The last section discusses the application of multi-scale methods for interpreting spatial ASS formation factors and examines the level of robustness of the mapping procedures in this study, including the uses of remotely sensed data and GIS. To conclude, this study proposes a conceptual framework for understanding the hydro-geomorphic controls upon ASS development and distribution in Central Java.

8.2 Anthropogenic Controls on Hydro-Geomorphic Processes and the Distribution of ASS

Rambut and Jajar Estuaries are both located in low-energy environments, where the characteristics of their geo-climatic region (GcR) provided the ideal environment for pyrite to form and accumulate in mangroves. Interestingly, the absence of pyrite in these estuaries is not consistent with what current mapping models and knowledge would predict (Dent, 1986; Fitzpatrick *et al.*, 2008c). Based on the results of this study, the absence of ASS can be explained by human-induced changes to coastal environments. The following sections outline the human influences on ASS development in both these estuaries which may be applied to other similar estuaries.

8.2.1 The Impact of Intensive Aquaculture in Coastal Lowlands on ASS

River-dominated estuaries are expected to have low pyrite concentration (Lin & *Melville*, 1994; Chapter 2, Section 2.5). Where present, pyrite is usually located beneath recent fluvial sediments, or develops in isolated areas with low-energy conditions but with a sufficient supply of sulfate and organic material for reduction (Dent, 1986; Lin & Melville, 1994). The paleo-geomorphic data for the northwestern part of Central Java, where the Rambut Estuary is located, shows high fluvial sedimentation during the early Quaternary era (Kloosterman, 1989; Verstappen, 2000) due to paleo-climatic change (Figure 8.1). The present ITCZ position, which controls the climate in Indonesia (Chapter 3, Section 3.3) shifted to the south because of the strong Asia anticyclone, during the early Quaternary era (glacial period). This shifting of the ITCZ decreased rainfall and resulted in long periods of drought in Java (Verstappen, 2000).

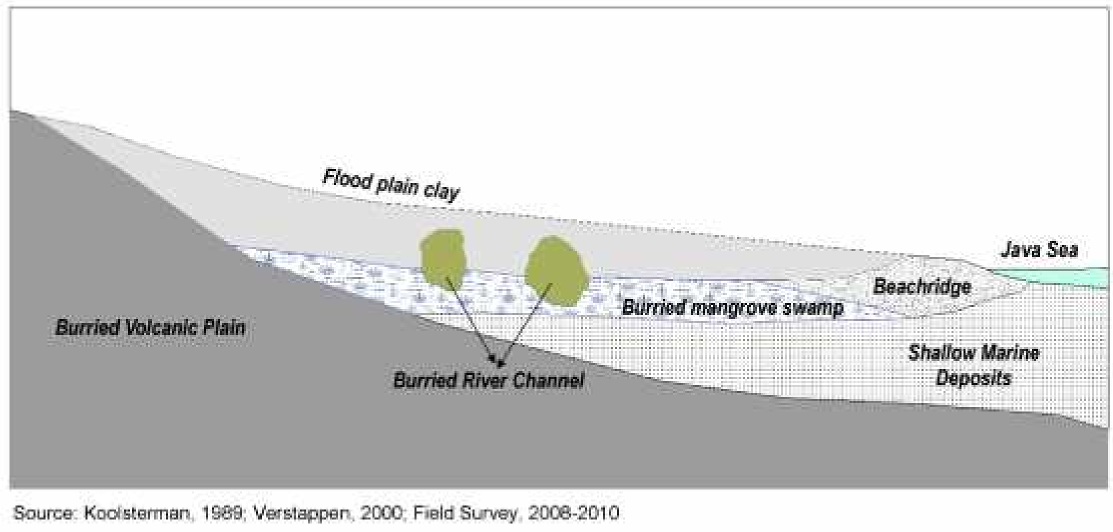

Figure 8.1. The development of coastal lowlands in Northwestern Central Java, including the Rambut Estuary, during the Holocene period.

Humid tropical conditions followed when the position of the ITCZ position moved back close to the current position during the interglacial or 11,400 years before present day (the sea level was 90-100 m lower than present). This change in the paleo-climate caused high chemical weathering and triggered extensive planation, massive erosion and sedimentation (Kloosterman, 1989). This influence continued through to the Holocene, when sea level rose and flooded the coast. Although the intensity of weathering and sedimentation are currently decreasing, the influence of fluvial sediment on coastal development is still dominant (Verstappen, 2000). The existing deltas in GcR-Northwest, such as Pemali, Comal and Bodri, show that high river energy and related high sedimentation, which influenced the development of the coast and estuaries. Deltaic deposits are a feature of estuaries where river energy dominance occurs (Bird, 2007). The dominance of fluvial processes may have reduced or prevented the formation of pyrite because of the low availability of sulfate. Under high river energy conditions, freshwater is likely to have reduced sulfate concentrations in the estuary as a result of dilution of marine waters and/or attenuation of lower energy marine incursion.

On the other hand, previous studies on aquaculture indicated that massive mangrove fringes existed since about year 1500 (as mentioned in Chapter 2) and decreased slightly in their extent until around the 1980s (due to coastal population development) just before the extensive development of brackish water aquaculture on the northern coast of Central Java (Hutabarat, 2008; Suharsono, personal communication 2010). This indicates that there was another period when the northwestern coast of Central Java shifted from high fluvial sedimentation into a low-energy environment with sufficient tidal influence that would allowed mangrove fringes to develop. There have not been any specific studies in Central Java to determine the time period in which this shift in energy conditions occurred. Brackishwater aquaculture existed from 1400 AD (Brown & Prayitno, 1987), indicating that this event was not recent in terms of land use history in the area, but was recent in terms of the geological history.

The aquaculture ponds the Rambut Estuary are situated in an environment that, under natural conditions, could possibly produce pyrite, such as in mangrove environment close to these ponds (Field observation, 2010; Appendix E.2). However, the continuous disturbance of the land by shrimp farming can oxidise pyrite, and oxidation products can be removed over time, as noted by Sammut *et al*., (2000) in ASS affected shrimp ponds. The absence of pyrite in several observed abandoned ponds indicates that the coastal environment surrounding Rambut Estuary has been exploited intensively because it occurs in an environment under which pyrite formation would have most likely occurred. Unsurprisingly, pyrite in this area is only associated with undisturbed mangrove areas where oxidation has not occurred and this supports the argument that over-developed areas have undergone past oxidation events that have reduced pyrite concentrations (Figure 7.1 and Appendix E2). This finding suggests that landuse history is an important factor in mapping ASS because human activities can deplete pyrite in environments. Basing mapping entirely on pyrite forming factors may lead to incorrect classification of present-day environments as PASS or AASS; accordingly, anthropogenic factors should not be ignored in mapping models.

A comparison of the physical characteristics in river-dominated estuaries with similar catchment morphometry in GcR-Northwest (Chapter 4, Section 4.4/Table 4.4), suggests that the sedimentation processes which determine the dominant energy conditions influences the development of pyrite in this type of estuary. These sedimentation processes are controlled by the size of catchments. Even though during the rainy season the small catchment estuary, like Rambut, is able to produce a pro-delta, indicating river domination (Ongkosongo, 2010), its energy is not as dominant as that of large catchments as mentioned in Chapter 4 (BPDASPS, 2007). Table 4.4 shows that there is a large difference between the minimum and maximum river discharges that corresponds to the wet and dry seasons, and there is a period during the dry season when tides temporarily dominate these type of estuaries. Salinity measurements during the dry season (Field observation, 2009 and Appendix A) support this finding. In brief, the opportunity for pyrite development in a river-dominated estuary with a small catchment occurs when energy conditions alternate between river and tidal energy, commonly between the rainy and dry seasons. During the dry season, when tidal water dominates, sufficient sulfate is present to enable sulfate reduction to pyrite.

Because there are many low-elevation landscapes adjacent to tidal water in the river-dominated estuaries in GcR-Northwest, it can be deduced that there are many places other than the Rambut Estuary that have a high probability of ASS occurrence based upon environmental conditions. This is supported by previous mangroves studies in Pemalang and other areas in the GcR-Northwest (Sukardjo, 2000) which recorded pyrite layers at a depth of 45 cm to 90 cm beneath the sediment surface in the existing mangrove clusters and fringes and some brackishwater ponds. However, there is no information on the ponds' current status in those previous studies. It is likely that the Rambut Estuary would have higher concentrations of pyritic sediment, if this environment did not experience intensive use of land for aquaculture. Despite the presence of organic material, sulfate and iron in aquaculture ponds (Appendix E.2), the formation of pyrite would most likely be minimal due to the pond dryouts and pond preparation that occurs between crops. The formation of monosulfides, a precursor mineral for pyrite, readily forms in the reduced environment, but these monosulfides are easily oxidized (Dent, 1986). The presence of shells within the areas surrounding the abandoned ponds is associated with years of aquaculture pond development which unearthed and spread shell materials (Field observation and interview, 2009). The shells are of marine and estuarine origins which indicate that this environment was once influenced by tidal conditions during its evolution. Under such conditions, pyrite should have formed and persisted under the anoxic and shallow watertable of this environment.

The absence of pyrite in some potential ASS areas might be partly due to its oxidation through past excavation. It was also possibly affected by a reduced supply of sulfate associated with fresh water (high river energy) in the wet season, diluting the concentration of seawater in abandoned ponds (Personal observation, 2009 and 2010). Information on the presence of pyrite layers from previous studies (Setyawan *et al*., 2008; Sukardjo, 2000) could be developed further by identifying their estuary types and by comparing their existing pond status to the ones in the Rambut Estuary.

8.2.2 The Effect of Dredging on ASS

The absence of pyrite in soils sampled in the Jajar Estuary, which is a tide-dominated estuary in GcR-Northeast, was not predicted. An earlier ASS study showed that tide-dominated estuaries have the highest probability of ASS presence compared to river- and wave-dominated estuaries (Lin *et al.*, 1995). A previous study also revealed that most mangrove forests in this regency contained reasonably high pyrite (Sukardjo, 2005). In addition, satellite imagery (Landsat ETM^+; ALOS AVNIR2) shows the coastal landscapes with mangrove fringes and clusters exist along Demak coast line (See chapter 4, Section 4.2). ASS was predicted to occur this environment because (1) the non-calcareous parent material in the upper catchment provides less carbonate in the sediment transported to the lowlands, and (2) the lowlands are exposed to low marine energy. Iron mottles were found below 50-100 cm in the soil profiles (Chapter 7, Figure 7.6B) also indicate there have been fluctuations in the height of the river surface in the

Jajar Estuary. If pyrite existed previously here, the watertable fluctuations may have enabled pyrite to oxidize leaving behind iron oxides as a byproduct.

Soil laboratory analysis of samples collected in Jajar Estuary did not detect pyrite in sediment samples (Appendix F.2). Some HGUs, which were predicted to have high pyrite concentration, such as those with mangrove fringes or backswamps, showed very low pyrite concentrations (0-0.001 %). Shells and grit were found in almost all of levee's surfaces (Chapter 7, Figure 7.6), reaching 5 km inland. This is also observed in some brackishwater pond environments in the Phillippines, subtidal estuarine environment in New South Wales, and also some laboratory experiments in Australia and USA, where the sufficient amount of existing shell grits were able to neutralise the low pH soil and water from 4 to 6 or 7 (van Bremmen, 1986; Corfield, 2000; Dent, 1993; Golez, 1995; Welch, 2007). This shell material (see Chapter 7), provides evidence of past environmental conditions which are related to estuarine evolution. The shell material evidence is indicative of the past hydro-geomorphic processes that shaped the Jajar Estuary and Demak.

Figure 8.2. (A) Previous marine environment of Demak area, located in GcR-Northeast (Muria Strait), in the 15th century (Soenarto, 2004). (B). The present alluvial plain of Demak area, developed when the marine environment evolved into a brackish-water swamp with mangroves. This transition was associated with high sedimentation fed by eroded material from the surrounding mountains.

Paleo-geomorphologic studies (Bellwood, 1987; Whitten & Soeriaatmadja, 1996; Tjia, 1970; Dunn *et al*., 1977, Sartono *et al*., 1978 and Sunarto, 2004) concluded that the Jajar Estuary was part of Muria Strait, the shallow marine environment that connected the Muria Mountains and Kendeng Hills (Figure 8.2). Intense weathering processes in the upper catchment of Muria and Kendeng, triggered by high rainfall intensity, resulted in intensive sedimentation of the Muria Strait (Sunarto, 2004). This sedimentation was also associated with a continuous supply of fresh water and changed the Muria Strait from a marine environment into a brackishwater, terrestrial environment. Subsequently, in this ‘previously marine environment’, mangroves had established, indicated by the shells observed in the sediment profiles (Chapter 7, Figure 7.7). These types of shells (*Terebralia sulcata, Turitella terebra,* and *Anadara granosa*) commonly lived in brackish water mud environments and sometimes attached to the trunks of mangroves (Dharma, 1988 in Sunarto 2004). The presence of these shells supports the finding of previous studies which stated that during the transition from a marine to a fluvial environment, Demak area was once a large extensive mangrove forest (Sartono *et al.*, 1978; Sunarto, 2004). The continued high sedimentation processes then gradually buried this mangrove forest, and its associated shell communities, and transformed this landform to an alluvial plain (Sunarto, 2004). Some soil profiles in Jajar Estuary (Appendix F.2) clearly show alluvium (brown to olive brown soil colour – 2.5Y 4/3) overlying estuarine sediments (very dark grey to black – 5Y 2.5/2, GLEY1 3/10GY), which provides further evidence of this transition from a marine to fluvially-dominated environment in which ASS were present only at depth i.e. beneath the alluvium.

It can be hypothesized that the shells found in the levee of Jajar River originated from the Jajar riverbed. Based on personal communication with several farmers and the local community, these shells were brought to the surface by dredging of the riverbed to supply material to build levees; the artificial levees were built to prevent overbank flow and protect adjacent land-use. This information was supported by data from the Demak Public Work Agency (2004) which show that Jajar estuary was dredged several times between 1995 to 1996, covering the distance from the estuary entrance to the Jajar inflatable dam (Figure 7.11), approximately 7 km upstream of the entrance (see Chapter 7, Section 7.2.2). This shell material, which is a rich source of calcium carbonate, enabled the soil to have a high acid buffering capacity (Beers, 1962; Baldwin and Mark, 2009). The soil analysis (Appendix 7.2.B) showed very little pyrite concentration (almost at detection limits) in the Jajar Estuary, despite the absence of a residual acid buffering capacity. It is probable that the calcium carbonate in the sediments neutralized any acidity produced from pyrite oxidation. Hence, ASS could not be well developed here or if ASS once existed, it has since been neutralized. The absence of pyrite in most of Jajar Estuary’s HGUs shows that dredging, as one of the common practices that can produce a sulfuric horizon through the exposure of pyrite (Fitzpatrick *et al*., 2007, McDonald *et al.*, 2009; Roy *et al*. 2001), has not created chronically acidic conditions in the Jajar Estuary.

The situation appears to be different in other estuaries in close proximity which have not undergone dredging. On the last visit to the Tuntang (Bunyaran) River (located to the west of the Jajar Estuary) and other estuaries surrounding it, the levees were still undisturbed, and mangrove fringes established downstream, up to 2 km from the estuary entrance (similar with the Jajar Estuary). Earlier research found that the pond and mangrove areas in Demak, covering the area from Sayung to Wedung, including Tuntang Estuary, had pyrite in the soil profiles from 30 to 100 cm deep (Sukardjo, 2000). In this study, field soil analysis also (Appendix F.3) showed that ASS was present as indicated by the strong reaction of hydrogen peroxide with the soil samples (higher than associated with sediments with a high organic content), and significant changes from pH to pH_{FOX}, averaging from 6 to 3 unit changes (Appendix F.4) which are indicative of pyrite being the source of the acidity (Field Observation, 2010). This strong mineral acidity is not associated with organic material; rather it suggests a mineral source because of the large drop in pH after forced oxidation; pyrite is the primary acid-producing mineral in this locality. Therefore, from comparing similar adjacent estuaries, which could be expected to have similar ASS formation and distribution pattern, human disturbances in the Jajar Estuary has resulted in low levels of detectable pyrite.

8.3 Natural Controls on Hydro-Geomorphic Processes and the Distribution of ASS

Serayu and Bengawan wave-dominated estuaries are influenced by the tropical monsoon creating dry and wet seasons with very high rainfall intensity (see Chapter 4, Section 4.2.1). The ASS found in these wave-dominated environments involved different hydro-geomorphic processes compared to similar environments in other parts of the world. For instance in Western Australia (Radke *et al.*, 2006) or New South Wales, Australia, wave-dominated estuaries have evolved with infilling processes within a large barrier estuary and inconsistent rainfall intensity and pattern (Rosicky *et al*., 2004b; Roy *et al*., 2001, 1984b), which enabled pyrite to form in the delta and pro-delta behind the sand barrier (Lin, 1998). The following sections will explain how these hydro-geomorphic characteristics differ between the Serayu and Bengawan Estuaries, which represent wave-dominated estuaries with a very large catchment (> 1000 km^2) and a medium size catchment (500 – 1000 km^2) respectively, and how this controls the development and distribution of ASS.

8.3.1. Seasonal Controls on the Distribution of ASS

As described in Chapter 4, Section 4.2.2 the Serayu Estuary is a wave-dominated estuary with a very large catchment (3700 km^2), with mixed volcanic and sedimentary parent rock material, and influenced by high rainfall intensity during rainy season. These physical and seasonal conditions generate high fluvial energy and very active alluvial processes on its lowlands, in the rainy season. Conversely, the river energy during the dry season was considered as negligible. The Serayu Estuary is also highly influenced by marine energy from the Indian Ocean. The combinations of high fluvial and marine energies usually do not provide optimal conditions for pyrite to develop because organic matter does not accumulate and reducing conditions do not occur. Where pyrite does sporadically occur, the concentration is usually less than that compared to concentrations in a tide-dominated estuary (Lin & Melville, 1994). Therefore, the results of this study show that the existence of high pyrite concentrations in this estuary, are worthy of further examination.

The alternate dominant energy forms during the rainy and dry seasons in the Serayu Estuary create a large range for discharge (300 – 1750 m^3/s) and sedimentation rates (750 - 4500 $ton/km^2/year$) (see Chapter 5, Table 5.6). Using several maps and multi-temporal remotely-sensed imagery, it was observed that the Serayu Estuary has experienced intensive change in the past 50 years compared to other estuaries on the south coast of Central Java (Figure 8.3). The seasonal river floods (5-10 years period) altered the estuary entrance from bending to the east (1973) to the west (2002). During a field visit in 2010, the sand barrier observed in year 2009 had gone. The consequences of these changes are the development of some new landforms. For example: oxbow lakes, as a result of a flood which cut a previous meandering channel (Verstappen, 2000; personal field and satellite imagery observation, 2009-2011); lagoon, where the floods cut off the previous bending estuary entrance (Figure 8.3, year 2002 image); and abandoned channels that then evolved into brackish water swamps (comparison of images between 1973 and 2002 in Figure 8.3). Some tributary rivers also underwent reduction in their cross sectional area due to high sedimentation caused by floods (comparison of 1993 and 2002 images in Figure 8.3). These changes indicate a highly dynamic system. The flows of these rivers were close to cease-to-flow because the water input is very little to none due to evaporation and sediment supply from the surrounding environment. Some of these tributaries were still part of the main the Serayu Estuary, but showed evidence that they are disconnecting.

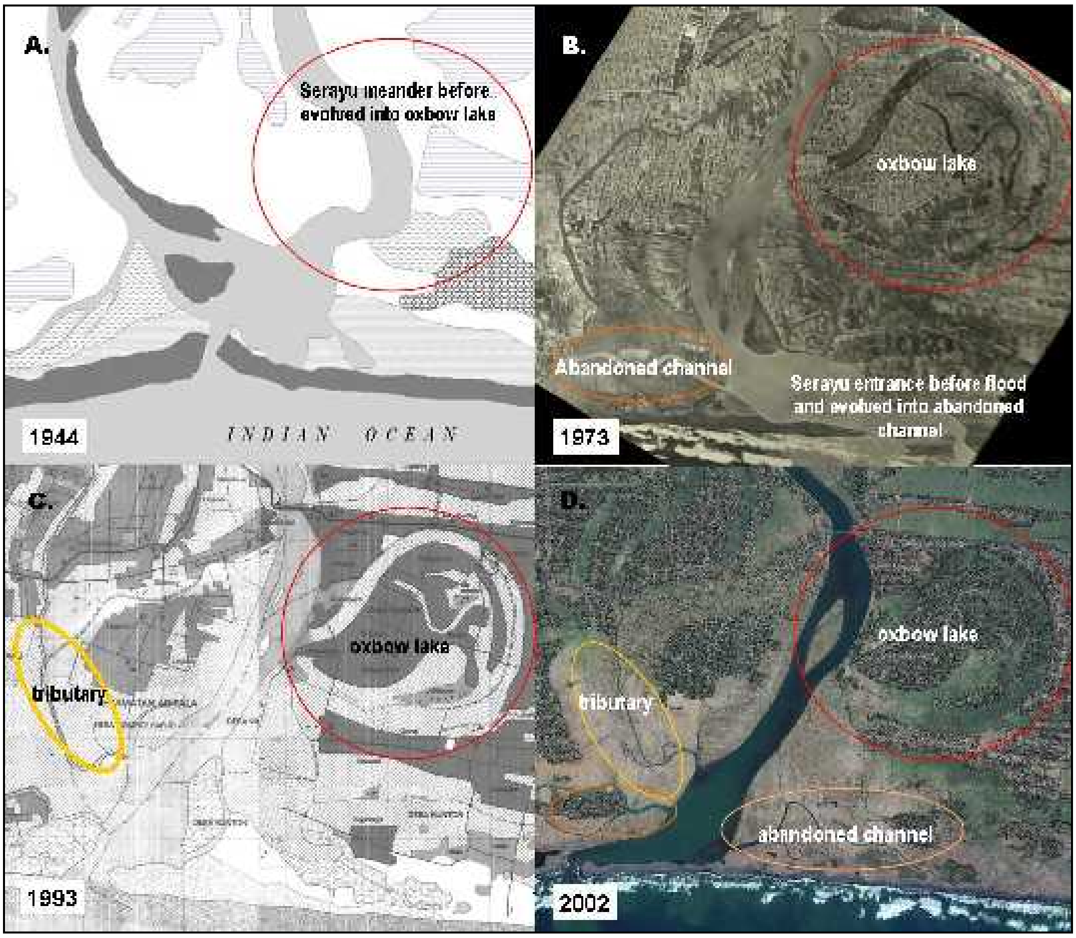

Figure 8.3. Series of Serayu estuary images and maps showing changes to the estuary shape over 70 years: (A). AMS Map, 1944; (B) Aerial Photograph, 1973; (C) Topographic Map, Bakosurtanal, 1993; and (D) Quickbird® imagery, 2002. The seasonal flood and wave energy dynamics created abandoned channels and brackish water tributaries.

The hydrodynamic processes of the Serayu Estuary described above, explain the existing low energy environment, despite dominant fluvial and marine energy. The presence of *Nypa fruticans* clusters (Chapter 7, Figure 7.12) in some new landforms indicates that the environment is suitable for pyrite to develop at this location. The distribution of pyrite concentration in the soil profiles, which ranged from medium (2-5%) to very high (>7 %), was associated with soil texture for different landforms. In brackish water swamps and oxbow lakes, their more sandy soil textures (sandy clay and sandy loam) indicated that there was once a high-energy environment in this location, resulting in less pyrite development (Chapter 7, Table 7.12). However, as mentioned in Chapter 2, the very low pyrite concentration in sandy soil can result in extreme acidity due to its low acid buffering capacity and high porosity (Dent, 1986). This condition leads to severe acidity of water (O'Shea *et al*., 2007; Miller *et al*., 2010), and means that even low concentrations of pyrite have to be managed to prevent oxidation and leaching.

Conversely, in the floodplain near the tributary, silty clay and silty clay loam were the dominant soil profiles (Appendices G.2 & G3), reflecting lower energy conditions and hence possible pyrite accumulation. The higher pyrite concentrations in tributaries indicated that these environments receive a constant supply of sulfate and organic matter, whereas the low pyrite concentration in the oxbow lake may be attributed to the presence of ricefields and the absence of a continuous sulfate input. As mentioned in Chapter 7 (Section 7.3.2) this oxbow lake also has a swamp with *Nypa fruticans* cluster (Map 7.20, Grid G2 & G3). This presence of *Nypa fruticans* indicates a brackishwater environment (Figure 7.19), as indicated in previous studies conducted by Bloomfield and Coulter (1973) in parts of Southeast Asia, including specific mangrove species and elevation differences of the lowlands (van Breemen, 1975; Dent 1986; and van de Kervie, 1972).

Despite marine energy being the dominant factor for estuary evolution in this wave-energy estuary, the ASS associated landform itself is a result of the combined influences of fluvial and marine energy controlled by a seasonal climate. This multi energy domination, emphasized by intensive use of land, meant some soil profiles did not have pyrite content in every single layer, as presented in the Bengawan Estuary (Chapter 7,

Figure 7.19 and 7.20). The function of landform evolution, in this case, controls the vertical distribution of the pyrite.

In brief, the soil texture, determined by the process of sedimentation, represents the energy involved in the development of a landform. The association between soil texture and pyrite concentration identified in the Serayu Estuary also explains the distinct hydro-geomorphic characteristic of each landform is the most important factor that affects pyrite formation, as also confirmed earlier in Chapter 2 (Section 2.1.1), by Dent (1986), and Bloomfield & Coulter (1973). Further discussion on how seasonal river and marine energy dominance influence the vertical distribution of pyrite are provided in section 8.4.2 and 8.4.3

8.3.2 The Influence of an Existing Barrier on Sedimentary Processes in a Wave-dominated Estuary

The Bengawan Estuary is a wave-dominated estuary with a pre-existing barrier and relatively low river energy, producing a variety of landforms, and hence more HGUs, compared to the Serayu Estuary (see Chapter 7, Section 7.2.4). The pre-existing barrier (Selok Hill), which slowed down the river flow, has generated different sedimentation rates and has created landforms with different types of soil textures, such as: lateral bar, mudflat, backswamp etc. (Appendices H.2).

During the rainy season, this meander sometimes experiences overbank flow because the river meander cannot accommodate the higher river discharge (BPDASPS, 2007). For this reason, this river meander was naturally diverted by normalizing its point bar southwest to accommodate the river flow. Consequently, the northern part of the meander area was cut off from the fresh water supply, creating a low energy brackish water environment and conditions suitable for the growth of a large *Nypa fruticans* forest (Chapter 5, Figure 5.13), reaching the Adiraja tributary (Figure 8.4.B).

Based on river salinity measurements (Appendix B), the *Nypa fruticans* distribution was limited by a change in salinity levels from very high to medium at the estuary entrance and from medium to very low (to fresh water) at about 6 km upstream of the entrance.

The high pyrite concentration found to a depth of 200 cm in *Nypa fruticans* fringes, 4 km upstream of the entrance, indicated that this environment had ideal salinity and energy levels for pyrite to form. In some of the *Nypa fruticans* environments in the southern part of the meander, which was cleared for agriculture and/or aquaculture, the pyrite concentrations were considerably high, reaching 3-5 % (Appendices G4, G5). Even though the salinity levels in the upper part of Bengawan's estuary entrance (100 up to 200 meters of the entrance) were similar to the one on the meander with *Nypa fruticans* forest, pyrite was not detected in this environment. The absence of pyrite in this estuary entrance environment was probably caused by high wave energy during dry season, creating a hyper-saline environment, and high river energy during the rainy season, causing less organic material supply, as was also observed in Serawak River (Andriesse, 1993). Therefore, even though a low-energy environment occurs at the equilibrium stage (between wave and river energy), the time to accumulate the pyrite was probably insufficient, and there is a lack of organic material (Appendices, H4, H5).

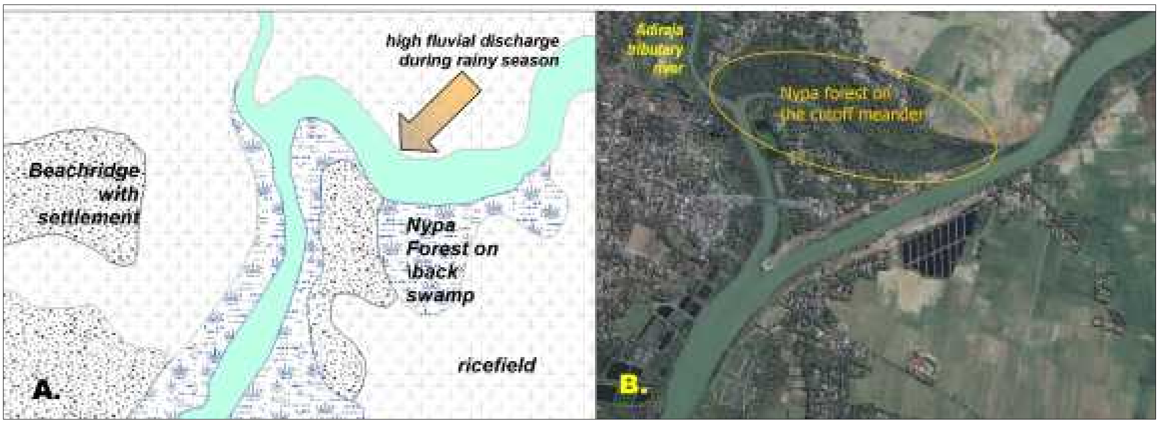

Figure 8.4. (A) Schemata of the Bengawan Estuary's meanders, before being diverted, show the existence of a backswamp (AMS, 1949). (B). After the point bar was normalized, the north part of meander became a low energy environment with Nypa fruticans forest (Quickbird, 2007).

The overbank flow, which occurred before river normalization, also generated the development of backswamps on the both sides of levees located south of the meander (Figure 8.4.A). After being normalized, these backswamps developed into *Nypa fruticans* fringes, and are now occupied by abandoned ponds and some remnant stands of *Nypa fruticans* (Figure 8.4.B). The pyrite concentration in this dominated sandy clay environment was considered high but was lower compared to that of the meander environment (sandy clay loam; Appendices H2, H3). This lower pyrite concentration might be caused by previous intensive used of ponds that were probably leaching some of pyrite oxidation products, as also suggested by Dent (1993); Sammut *et al.* (1996, 2000); and Gosavi *et al.* (2004).

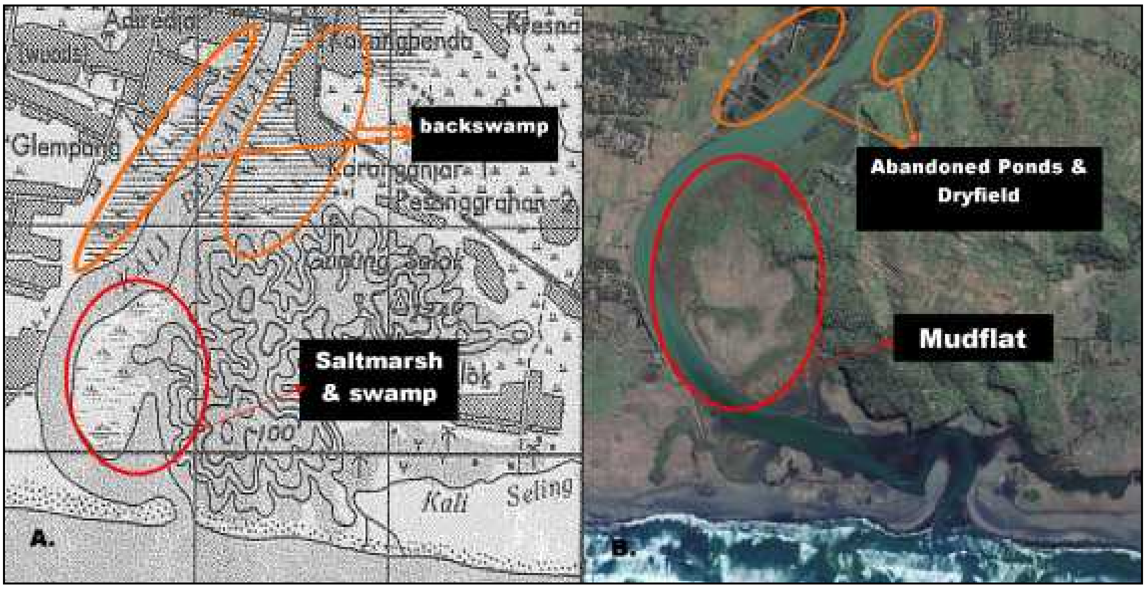

Figure 8.5. (A). The saltmarsh/swamp and backswamp present on the west and north of Selok hills (AMS, 1949). (B) The previous saltmarsh/swamp and backswamp transformed into mudflats and abandoned ponds (Quickbird, 2007).

The slowing down of the Bengawan River flow caused by the Selok Hills also produced a mudflat which was formed on the west side of this pre-existing barrier. This mudflat was a result of landform transformation from a swamp or a saltmarsh before (AMS, 1949) to a lateral bar and then mudflat due to high sedimentation from fluvial discharge and the Selok Hill denudational processes (Personal Observation, 2010; Figure 8.5.A). The soil analysis result shows variable ASS distribution in this mudflat. As described in Appendices H4 & H5, despite their similar texture (mostly sandy clay), the pyrite concentrations among the HGUs were diverse (0.5 – 4 %).

On the field visits during the dry seasons, the mudflat was mostly occupied by dryfields with various crops (Figure 8.5.B). During the rainy season, flooding inundated the outer area of the mudflat (close to the river). Salinity measurements for the inundated area showed that water salinity could be classified as brackish (5 -30 ppm during high tide - Appendix B). The stable area (non-inundated) in the middle of mudflat was mostly used for ricefields, utilizing river water from upstream transported by traditional irrigation canal system.

Figure 8.6 The Bengawan Estuary mudflat, with ricefields (A) and dry-field (B) landuses.

Mud lobster mounds were present in this mudflat during the dry season (Figure 8.6) indicating that conditions for pyrite formation were present, in this case reaching more than 2.5 % (Appendix H5). Mud lobster (*Thalassina anomala*) mounds are well known as pyrite biological indicator (Chapter 2; Dent, 1986). The area utilized for agriculture had lower pyrite concentration (below 1%), even though mangrove and *Nypa fruticans* had occupied this area in the past. The pyrite concentration variation across this area was a result of the continuous sulfate supply and intensity of anthropogenic land-use.


Figure 8.7 Lobster mounds on the Bengawan Estuary mudflat, on the west side of Selok Hill, during the dry season (left). The area was inundated during the rainy season (right).

As with the Serayu Estuary, the dry and rainy seasons have influenced landform development in the Bengawan Estuary, even though the river energy level is not as high as in the Serayu Estuary. The pre-existing barrier (Selok Hill) created a low-energy environment, shown by the presence of *Nypa fruticans* forest upstream (Chapter 5,

Figure 5.13), leading to more HGUs with ASS detected in the Bengawan Estuary. Medium catchment size and alternating seasonal energy factors in the Bengawan estuary, allowed ASS environments to develop, such as in fluvial-dominated estuaries observed in the Pearl River Delta (Lin, 1998). The existence of ‘rocky islands’ scattered in this high fluvial energy delta increased sedimentation, shown by the sediment accumulation surround it. The low-energy environment, where the sediment accumulated, created conditions suitable for pyrite to form which was similar to what occurred at Selok Hill. This example, where the existing landform has affected sedimentation processes, supports the conclusion that the Selok Hill pre-existing barrier is the main control on formation of pyrite in the Bengawan Estuary. The absence of pre-existing barriers in other estuaries with similar physical characteristics (Wawar, Cokroyasan, Bogowonto etc.; Chapter 5, Section 5.3) could provide less suitable conditions for pyrite to develop, because they are classified as wave-dominated estuaries and seasonal intermittently open and close (but mostly open) estuaries which minimize the development of ideal environment for pyrite to develop (Chapter 4, Section 4.4.3).

8.4 Factors Controlling Properties of ASS within Profiles

In this study, landforms had different ASS properties in different estuaries. ASS profiles from the same HGU but in a different type of estuary also showed distinct properties in their layers. The result of synthesizing the relationship between distribution patterns of ASS and the present hydro-geomorphic processes has revealed that the development of pyrite is influenced primarily by the estuarine characteristics. Based on statistical analysis (Chapter 7, Section 7.3) the concentration of pyrite was likely controlled by different energy levels that occurred in each estuary. Hence, while previous sections discussed the influence of hydro-geomorphic processes on the distribution of ASS, discussion below refers to the hydro-geomorphic processes in each estuary and its HGU with reference to pyrite vertical distribution.

8.4.1 Hydro-geomorphic Controls on Low- to Non- pyritic Layers

In this study, the absence of ASS was influenced by natural hydro-geomorphic processes and land-use, which either triggered pyrite oxidation or prevented the development of pyritic sediment.

HGUs without ASS were mainly located in fluvial plains, levees, foredunes and beach ridges, where their land formations were dominated by high fluvial and marine (wave) energy, and in the case of dunes, wind-driven sedimentation. Landforms that commonly formed under high wave energy were usually unstable and do not allow sediment and organic matter to accumulate slowly, thus it prevents the vegetation to colonize (Dent, 1986). Interestingly, some of these landforms also contained layers with low pyrite concentrations, mostly in their lower horizons which represented past environments and their processes. These low pyrite layers were probably formed in lower energy environment that possibly occurred before high fluvial or marine energy landforms formed. The formation of high energy landforms then disturbed the pyrite layers, causing this layer oxidised and its product (i.e. sulfuric acid) washed during this process, as was also observed in other estuaries where floodplain overlying pyrite sediment (Diemont *et al*., 1992; Lin & Melville, 1994; Minh *et al*., 1997). Unless disturbed, this low pyrite concentration might have a low potential hazard when preserved in finer soil texture (Pons & van Breemen 1982). However, as mentioned earlier, the small concentration of pyrite in sandy texture soil could enable leaching of the pyrite oxidation products easily, leading to higher potential hazard, for example: due to water table fluctuation, even though in a non-disturbed environment (Dent, 1986; O'Shea *et al*., 2007; Miller *et al*., 2010).

On the other hand, the soil profiles which have low (and very low) level pyrite concentration layers (below 1 %), observed in 10 cm soil depth increments, showed that their environments were not exposed to a high supply of sulfate and organic matter (Appendix H). Landforms with low pyrite concentration have distinct hydro-geomorphic processes compared to landforms without ASS. Detailed explanation of the processes that influence pyrite concentrations through the soil profiles is provided below. There were two types of soil profiles with layers of low pyrite concentration:

soil profiles which had ASS contents in all of their layers; and soil profiles which had only one or several layers containing ASS. Analysis of the first group of soil profiles which in the four observed estuaries, indicated that the vertical distribution of this low ASS content was mostly controlled by energy conditions (seasonal, high/ebb-tide periodic, etc.) which determined the availability of sulfate and organic matter (Chapter 7, Section 7.3). In the Rambut Estuary, for instance, one example of a soil profile with ASS in all layers showed layers located below 40 cm (five cm below sea-level; field observation, 2010) had higher pyrite concentration compared to the upper 40 cm layers (Figure 7.3). This river-dominated estuary attenuates marine energy further inland even during the dry season (personal observation, 2010; Setyawan *et al*., 2008). Thus, the ideal salinity level for ASS development was only available close to the estuary entrance (Appendix E.3), which provided enough sulfate from the seawater, as suggested by Dent (1986) and Lin & Melville (1993) as a determinant of pyrite formation. Clearly, the fluvial dominance of the middle to upper estuary was not conducive to pyrite formation due to the lack of sulfate-rich waters.

One other example of layers of low pyrite concentration in soil profiles was shown in the lower part of levee in the Jajar Estuary (Figure 7.8) which only had pyritic layers in the middle part of its soil profile (Chapter 7, Section 7.2.2, Table 7.4). The laboratory results showed that the TPA value ranged from 20 - 146 mol H^+/ton with pyrite concentration between 0.10 – 0.80 % in those layers. These pyrite concentrations were considered low compared to similar sediment, which was commonly more than 2 % (Lin & Melville, 1993; Sukardjo, 2000). While this environment allowed pyrite to develop, the absence of pyrite (0.01 % or considered as 0 %) in the upper 50 cm and the lower 100 cm soil profiles (80 cm below average sea level) was also questionable.

The morpho-chronology of the Jajar Estuary (Section 8.2.2) suggests that the current landform dominating this area was a floodplain covering mangrove sediment, indicated by the observed shells belonging to a species that occupied mangrove environments to a depth of about 3-4 m in the estuarine environment (Field observation, 2010; Sunarto, 2004). Therefore, the occurrence of shell grit on the top layers was believed to have originated from the dredging material, as discussed earlier in Section 8.2.2. For the new mangrove fringe, the low pyrite concentration in the upper layers of the profile might be influenced by the occurrence of carbonate from this dredging material that exceeded the ASS formation capability or neutralized the acid if the pyrite in the soil oxidised. The middle part of the soil profiles in these new mangrove clusters, however, probably have not been contaminated by carbonate concentration from the dredging material or represented a different environmental setting when these layers were the original soil surface (Figure 7.6.A).

Previous studies (Dent, 1986; Andriesse, 1993) suggesting that pyrite formation was possibly influenced by seasonal river energy levels that control the water fluctuation, and depth and duration of flooding, also support the prediction on how alternating low pyrite layers occurred in some HGU profiles in Jajar Estuary. The existing orange-brownish mottles on some layers of HGU (Figure 7.6.B) were related to the presence of iron and could indicate water table fluctuation, especially in an estuarine environment (Joffe, 1968; Fitzpatrick, 2007; Khan *et al*., 2012; Satheeshkumar & Khan, 2012). The salinity level changes between both seasons, perhaps causing the salinity of top water column (< 100 cm depth, suggested by Savenije, 2005) was lower during the rainy season, thus all soil profiles on levees were influenced by this condition. Besides the past environments that are suitable for pyrite to form, the high pyrite concentrations in the middle layers of levee have been probably maintained by the continuity of inundation by brackish water. Therefore, these layers have a more stable environment in terms of water fluctuation and disturbance level that prevent this pyrite layer from oxidising The different soil textures between upper (sandy loam) and middle/lower layers (silty clay loam) also indicated different hydro-geomorphic processes occurred in the past, especially with the respect to the type of energy involved (see section 8.3.1).

An inflatable dam (Chapter 7, Figure 7.11) also indicates that high salinity estuarine water occasionally occurred in the Jajar Estuary. This dam, as mentioned in Chapter 7, was built to prevent seawater intrusion and to protect upstream farmland, especially during high tide in the dry season where there is no significant fresh water input (Public Work, 1996). The presence of *Avicennia alba* and *Avicennia marina* instead of *Rhizopora* or *Nypa fruticans*, also reflects a high-salinity environments in some parts of the estuary. Salt intrusion and various flow characteristics on various depth of water column between dry and rainy seasons, commonly occurred in this type of estuary (Setyawan *et al.*, 2008; Savenije, 2005; Knighton, 1998). This water column condition probably influenced the varying pyrite concentration in the soil along the river. This finding is supported by Ritsema *et al.* (1992) which examined more drainage effects upon the formation of pyritic layers column in Netherland and Indonesia.

Higher concentrations of pyrite at depth reflect different environmental conditions when this soil layer formed. It might also reflect a lower energy environment when this was the original surface. Lower levels of pyrite in upper layer might be explained by regular oxidation during a drier period, higher energy conditions reducing accumulation of organic matter, or greater fluvial dominance. Changes in texture can be an indication of process and environmental change, since they represent the energy involved in sedimentation processes. The intensive use of land, for instance: dryfields and ricefields in mudflats (Figure 7.8), was also possibly one of the causal factors that decreased the pyrite concentration in the upper soil layers.

8.4.2. Fluvial Energy Controls on ASS Development

In the Serayu Estuary, as mentioned in Section 8.3.1, despite highly dynamic river conditions during the rainy season, some landforms favorable for pyrite formation were present. These landforms included large and small tributary banks, oxbow lakes, some levees, abandoned channels and backswamps. These low-energy environments, which developed later after a massive flood (high fluvial energy) occurred (Section 8.3.1; Figure 8.3), generated soil profiles that have high pyrite concentration layers (4-9%).

8.4.2.1 Intensive Pyrite Vertical Development in Tributary Environments

For tributary banks, the soil profiles that contained high pyrite concentrations indicated conditions for pyrite formation were met in all layers. The soil profiles reached more than 2 meters below the surface, with soil surfaces located about 10 cm higher than tributary river water level (Chapter 7.2.3.B). There were two processes of pyrite development that possibly occurred in this tributary, if referring to the hydrodynamic process of Serayu portrayed in Figure 8.4. First, during coastal plain evolution, the pyrite formed in the landscape as it evolved. The tributary banks with the pyrite content layers were then exposed by a river's capacity to incise, as was also observed by Lin *et al.* (1995) and Preda and Cox (2004), in Australian estuarine tributaries. Second, there was possibly no pyrite formed during the beginning of high fluvial energy sedimentation. However, the tributary channels enabled brackish water (which contains sulfate) to enter the adjacent landscape. Therefore, pyrite could form in this landscape, as was also observed in Kalimantan by Ritsema *et al.* (1992).

The existence of *Nypa fruticans* along this tributary (Figure 7.11) signifies that the brackishwater river continuously supplies sulfate to the adjacent lands (soil) under low energy conditions, therefore pyrite was able to form at high concentrations. This condition is similar to a study in Kalimantan where lateral inflow from sulfate bearing estuarine waters enabled the development of pyrite in adjacent river banks (Andriesse, 1993). The floodplain with settlement and ricefields surround this tributary bank which did not have any pyrite layers in the soil profiles (Appendix G4), indicated that the pyrite development only occurred in the land that was adjacent to the tributary. The mostly sandy clay textured soil in this tributary signifies interlayering of marine and estuarine sediment (Dent, 1986) that shows the past marine and fluvial processes. Thus, the pyrite development in this tributary was likely associated with the second process mentioned in previous paragraph.

There was a difference in pyrite concentration in floodplain landforms with ricefields adjacent to Serayu's large and small tributary banks, HGU-S4/R1 and HGU-S4/R2 respectively (Figure 7.11). The soil profiles located at the edge of the large tributary (pyrite: 0.20 to 0.40 %) had lower pyrite concentration compared to the small tributary (1-9%). The soil layers of the large tributary had alternating layers with the highest pyrite concentration (0.37-0.40%) in the uppermost 10 cm and 40-50 cm soil layers, with greyish soil colour (GLEY1 4/10Y), and lower pyrite concentration (0.20-0.23%), at a depth of 10-40 cm and below 50 cm depth with brownish soil colour (2.5Y 4/3) (Figure 7.13, Graph B). The lower pyrite in this large tributary bank might be influenced by more dynamic interactions between fresh and brackish water (higher energy environment compared to the small tributary), because it was located closer to the main Serayu River (Figure 7.10, Grid D3 & E3).

The gleyish colour soil in the uppermost 10 cm of the large tributary bank with ricefields (see Chapter 7.2.3) indicated a continuously waterlogged environment. The similar range of pyrite concentration in these alternating layers indicates that before being occupied for agricultural purposes the pyrite layers might have been developed as a single layer. An undeveloped floodplain soil profile from the Bengawan Estuary (HGU-B11) has consistent soil colour and texture, and pyrite concentration in its profiles (Appendix G.2). In floodplains with ricefield cultivation, ploughing and inundation were involved and these disturbed soil layers, mixing pyrite and non-pyrite layers. Despite these disturbances, surprisingly, there was not any AASS found in this floodplain with ricefields, compared to other ricefields in tidal environments in Mekong and Kalimantan (Husson, *et al.*, 2000; Anda *et al.*, 2009). The absence of AASS might be related to leaching processes following drainage, shown by the low pH (4 to 5) and medium redox value (around 50 to 100 mV). This pH and redox potential indicated that there were alternating processes of oxidation and reduction during drainage and inundation phases in this ricefields (Appendix G.5), as was also observed by Vegas-Vilarrubia *et al.* (2008), and Husson *et al*. (2000) in a study of pyrite concentration in all ricefields cultivation phases in deltaic environments in Spain and Vietnam, and were also defined by Krauskopf (1967) and Zhi-guang (1985). Despite this AASS leaching, the plant rotation pattern and high rainfall climate, allowed continuous inundation of the ricefields during the cropping phase. This condition has prevented the remaining pyrite from oxidizing, as is the case in other waterlogged ricefields (Dent, 1986).

AASS was not found in the soil layers that bordered the small tributary (HGU-S4/R2), despite high pyrite concentrations (Figure 7.11, right graph and Appendices G4 & G5). The pyrite concentrations were less than 1% from 0-40 cm in depth but gradually increased from 40 cm below the surface, reaching 9%, which was considered as very high. The fluctuations of the water table in the upper 40 cm layers during the rainy and the dry season might explain this low pyrite concentration layer, as higher pyrite concentration layers occurred deeper beneath the water table (measured during the dry season) where oxidation was limited. Water table fluctuations in some ASS, triggers oxidation during periods of lowered water tables and then seasonal leaching of acidity when the water table is higher (Cook *et al*., 1999; Hicks *et al*., 2002; Smith *et al*., 2003; Fitzpatrick *et al.*, 2010).

The lower layers, where the pyrite concentration was higher (4-9 %), were possibly once a surface environment where organic material would have accumulated and provided energy for reducing bacteria to convert sulfate to sulfide. This former surface environment would have been exposed to a supply of sulfate from the tidal action that formerly inundated this relict surface. The redox value between (-)100 to (-) 50 on neutral pH value, also indicated that the upper layer of the small tributary bank was mostly in a moderate reducing environment, whereas the high pyrite concentration at the depth 40 cm has redox potential value below (-) 100 mv, indicating a strongly reduced environment, following redox classification by Zhi-guang (1985) in Thomas *et al.* (203). Fresh water input in this small tributary river was available during the dry season through irrigation (from dam) and was more abundant during the rainy season (personal observation, 2009). In observing the pyrite values that were directly proportional to the depth, it is presumed that the soil layers' stability for the formation of pyrite increases with the depth. The presence of *Nypa fruticans* clusters in this HGU also indicated that the continuous low energy of brackish water has influenced the pyrite layers development. The stability of water column salinity, as suggested by Dent (1986), also influenced the soil characteristics of each layer, since it is related to the energy level, even in a small-scale environment.

8.4.2.2 Pyrite Vertical Development in Oxbow Lake and Backswamp

Oxbow lake landform in the Serayu Estuary (HGU-S10) had been infilled and was transforming into a swamp. It has also been intensively utilized for ricefields (Figure 7.8, Grid G2 & G3, and 7.10). This HGU was predicted to have ASS, due to the presence of *Nypa fruticans* clusters (HGU-S11) and the past conditions that would have been well suited to pyrite formation (ie. low energy conditions, accumulation of organic material and a supply of sulfate). The *Nypa fruticans* cluster was influenced by the water salinity level of the Serayu River (Chapter 7.2.3.B). This cluster also indicated that the previous meandering river was saline to brackish before the meander was cutoff and the oxbow lake formed (AMS, 1949; NSMA, 2001; Verstappen, 2000). However, the soil analyses show very low pyrite concentration (Appendix G.4). From the field observations, the elevation of the oxbow lake was lower compared to its surrounding environment including natural levees, beach ridge and the fluvial plain. Thus, rainfall and runoff are captured in this landform. In addition, the agricultural system in this oxbow lake applies regular water circulation using a fresh water irrigation system. Therefore, a continuous supply of fresh water has decreased the oxbow lake water salinity even though rice cultivation has maintained waterlogged environment in this HGU.

Some clusters of *Nypa fruticans* (HGU-S11) that were located in the northern part (point bar) of this oxbow lake (Figure 7.13, Grid G2, E2), were identified as potential environments for ASS development. Unfortunately, these landforms were not sampled in this study, as they were inaccessible. However, it is possible for pyrite to develop at these sites if they are not cultivated for ricefields or other land-uses, and the sediment is allowed to build up, in the process to become an infilled channel. Therefore, this HGU is appropriately classified as 'future possibility of ASS occurrence' which is close to PASS. This environment could be ideal for a future ASS development process study, if its environmental factors are controlled, especially if vegetation colonization is maintained as also suggested by Dent (1986) in his study in Gambia.

Medium pyrite concentration (1-2 %) in landforms shaped by higher river energy was also found in backswamps with ricefields (HGU-B11 and HGU-B12) (Figure 7.16, Graph a and b). These were located more than 2.5 km from the Bengawan Estuary entrance. These HGUs were first classified as floodplain near the main river ($\pm$<100), but based on the morpho-chronology of the Serayu River showing the high fluvial energy during rainy season causes overbank flow that affected this part of floodplain (Section 8.3.2), this landform was then reclassified as backswamp. The soil results showed that soil properties in this backswamp have clay texture (silty and sandy clay) and gleyish colour (GLEY1 2.5/10Y), compared to brownish (2.5Y 4/3-5/3) and sandier texture commonly found in floodplain profiles. The fine texture and brightness tone of this area on the QuickBird® imagery also indicated that this type of environment has been continuously inundated (Campbell, 2010).

After verification with the AMS (1949) map (Figure 8.4A), this HGU was indeed a backswamp with a *Nypa fruticans* fringe fed by a regular overbank flow (Section 8.3,2). The development of levees, after the Bengawan meander normalized, then restricted brackish water input in the backswamps. The sandy clay and sandy silty clay soil textures in these backswamps were different compared to backswamps found in the infilled Holocene estuarine sediments along the central coast of Australia (Roy, 1984a; Lin & Melville, 1993, Milford, 1997), marine clay sediment underlying peat as part of Holocene sea level rise in southeast Thailand (Okubo, *et al,* 2003), or heavy clay in tidal backswamp in central Kalimantan (Anda *et al.*; 2009).

The presence of sandy textured soils in the Bengawan backswamp indicates the influence of recent marine energy. This was further demonstrated by the presence of sandy-textured mid-channel bars reaching 4 km up stream during the dry season (Chapter 7, Table 7.13). Therefore, even though the pyrite concentration in Bengawan backswamps is lower compared to other previously mentioned clayish backswamps (3-5%), the sandy texture of backswamps also has more potential hazard to the estuarine environment because of the low-acid neutralising capacity and high permeability of sands (White *et al*., 1995). The severe acidity, Fe and Al in permeable sandy soils can be easily leached into the surrounding environment by rainfall and flood, and delivered to nearby environments via natural and artificial drainage systems (Dent, 1986; Sammut *et al*., 1996; Johnston *et al.*, 2005).

8.4.2.3 Pyrite Vertical Development in Mudflat Environments

Three HGUs in mudflats (Figure 7.16, Grid B3 and B4) formed as a result of the river flow being blocked by Selok Hill. These landforms had a range of pyrite concentrations, related to their position on the Bengawan River (horizontal distribution) as result of past sedimentation processes. The mudflat with ricefields (HGU-B7) had upper soil layers (0-20 cm depth) dominated by dark greyish brown (2.5Y 3/2), sandy clay soils; followed by black to very dark grey (5Y 2.5/1 – 5Y 3/1), silty and sandy clay loam, below 20 cm depth (Appendix F.2). The brownish colour soil on the upper layers was interpreted as an alluvium layer, as found on undisturbed floodplain with unused land (HGU-B10 and Appendix F.2). The very dark grey brownish soil located underneath might represent layers that have moderately reducing environment, shown by slightly acid pH (6.5 - 7) and low Redox potential (0 - (-100) mv). The continuous sulfate supply during the sedimentation processes, despite water table fluctuation, might also maintain the development of pyrite in this very dark grey layers (Section 8.4.2.3).

Different pyrite concentrations in mudflats with dry fields and with unused-land (HGU-B6 and B8 respectively) reflected the influence of different land-uses on the vertical distribution of pyrite as suggested by Dent & Ponds (1995). HGU-B6 is located in the middle of the mudflat environment where seasonal inundation was associated with floods, but did not occur during rainy season (Field observation, 2009, 2010). The soil profiles in these inner parts of the mudflat were expected to have stable and higher pyrite concentration because of the more stable environment, compared to those of the outer area (HGU-B8). However, the dryfield agricultural activities have highly disturbed the soil profiles to a depth of 50-75 cm which has exposed pyrite to oxidation and modified the soil profile (Figure 7.17, Graph 3). Compared to the unused-land mudflat (Figure 7.17, Graph 1), the similar range of pyrite concentrations on the mudflat with ricefields from the surface to the bottom soil profiles indicated that there was less disturbance to deeper pyrite bearing layers.

Soil profiles with low pyrite concentration (0.1- 2 %) were mostly situated on the outer mudflat (Figure 7.18; Figure 8.8), despite the existence of mangrove and *Nypa fruticans* fringes. The variable pH and Redox potential values within the soil profiles demonstrate alternating oxidation and reduction conditions, which was possibly influenced by seasonal river water level fluctuation. The average pyrite concentration was below 0.5 % (Appendices, H.4 & H5) at a depth of 0 - 30 cm. Low pH_F (4-5) and medium redox potential (0 - (-50) mV) indicate that this environment had previously oxidized but then was buried by sediments from floods and returned to a reducing environment. The lower soil horizons, however, show neutral pH (6.5 – 7.5) and low Redox potential (below (-) 100 mV), representing a moderately reducing environment that developed low to medium pyrite concentration (more than 1.5 %). Therefore, the outer mudflat has been influenced by seasonal river water level fluctuation and the timing of flood inundation, which according to Dent (1986) could cause instability in the rate of sedimentation vertically; in times of stable tidal zone environment, pyrite layers may accumulate.

Figure 8.8 The Nypa fruticans fringes in the outer part of the Bengawan Estuary mudflat environment, showing the inundation that occurred during the rainy season (Field observation, October 2010).

This process is possibly disrupted by high fluvial energy during the rainy season. As a result, the pyrite in the upper and middle layers was diminished to only 0.25 % (Figure 7.17, Graph B). However, given that this environment contained sandy textured soils, the low pyrite concentration was not surprising. This leaching of pyrite oxidation products in the sandy soil causes a very low pyrite concentration in this environment (O'Shea *et al.*, 2007; Miller *et al.*, 2010). There is a need to investigate the time lapse between low and high fluvial energy (dry and rainy season), in terms of continuous supply of sulfate and whether this type of environment provides enough time for pyrite to form.

The ability of river energy to transfer cubic and framboidal pyrite and their associated soil materials from one ASS landform (HGU with ASS present) to another non-ASS landform (HGU where ASS is absent) is probable. This was shown to have occurred in wash over deposits which were located at the southernmost part of the mudflat environment (HGU-B8.B). As seen on Map 7.14-Grid B4, this HGU is located just beside a mudflat with a dryfields (HGU-B6) which has pyrite in almost all profile layers. This wash over coincidentally had almost similar colour and texture to the top 40 cm pyrite layers of HGU-B8.B. Therefore, the pyrite layers on the upper layer of HGU-B8.B were possibly transferred from the soil material of the mudflat (HGU-B6) during the rainy season through overland flow or surface erosion. This conclusion could be supported by the occurrences of the non-ASS soil layers in the washover located closer to the entrance (HGU-B5) situated in a high energy environment caused by the confluence of river and marine energy. These layers have similar soil colours (5Y 2.5/1 – black) and textures (sandy clay – sandy clay loam) to the lower part of layers on HGU-B8.B, and there was not any detectable pyrite. This process is very common in southern Kalimantan, where overland flow and intensive rainfall and runoff have entrained acid producing soils and deposited the materials away from their source or transferred the soil acidity laterally through the sub-surface environment (Hoyer and Hobma, 1989; De Wit, 1990).

8.4.3 Marine Energy Controls on Pyrite Vertical Distribution

The swales are the only marine energy landform that contained ASS in this study (Chapter 7, Section 7.2.3.B). These landforms were located up to 4 km inland (Figure 7.8 and 7.17; Row 1). Swales in both the Serayu and Bengawan Estuaries had medium to high pyrite concentration in their soil profiles (Appendix H.5). The soil results indicate that proximity to a supply of sulfate determines the concentration of pyrite in the soil profile; the further away from the sources the lower the pyrite concentration (Appendices H.4 & H5). The swales closer to the estuary and coastline have more evenly distributed pyrite concentration in their soil profiles than those further away (Figure 7.9, Graphs 1&2). The continuous supply of sulfate through seasonal brackishwater floods (Public Work, 2005) and inundation from ricefield irrigation (Appendix A), perhaps maintains the environment for pyrite development, as has been described in backswamp ricefields in Kalimantan (Anda *et al.*, 2009). This soil profiles showed neutral pH_F on all layers, and the Redox potential values ranged from (-) 30 to (-) 90 mV on their top 30 cm layers, and an average of (-) 300 mV for depth of below 30 cm. These soil properties demonstrate the strongly reducing environment that might occur during ricefields cultivation and also during floods caused by overbank flow (field survey, 2009 & 2010).

For swales with ricefields located farther from the estuary entrance (HGU-B16/BS), layers containing pyrite were interlaced with layers with no pyrite (Appendix H.4). The layers with pyrite content have pH_F neutral (6.5 – 7) and Redox potential values of 30-100 mV, with similar values after hydrogen peroxide treatment indicating the beginning of continuous oxidation environment after its weak reduction (Hanhardt & van Ni, 1992; Thomas, 2011). On the other hand, the layers with no detectable pyrite showed high Redox potential (in average of above 300 mV) with pH_F of neutral to slightly acid (5.8 – 6.9) (Appendices G.4 & G.5), presenting active Fe^{+} oxidation (Schmidt *et al.*, 2011). Hence, this active oxidation layer was presumed to be located at the surface in the past, then ploughing during the beginning of cultivation (Fieldwork, 2009) mixed this non-pyrite layer deeper.

The various pyrite concentrations in the soil layers in the swales, despite their current land-uses, represent the past environment when this layer formed. The coastal environment in the Serayu and Bengawan River had been sufficiently supplied with sulfate during coastal evolution. As briefly described in Section 2.1.2, the beach ridge and swale systems along the western south coast of Central Java existed since the end of the Pleiocene (Verstappen, 2000). This beach ridge and swale system was formed from the tectogene in the southern tilted zone (Verstappen, 2000), instead of global Holocene sea fluctuation suggested by Goffau and Van der Lindern (1982). It also was not dominated by decadal fluctuation in wind patterns (Verstappen, 2000). However, taking into account the timing of the southern tilted zone stability and of the Holocene sea level fluctuations (Chapter 4), the lower part of these beach ridge and swale system probably have been developed a further 5000 – 10,000 years ago (Verstappen, 1997, 2000; Sunarto, 2011). Therefore, the swale with pyrite present inland formed when Holocene sea level rose and sediments were further accumulated along ridges as a result of wind entraining sediments accumulating along the shoreline. During this time, tidal inundation of the swale environment would have occurred. This condition is similar to other ASS found on a swale a few kilometers inland indicating that seawater inundation of the swale in the same period in Malaysia (Roslan *et al.*, 2010; Suswanto *et al.,* 2007; Tjia *et al.*, 1977) and Thailand (van Breemen and Harmsen, 1975).

The low energy swale environment system, despite being used for agriculture, had some hydro-geomorphic units which met the conditions for pyrite to develop, demonstrated by the presence of pyrite layers in all sampled soil profiles and by several *Nypa fruticans* clusters in the middle of swales (Chapter 5, Section 5.4.3). Subsequent development of the swale for agriculture, and a dominance of freshwater inputs from irrigation and rain, have arrested further pyrite development and has induced pyrite oxidation (largely through agriculture). However, since this landform developed, tidal flushing remained inactive due to its present-day hydrological disconnection from tides. Therefore, the current sulfate supply that determines and maintains the pyrite vertical development and distribution are more related to their distances from the sea or river, as these are the main brackishwater resources. Therefore, the current sulfate supply that determines and maintains the vertical development and distribution of pyrite is more related to the distance to the sea or river, as these are the primary brackishwater resources.

8.5 Dominant Environmental Factors in Pyrite Development and Distribution

The concentrations of pyrite in each estuary type and HGUs are related to the hydro-geomorphic factors of each estuary. Statistical analysis described in Chapter 7 (Section 7.3 and 7.4) identified factors influencing ASS presence and absence in HGUs. According to the PCA loading and factors (score) plot (Figure 7.21 and 7.22, Table 7.11), the HGU with ASS present were mostly situated in estuary zone 2 and 3 (tidal zone and river deposition). These estuary zones (Figure 7.22) were influenced by low to medium river energy, low to high tide energy, and low to no wave energy, supporting the synthesis result based on soil analysis and its hydro-geomorphic spatial characteristics. It means that the energy level involved in the HGUs influences the formation of ASS.

The presence of ASS was also controlled by the existing soil properties shown by the PC1 values, which were strongly correlated with five original variables (Table 7.12).

This PC1 accounted for 0.32 of the variation (eigenvalue : 4.57) with strong negative loading of pH_F, pH_{FOX} and Redox, and positive loading of carbon organic, organic matter. It means that the pyrite concentration increases with decreasing pH_F, pH_{FOX} and Redox but increasing carbon organic and organic matter. However, in the Bengawan Estuary loading plot, because the pH_F values were commonly neutral to slightly acid, the strongly correlated eigenvectors values only shown in pH_{FOX} (-0.433) and Redox (-0.314). It indicates that most of the pyrites present in the Bengawan Estuary have not been oxidized.

The PCA score loading (Table 7.12) also supported the results of the soil analysis showing that the distances of the HGU from the sources of sulfate (brackish water river) indeed influenced the development and distribution of pyrite. In the Serayu Estuary, the different pyrite concentrations between swales and riverbanks are related to distance from the sources of sulfate, discussed in section 8.4.3 and 8.4.2.1 respectively, are reflected by the large contribution of the 'distance to the river (m)' factor to PC2 (-0.601). This negative eigenvector value indicates that the closer (the less) the distance to the source of sulfate supply (river), the more opportunity for pyrite to develop. In the Bengawan Estuary, however, 'distance to river' factor did not contribute to the presence of ASS significantly (0.131). The development of low energy environments, because of the effect of the pre-existing barrier in the Bengawan Estuary, accounts for differences compared to the Serayu Estuary. Hence, the distance (factor) of the HGU to the sources of sulfate was not a strong factor for the presence of HGU with ASS. The sedimentary processes that develop distinct soil properties among the HGU soil layers have more control on pyrite development, than distance to sulfate source.

8.6 Evaluation of Using Multi-Scale Remote Sensing Data and GIS Analysis for Robust ASS Mapping Method

8.6.1 The Use of Multi-resolution Remotely Sensed Data to Acquire Hydro-geomorphic information

A central aim of this thesis is to establish a new robust mapping method using remote sensing and GIS through multi-scale approaches not commonly applied in previous ASS mapping studies in an effort to improve the accuracy and rapidity of mapping ASS (see Section 2.3). It was described comprehensively in Chapter 2 (Section 2.3.1) that the development of ASS mapping methods commonly involves either high-end technology for remotely sensed data or only single remote sensing data and a GIS approach to gain optimal information related to the development and distribution control factors of ASS. However, advanced technology for remote sensing data will not be easy to apply in a developing country like Indonesia. Conversely, single remote sensing data to map ASS is not always the best option because of the limitations of spectral range, spatial resolution and time of acquisition in representing the hydro-geomorphic properties. The three levels of mapping approaches described in Chapter 4, 5 and 6, showed that using more remote sensing of multi-resolution data in ASS mapping enabled this study to obtain more comprehensive hydro-geomorphic information at different scales of detail.

In remote sensing applications for mapping, high-level interpretation techniques, knowledge and experiences are important to obtain high accuracy (Lillesand *et al.*, 2000; Campbell & Wynne, 2010). In this study, one important stage in applying remote sensing was selecting and preparing the appropriate remotely sensed data for each stage (scale) of analysis. From this study, it is concluded that the data selection process needed a researcher who not only holds technical skills in remote sensing, but also has expertise in land-use or landform interpretation skills. Furthermore skill is also required to select the right hydro-geomorphic information suitable for the required data scale (regional, catchment and estuarine levels). The suitability of the required data for each level of analysis is important to avoid generalization or overly detailed information in producing the map and to increase the accuracy (McKenzie *et al.*, 2008).

The used of SRTM (Shuttle Radar Topography Mission), and Landsat ETM^+ in this current study showed an important contribution in validating existing watersheds' data, provided by Indonesian Department of Forestry (2007). In Chapter 4, Section 4.3.1, it was explained that the validation that included a DEM generated from the SRTM was able to determine topographic features including slopes and relief for regional scale analysis (Scale 1:100,000). This DEM also provided clearer topographic features together with the land-cover information of the relief, when combined with Landsat

ETM$^+$. The comparison between the new watersheds delineated from this DEM plus Landsat ETM$^+$ and the one provided by the Indonesian government present some minor boundaries dissimilarities. They included the detail of ridge boundaries, which could influence interpretation of the catchment size. This dissimilarity is negligible in small scale mapping, but will lead to problems with political boundaries if applied at a larger scale (scale above 1:25,000). The small inaccuracy in the watershed layers could lead to technical problems when conducting GIS analysis, especially when it is superimposed on a large range of spatial data information. Therefore, the decision to utilize the newest updated watershed layer was taken, because this current study applied it as the basic unit in Geo-climatic Region level (section 4.3.1).

The evaluation of applying the three multi-spectral remote sensing data to see their ability to support the development of a robust ASS mapping method showed that Landsat ETM$^+$ produced the best band combination (composite) for signalizing landform features (slope, geological structure, drainage pattern), at the medium scale (1: 100,000). The combination of multi-temporal data, including the geological and geomorphic map and the Landsat ETM$^+$ imagery, also showed a better synoptic view of the morpho-chronology or landform evolution in the coastal environments, such as: the meandering-channels and the previous position of the Serayu River compared to the SPOT-5 and ALOS AVNIR-2 (Figure 8.9; Figure 8.9.A). SPOT-5 is not able to provide more detail landform features despite its higher spatial resolution (Figure 8.9.B) compared to Landsat ETM$^+$. However, with ALOS AVNIR-2, detailed landforms can be identified and produces sharper vegetation and land-use features (Figure 8.9.C). Therefore, the use of Landsat ETM$^+$ together with ALOS AVNIR-2 to support mapping in the second stage of the methods, the estuary classification, provided more accurate interpretation in this study.

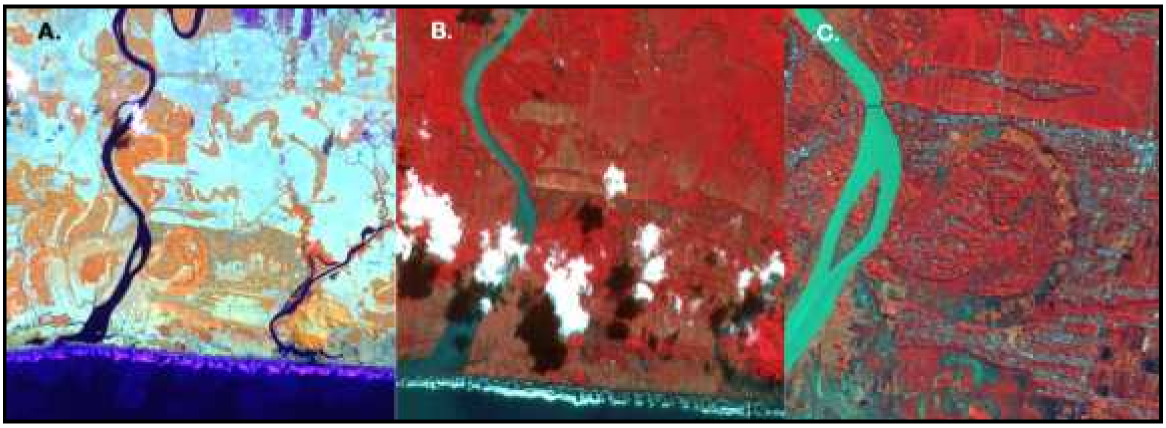

Figure 8.9 The Serayu estuarine system from different spatial resolution imageries: (A) Landsat ETM+, 30 m; (B) SPOT-5, 20 m; (C) ALOS AVNIR-2, 10 m.

In coastal areas where aquaculture dominates, as shown in Figure 8.10, this study also showed that a higher number of bands in the Landsat ETM^+ with 30 m spatial resolution provided more spectral options to select band composites to differentiate between water bodies, wetlands and dryland compared to the SPOT-5 image. The experiment to composite images in this study revealed that the Landsat ETM^+ spectral composite of 453 (Figure 8.10.A), supported 754 spectral composite, presented the best band composites for signalizing more detailed objects between wetlands, vegetation, soil and different types of land-uses for visual interpretation. The presence of two far infra-red (TM4 and TM5) and far infra-red (TM7) bands provided more detail in the variation of vegetation and soil/vegetation. The uses of SPOT-5 and ALOS AVNIR-2 were possible but not that effective when applied to determining the landforms, despite their higher resolution (10-20 and 10 m respectively). The SPOT-5, with its near- and mid-infrared was more effective to differentiate water bodies and land, and to identify vegetation types, but not different levels of soil moisture due to the absence of a blue band (Jensen, 2007). As the blue spectrum penetrates clear water better than other spectrums, different features of water bodies (turbidity, the use of water body) also could not be differentiated well in SPOT-5 (Figure 8.10.B).

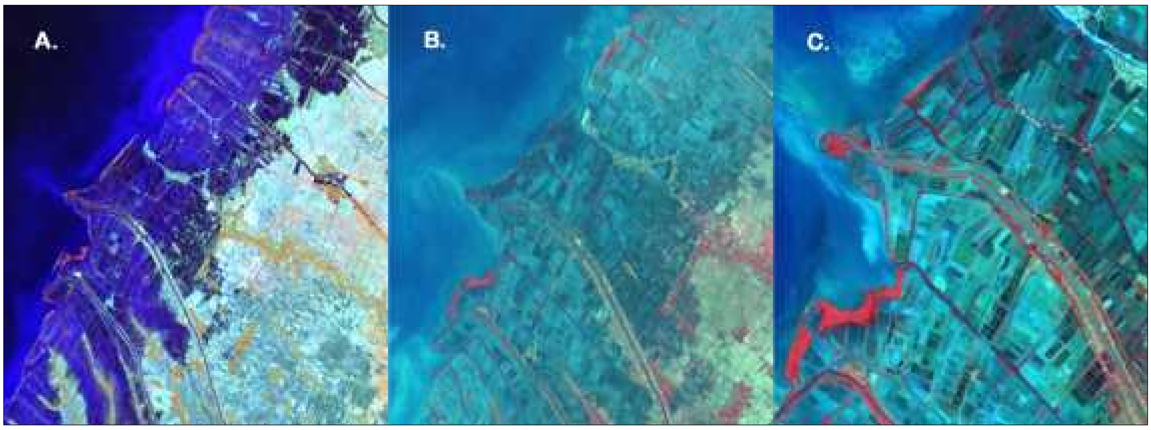

Figure 8.10. The comparison of the estuary with dominant aquaculture land-uses, in the Jajar Estuary from the band composites of (A) Landsat ETM+ 453; (B) SPOT-5 452; and (C) ALOS AVNIR-2 432.

On the other hand, ALOS AVNIR-2 imagery, with its higher spatial resolution, and the existence of the blue band, determined more detailed types of land-uses which were related to aquaculture ponds and rice-fields. For aquaculture mapping purposes, the use of ALOS AVNIR-2 imagery provided more wetland spectral differences which enabled this study to classify pond conditions at medium spatial scales (1:50,000 – 1:25,000) (Figure 7.17.C). The differences in tone and brightness on the pond objects as were validated in the field, showed different uses and characteristics of ponds. The brighter are the ponds objects in this ALOS AVNIR-2 imagery, the higher sediment content in these ponds. The brighter ponds are at the preparation stage, drying stage or abandoned ponds, whereas the darker ones show less sediment, which are mostly active ponds (Field survey, 2010). The distance of the ponds from the Jajar River and coastline, however, needed to be considered during visual interpretation. This study shows that some objects with similar brightness to the aquaculture ponds were ricefields when these were located further from Jajar River and coastline (Chapter 5). This finding demonstrates the need of tone, association and site elements as key interpretations of ricefield in area where ponds are also located.

The soil analytical results showed that QuickBird® satellite imagery was able to distinguish between landform types in estuarine environments up to a scale 1:10,000. This imagery is also able to identify different level of inundation of existing landforms, based on the colour and texture on the imagery (Figure 7.14). The darker features were associated with the sulfate supply sources (estuary and sea) and show that these environments experienced continuous inundation compared to landforms which appeared brighter. Even though this study did not statistically measure the correlation level between the features' tone on the QuickBird® imagery and pyrite presence and absence, there is a trend showing that the darker the tone of areas near a sulfate source, the higher the pyrite concentrations are. This finding is significant and should be further explored, especially in spectral analysis utilizing high-resolution satellite imagery and spectro-radiometer to identify more detailed soil characteristics (Campbell and Wynne, 2010).

8.6.2 The Efficiency of Multi-level Approach in Gaining Hydro-geomorphic Information at Different Scales

At the first level of determining the Geo-climatic region (GcR), application of a comprehensive approach to investigate the regional diversity of hydro-geomorphology effectively identified the ASS formation process in Central Java. It was shown by the high accuracy of the presence of ASS assessments before and after HGU validation described in Chapter 6 and 7 (Table 6.6-6.12 and 7.14). The integrated information on geology, geomorphology and agro-climate was classified systematically using a GIS multistage aggregation approach based on watershed (Figure 4.9) also demonstrates this accuracy. This approach facilitated this study in identifying commonalities between different physical aspects, using large sets of data such as: climate, regional geology, soils and catchment characteristics within the Geo-climatic Region (GcR) (Chapter 4). The decision to set the watershed, as discussed earlier, to control the boundary of mapping unit during data aggregation proved to be reasonable and compulsory in this level concerning the large data involved. The common GIS overlay analysis combines layers of spatial data without regarding the control boundary in creating a mapping unit (McKenzie *et al.*, 2008). In fact, this study found that when applying this GIS analysis in a large data set, complexity and confusion would rise in identifying the accurate boundary to determine a mapping unit based on aggregation approach (see Section 4.3.1). This occurred because the mapping units for geology, geomorphology and agro-climate maps are different; hence one unit in geology, for example, could be two or more units in geomorphology, as presented in Table 4.4, 4.5 and 4.6. Therefore, it is important to decide what mapping unit is to be used in a mapping process before applying a GIS analysis. In addition, the approach used to set this mapping unit has to be relevant to the conceptual background of a study (in this case a hydro-geomorphic approach) as also suggested by Bochco *et al.* (2001) and Minar & Evan, (2008) in their studies of multi-scale geomorphology mapping.

This study has also shown that the GcR classification facilitates detailed mapping that considers more detailed factors and their interactions in terms of landform evolution and soil development. As mentioned in Chapter 4, the next level of the methods, which involved estuary classification and selection that utilized the understanding of coastal landform evolution approach, assisted this study to gain as much as possible information from the existing data to minimize sophisticated field work procedures, due to limited resources in Indonesia. This approach was taken bearing in mind the resources and scale of this current study do not correspond to a large project for estuary classification such as conducted by Roy *et al.* (2001) which covered almost all estuaries in New South Wales; Geoscience Australia (2003) for many estuaries in all Australian states, or by Merry *et al.* (2003) in CSIRO South Australian Inventory of Acid Sulfate Soil Risk (Atlas). Therefore, the GcR will facilitate the project or in the future work conducted by a local government agency to assist classifying estuary using more robust methods.

The landscapes of selected estuaries in this present study were effectively used to represent combinations of specific hydro-geomorphic processes which occurred over a very large range of time periods. These periods covered the time range that represents the *Holocene*. However, the Holocene sea level rise information was not adequate to explain some ASS formation in Indonesia. For example, major sedimentation during paleo-climatic conditions until recently, paleo-tectonic activity, and the dynamic hydro-geomorphic processes discussed in the present study, are not covered by other research. Adding regional information on paleo-geomorphic and estuarine hydro-dynamic processes, on top of the GcR information, has enabled this study to identify and explain a different pattern of ASS distribution than would be expected using the soil forming knowledge of other studies (Section 8.2-8.3). This approach has also shown that ASS can occur or not be present in certain landforms that would be described differently by other approaches (Chapter 7). The first stage of the method (geo-climatic approach) in this current study provides valuable information on the paleo-geomorphology, estuarine morpho-chronology (or evolution), and recent hydro-dynamic conditions.

The results of this study show that the estuary classification method is able to capture information that could be dated to centuries, years and present conditions which were represented by Rambut, Jajar, Serayu and Bengawan estuaries respectively. This current study was also able to examine how various land-uses and temporal landscape changes could control the development of pyrite, by comparing these distinct (highly disturbed) selected estuaries with common (less to undisturbed) estuaries in the same GcR, as applied to the Jajar and Tuntang Estuaries (Section 8.2.2). The findings of this study show that pyrite concentrations and patterns of distribution can be related to different land-uses and landscape history. At a more detailed level, this method is able to identify complex environmental factors influencing the development of ASS. This approach is able to provide further information when the finding of ASS presence and absence are unexpected, for example in Rambut and Jajar Estuaries where ASSs are unexpectedly absent (Appendices E.3 & F.3).

Based on the results of this study, this multi-scale method is also effective in investigating the occurrence of ASS in environments which underwent change due to paleo-geomorphic and hydro-geomorphic processes, by adding the paleo-geomorphic parameter at the Geo-climatic Region level (Section 8.2.1 and 8.2.2). In the first step of the GcR establishment, this study only considered the Holocene sea level rise as a factor in identifying ASS probability sites, as applied in other ASS studies (Dent & Ponds, 1995; McDonald *et al.*, 2009**).**

For instance, as mentioned section 7.2, the tide-dominated estuary characterized as containing low energy environments, commonly has higher potential for pyrite accumulation compared to wave or river dominated estuaries (Lin, 1994; Roy *et al.*, 2001). Therefore, when this study unexpectedly showed that in some estuaries and landforms which were commonly ideal for pyrite development, the ASS concentration was negligible or was not found, it is important to consider both ASS and non-ASS landforms when doing sampling. This sampling approach, subsequently should be a compulsory procedure to review broader (GcR) ASS mapping. The soil sampling approach in which landforms identified with ASS absence and presence, in this current study, are rarely conducted in previously mentioned ASS studies (Lin, 1995, 1996, 1998, 2012; Fitzpatrick *et al*., 2000; 2012; Eden *et al.*, 2012; Fanning *et al*, 2012; Beucher *et al*., 2012). In aquaculture, specifically, the ASS mapping has mostly focused on the common ASS occurrence landforms and/or ASS problem pond sites (Bregt & Gesink, 1992; Golez, 1995; Gosavi *et al*., 2004; Hashidoko *et al.*, 2007), or only applies a single level (scale) mapping method. This single level mapping method is still regularly applied in recent times. A related ACIAR project (FIS/2002/076) involving UNSW, RICA and GMU (2008) has, however, undertaken research which has involved both ASS and non-ASS geomorphic units in its mapping program. However, in this project, the ASS were mostly found only in the commonly assigned ASS landforms of other regions in Indonesia where coastal processes have differed to those of the present study site. In this current study there are many more landform types that show that ASS is present (Chapter 7).

8.7 Summary

In this study, complex combinations of environmental factors influence sedimentary pyrite concentrations. The hydro-geomorphic processes that occurred in different types of estuaries significantly controlled the development of ASS. However, low energy environments controlled by landform types played a major role on the development of environments suitable for pyrite formation. The sulfate supply availability provided by permanent or seasonal sea water inundation influenced the vertical distribution of pyrite. The low energy environments, as a result of high energy river, tide or wave conditions, permanently or seasonally, determined the variety of soil characteristics in their soil layers.

The uses of multi-stage and multi-scale mapping methods have assisted this study to effectively map the horizontal and vertical distribution of pyrite. The multi-stage approach, which provides multi-scale hydro-geomorphic information, is effective to map ASS at various determined scales. The finding on the best remotely sensed data to extract the features of different condition of aquaculture ponds, indicates the importance of remotely sensed data selection to minimize the use of high cost data, especially for developing countries. Further image processing analysis related to soil properties will be established easily from the results of this study.

In summary, the use of a multi-stage ASS mapping approach in this study is reasonably robust to provide a valid procedure to map the horizontal and vertical distribution of ASS in coastal lowlands and improves on approaches used in previous studies.

CHAPTER 9

CONCLUSION

9.1 INTRODUCTION

This chapter reviews and discusses this study's research contribution to ASS mapping knowledge, estuary classification for Central Java, and controls on ASS formation. It includes the major findings, an overview of the originality and significance of the research, outlines the potential outcomes from the uptake of the findings, and provides direction for future research. The chapter also makes recommendations based on the HGU – pyrite concentration relationships identified by the ASS mapping methods developed in this study, to create more robust and rapid remote sensing and GIS methods used for ASS mapping and to support sustainable development of coastal resources.

9.2 Major Findings

This thesis set out to develop an understanding of the distribution and formation of ASS based on hydro-geomorphic controls, principally sedimentary processes driven by hydrology, and the subsequent formation of pyrite-bearing coastal landscapes in Central Java. This overall objective was achieved by producing an estuary classification scheme for Central Java that was then used to identify the relationship between landform development processes and pyrite concentration in soil layers, and by investigating how these factors interact to produce ASS in different HGUs. The research also effectively used a combination of field, laboratory and remotely sensed data as well as GIS mapping methods to produce more accurate spatial representation of ASS in coastal landscapes. More details on the achievement of the specific objectives in this study are provided in the sub-sections below.

9.2.1 Multi-level Mapping Method and Estuary Classification

The first specific objective of this study was to provide a method to derive the multi-level information on hydro-geomorphic processes that control ASS development through the establishment of an estuary classification scheme for Central Java, based on

Geo-climatic Regions (GcR); this was necessary to underpin more accurate and rapid mapping of ASS. This study developed mapping methods that will enable researchers and decision makers to produce more accurate maps to identify ASS and some of their key characteristics based on hydrological and geomorphological information. This was achieved through the outputs of Chapter 4, 5 and 6.

The provision of remote sensing data selection at every scale of mapping enables soil researchers to choose appropriate remote sensing data required to produce ASS maps. The multi-level mapping method used in the present study also provided an approach to predict information on the vertical and horizontal distribution of pyrite in each HGU, which complements existing approaches to mapping ASS (Bregt & Gesink, 1992; Ahmed & Dent, 1997; Husson *et al.*, 2000; Tarunamulia, 2008; ACIAR, 2011; Fitzpatrick *et al*. 2003; Beucher *et al.*, 2012). The past studies have largely only indicated the presence and absence of ASS; where the depth of ASS presence is alluded to, it is not presented in relation to soil -landform forming processes.

In addition to this, this thesis, for the first time, provided a classification scheme for the estuaries of Central Java (Chapter 6) with a potential for application across Indonesia and countries that have similar hydro-geomorphic setting. This scheme provides an estuary classification approach that can be useful to other forms of land development, research and wider environmental management. Environmental management decision making in Indonesia has not, to date, utilised an estuary classification scheme. Different estuary types will require different management approaches and this new classification scheme could enable decision makers to target appropriate efforts based on understanding of estuary development processes. This estuary classification process also introduced criteria for river, tidal and wave energy levels based on concepts of estuary classification (Boyd *et al.*, 1992; Haslett, 2000; and Bird, 2007) and the coastal conditions in Indonesia (Ongkosongo, 2010), which have not been integrated in any previous studies.

This study described four estuary types for Central Java: river-dominated estuary (Rambut Estuary); tide-dominated estuary (Jajar Estuary); wave-dominated estuary

(Serayu Estuary) and wave-dominated estuary with pre-existing barrier (Bengawan Estuary). This study's estuary classification procedures identified a new type of estuary, the wave-dominated estuary with pre-existing barrier, which is useful for interpreting the ASS development process in this estuary type. The wave-dominated estuaries with seasonally high river energy were found on the relatively high energy south coast of Central Java. The tide-dominated estuaries with low and medium river energy were located in the north coast of Central Java. Both coasts had estuaries with a range of energy levels which influenced sedimentation. Different river energy provided different erosional and depositional processes which influence the pyrite accumulation process. Low river energy levels results in greater pyrite accumulation compared to high river energy environments.

9.2.2 Hydro-geomorphic Units (HGUs), and ASS Development and Distribution

This second objective of this study was to define differences in vertical and horizontal trends in the physical and chemical properties of coastal sediments in intertidal and supra-tidal areas. This objective was achieved in Chapter 7 and 8. The results of the soil field and laboratory analyses showed that different hydro-geomorphic characteristics in each HGU determined the development, distribution and properties of ASS, both vertically and horizontally. The HGUs that represented different types of landforms, land-uses, vegetation and hydrological characteristics showed a consistent association with the presence of the pyrite. The common landforms, where ASS were present, were backswamps, swales, oxbow-lakes, abandoned channels, saltmarshes and mudflats. These landforms were developed in low-energy environments creating vegetated tidal flats which were suitable for pyrite to accumulate. In high-energy environments, such as: beach ridges, sandy shore faces, washovers and mid-channel bars, the conditions didn't favour pyrite formation. Some landforms showed potential for development of pyrite did not have any ASS in every estuary in which they were recorded, these were lateral bars, levees, swales, abandoned channels and floodplains. This complexity hasn't been identified in previous studies, which did not compare pyrite formation of different estuary types (Lin *et al.*, 1995; Lin & Melville, 1994, 1995; Fitzpatrick *et al.,* 2008, Fanning, 2009), and have drawn simplistic conclusions about ASS presence in certain landforms.

Different pyrite concentrations in the ASS profiles present evidence of past environmental conditions which were related to estuarine evolution. High pyrite concentrations are found in low-energy environments, where there is sufficient opportunity for brackish water vegetation to establish and for pyrite to accumulate; these environments accrete sediments and organic material creating a reducing environment for pyrite to form. In high-energy environments where the supply of organic material is lower or reducing conditions are less likely to occur, pyrite accumulation is expected to be low. The occurrence of ASS layers in high wave and river energy environments suggest sedimentary processes that involved intermittent low energy conditions occurred before a high-energy environment developed. This is in contrast with the information derived from some previous mapping methods (Lin *et al*., 1995, 1998; Lin & Melville 1994) that predicted ASS to be present only in estuaries currently with low energy. This finding again shows that an understanding of estuarine morpho-chronology is important for ASS mapping as demonstrated by the complex river dynamic of the Serayu Estuary (Chapter 8). More detailed understanding of soil and landforms within the HGUs for each estuary type will enable more efficient ASS mapping by targeting landforms where ASS may be present; and this can be applied to other estuaries. The ability of the HGU to represent the formation of ASS is significant in reducing the amount of fieldwork and data analysis required to understand where these soils occur, and what their chemical and physical properties are likely to be.

Field validation confirmed the presence of ASS predicted in HGUs, except in areas where anthropogenic activities dominated the estuary, for example in Rambut and Jajar Estuaries which are densely populated and highly developed. Intensive aquaculture ponds and dredging activities were the main factors contributing to the absence of ASS in these estuaries. Therefore, it is critically important to not exclude anthropogenic factors when mapping ASS at least for Indonesia where a large population is intensively utilizing the coastal soil resources.

9.2.3 ASS Mapping Model

The third specific objective of this study was to create a scientifically robust ASS mapping model incorporating knowledge on the relationship between soil and landform formation in Central Java estuaries. This ASS mapping model was formulated systematically through Chapters 4 to 7, by involving multi-level mapping methods, field observations, and remote sensing and GIS analyses, to produce more accurate ASS distribution maps based on the HGUs. Past studies on pyrite formation and oxidation were conducted in Australia, Indonesia, Thailand and Vietnam (Konsten *et al.*, 1994; Willet *et al.*, 1992; Minh *et al.*, 1997; White *et al.*, 1997; Anda, 2008), but none of them focused on ASS mapping schemes involving soil-landscape relationships. Estimating the depth at which pyrite occurs, using the HGU-ASS distribution maps, can enable land users to avoid this layer being exposed during coastal lowland development. This ASS mapping model was also able to identify the areas with and without ASS. Planning policies can describe areas without ASS as minimum risk for development and environmental impacts, and zone areas with ASS for limited or no development. The simple, efficient and comprehensive maps of ASS distribution, from this mapping method, will support aquaculture land sustainability and capability assessment, and local management planning for coastal resources.

9.3 Potential Outcomes from Uptake of the Findings

The results of this study have potential for adoption by research and government agencies involved in planning, environmental management and development. This thesis has made a significant and original contribution to knowledge by providing a scientific basis for a clearer and better understanding of soil forming processes for ASS in estuarine systems in Central Java. The establishment of GcRs, an estuary classification scheme and associated HGU, using spatial approaches, has simplified the complexity of ASS development processes in Central Java. The estuary classification scheme, in its own right, is a significant contribution and has wider application than soil mapping. The mapping method used in this study was designed in a very simple way so it could be widely adopted. Future application of this method in other parts of Indonesia will complement the mapping of ASS enabling a broader assessment of land capability in Indonesia. The methods developed by this study have broader application and can be adopted in other developing countries, as well as developed countries, where access to field sites and where resources to support field-based mapping are limited. Similarly, the processes described here for the formation of ASS could potentially occur in countries with a similar environmental setting, that is, in areas where similar estuary types, as described in Chapter 5, occur and where there are parallel hydro-goeomorphic processes.

Another potential outcome is the adoption of the estuary classification scheme which will enable decision makers and researchers to utilize a category-based system to classify estuaries in Indonesia. The government will benefit from the adoption of this method and increase the efficiency of ASS mapping. The adoption of the mapping method will also potentially lead to positive environmental outcomes. Soil and water are two fundamental resources for human life and also for ecosystem health. The reduction in the development of ASS will reduce the amount of acid and metals that is discharged into the environment.

The use of accurate ASS distribution maps by local government agencies (e.g. Regional Planning and Developments Agency; Regional Agency of Marine and Fisheries) will assist the community to manage their decisions. Best management practices and regional planning policies can utilise the findings of this study to avoid over utilization of coastal resources. Communities may also benefit through reduced conflict over resources use due to a better understanding of environmental constraints on land use. Government will be able to help farmers to choose the most suitable sites for aquaculture development and improve their productivity. It is important for farmers to avoid developing areas that present high risk, as is the case of ASS (Dieberg and Kiattisimkul, 1996; Sammut & Hanafi, 2000; Powell & Martens, 2005). In brief, by using the ASS mapping method developed by this study, there will be an improvement in aquaculture development decisions especially for people who work on intensive/semi-intensive farming. The mapping can also enable farmers to change to more appropriate land practices or to relocate aquaculture ponds to the hinterland or above the intertidal area. Other land practices stand to benefit from a knowledge of where ASS occur.

9.4 Limitations and Recommendations for Future Work

9.4.1. Limitations

The simple approach to ASS mapping utilized in this study has many practical applications. However, interpreting landforms types in multi-resolution satellite imageries is not always a simple task that can be conducted by every researcher. Highly skilled remote sensing and GIS experts with knowledge of geomorphology are needed to interpret landform types and soil forming processes. Similarly, to understand the hydro-geomorphic processes related to landform development, researchers need sound knowledge of hydrology and geomorphology.

Field surveys conducted in different seasons would describe hydro-geomorphic processes. Therefore, this type of study could be extended over a longer time period and involve more researchers from different fields to gather and analyse data over time using the findings of this project.

In this study, multi-temporal, remotely-sensed data were used to identify seasonal land-use differences for the dry and rainy seasons. However, soil samples were only taken during the dry season due to access issues in the rainy season. In fact, some HGUs have different conditions and land-use during different seasons which could influence vertical pyrite distribution, particularly in the upper soil layers where cultivation disturbs the soil profile. Therefore, this may limit interpretation of ASS presence and absence in some seasonally cultivated landform.

9.4.2 Recommendation for Future Work

Based on the results and the discussion of advantages and limitations of this study several areas for further research to improve the understanding of pyrite formation in HGUs are suggested:

1. The ASS distribution mapping in this study will be improved by involving more detailed soil sampling and analysis in the terrains that are undergoing continuous disturbance by humans, for example in ricefields where there is a cycle of soil usage. These different cycles can influence the variability of pyrite concentrations with a particular emphasis on contemporary pyrite formation and oxidation. Such a study would generate useful information that would add to the understanding of pyrite formation and oxidation under cultivation and also underpin strategies to remediate soils to increase productivity and reduce environmental impacts.

2. Improving the knowledge on estuary evolution and its role in ASS formation by involving stratigraphy in more detail and dating of soil layers.
3. Expanding the study areas (estuaries) which have more diverse mangrove species (and other brackish water vegetation types) with their significant distribution in a relatively large area will facilitate the development of this future research in investigating the role of different type of fauna in development of pyrite, supported by PCA statistical approach as has been initiated in this study.
4. Developing further research in other types of estuaries to examine whether the robust ASS mapping method developed in this study is applicable and whether there are different HGU characteristics that produce different types of ASS in other environments.
5. Developing a map and GIS database available for the decision-makers so they can assess the presence of ASS in coastal environments.
6. Exploring and identifying more advanced remote sensing and GIS analysis to refine the methods applied in this study. The use of remote sensing and GIS in this study was limited to visual interpretation that was labour-intensive in regards to interpreting land-use and landforms at different scales and on different types of remotely-sensed data, and to convert them into a digital format/layers. Appropriate digital image processing includes multi-spectral analysis for land-use mapping, object-oriented multi-resolution image segmentations for land-use, and landform mapping approaches. Other GIS modelling, such as artificial neural networks, decision tree analysis and data mining analysis for ASS mapping could be incorporated in the multi-level ASS mapping methods. Digital elevation models (DEMs) and flow accumulation methods could be used to derive the hydro-geomorphic information in order to define areas affected by inundation under different scenarios (seasonal or human control). Recent advanced ASS mapping studies (Huang *et al*; 2014; Beucher *et al*., 2013; Familiar, 2012) focus upon the relationship between spectral characteristics and soil analysis results without considering soil landscape evolution thereby missing opportunities to describe associations between soils and landforms. The use of high-resolution satellite imagery data could also

enhance the rapid assessment of ASS because it is able to provide more accurate information on vegetation types (in this case species of mangrove) through visual or digital image interpretation. The type of mangroves species that are related to the salinity levels and soil texture will provide more detailed information on how ASS develop in certain type of soil textures.

7. It is proposed that the National Thematic Maps of Coastal Environment workgroup should utilize the methods and maps from this study. The Indonesian coastal environmental maps which are commonly provided at a scale of 1: 100,000 and 1:50,000 (National Agency of Geo-spatial Information - BIG, 1994) do not provide information on the spatial distribution of ASS, despite their use as a foundation for coastal land-use planning. The outputs of the present study address the multi scale information ASS distribution from 1:250,000 to 1:50,000 and will complement the thematic mapping program that was recently established by in 2014; the results will be promulgated to this agency by the author and through ACIAR's extension activities. The adoption of the outputs from this research by BIG will foster adoption of the outputs by other government agencies (e.g. Ministry of Marine Affairs and Fisheries, Ministry of Forestry, and the Ministry of Agriculture), because they will utilize the maps produced by BIG as a standard and reliable mapping data resource.

9.5 Final Comments

This study revealed that the hydrogeomorphic processes that underpin development of landforms, vegetation and anthropogenic activities, significantly influenced the level and pattern of pyrite accumulation in different types of estuaries of Central Java. This ASS mapping method using multi-level mapping approaches captures optimum hydro-geomorphic information to interpret both landscape and ASS development processes. As a result, improved land capability and site selection criteria for brackish water aquaculture will improve both the planning and development of coastal resources in Indonesia.

REFERENCES

REFERENCES

Agus, F., Wahyunto, S.H., & Watung, R.L. (2004). *Environmental Consequences of Land Use Change in Indonesia*. Conference of International Soil Conservation Organization, Brisbane, Australia.

Ahern, C. R., Blunden, B., & Stone, Y. (Eds). (1998a). *Acid Sulfate Soils Laboratory Methods Guidelines*. The Acid Sulfate Soil Management Advisory Committee, Wollongbar, NSW, Australia.

Ahern, C. R., Stone, Y., & Blunden, B. (1998b). *Acid Sulfate Soils Assessment Guidelines.* The Acid Sulfate Soil Management Advisory Committee, Wollongbar, NSW, Australia.

Ahern, C.R., McElnea, A.E., & Sulivian, L.A. (2004). *Queensland Acid Sulfate Soils Manual*. Department of Natural Resources, Mines and Energy, Indooroopilly, Queensland, Australia.

Ahmad, D. S. (2009). Diversity of *Sonneratia alba* in coastal area of Central Java based on isozymic patterns of esterase and peroxidase. *Nusantara Bioscience*, *1,* 92-103.

Ahmad, D. S., Susilowati, A., & Wiryanto (2002). Relic habitat of mangrove vegetation in South Coast of Java. *Biodiversitas, 3(2),* 242-256.

Ahmed, F.B., & Dent, D.L. (1997). Resurrection of soil survey: A case study of the acid sulphate soil of the Gambia. II. Added value from spatial statistics. *Soil Use and Management*, *13,* 57-59.

Aldrian, E., & Susanto, R.D. (2003). Identification of three sominant rainfall regions within Indonesia and their relationship to sea surface temperature. *International Journal of Climatology*, *23(12),* 1435-1452.

Allen, J.R.L., & Pye, K. (1992). *Saltmarshes: Morphodnamics, Conservation, and Engineering Significance.* Press Syndicate of the University of Cambridge, Cambridge.

Alongi, D.M. (2002). Present state and future of the world's mangrove forest. *Environmental Conservation, 29(3),* 331–349.

AMS (1949). Map of Serayu River, Index: 4820-Jatilawang, US Army Mapping Service.

Anbazhagan, S., Ramasamy, S.M., & Gupta, S.D. (2005). Remote sensing and GIS for artificial recharge study, runoff estimation and planning in Ayyar Basin, Tamil Nadu, India. *Environmental Geology, 48,* 158–170.

Anda, M., Siswanto, A.B., & Subandiono, R.E. (2009). Properties of organic and acid sulfate soils and water of a 'reclaimed' tidal backswamp in Central Kalimantan, Indonesia. *Geoderma*, *149(1-2),* 54-65.

Andriesse, W. (1993). Acid sulphate soils: Diagnosing the illness. In D.L. Dent and M.E.F. Van Mensvoort (Eds). *Selected Papers of the Ho Chi Minh City Symposium on Acid Sulphate Soils* (pp. 11-29), ILRI, Netherlands.

Ardjosoediro, I., & Franz, G. (2007). *A Value Chain Assessment of the Aquaculture Sector in Indonesia*, AMARTA, Indonesia.

Astrom, M. (2001). Effect of widespread severely acidic soils on spatial features and abundance of trace elements in streams. *Journal of Geochemical Exploration*, *73,* 181-191.

Astrom, M., & Corin, N. (2003). Distribution of rare earth elements in anionic, cationic and particulate fractions in boreal humus – Rich streams affected by acid sulphate soils. *Water Research, 37,* 273–280.

Atkinson, G., Naylor, S.D., Flewin, T.C., Chapman, G.A., Murphy, C.L., Tulau, M.J., Milford, H.B. & Morand, D.T. (1998). *DLWC Acid Sulfate Soil Risk Mapping*. Department of Land and Water Conservation. Australia.

Avery, B.W. (1980). *Soil Classification for England and Wales*. Soil Survey, Technical Monograph, UK.

Babar, Md. (2005). *Hydrogeomorphology*. New India publishing Agency, Pitam Pura, New Dehli.

Bakosurtanal. 1998. Topography Maps of Central Java. Indonesia: Cibinong, Bogor.

Bala, B.K., & Hossain, M.A. (2009). Modeling of food security and ecological footprint of coastal zone of Bangladesh. *Environment, Development and Sustainability - A Multidisciplinary Approach to the Theory and Practice of Sustainable Development, 12(4),* 511-529

Baldwin, D. S., & Mark, F. (2009). Rehabilitation options for inland waterways impacted by sulfidic sediments – A Synthesis. *Journal of Environmental Management*, *91,* 311–319.

Barbiero, L, Mohamedou, A.O., Roger, L., Furian, S., Aventurier, A.J., Rémy, C., & Marlet, S. (2005). The origin of vertisols and their relationship to acid sulfate soils in the Senegal Valley. *Catena, 59,* 93–116.

Barbier, E.B., Hacker, S.D., Kennedy, C., Koch, E.W., Stier, A.C., & Silliman, B.R. (2011). The value of estuarine and coastal ecosystem services. *Ecological Monographs*, 81(2), 169–193.

Barson, M., & Lesslie, R. (2004). Land management practices – why they are important and how we know this. *National Workshop on Land Management Practices Information Priorities, Classification and Mapping, - Towards an Agreed National Approach*. Bureau of Rural Sciences, Canberra.

Behrens, T., Förster, H., Scholten, T., Steinrücken U., Spies, E. & Goldschmitt, M. (2005). Digital soil mapping using artificial neural networks. *Journal Plant Nutrition and Soil Science, 168(1),* 21–33.

Bellwood, P. (1987). The prehistory of Island Southeast Asia: A multidisciplinary review of recent research. *Journal of World Prehistory, 1(2),* 171-224.

Bemmelen, R.W. van (1949). *The Geology of Indonesia*. Martinus Nijhoff, The Hague.

Benjamin, C., & Robert, H. (2007). Cretaceous to late Miocene stratigraphic and tectonic evolution of West Java. *Proceedings of Indonesian Petroleum Association*, Indonesia.

Berdin, R.D., Sirinan, F.P., & Maeda, Y. (2003). Holocene relative sea-level changes and mangrove response in Southwest Bohol, Philippines. *Journal of Coastal Research, 19* (2), 304-313.

Berner, R.A. (1984). Sedimentary pyrite formation: An update. *Geochimica Cosmochimica Acta, 48,* 605-615.

Bertels, L, Vanderstraete, T., van Coillie, S., Knaeps, E., Sterckx, S., Goossens, R., & Deronde, B. (2008). Mapping of coral reefs using hyperspectral CASI Data - A case study: Fordata, Tanimbar, Indonesia. *International Journal of Remote Sensing, 29,* 2359–2391.

Bescansa, P. & Roquero, C. (1990). Characterization and classification of tidal marsh soils and plant communities in North-West Spain. *Catena, 17(4-5),* 347–355.

Beucher, A., Österholm P., Martinkauppi A., Edén P., & Fröjdö S. (2012). *Artificial neural network for acid sulfate soil mapping: Application to the Sirppujoki River catchment area, south-western Finland*. Åbo Akademi University, Finland Geological Survey of Finland, Kokkola, Finland.

Beveridge M.C., & Brooks, A.C. (2008). Impact of long-term training and extension support on small-scale carp polyculture farms of Bangladesh. *Journal of the World Aquaculture Society, 39(4),* 441-453.

Beveridge, M.C.M. (2007). *Cage Aquaculture*. Fishing News Books, Blackwell Science, Fifth Edition, Oxford.

Bird, E.F. (2007). *Coastal Geomorphology: An Introduction*. John Wiley and Sons, LTD, London.

Bird, E.F., & Ongkosongo, O.T.R. (2000). *Environmental Change of the Coast of Indonesia*. United Nations, University of Tokyo.

Black, P. E. (1990). *Watershed Hydrology*. Prentice Hall Inc., Englewood Cliffs, New Jersey.

Bloomfield, C., & Coulter, J.K. (1973). Genesis and management of acid sulfate soils. *Advance Agronomy, 25,* 265-326.

BMG (2000). Meteorology Data of Java from Year 2000 – 2020. National Agency of Meteorology and Geophysic, Jakarta, Indonesia.

BPDASPS (2007). Profil Balai Besar Wilayah Sungai Pemali Juana (Pemali Juana River Profiles), Direktorat Jenderal Sumberdaya Air, Departemen Pekerjaan Umum (Water Resources General Directorate, Department of Public Work).

BPDASSO (2010). Profil Balai Besar Wilayah Sungai Serayu Opak (Serayu Opak River Profiles), Direktorat Jenderal Sumberdaya Air, Departemen Pekerjaan Umum (Water Resources General Directorate, Department of Public Work).

Bocco, G., Mendoza, M., & Velazques, A. (2001). Remote sensing and GIS-based regional geomorphological mapping – a tool for land use planning in developing countries, *Geomorphology*, *39(3-4),* 211-219.

Boman, A., Åström, M., & Fröjdö, S. (2008). Sulfur dynamics in boreal acid sulfate soils rich in metastable iron sulfide - The Role of Artificial Drainage, *Chemical Geology*, *255,* 68–77.

Bortone, S.A (2005). *Estuarine Indicators*. CRC Marine Science Press, Washington D.C.

Bowmen, W.D. (2012). Nitrogen critical loads for alpine vegetation and soils in Rocky Mountain National Park, *Journal of Environmental Management*, *103,* 165-171.

Boyd, C.E. (2002). Mangrove and coastal aquaculture. In Stickney, R.R. & McVey, J.P. (Eds.), *Responsible marine aquaculture* (pp. 145-158). CAB International Publishing.

Boyd, R., Dalrymple, R.W., & Zaitlin, B.A. (1992) Classification of clastic coastal depositional environments, *Sedimentary Geology*, *80,* 139–150.

Brinkman, R., & Pons, L.J. (1972). Recognition and prediction of acid sulfate soil conditions. In Dost, H. (Ed.), *Acid Sulphate Soil: Proceedings of an International Symposium* (pp.169-203). Publication of International Institute for Land Reclamation and Improvement (ILRI), Wageningen.

Brinkman, R., Nguyen, B.V., Tran, K.T., Do, P. H., & Van Mensvoort, M.E.F. (1993). Sulphidic materials in the western Mekong Delta, Vietnam. *Catena*, *20,* 317-331.

Bregt, A.K., & Gesink, H.J. (1992). Mapping the conditional probability of soil variables. *Geoderma*, *53,* 15-29.

Brewer, R., & Walker, P.H. (1969). Weathering and soil development on a sequence of river terraces. *Australian Journal of Soil Research*, *20,* 293–305.

Brownswijk, J. J. B., Groenenberg, J.E. ,Ritsema, C.J., van Wijk, A.L.M., & Nugroho, K. (1995). Evaluation of water management strategies for acid sulphate soils using a simulation model: A case study in Indonesia. *Agriculture Water Management*, *27,* 125–142.

Brownswijk, J. J. B., Nugroho, K., Aribawa, I.B., Groenenberg, J.E., & Ritsema, C.J., (1993). Modeling of oxygen transport and pyrite oxidation in acid sulphate soils. *Journal of Environmental Quality, 22(3)*, 544-554.

Brown, J.H., & Prayitno, B. (1987). Backyard fish farming in Java, Indonesia. *Community Development Journal*, *22(3),* 237-241.

Bruijnzeel, L.A. (2004). Hydrological functions of tropical forest: Not seeing the soil for the trees? *Agriculture, Ecosystems and Environment*, *104,* 185–228.

Buchanan, S., Triantafilis, J., Odeh, I.O.A., & Subansinghe, R. (2012). Digital soil mapping of compositional particle-size fractions using proximal and remotely sensed ancillary data. *Geophysics*, 77(4), 201-211.

Bullock, D.S., & Bullock, D.G. (2000). Economic optimality of input application rates inprecision farming. *Precision Agriculture*. *2,* 71–101.

Bulluck III, L.R., Brosius, M., Evanylo, G.K., & Ristaino, J.B. (2002). Organic and synthetic fertility amendment influence soil microbial, physical and chemical properties on organic and conventional farms. *Applied Soil Ecology*, *19(2),* 147-160.

Burgess, T.M. & Webster, R. (1980). Optimal interpolation and isarithmic mapping of soil properties. II. Block kriging. *Journal of Soil Science*. *31*, 333-341.

Burrough, P. A., & McDonnell, R. (1998), *Principles of Geographical Information Systems.* Clarendon Press, Oxford.

Burton, E. D., Bush, R.T., & Sullivan, L.A. (2006). Elemental sulfur in drain sediments associated with acid sulfate soils. *Applied Geochemistry*, *21,* 1240–1247.

Burton, E. D, Bush, R.T., Sullivan, L.A., & Johnston, S.G. (2008). Mobility of arsenic and selected metals during re-flooding of iron- and organic-rich acid-sulfate soil. *Chemical Geology*, *253,* 64–73.

Bush, T.B., & Sullivan, L.A. (1999). Pyrite micromorphology in three Australian Holocene sediments. *Australian Journal of Soil Research, 37(4),* 637.

Bush, T.B., Fyfe, D., & Sullivan, L.A. (2004). Occurrence and abundance of monosulfidic black ooze in coastal acid sulfate soil landscapes. *Australian Journal of Soil Research*, *42,* 609 – 616.

Butler, B. E. (1958). Depositional Systems of the Riverine Plain in Relation to Soils. *C.S.I.R.O. Australian Soil Publication,* No. 10.

Butler, B. E. (1959). Periodic Phenomena in Landscapes as a Basis for Soil Studies. *C.S.I.R.O. Australian Soil Publication,* No. 14.

Camacho, A. S. & Bagarinao, T. U. (1987). Impact of fishpond development on the mangrove ecosystem in the Philippines. In *Mangroves of Asia and the Pacific: Status and Management,Technical Report UNDP/UNESCO Research and Training Pilot Programme on Mangrove Ecosystems in Asia and the Pacific* (RAS/79/002) (pp. 373 – 405). Natural Resources Management Center and National Mangrove Committee, Ministry of Natural Resources, Philippines.

Cambule, A.H., Rossiter, D.G. , & Stoorvogel, J.J. (2013). A methodology for digital soil mapping in poorly-accessible areas. *Geoderma*, *192,* 341–353.

Campbell, J.B. (2011). *Introduction to Remote Sensing*. Taylor and Francis, London, New York

Campbell, J.B., & Wynne, R.H. (2010). *Introduction to Remote Sensing*. The Guilford Press, New York.

Caratini, C., & Tissot, C. (1988). Paleogeographical evolution of the Mahakam Delta in Kalimantan, Indonesia during the Quaternary and Late Pliocene. *Review of Paleobotany and Palynology*, *55,* 211-228.

Carbonel, P., & Moyes, J. (1987). Late Quaternary paleoenvironments of the Mahakam Delta (Kalimantan, Indonesia). *Palaeogeography, Palaeoclimatology, Palaeoecology*, *61,* 265-284.

Carré, F., McBratney, A.B., Mayr, T., & Montanarella, L. (2007). Digital soil assessments: Beyond DSM. *Geoderma*, 142, 69–79

Carter, R.W.G. (1988). *Coastal Environment, An Introduction to the Physical, Ecological and Cultural System of Coastlines*. Academic Press, Toronto.

Carter R.W.G., & Woodroffe, C.D. (1994). *Coastal Evolution*, University Press, Cambridge University, UK.

Chang, K. (2002). *Introduction to Geographic Information Systems*. McGraw-Hill Publishing Company, New York.

Chen, S., Qinhuo, L., Chen, L., & Wang, J. (2004). Remote Sensing and DEM – Based Approach for Updating Acid Sulphate Soil Distribution: an example in Pearl River Estuary, South China. In Gao, W. and David, R. S. (Eds.). *Remote Sensing and Modeling of Ecosystems for Sustainability (pp 70-77)*, Proceeding of SPIE, Bellingham.

Chiem, N.H. (1993). Geo-pedological study of the Mekong Delta. *Southeast Asian Studies, 31(2),* 158-186.

Choe, E., Meer, F. van der, & Ruitenbeek, F. van (2008). Mapping of heavy metal pollution in stream sediments using combined geochemistry, field spectroscopy, and hyperspectral remote sensing: A case study of the Rodalquilar mining area, SE Spain. *Remote Sensing of Environment, 112,* 3222 – 3233.

Chong, V.C., Sasekumar, A., Leh, M.U.C., & D'Cruz, R. (1990). The fish and prawn communities of a Malaysian coastal mangrove system, with comparisons to adjacent mud flats and inshore waters. *Estuarine Coast and Shelf Science. 31,* 703-722.

Chorley, R.J. (1972). *Spatial Analysis in Geomorphology*. British Geomorphological Research Group, Methuen & Co Ltd, London.

Christanto, N., Hadmoko, D.S., Westen, C.J., Lavigne, F., Sartohadi, J., & Setiawan, M.A. (2009). Characteristic and Behavior of Rainfall Induced Landslides in Java Island, Indonesia: an Overview. *Geophysical Research Abstracts*, *11,* 4069-4070.

Claff, S.R., Sullivan, L.A., Burton, E.D., Bush, R.T., & Johnston, S.G. (2011). Partitioning of metals in a degraded acid sulfate soil landscape: Influence of tidal re-inundation. *Chemosphere, 85(8),* 1220-1226.

Cloke, I.R., Milsom, J., & Blundell, J.M. (1999). Implications of gravity data from East Kalimantan and the Makassar Straits: A solution to the origin of the Makassar Straits? *Journal of Asian Earth Science*, *17,* 61-78.

Cogger, C.G., Kennedy, P.E., & Carlson, D. (1992). Seasonally saturated soils in the puget lowland II: Measuring and interpreting redox potentials. *Soil Science*, *154 (1)*, 50-58.

Cook, F.J., Hick, W., Gardner, E.A., Carlin, G.D., & Froggatt, D.W. (2000). Export of acidity in drainage water from acid sulfate soils. *Marine Pollution Bulletin*, *41,* 319-326.

Corbane, C., Raclot, D, Jacob, F., Albergel, J., & Andrieux, P. (2008). Remote sensing of soil surface characteristics from a multiscale classification approach. *Catena*, *75*, 308 – 318.

Corfield, J. (2000). The effect of acid sulphate run-off on a subtidal estuarine macrobenthic community in the Richmond River, NSW, Australia. *Journal of Marine Science*, *57(5)*, 1517-1523.

CSR (1983). Indonesian Soil Classification 1983. Indonesian Soil Research Centre.

CSR (2000). Indonesian Soil Classification 2000. Indonesian Soil Research Centre.

Dalrymple, R., Zaitlin, B.A., & Boyd, R. (1992). Estuarine facies models: conceptual basis and stratigraphic implications. *Journal of Sedimentary Research*, ***62(6)***, 1130-1146.

Dam, M.A.C., Suparan. P., Nossin, J.J., & Voskuil, R. (1996). A Chronology for geomorphological gevelopment in the greater Bandung area, West-Java, Indonesia. *Journal of Southeast Asian Earth Science*, *14,* 101 – 115.

Danoedoro, P. (2006). *Versatile Land-use Information for Local Planning in Indonesia*, PhD Thesis, Centre for Remote Sensing and Spatial Information Science (CRSSIS), School of Geography, Planning and Architecture, University of Queensland.

Datta, D., Chattopadhyay, R.N., Guha, P. (2012). Community based mangrove management: A review on status and sustainability. *Journal of Environmental Science, 107,* 84-95.

David, M. Theobald, Don L. S., White, D., Urquhart, N.S., Olsen, A.R., & Norman, J.B. (2007). Using GIS to generate spatially balanced random survey designs for natural resource applications. *Environmental Management*, *40,* 134 – 146.

Davis, R.A, Jr. (1997). *The Evolving Coast.* A Scientific American Library, New York.

Davies, J.L. (1964). A morphogenic approach to world shorelines. *Geomorphology, 8,* 27-42.

Davies, J.L. (1980). *Geographical variation in coastal development*. 2nd edition, Longman, New York.

Davydova, N.N., Subetto, D. A., Khomutova, V. I., & Sapelko, T.V. (2001). Late Pleistocene – Holocene paleolimnology of three Northwestern Russian lakes. *Journal of Paleolimnology*, *26,* 37 – 51.

DeMers, M.N. (2000). *Fundamentals of Geographic Information Systems*. John Wiley, Technology & Engineering, New York, Chichester.

Dent, D.L. (1986). *Acid sulphate soils: a baseline for research and development,* International Institute for Land Reclamation and Improvement ILRI, Wageningen, The Netherlands.

Dent, D.L. (1991). Reclamation of acid sulphate soils. *Advance Soil Science, 17,* 79-122.

Dent, D.L. (1993). Bottom-up and top-down development of acid sulphate soil, *Catena*, *20(4)*, 419-425.

Dent, D.L., & Ahmed, F. (1995). Resurrection of soil survey: A case study of acid sulphate soils on the flood plain of the River Gambia I - data validation, taxonomic and mapping units. *Soil Use Management*, *11 (2)*, 79-122.

Dent, D.L., & Pons, L. J. (1995). A world perspective on Acid Sulphate Soils. *Geoderma*, *67,* 263 – 276.

De Vries, W., Kros, J., & Salm, C. (1995). Modelling the impact of acid deposition and nutrient cycling on forest soils. *Ecological Modelling*, *79*, 231-254.

De Wit, P.A.J.W. (1990). *Hydrological Research in Unit Tatas*. LAWOO/AARD Scientific Report, 25. Research Program on Acid Sulfate Soil in Humid Tropics, LAWOO, Wageningen.

DGA (1994). *Aquaculture Production Statistics 1994* (pp. 124). Jakarta, Indonesia: Directorate General of Aquaculture.

DGA (2003). *Aquaculture Production Statistics 2001* (pp. 243). Jakarta, Indonesia: Directorate General of Aquaculture.

DGA (2004a). *Aquaculture Production Statistics 2003* (pp. 121). Jakarta, Indonesia: Directorate General of Aquaculture.

DGA (2004b). *Masterplan of Brackish Water Area Development Program 2004* (pp. 272). Jakarta, Indonesia: Directorate General of Aquaculture.

DGA (2004c). *Masterplan of Mariculture Area Development Program 2004* (pp. 137). Jakarta, Indonesia: Directorate General of Aquaculture.

DGA (2014). *Aquaculture Production Statistics 2013*. Jakarta, Indonesia: Directorate General of Aquaculture.

DGWR (2013). *River Management in Indonesia.* Jakarta, Indonesia: Directorate General of Water Resources.

Dieberg, F.E., & Kiattisimkul, W. (1996). Issues, impacts, and implications of shrimp aquaculture in Thailand. *Environmental Management*, *20 (5)*, 649-666.

Diemont, H., Pons, L.J., & Dent, D.L. (1992). Standard profiles of acid sulphate soil. In D.L. Dent, & M.E.F. van Mensvoort (Eds.), *Acid Sulphate Soils, selected papers of the Saigon Symposium* (pp. 263-276). Wageningen: ILRI.

Dijk, A.I.J.M., Bruijnzee, L.A., & Purwanto, E. (2004). *Conserving Soil and Water for Society: Sharing Solutions*, *218* (pp. 1-6). Soil conservation in upland Java, Indonesia: Past failures, recent findings and future prospects, 13th International Soil Conservation Organisation Conference–Brisbane.

DoF (2006). *The* Central Java *Green Belt Mangrove Corridor Program*: *Report*. Indonesia: Regional Agency of Forestry (Dinas Kehutanan Jawa Tengah).

DoF (2007). *Statistic of Central Java Forestry* (pp. 93). Indonesia: Regional Agency of Forestry (Dinas Kehutanan Jawa Tengah).

Dosmet, P.J.J., & Govers, G. (1996). A GIS procedure for automatically calculating the USLE LS factor on topographically complex landscape units. *Journal of Soil and Water Conservation,* 51 (5), 427-433.

Drury, L.W., & Roman, D. (1982). Chronological correlation of interglacial sediments of the Richmond River valley, New South Wales. In W. Ambrose, & P. Duerdin (Eds.), *Archaeometry: An Australasian Perspective* (pp. 290-296). Australia: Department of Prehistory Research School of Pacific Studies Australian National University.

Drummond, M.A., & Loveland, T.R. (2010). Land-use pressure and a transition to forest-cover loss in Wastern United States. *BioScience, 60*(4), 286-298.

Dunn, F.L., & Dunn, D.D. (1977). Maritime adaptations and exploitation of marine resources in Sundaic Southeast Asian prehistoric. *Modern Quaternary Research in Southeast Asia, 3,* 1-28.

Dunn, J.R., Ridgway, K.R. (2002). Mapping ocean properties in regions of complex topography. *Journal of Deep-Sea Research I, 49,* 591 – 604.

Dutrieux, E. (1991). Study of the ecological functioning of the Mahakam Delta (East Kalimantan, Indonesia), notes and discussions. *Estuarine Coastal and Shelf Science,* 32, 415 – 420.

Dwivedi, R.S., Ramana, K.V., Thammappa, S.S., & Singh, A.N. (2001). The utility of IRS-1C LISS-Ill and PAN-merged data for mapping salt-affected soils. *Photogrammetric Engineering and Remote Sensing, 67*(10), 1167-1176.

Earth Trend. (2003). *Coastal and Marine Ecosystems: Indonesia*. Earth Trends Country Profiles. Accessed 26 October 2009. doi : www.earthtrends.wri.org.

Ellison, J. (2005). Holocene palynology and sea-level change in two estuaries in Southern Irian Jaya. *Palaeography, Palaeclimatology, Palaeoecology, 220,* 291 – 309.

Endreny, T.A, Wood, E. F., & Lettenmaier, D. P. (2000). Satellite-derived digital elevation model accuracy: Hydrogeomorphological analysis requirements. *Hydrological Processes, 14,* 1-20.

Engelen, G. B. (1980). The Serayu valley project, Central Java, Indonesia. *Geo Journal, 4(1),* 71-75.

Engle, V.D., Kurttz, J.C., Smith, L.M., Chancy, C., & Bourgeois, P. (2007). A classification of U.S. estuaries based on physical and hydrologic attributes. *Environmental Monitoring and Assessment, 129 (1-3),* 397-412.

Erwidodo, & Rina, O. (2005). *Indonesia's Shrimp Exports: Meeting the Challenge of Quality Standards*. Foreign Agricultural Service USDA.

Everaarts, J.M., J.P., Kastoro, W., Fischer, C.V., Razak, H., & Sumanta, I. (1989). Copper, zinc and cadmium in benthic organism from the Java Sea and estuarine and coastal areas around East Java. *Netherlands Journal of Sea Research, 23,* 415-426.

Facchinelli, A., Sacchi, E., & Mallen, L. (2001). Multivariate statistical and GIS–based approach to identify heavy metal sources in soils. *Environmental Pollution, 114,* 313 – 324. Amsterdam: Elsevier Science Publication.

Fanning, D. S., & Burch, S. N. (2000). *Reclamation of Drastically Disturbed Lands, Coastal Acid Sulfate Soils* (pp. 921-937). College Park, Maryland, USA: University of Maryland.

Fanning, D. S., Rabenhorst, M.C., Balduff, D.M., Wagner, D.P, Orr, R.S., & Zurheide, P.K. (2009). An acid sulfate perspective on landscape/seascape soil mineralogy in the U.S.Mid-Atlantic Region. *Geoderma*. Elsevier Science, Ltd.

FAO (1972). FAO/UNESCO Soil Legend. Rome: Food and Agriculture Organisation.

FAO (2007). The world's mangroves 1980–2005. *FAO Forestry Paper, 153*. Rome: Food and Agriculture Organization of the United Nations.

FAO (2009). *Fish as Feed Inputs for Aquaculture: Practices, Sustainability and Implications*. Rome: Food and Agriculture Organisation of the United Nations.

Ferreira, T.O., Vidal-Torrado, P., Otero, X.L., & Macias, F. (2007). Are mangrove forest substrates sediments or soils? A case study in southeastern Brazil. *Catena*, *70 (1),* 79-91.

Fetter, C.W. (2001). *Applied Hydrogeology*. Upper Saddle River, New Jersey: Prentice-Hall, Inc.

Fitzgerald, W.J. (2000). Integrated mangrove forest and aquaculture systems in Indonesia. In J.H. Primavera, Garcia, L. M. B., Castaños, M. T. & Surtida, M. B. (Eds.), *Mangrove-friendly Aquaculture* (pp. 21-34). Proceedings of the workshop on mangrove-friendly aquaculture organized by the SEAFDEAC Aquaculture Department, Januari 11-15, Iloilo City, Phillipines.

Fitzpatrick, R.W., Fritsch, E., & Self, P.G. (1996). Interpretation of soil features produced by ancient and modem processes in degraded landscapes: Development of saline sulfidic features in non-tidal seepage areas. *Geoderma, 69,* 1-29.

Fitzpatrick, R.W., Powell, B., McKenzie, N.J., Maschmedt, D.J., Schoknecht, N., & Jacquier, D.W. (2003). Demands on soil classification in Australia. In: Eswaran, H., Rice, T., Ahrens, R., Stewart, B.A. (Eds.), *Soil Classification A Global Desk Reference*. CRC Press, ISBN 0-8493-1339-2.

Fitzpatrick, R.W., Hicks, W., Marvanek, S., Raven, M., Dahlhaus, P., & Cox, J. (2007). *Scoping Study of Coastal and Inland Acid Sulphate Soils in the Corangamite CMA*. Australia: CSIRO Land and Water Science Report.

Fitzpatrick, R.W., Powell, B., & Marvanek, S. (2008a). Atlas of Australian acid sulfate soils. In R.W. Fitzpatrick & Paul Shand (Eds.), *Thematic Volume: Island Acid Sulfate Soil Systems Across Australia* (chapter 2: 12 pp). Perth, Australia.

Fitzpatrick, R.W., Marvanek, S., Shand, P.,Merry, R., & Thomas, M. (2008b). *Acid Sulfate Soil Maps of the River Murray below Blanchetown (Lock 1) and Lakes Alexandrina and Albert when Water Levels were at Pre-Drought and Current Drought Conditions*. Australia: CSIRO Land and Water Science Report.

Fitzpatrick, R.W., Powell, B., & Marvanek, S. (2008c). Atlas of Australian acid sulfate soils. In Fitzpatrick, R. & Shand, P. (Eds.), *Island Acid, Sulfate Soil Systems Across Australia* (pp 75-89). CRC LEME Open File Report No. 249. (Thematic Volume). Perth, Australia: CRC LEME,

Fitzpatrick, R.W., Baker, A.K.M., Shand, P., Merry, R.H., Grealish, G., & Mosley, L.M. (2012). A modern soil-lansdcape characterization approach to reconstructing and predicting pedogenic pathways of inland acid sulfate soils. *Proceeding 7th International Acid Sulfate Soil Conference.* Finland: Vaasa.

Fortin, M.J., & Mark, D. (2005). *Spatial Analysis: A Guide for Ecologists*. Australia: Cambridge University Press.

Fox, G.A., & Metla, R. (2005). Soil property analysis using principal components analysis, soil linear, and regression models. *Soil Science Society of America Journal, 69(6),* 1782- 1787.

Fresco, L.O., & Kroonenberg, S.B. (1992). Time and spatial scales in ecological sustainability. *Land Use Policy, 9,* 155-182.

Fritsch, E. & Fitzpatrick, R.W. (1994). Interpretation of soil features produced by ancient and modern processesin degraded landscapes: A new method for constructing conceptual soil-water-landscape models. *Australian Journal of Soil Research, 32,* 880–885.

Fulthorpe, C.S. (2008). Pre-quaternary sea-level changes: records and processes. *Basin Research, 20,* 161-162. Blackwell Publishing Ltd.

Gerrard, J. (1992). *Soil Geomorphology*. 2-6 Boundary Row, London SE1 8HN, UK: Chapman & Hall.

Gessler P. E., Chadwick, O. A. ,Chamran, K., Althouse, L., & Holmes, K. (2000). Modeling soil–landscape and ecosystem properties using terrain attributes. *Soil Science Society of America Journal, 64(6),* 2046-2056.

Gessler, P.E., Moore, I.G., McKenzie, N. J., & Ryan, P.J. (1995). Soil-landscape modelling andspatial prediction of soil attributes. *International Journal of Geographical Information Systems, 9 (4),* 421-432.

Getis, A., & Ord, J.K. (1996). Local Spatial Statistics an Overview. In Longley, P., & Batty, M., *Spatial Analysis: Modelling in a GIS Environment* (pp. 263 – 277.). Canada: John Willey & Sons.

Goffau, A. de, & Linden, P. van der. (1982). Later tertiary and quaternary landscape development, of the Kroya Beach ridge area, (South Central Java, Indonesia). *Geologie en Mijnbouw*, *6 (1-2),* 131-140.

Golez, N. V. (1995). Formation of acid sulfate soil and its implications to brackishwater ponds. *Aquacultural Engineering*, *14(4),* 297-316.

Gosavi, K., Sammut, J., Gifford, S., & Jankowski, J. (2004). Macroalgae biomonitors of trace metal contamination in acid sulfate soil aquaculture ponds. *Science of the Total Environment, 324,* 25-39.

Graaf, G.J. de, & Xuan, T.T. (1998). Extensive shrimp farming, mangrove clearance and marine fisheries in the Southern Provinces of Vietnam. *Mangroves and Salt Marshes, 2 (3),* 159-166.

Granados, F.L., Jurado-Exposito, M., Pena-Barragan, J.M., & Garcia-Torres, L. (2005). Using geostatistical and remote sensing approaches for mapping soil properties. *European Journal of Agronomy, 23,* 279 – 289.

Green, R., MacDonald, B.C.T., Melville, M.D., & Waite, T.D. (2006). Hydrochemistry of episodic drainage waters discharged from an acid sulfate soil affected catchment. *Journal of Hydrology, 325,* 356–375.

Grieve, I. C. (1999). Effects of parent material on the chemical composition of soil drainage waters. *Geoderma, 90,* 49–64.

Gruijter, J.J. de Brus, D.J., Bierkens, M.F.P., & Knotters, M. (2006). *Sampling for Natural Resource Monitoring*. Berlin: Springer-Verlag.

Gupta, A. (2007). *The Large River: Geomorphology and Management*. England: John Willey and Sons.

Haberle, S.G., & Ledru, M.P. (2001). Correlations among charcoal records of fires from the part 16,000 years in Indonesia, Papua New Guinea, Central and South America. *Quaternary Research, 55,* 97 – 104.

Hamada, J., Yamanaka, M.D., Matsumoto, J., Fukao, S., Winarso, P.A., & Sribimawati, T. (2002). Spatial and temporal variations of the rainy season over Indonesia and their link to ENSO. *Journal of the Meteorological Society of Japan, 80(2),* 285-310.

Hanafi, A., & Ahmad, T. (1999). *Shrimp Culture in Indonesia: Key Sustainability and Research Issues*. Maros, Indonesia: Research Institute for Coastal Fisheries.

Hanhart, K., & van Ni, D. (1993). Water management on rice fields at Hoa An in the Mekong Delta. In Dent, D.L., van Mensvoort, M.E.F. (Eds.), *Selected Papers of the Ho Chin Minh City Symposium on Acid Sulphate Soils* (pp. 161–175) Vol. 53. Wageningen, The Netherlands: ILRI Publication.

Haraguchi, A. (2007). Effect of sulfuric acid discharge on river water chemistry in peat swamp forest in Central Kalimantan, Indonesia. *Limnology, 8,* 175-182.

Haraguchi, A., Akioka, M., & Shimada, S. (2005). Does pyrite oxidation contribute to the acidification of tropical peat? A case study in a peat swamp forest in Central Kalimantan, Indonesia. *Nutrient Cycling in Agroecosystems, 71,* 101 – 108.

Hariati, A. M., Wiadnya, D.G.R., Tanck. M.W.T., Boon, J.H., & Verdegem, M.C.J. (1996). Penaeus monodon (Fabricius) production related to Water Quality in East Java, Indonesia. *Aquaculture Research, 27,* 255 – 260.

Harris, R. (2006). Rise and fall of the eastern great Indonesian arc recorded by the assembly, dispersion and accretion of the Banda Terrane, Timor. *Gondwana Research, 10,* 207 – 231.

Hart, B.T. (2004). Environmental risks associated with new irrigation schemes in Northern Australia. *Ecological Management & Restoration, 5 (2),* 106-110.

Hart, B. T., Day, G., Sharp-Paul, A., & Beer, T. (1988). Water quality variations During a flood event in the Annan River, North Queensland. *Australian Journal of Marine Freshwater Resources, 39,* 225-43.

Hart, B. T., Ottoway, E. M., & Noller, B. N. (1987). Magela creek system, Northern Australia I 1982-1983 wet season water quality. *Australian Journal of Marine and Freshwater Research, 38,* 261-88.

Hashidoko, Y, Kitagawa, E., Iwahashi, H., Purnomo, E., Hasegawa, T., & Tahara, S. (2007). Design of sphingomonad-detecting probes for a DNA aArray, and its application to investigate the behavior, distribution, and source of rhizospherous spingomonas and other sphingomonads inhabiting an acid sulfate soil paddock in Kalimantan, Indonesia. *Bioscience, Biotechnology and Biochemistr*y, *71,* 343 – 351.

Haslett, S.K. (2000). *Coastal System: Introductions to Environment Series*. London: Routledge.

Hayes, M.O. (1975). Morphology of sand accumulation in estuaries: an introduction to the symposium. *Estuarine Research, 2,* 3-22.

Hazelton, P. A., & Murphy, B.W. (2007). *Interpreting Soil Test Result: What Do All The Numbers Mean?* Coolingwood: NSW Department of Natural Resources, CSIRO Publishing.

Hengl, T., & Rossiter, D.G. (2003). Supervised landform classification to enhance and replace photo-interpretation in semi-detailed soil survey. *Soil Science Society of America Journal, 67 (6),* 1810-1822.

Hewitt, A.E. (1993). Predictive modelling in soil survey. *Soils Fertilizers, 56,* 305-304

Hicks , W.S., Bowman, G.M., & Fitzpatrick, R.W. (1999). East Trinity, acid sulfate soil part 1, environmental hazard. *CSIRO Land Water and Water Technical Report 14/99, Australia*.

Hinrichs, S., Nordhaus, I., & Geist Status, S.J. (2009). Diversity and distribution patterns of mangrove vegetation in the Segara Anakan Lagoon, Java, Indonesia. *Regional Environmental Change*, *9 (4),* 275-289.

HODIN (2008). *Tidal Range Data 1995 – 2010*. Indonesia: Dinas Hidro-Oseanografi (Hydro-oceanographic Office of Indonesia).

Hoekstra, P. (1988). Coastal hydrodynamics, geomorphology and sedimentary environment of two major Javanese river deltas. Program and Preliminary result from snellius II expedition (Indonesia). *Journal of Southeast Asian Earth Science, 2 (2),* 95-106.

Hoekstra, P., Nolting, R.F., & Van der Sloot, H.A. (1989). Supply and dispersion of water and suspended matter of the Rivers Solo and Brantas into the coastal waters of East Java, Indonesia. *Netherlands Journal of Sea Research, 23 (4),* 501 – 515.

Hoffman, R.R., & Markman, A.B. (2001). *Interpreting Remote Sensing Imagery: Human Factors*. USA: Lewis Publisher.

Hole, F.D., & Campbell J. B. (1985). *Soil Landscape Analysis*. London, England: Routlege& Kegan Paul plc.

Horton, B.P., Whittaker, E., & Thomson, K.H. (2005). The development of a modern foraminifera data set for sea-level reconstructions, Wakatobi Marine National Park, Southeast Sulawesi, Indonesia. *Journal of Foraminiferal Research, 35 (1),* 1 – 14.

Hoyer, A., & Hobma, T.W. (1989). *Results on Water Management Experiments in Unit Tatas*. LAWOO/AARD Scientific Report, No.12, Research Program on Acid Sulfate Soil in Humid Tropics, LAWOO, Wageningen.

Hume, M.T., Snelder, T., Weatherhead, M., & Liefting, R. (2007). A controlling factor approach to estuary classification. *Ocean and Coastal Management, 50,* 905-929.

Husson, O., Verburg, P.H., Phung, M.T., & Mensvoort, M.E.F. van (2000). Spatial variability of acid sulphate soils in the plain of reeds, Mekong Delta, Vietnam. *Geoderma, 97,* 1-19.

Hutabarat, J. (2008). *Coastal Aquaculture Development in Central Java, Its Prospects and Problems*. Presented paper in international symposium: "Development and Conservation of Desired Ecological Coastal Zone" held by Research Institute of Marine Science and Technology, Korea Maritime University-Busan South Korea.

Hutagalung, H.P. (1987). Mercury content in the water and marine organisms in Angke Estuary, Jakarta Bay. *Bulletin of Environmental Contamination and Toxicology, 39,* 406 – 411.

Hyne, R.V., & Scott, P.W. (1997). Toxicity of acid sulphate soil leachate and aluminium to the embryos and larvae of Australian Bass (*Macquaria novemaculeata*) in estuarine water. *Environmental Pollution, 97(3),* 221-227.

Ibrahim, Z.Z., Loi, L.S., & Abdullah, R. (1996). Classification of Malaysia estuary for develoment planning, aquatic conservation. *Marine and Freshwater Ecosystems, 6 (4),* 195 – 203.

IBS (2003). *Indonesian in Numbers (Indonesia dalam Angka) 2002*. Indonesian Bureau of Statistics.

IBS (2009). *Indonesian in Numbers (Indonesia dalam Angka) 2008*. Indonesian Bureau of Statistics.

IBS (2010). *Statistics of Indonesia 2009*. Indonesian Bureau of Statistics.

IBS (2012). *Indonesian in Numbers (Indonesia dalam Angka) 2011*. Indonesian Bureau of Statistics.

Ilman, M, Iwan, T.C.W., & Suryadiputra, I.N.N. (2011). *State of the Art Information on Mangrove Ecosystem in Indonesia*. Wetland International Indonesia Program.

Islam, S.N. (2014). An analysis of the damages of Chakoria Sundarban mangrove wetlands and consequences on community livelihoods in south east coast of Bangladesh. *International Journal of Environment and Sustainable Development. 13(2),* 153-171**.**

Islam, G.M., Islam, A., Rahman, M., Lazar, A., & Mukhopadhyay, A. (2014). Implications of agricultural land use change to ecosystem services in the Ganges delta. *Journal of Environmental Management*, in press.

Jackson, D.W.T., Cooper, J.A.G., & Del Rio, L. (2002). Geological control of beach morphodynamic state. *Marine Geology*, *216 (4),* 297–314.

Jakobs, A.L., & Baker, D.E. (2004). Sustainable soil management – The management of soil growing media during the planning and design of road projects (pp. 1-6) in Queensland Australia. *Conserving Soil and Water for Society: Sharing Solutions* (No.1009). Australia: Queensland Department of Main Roads.

Jennerjahn, T.C., Ittekkot, V., Klopper, S., Adi, S., Nugroho, A.P., Sudiana, N., Yusmal, A., Prihartanto, & Gayw-Haake, B. (2004). Biogeochemistry of a tropical river affected by human activities in its catchment: Brantas River estuary and coastal water of Madura Strait, Java, Indonesia. *Journal of Estuarine, Coastal and Shelf Science, 60,* 503–514.

Jensen, J.R. (2007). *Remote Sensing Of The Environment: An Earth Resource Perspective*. New York: Pearson Prentice Hall.

Johnson, D.B. (2010). The biogeochemistry of biomining. *Geomicrobiology: Molecular and Environmental Perspective,* 401-426.

Johnston, S.G., Bush, R.T., Keene, A.F., Sullivan, L.A., Burton, D.,Martens, M., McElnea, L.P., & Wilgraham, S.T. (2009b). Contemporary pedogenesis of severely degraded tropical acid sulfate soils after introduction of regular tidal inundation. *Geoderma, 149,* 335–346.

Johnston, S.G., Bush, R..T., Sullivan, L.A., Burton, E.D., Smith, D., Martens, M., McElnea, A.E., Ahern, C.R., Poweel, B., Stepens, L.P., Wilgraham, S.T., & Hell, S. Van. (2009a). Changes in water quality following tidal inundation of coastal lowland acid sulfate soil landscapes. *Estuarine, Coastal and Shelf Science, 81,* 257 – 266.

Johnston, S.G., Slavich, P.G., & Hirsta, P. (2005). The impact of controlled tidal exchange on drainage water quality in acid sulphate soil backswamps. *Agricultural Water Management, 73,* 87–111.

Joseph, V., Thornton, A., Pearson, S., and Pauli, D. (2013). Occupational transition in three coastal villages in Central Java, Indonesia, in the context of sea level rise: a case study. *Natural Hazard, 69 (1),* 675-694.

Jonnel, M., Henriksson, P. (2014). Mangrove–shrimp farms in Vietnam—Comparing organic and conventional systems using life cycle assessment. *Aquaculture, in press.*

Kawaguchi, K., & Kyuma, K. (1976). Paddy soils in Tropical Asia: Characteristics of paddy soils in each country (part 6). *South East Asian Studies, 14 (3),* 177-192.

Khan, F.R., Misra, S.K., Gracia-Alonso, J., Smith, B.D., Strekopytov, S., Rainbow, P.S., Luoma, S.N., & Valsami-Jones E. (2012). Bioaccumulation dynamic and modeling in an estuarine invertebrate following aqueous exposure to nanosized and dissolved silver. *Environmental Science and Technology, 46(14),* 7621-7628.

Kinsela, A.S., & Meville, M.D. (2004). Mechanisms of acid sulfate soil oxidation and leaching under sugarcane cropping. *Soil Research, 42 (6),* 569–578.

Kerry, R., & Oliver, A.O. (2011). Soil geomorphology: Identifying relations between the scale of spatial variation and soil processes using the variogram. *Geomorphology, 130 (1-2),* 40–54.

Knighton, D. (1998). *Fluvial Forms and Processes*. London: Hodder Arnold.

Koentjaraningrat, R.M. (1961). *Some Social Anthropological Observations on Gotong Royong Practices in Two Villages of Central Java*. Ithaca: Cornell University.

Kongkeo, H. (1997). Comparison of intensive shrimp farming systems in Indonesia, Philippines, Taiwan, and Thailand. *Aquaculture Research, 28,* 789 – 796.

Konsten, C.J.M., van Breemen, N., Supping, S., Aribawa, I.B., & Groenenberg, J.E. (1994). Effects of flooding on pH of rice-producind, acid sulfate soil in Indonesia. *Soil Science Society of American Journal. 58,* 871-883.

Kopp, H., Flueh, E.R., Petersen, C.J., Weinrebe, W., & Witter, A. (2006). The Java margin revisited: Evidence for subduction erosion of Java. *Earth and Planetary Science Letters, 242,* 130 – 142.

Koropitan, A.F., & Ikeda, M. (2008). Three-dimensional modeling of tidal circulation and mixing over the Java Sea. *Journal of Oceanography, 64(1),* 61-80.

Krampe, K. (1982). *Prospects of Groundwater Development for Rural Water Supply in Central Java Province Indonesia* (pp. 230). Technical Report, German Agency for Technical Cooperation an World Health Organization, Hannover.

Kulkova, M.A., & Matzurkeyich, A.N. (2001). Chronology and palaeoclimate of prehistoric sites in Western Dvina-Lovat Area of North-Western Russia. *Absolute Geochronometria, 20,* 87 – 94.

Kusmana, C., & Onrizal, D. (1998). *Mangrove forest inventory in five provinces: West Java, Central Java, East Java, Lampung and North Sumatra*, Bogor: Faculty of Forestry, Bogor Agricultural University.

Kusumastanto, T., & Jolie, C.M. (1998). A multiperiod programming evaluation of brackishwater shrimp aquaculture development in Indonesia 1989/1990–1998/1999. *Aquaculture, 159 (3-4),* 317–331.

Koolsterman, F.H. (1989). *Groundwater Flow Systems in the Northern Coastal Lowlands of West- and Central Java, Indonesia: An Earth-scientific Approach*. Indonesia: Kanisius.

Krauskopf., K.B., & Bird, D.K. (1967). *Introduction to Geochemistry*. New York: McGraw Hill. Inc.

Lane, S. N., Westaway, R.M., & Hicks, D.M. (2003). Estimation of erosion and deposition volumes in a large, gravel-bed, braided river using synoptic remote sensing. *Earth Surface Processes and Landforms, 28,* 249 – 271.

Larssen, T., Duan, L., & Mulder, J. (2011). Deposition and leaching of sulfur, nitrogen and calcium in four forested catchments in China: implications for acidification. *Environmental Science and Technology, 45(4),* 1192-1198.

Le, T.M.H., Collins, R.N., & Waite, T.D. (2008). Influence of metal ions and pH on the hydraulic properties of potential acid sulfate soils. *Journal of Hydrology, 356,* 261– 270.

Lee, S., & Choi, J. (2004). Landslide susceptibility mapping using GIS and the weight-of-evidence model. *International Journal of Geographical Information Science,* 18 (8), *789-814.*

Lee, S.Y., Primavera, J.H., Dahdouh-Guebas, F., McKee, K., Bosire, J.O., Cannicci, S., Diele, K., Fromard, F., Koedam, N., Marchand, C., Mendelssohn, I., Mukherjee, N., & Record, S. (2014). Ecological role and services of tropical mangrove ecosystems: a reassessment. Global Ecology and Biogeography, 23(7), 726-743.

Lesslie, R., Barson, M., & Smith, J. (2014). Land use information for integrated natural resources management – a coordinated national mapping program for Australia. *Journal of Land-use Science, 1 (1),* 45-62.

Lillesand, T.M., Kiefer, R.W., & Chipman, J.W. (2004). *Remote Sensing and Image Interpretation*. New York: John Willey & Sons.

Li, Z., Saito, Y., Mao, L., Tamura, T., Song, B., Zhang, Y., Lu, A., Sieng, S., Li, J. (2012). Mid-Holocene mangrove succession and its response to sea-level change in the upper Mekong River delta, Cambodia. *Quaternary Research, 78* (2), 386-399.

Lin, C. (1998). Chemical controls on acid discharges from acid sulfate soils under sugarcane cropping in an Eastern Australian estuarine floodplain. *Environmental Pollution, 102 (1-2),* 269–276.

Lin, C. (2012). Climate change adaptation in acid sulfate landscapes. *American Journal of Environmental Science, 8 (4),* 433-442.

Lin, C., & Melville, M. D. (1993). Control of soil acidification by fluvial sedimentation in an estuarine flood plain, Eastern Australia. *Sedimentary Geology, 85,* 271-284.

Lin, C., & Melville, M.D. (1994). Acid sulphate soil-landscape relationships in the Pearl River Delta, Southern China. *Catena, 22,* 105-120.

Lin, C., Melville, M.D., & Hafer, S. (1995). Acid sulphate soil-landscape relationships in an undrained, tide-dominated estuarine floodplain, Eastern Australia. *Caten*a, *24,* 177-194.

Liu, H., & Lei, W. (2008). Mapping detention basins and deriving their spatial attributes from airborne LIDAR data for hydrological applications. *Hydrological Processes, 22,* 2358 – 2369.

Ljung, K., Maley, F., Cook, A., & Weinstein, P. (2009). Review article: Acid sulfate soils and human health - A millennium ecosystem assessment. *Environment International, 35,* 1234–1242.

Logsdon, S.D., Clay, D., Moore, D., & Tsegaya, T. (2008). *Soil Science: Step-by-step Field Analysis*. Madisson, USA: Soil Science Society of America.

Longley, P.A., M.F. Goodchild, D.J. Maguire & D.W., Rhind. (2001). *Geographic Information Systems*. London: John Wiley & Sons,.

Lu, L., Wang, R., Chen, F., Xue, J., Zhang, P., & Lu, J. (2005). Element mobility during pyrite weathering: Implications for acid and heavy metal pollution at mining impacted sites. *Environmental Geology*, *49,* 82-89.

Madan, K.J., Chowdhury, A., Chowdary, V.M., & Peiffer, S. (2007). Groundwater management and development by integrated remote sensing and geographic information systems: Prospect and constraints. *Water Resource Management*, *21,* 427 – 467.

Madsen, H.B., Jensen, N.H., Jakobsen, B.H., & Platou, S.W. (1985). A method for identification and mapping potentially acid sulfate soils in Jutland Denmark. *CATENA Verlag, 12*, 363-371.

Mallants, D., Mohanty, B.P.Jacques, D., & Feyen, J. (1996). Spatial variability of hydraulic properties in a multi-layered soil profile. *Soil Science, 161 (3),* 167-181.

Maltby, E. (1986). *Waterlogged Wealth*. Earth Library Collection: Natural Resources Management.

Mantra, I.B. (1982). Population and rural settlement in the Segara Anakan Region. In E. C. F. Bird, A. Soegiarto, & K. A. Soegiarto, (Eds.), *Workshop on coastal resources management in the Cilacap Region* (pp. 86-92). Indonesian Institute of Sciences and the United Nations University, Jakarta.

Marfai, M.A., & Lorenz, K. (2008). Potential vulnerability implications of coastal inundation due to sea level rise for the coastal zone of Semarang City, Indonesia. *Environmental Geology, 54,* 1235 – 1245.

Mark, A., Rosicky, M., Sullivan, L.A., Slavich, P.G., & Hughes, M. (2004). Soil properties in and around acid sulfate soil scalds in the coastal floodplains of New South Wales Australia. *Australian Journal of Soil Research*, *42,* 595 – 602. Australia: CSIRO Publishing.

Martosubroto, P., & Naamin, N. (1997). Relationship between tidal forest (mangroves) and commercial shrimp production in Indonesia. *Marine Reseacrh Indonesia, 18,* 18-86.

Mary, J. Kraus. (1998). *Development of Potential Acid Sulfate Paleosols in Paleocene Floodplains, Bighorn Basin, Wyoming, USA*. USA: Department of Geological Sciences, University of Colorado.

Mastaller, M. (1996). Destruction of mangrove wetlands - causes and consequences. natural resourses and development. *Institute for Scientific Co-operation, Tübingen, 43/44,* 37–57.

Matsumoto, E., Suvijanto, Y. Kaida, & Y. Takaya. (1974). Environmental conditions of three representative villages in Central Java (special issue, the natural environment and the socio-economic behavior of farmers in Thailand and Java: A preliminary summary report on "Nature and Man Project" of Kyoto University Center for Southeast Asian Studies. *Southeast Asian Studies*, 12, 3.

Matthew, R.K. (1985). *Quaternary Sea Level: Sea Level Change*. National Academy of Science, accessed 14 April 2009. doi : www.nap.edu/catalog/1345.html

Matthew, E.K., Panda, R.K., & Nair, M. (2001). Influence of subsurface drainage on crop production and soil quality in a low-lying acid sulphate soil. *Agricultural Water Management, 47,* 191 – 209.

Mawardi, I. (2010). River basin watershed damage and decrease the carrying capacity of water resources in Java as well as efforts to handle (in Indonesian language). *Hidrosfer Indonesia Journal*, *10 (2),* 1-8.

Mayr, T., & Hollis, J. (1998). *New Technologies for Soil Mapping*. European Soil Bureau, Research Report No.7.

McBratney, A.B., & Gruijter, J.J. (1992). A continuum approach to soil classification by modified fuzzy k-means with extragrades. *Journal of Soil Science, 43(1),* 159-175.

McBratney, A.B., Hart, G.A., & McGarry, D. (1991). The use of region partitioning to improve the representation of geostatistically mapped soil attributes. *Journal of Science*, *42 (3),* 513-515.

McBratney, A.B., Hart, G.A., & McGarry, D. (1992). The use of region partitioning to improve the representation of geostatistically mapped soil attributes. *European Journalof Soil Science*, *42 (3),* 513–532.

McBratney, A.B, Mendonça M.L, & Santos, M. B. (2003). On digital soil mapping. *Geoderma, 117 (1–2),* 3–52.

McBratney, A.B., & Odeh, I.O.A. (1997). Application of fuzzy sets in soil science: fuzzy logic, fuzzy measurements and fuzzy decisions. *Geoderma*, *77 (2–4),* 85–113.

McDonald, B.C.T., Reynolds, J.K., Kinsela, A.S., Reilly, R.J., van Oploo, P., Waite, T.D., & White, I. (2009). Critical coagulation in sulfidic sediments from an East-Coast Australian acid sulfate landscape. *Applied Clay Science, 46,* 166–175.

McDonald, M.L. (1996). A multi-attribute spatial decision support system for solid waste planning. *Computers, Environment and Urban Systems, 20 (1),* 1–17.

McDonald, R., & Isbell, R.F. (2009). Soil and Land Survey (pp. 198). Field Handbook 2nd (Eds.), Inkata Press, Melbourne. In National Committee on Soil & Terrain (Eds.), *Australian Soil and Land Survey Field Handbook* (3rd Ed). Melbourne, Australia: CSIRO Publishing.

McKenzie, N.J., D.W., Jacquier, L.J., Ashton, & Cresswell, H.P. (2000). *Estimation of Soil Properties Using the Atlas of Australian Soil*. Canberra: CSIRO Land and Water, ACT Technical Report 11/00.

McKenzie, N.J., Grundy, M.J., Vebster, R., & Ringrose-voase, A.J. (2008). *Guidelines of Surveying Soil and Land Resources*. Melbourne: CSIRO.

Melati, F.F., Hendrawan, D., & Sitawati, A. (2007). *Land Use and Water Quality Relationships in the Ciliwung River Basin, Indonesia* (pp. 575 – 582). International Congress on River Basin Management.

Merry, R.H., Fizpatrick, R.W., Barnet, E.J., Davies, P.J., Fotheringham, D.G., Thomas, B.P., & Hicks, W.S. (2003). *South Australian Inventory of Acid Sulfate Soil Risk (Atlas)*. Australia: CSIRO.

Milford, H. (1997). Acid sulfate soil risk maps of the Tucabia and Tyndale 1:25000 map sheets. NSW Separtment of Land and Water Conservation. NSW Government, Sydney.

Milliman, J.D., & Meade, R.H. (1983). World-wide delivery of sediment to the oceans. *Journal of Geology, 91 (1),* 1–21.

Milliman, J.D., & Farnsworth, K.L. (2011). *River Discharge to the Coastal Ocean: a Global Synthesis.* Cambridge University Press.

Miller, F.S., Kliminster, K.L., Degens, B., & Fims, G.W. (2010). Relationship between metal leached and soil type from potential acid sulphate soil under acidic and neutral conditions in Western Australia. *Water Air Water Pollution, 205 (1-4),* 33-147.

Milne, G. (1935). Some suggested units of classification and mapping particularly for East African soils. *Soil Research, 4 (3),* 127-145.

Minar, J., Evan, I.S. (2008). Elementary forms for land surface segmentation: the theoretical basis of terrain analysis and geomorphological mapping. *Geomorphology, 95 (3-4),* 236-259.

Minh, L.Q., Tuong, T.P., Van Mensvoort, M.E.F., & Bouma, J. (1997). Contamination of surface water as affected by land use in acid sulfate soils in the Mekong River Delta, Vietnam. *Agriculture, Ecosystems & Environment, 61 (1),* 19–27.

MMAF (2008). Center of Data and Statistics 2007. Jakarta, Indonesia: Ministry of Marine Affairs and Fisheries

MMAF (2009). Center of Data and Statistics 2008. Jakarta, Indonesia: Ministry of Marine Affairs and Fisheries.

MMAF (2011). *Marine and Fisheries in Figure*. Indonesia: Ministry of Marine Affairs and Fisheries.

MoF (2007). *Mangrove Rehabilitation Program on the North Coast of Central Java*. Annual Report from Central Java Ministry of Forestry.

Momon, S. Imanudin, Armanto, M.E., & Susanto, R.H. (2009). *Developing Strategic Operation of Water Management in Tidal Lowland Agriculture Areas of South Sumatera, Indonesia*, Indonesia: Sriwijaya University.

Mondal, S.M. (2007). Groundwater prospects evaluation base on hydrogeomorphological mapping using high resolution satellite image: A case study in Uttarakhand. *Journal of Indian Social Remote Sensing, 36,* 69-76.

Moore, I.D., Gessler, P.E., Nielsen, G.A., & Peterson, G.A. (1993). Soil attribute prediction using terrain analysis. *Soil Sci. Soc. Am. J., 57,* 443-452.

Moore, I.D., & Wilson, J.P. (1992). Length-slope factors for the revised Universal Soil Loss Equation: simplified method of estimation. *Journal of Soil and Water Conservation, 47,* 423-428.

Moran, C.J., & Bui, E.N. (2002). Spatial data mining for enhanced soil map modelling. *International Journal Geography Inf. Sci*., *16 (6),* 533–549.

Mulder, V.L., De Bruin, S., Schaepman, M.E., & Mayr, T.R. (2011). The use of remote sensing in soil and terrain mapping. *Geoderma, 162,* 1-15.

Munsell (2000). *Munsell Soil Color Charts*. Michigan: Munsell Color X-rite.

Murgese, D.S., Deckker, P. de (2005). The Distribution of Deep-Sea Benthic Foraminifera in Core Tops from the Eastern Indian Ocean. *Marine Micropaleontology, 56,* 25 – 49.

Murphy, B.W., & Charman, P.E.V. (1994). *SOILS: Their Properties and Management, Soil Conservation Handbook for New South Wales*. Sydney, Australia: Sydney University Press.

Murphy, P.N.C., Oglive, J., Meng, F. R., & Arp, P. (2008). Stream network modeling using Lidar and photogrammetric digital elevation models: A comparison and field verification. *Hydrological Processes, 22(12),* 1747 – 1754.

Mu'tamar, M., Eriyatno, Machfud, Soewardi, K. (2013). Agent-Based Simulation Model for the Sustainability of Minapolitan: A Case Study of Shrimp Agroindustry. *Journal of Economics and Sustainable Development, 4(4).*

Muttitanon, W., & Tripathi, N.K. (2005). Land use/land cover changes in the coastal zone of Ban Don Bay, Thailand using Landsat 5 TM data. *International Journal of Remote Sensing, 26 (11),* 2311-2323.

Naylor, R.L., Goldburg, R.J., Primavera, J.H., Kautsky, N., Beveridge, M.C.M., Clay, J., Folke, C., Lubchenco, J., Mooney, H., & Troell, M. (2000). Effect of aquaculture on world fish supplies, review article. *Nature, 405,* 1017-1024.

Neal, R.S., Coyle, S.D., Tidwell, J.H., & Boudreau, B.M. (2010). Evaluation of Stocking Density and Light Level on the Growth and Survival of the Pacific White Shrimp, *Litopenaeus vannamei*, Reared in Zero-Exchange Systems. *Journal of the World Aquaculture Society, 41(4),* 533-544.

Neyberg, M.E., Osterholm, P., & Nystrand, M.I. (2011). Impact of acid sulfate soils on the geochemistry of rivers in south-western Finland. *Environmental Earth Sciences, 10(11),* 1216-1224.

Noorfwijk, M. Van, Tomich, T.P., & Verbist, B. (2002). Negotiation support models for integrated natural resource management in tropical forest margins. In Campbell, B.M., Sayer, J.A., *Integrated Natural Resource Management* (pp. 87-108). CABI Publishing.

Nordmyr, L. (2008). Estuarine behaviour of metal loads leached from coastal lowland acid sulphate soil. *Marine Environmental Research, 66,* 378–393.

Notohadiprawiro, T. (1989). Farming acid mineral soils for food crops: An indonesian experience. In Craswell, E.T., and Pushparajah, E., *Management of Acid Soils in the Humid Tropics of Asia* (pp. 62-68). Canberra: ACIAR.

Nurdjana. (2006). *The Status of Shrimp Culture, Diseases and Their Impact on Production in the Province of Central Java* (pp. 22). Oral Presentation on "Pertemuan Teknis. Pengembangan Sistem Pengendalian Penyakit Udang di BBAP", Jepara, 1–3 October. Jawa Tengah, Semarang, Indonesia.

Oborn, I. (1989). Properties and classification of some acid sulfate soils in Sweden. *Geoderma, 45,* 197 – 219.

Oenema. (1990). Pyrite accumulation in salt marshes in the Eastern Scheldt, Southwest, Netherlands. *Biogeochemistry, 9,* 75-98.

Oktaviani (2007). *Contract Farming Option for Shrimp Production in Eastern Indonesia*. Final Report, SADI-ACIAR Project.

Okubo, S., Takauci, K., & Chakranon. (2003). Land characteristics and plant resources in relation to agriculture land-use planning in humid tropical stand plain, Southeastern Thailand. *Landscape and Urban Planning, 65 (3),* 133-148.

Oldak, A., Jackson, T.J., Stark, P., & Elliot, R. (2002). Mapping near-surface soil moisture on regional scale using ERS-2 SAR data. *International Jornal of Remote Sensing, 24 (22),* 4579 – 4598.

Oliveira, M.L., Ward, C.R., Izquierdo, M. (2012). Chemical composition and minerals in pyrite ash of an abandoned sulphuric acid production plant. *Science of The Total Environment, 430,* 34-47

Ongkosongo, O. S. R. (1979). *The nature of coastline changes in Indonesia*. Workshop on Coastal Geomorphology, UNESCO, Singapore-Malaysia.

Ongkosongo, O.S.R. (1982). The nature of coastline changes in Indonesia, lndonesian. *Journal of Geografi, 12,* 1-22.

Ongkosongo, O.S.R. (2010). *Estuary, Entrance and Delta in Indonesia*. Jakarta: Lembaga Ilmu Pengetahuan Indonesia, Pusat Penelitian Oseanografi.

O'Shea, B., Jankowski, J., & Sammut, J. (2007). The source of naturally occurring arsenic in a coastal sand aquifer of eastern Australia. *Science of The Total Environment, 379 (2-3),* 151-166.

Oudot, J., & Dutrieux, E. (1989). Hydrocarbon weathering and biodegradation in a tropical estuarine ecosystem. *Marine Environmental Research, 27,* 195 – 213.

Palacios, Orueta, & Ustin, S.L. (1998). Remote sensing of soil properties in the Santa Monica Mountains I: Spectral analysis. *Remote Sensing Environment, 65,* 170 – 183.

Palmer, S.M., Driscoll, C.T., & Johnson, C.E. (2004). Long-term trends in soil solution and stream water chemistry at the hubbard brook experimental forest: Relationship with landscape position. *Biogeochemistry, 68,* 51–70. Kluwer Academic Publisher

Pannekoek, A.J. (1949). Outline of the geomorphology of Java. *Tijdschr.Kon.Ned.Aard.Gen., LXVI,* 270-326.

Partadiredja, Atje. (1969). An economic survey of Central Java. *Bulletin of Indonesian Economic Studies, 5: 3,* 29-46.

Pattanaik, C., & Prasad, S.N. (2011). Assessment of aquaculture impact on mangroves of Mahanadi delta (Orissa), East coast of India using remote sensing and GIS. *Ocean & Coastal Management, 54(11),* 789-795.

Paul, B.G., & Vogl, C.R. (2011). Impacts of shrimp farming in Bangladesh: Challenges and alternatives. *Ocean & Coastal Management, 54(3),* 201-211.

Perillo, G.M.E. (1995). Geomorphology and sedimentology of estuaries: An introduction. *Development in Sedimentology, 53,* 17-47.

Pennock, D.J., & Veldkamp, A. (2006). *Advances in Landscape-Scale Soil Research, 133 (1-2),* 1-5.

Poernomo, A. (1992). *Site Selection for Sustainable Shrimp Ponds* (pp. 38). Jakarta: Central Research Institute for Fisheries.

Pons, L.J. (1973). Outline of the genesis, characteristics, classification and improvement of acid sulphate soils (pp. 3-27). In H. Dost (Ed.), *Acid Sulphate Soils*. Proc. 1st Int. Syrup, 13-20 August 1972. Wageningen: Wageningen ILRI Publication 18.

Pons, L.J. & Fiselier, J.L. (1991). Sustainable development of mangroves. *Landscape Urban Planning, 20,* 103-109.

Pons, L.J. & van Breemen, N. (1982). Factors influencing the formation of potential acidity in tidal swamps. In H. Dost (Ed.), *Proceeding of 2nd International Symposium of Acid Sulfate Soils* (pp. 37-51). Wageningen: ILRI Publication 13.

Pons, L.J. & van der Kevie, W. (1969). *Acid Sulphate Soils in Thailand*. Bangkok: Soil Survey Rept SSR 81, Land Development Departement

Pons, L.J. & Zonneveld, I.S. (1965). *Soil Ripening and Soil Classification*. Wageningen: ILRI Publication L3.

Powell, B., & Martens, M. (2005). A review of acid sulfate soil impacts, actions and policies that impact on water quality in Great Barrier Reef catchments, including a case study on remediation at east trinity. *Marine Pollution Bulletin, 51,* 149–164.

Preda, M., & Cox, M.E. (2004). Temporal variations of mineral character of acid-producing pyritic coastal sediments, Southeast Queensland, Australia. *Science of the Total Environment, 326 (1-3),* 257-269.

Primavera, J.H. (1995). Mangroves and Brackish Water Pond Culture in the Philippines. In Y. S. Wong, & N. E. Y. Tam, (Eds.). *Asia Pasific Symposium on Mangrove Ecosystems* (pp. 303 – 309). Kluwer Academic Puclisher, Belgia.

Primavera, J.H. (1997). Socio-economic impacts of shrimp culture. *Aquaculture Research, 28,* 815–27.

Primavera, J.H. (2005). Mangroves, fishponds, and the quest for sustainability. *Science, 310,* 57-59.

Primavera, J.H. (2006). Overcoming the impacts of aquaculture on the coastal zone. *Ocean and Coastal Management, 49,* 531-545.

Pubellier, M., Bader, A.G., Rangin, C., Deffontaines, B., & Quebral, R. (1999). Upper plate deformation induced by subduction of a volcanic arc: The snellius plateau (Molucca Sea, Indonesia and Mindanao, Philippines). *Tectonophysics, 304,* 345 – 368.

Pullin, R.S.V., Rosenthal, H., & Maclean, J.L. (1993). *Environmental and Aquaculture in Developing Countries*. Germany: International Centre for Living Aquatic Resources Management.

Purbo, Hadiwidjoyo., & R., Sukardi. (1974). Groundwater potential of areas underlain by volcaniclastic rock examples from Indonesia. *Bulletin AAPG, Vol. 58.*

Puri, S. (1985). *Response of aquifer to monsoon rainfall in Central Java Indonesia*. In Quinones, F. & Sanchez, A.V. (Eds), Proceeding of International Symposium on Tropical Hidrology and 2nd Caribbean Island Water Resources Congress (pp. 41 – 45). San Juan, Puerto Rico.

Purnomo, E., Mursyid, A., Syarwani, M., Jumberi, A., Hashidoko, Y., Hasegawa, T., Honma, S., & Osaki, M. (2005). Phosphorus solubilizing microorganisms in the rhizosphere of local rice varieties grown without fertilizer on acid Sulphate soils. *Journal of Science Plant Nutrient, 51,* 679 – 681.

Radke, L., Brooke, B., Ticehurst, C., & Murray, E. (2006). *Major Achievements of the Comparative Geomorphology of Estuaries Project*. Australia: Cooperative Research Center for Coastal Zone, Estuary and Waterway Management, CSIRO Publishing.

Ray, R.D., Egbert, G.D., & Erofeeva. (2005). A brief overview of tides in the Indonesian Seas. *Oceanography, 18 (4),* 62-73.

Rayment, G. E. & Higginson, F. R. (1992). *Australian Laboratory Handbook of Soil and Water Chemical Methods - Australian Soil and Land Survey Handbook*. Melbourne & Sydney: Inkata Press.

Repetto, R. (1986). Soil loss and population pressure on Java. *Ambio, 15(1)*, 14-18.

Revelle, R.R. (1990). *Sea Level Change*. Washington D.C: National Academy Press.

Ritsema, C.J., Groenenberg, J.E., & Bisdom, E.B.A. (1992). The transformation of potential into actual acid sulphate soils studied in column experiments. *Geoderma, 55,* 259 – 271. Amsterdam: Elsevier Science Publisher.

Rochford, D.J. (1959). Classification of Australian estuarine systems. *Archives of Oceanography and Limnology, 11,* 171 – 177.

Rompaey, A.J.J., Verstraeten, G., Oost, K. Van, Govers, G., & Poesen, J. (2001). Modelling mean annual sediment yield using distributed approach. *Earth Surface Processes and Landforms, 26,* 1221–1236.

Rose, C. W. (1929). *An Introduction to the Environmental Physics of Soil, Water, and Watersheds*, UK: Cambridge.

Rosicky, M., Sullivan, L., Slavich, P., & Hughes M. (2004a). Factors contributing to the acid sulfate soilscalding process in the coastal floodplains of New South Wales, Australia. *Australian Journal of Soil Science, 42,* 587–94.

Rosicky, M., Sullivan L., Slavich, P., & Hughes, M. (2004b). Soil properties in and around acid sulfate soilscalds in the coastal floodplains of New South Wales, Australia. *Australian Journal of Soil Science, 42,* 595–602.

Roslan, I., Shamshuddin, J., Fauziah, C.I., & Anuar, A.R. (2010). Occurrence and properties of soils on sandy beach ridges in the Kelantan–Terengganu Plains, Peninsular Malaysia. *Catena, 85,* 55-63.

Rosseti, D.F., Valeriano, M.M., & Thales, M. (2007). An abandoned estuary within Marajo Island: Implication for late quaternary paleogeography of Northern Brazil. *Estuary and Coast, 30,* 813-826.

Rossiter, D. (2004). Digital soil resources inventories: Status and prospects. *Soil Use and Management, 20 (3),* 296-301.

Rossiter, D. (2008). Digital soil mapping as a component of data renewal for areas with sparse soil data infrastructures. In Hartemink, A.E., McBratney, A. and de Lourdes Mendonca-Santos, M. (Eds.). *Digital Soil Mapping with Limited Data* (pp 69-80). Berlin : Springer.

Roy, P.S. (1984a). Holocene sedimentation histories of estuaries in southeastern Australia (pp. 23-60). In Hodgkin, E. P. (Eds.), Bulletin of *Estuarine Environments of the Southern Hemisphere*. Western Australia: Departement of Conservation and Environment.

Roy, P. S. (1984b). New South Wales estuaries - their origin and evolution (pp. 99-121). In Thom, B. G., (Eds.), *Developments in Coastal Geomorphology in Australia*, NSW: Academic Press.

Roy, P. S. (1993). *Late Quaternary Geology of the Hunter Delta - A Study of Estuarine Valley-Fill Sequences* (pp 31). Unpublished report.

Roy, P.S. (1994). *Holocene estuary evolution – stratigraphic studies from Southeastern Australia.* Society for Sedimentary Geology (SEPM) Special Publication.

Roy, P. S., & Crawford, E. A. (1977). *Significance of Sediment Distribution in Major Coastal Rivers, Northern NSW* (pp. 177-184). Third Australian Conference on Coastal and Ocean Engineering.

Roy, P. S., & Crawford, E. (1981). Holocene geological evolution of the Southern Botany Bay-Kurnell Region, central New South Wales Coast. *Geological Survey of New South Wales Record, 20,* 159-250.

Roy, P. S., Thom, B. G., & Wright, L. D. (1980). Holocene sequences on an embayed high-energy coast: An evolutionary model. *Sedimentary Geology, 26,* 1-19.

Roy, P.S., Williams, R.J., Jones, A.R., Yassini, I., Gibbs, P.J., Coates, B., West, R.J., Scanes, P.R., Hudson, J.P., & Nichol, S. (2001). Structure and function of south-east Australian estuaries. *Estuarine, Coastal and Shelf Science, 53,* 351-384.

Rudiyanto, A. (1999). Marine and coastal management in Indonesia: A planning approach. *Maritime Studies, 106,* 1-9.

Rudiyanto, A. (2001). Managing marine and coastal resources: Some comparative issues between Australia and Indonesia. *Maritime Studies, 118,* 6-28.

Runtunuwu, E., & Pawitan, H. (2007). Hydrometeorologial monitoring network of Java Island and hydrologic characteristics of the major river basin. *Proceeding of International Workshop on Integrated watershed management for Sustainable Water Use in a Humid Tropical Region.* Tsukuba: JSPS-DGHE Joint Reseach Project.

Ryan, D.A., Heap, A.D., Radke, L., & Heggle, D.T. (2003). *Conceptual Model of Australia's Estuaries and Waterways: Applications for Coastal Resources Management* (pp 135). Canberra: Geoscience Australia Record 2003/2009, Geoscience, Commonweatlh of Australia.

Salama, R.B., Bartle, G.A., Williamson, W.R., Watson, G.D., & Knapton, A. (1997). *Hydrogeomorphology and Hydrogeology of the Upper Kent River Catchment and Its Controls on Salt Distribution and Patterns of Ground Water Discharge*. CSIRO Land and Water Science Report No. 27/97.

Sammut, J. (1999). Amelioration and management of shrimp ponds in acid sulfate soils. In: Smith, P.T. (Ed.), *Towards Sustainable Shrimp Culture in Thailand and the Region*. Proceedings of a workshop held at Hat Yai, Songkhla, Thailand. Australian Centre for International Agricultural Research, Canberra, Australia..

Sammut, J., & Hanafi, A., (2000). *Rehabilitation and Management of Shrimp Ponds Constructed in Acid Sulphate Soils.* Thematic review on coastal wetland habitats and shrimp aquaculture, A report for world bank, Network of aquaculture centres in Asia-Pacific, World Wildlife Fund and Food Agriculture Organization of the United Nations Consortium Program on Shrimp Farming and the Environment.

Sammut, J & Mustafa, A (2011). *Land capability assessment and classification for sustainable pond-based aquaculture systems: FINAL REPORT*. Australian Centre for International Agriculture Research, Canberra, Australia.

Sammut, J., White, I., & Melville, M.D. (1996). Acidification of an estuarine tributary in Eastern Australia due to drainage of acid sulfate soils. *Marine and Freshwater Research, 47,* 669–684

Sanderson, P.G., & Taylor, D.M. (2003). Short-term water quality variability in two tropical estuaries Central Sumatera. *Estuaries, 26 (1),* 156-165.

Sandilyan, S. & Kathiresan, K. (2012). Mangrove conservation: a global perspective. *Biodiversity and Conservation, 2,* 3523-3542.

Sartono, S., Hidayat, S., Zainm, J., Nababan, U.P., & Djubiantono, T. (1978). *Undak Sungai Baksoko Berdasarkan Analisis Foto Udara, Proyek Pengendalian dan Penggalian Purbakala*. Indonesia: Departmen Pendidikan dan Kebudayaan.

Sarwani, M., Lande, M., & Andriesse,W. (1993). Farmers' experience in using acid sulfate soils: some examples from tidal swampland of southern Kalimantan, Indonesia (pp. 113–222). In Dent, D, Van Mensvoort, M., (Eds.), *Selected papers of the Ho Chi Minh City Symposium on Acid Sulfate Soils.* Ho Chi Minh City, Vietnam: ILRI Puiblications.

Satheeshkumar, P., & Khan, A.B. (2012). Identification of mangrove water quality by multivariate analysis methods in Pondicherry coast, India. *Environmental Monitoring and Assesment, 184(6),* 3761-3774.

Savenije, H.H.G. (2005). *Salinity and Tides in Alluvial Estuaries* (1st Edition). Amsterdam, Boston: Elsevier.

Scheidegger, A.E. (1973). Hydro-geomorphology. *Journal of Hydrology*, *20,* 193-215.

Scholten (Eds.). (2007). *Mangrove Guidebook for Southeast Asia*. Dharmasarn Co. Ltd. doi: 974-7946-85-8.

Schmidt, H., Eickhorst, T., Tippkotter, R. (2011). Monitoring of root growth and redox conditions in paddy soil rhizotrons by redox electrodes and image analysis. *Plant and Soil, 341(1-2),* 221-232.

Schriek, T., Passmore, D.G., Rolao, J., & Stevenson, A.C. (2007). Estuarine fluvial floodplain formation in the holocene lower tagus valley (Central Protugal) and implication for quaternary fluvial system evolution. *Quaternary Science Review, 26*, 2937-2957.

Schum, S.A. (1981). Evolution and response of the fluvial system, sedimentological implications. *Society of Economic Palaeontologists and Mineralogist Special Publications, 31,* 19-29.

Schuster, W.H. (1952). *Fish Culture in Brackish-Water Ponds of Java, Indo-Pacific, Fisheries*. Council Special Publication No. 1.

Scull, P., Franklin, J., Chadwick, O., & McArthur, D. (2003). Predictive soil mapping: A review. *Progress in Physical Geography, 27(2),* 171 – 197.

See, S.W., Balasubramanian, R., Rianawati, E., Karthikeyan, S., & Streets, D.G. (2007). Characterization and source apportionment of particulate matter ≤ 2,5 µm in Sumatra, Indonesia during a recent peat fire episode. *Environmental Science and Technology*, *41(10),* 3488-94.

Setyawan, D.S., Winarno, K., & Indrowuryatno, Wiryanto. (2008). Mangrove along Central Java coast: 3 Profile Diagram of Vegetation. *Biodiversity*, *9(4),* 315-321.

Shackelton, N.J. (1987). Oxygen isotop, ice volumes and sea level. *Quaternary Science Reviews, 6*, 183-190.

Shamshuddin, J., Muhrizal, S., Fauziah, I., & Husni, M.H.A. (2004). Effects of adding organic materials to an acid sulfate soil on the growth of cocoa (*Theobroma cacao L.*) seedlings. *Science of the Total Environment*, *323,* 33–45.

Shi, X., Aspandiar, M., & Oldmeadow, D. (2014). Spectral reflectance variations and mineral transformations during the formation of acid sulphate soil in an incubation experiment. *International Journal of Remote Sensing, 35(23),* 7959-7977.

Shi, Y., Zhang, G., Liu, J.,Zhu, Y., & Xu, J. (2011). Performance of a constructed wetland in treating brackish wastewater from commercial recirculating and super-intensive shrimp growout systems. *Bioresource Technology, 102(20),* 9416-9424.

Short, A.D. (1989). Chenier research on the Australian coast. *Marine Geology, 90 (4),* 345-351.

Simpson, H.J., Ducklow, H.W., Deck, B., & Cook, H.L. (1983). Brackish Water Aquaculture in Pyrite-Bearing Tropical Soils. *Aquaculture, 34,* 333–350. Elsevier Science Publishers.

Simoen, S. (2000). Monitoring of sea-water instrusion into coastal aquifer using geoelectrical sounding: A case study of the northern coastal area of Central Java, Indonesia. *The Indonesian Journal of Geography, 32(80),* 167 – 187.

Siswanto, A. B., Markus, Anda, & Subandiono, R. E. (2009). Properties of organic and acid sulphate soils and water of a 'reclaimed' tidal backswamp in Central Kalimantan, Indonesia. *Geoderma, 149,* 54–65. Amsterdam: Elsevier Science Publishers.

Skidmore, A.K., Watford, F., Luckananurug, P., & Ryan, P.J. (1996). An operational GIS expert system for mapping forest soils. *Photogrammetric Engineering & Remote Sensing, 62(5),* 501-511.

Smith, J., Janskowski, J., & Sammut, J. (2006). *Natural Occurrences of Inorganic Arsenic in the Australian Coastal Groundwater Environment, in Managing Arsenic in the Environment*. Australia: CSIRO Publishing.

Smith, J., van Oploo, P., Marston, H., Melville, M.D., & Macdonald, B.C.T. (2003). Spatial distribution and management of total actual acidity in an acid sulfate soil environment. *Catena, 51,* 61– 79.

Soegiarto, A. (1976). Indonesia. In K.K. Szekielda, & B.Breuer (Eds.), *Development and Management of Resources of Coastal Areas* (pp. 143-151). Utrecht.

Soewarno. (1999). *Hydrology of River Discharge Data Measurement and Management (Hydrometry)*. Bandung: Nova.

Sohlenius, G., & Oborn, I. (2004). Geochemistry and partitioning of trace metals in acid sulphate soilsin Sweden and Finland before and after sulphide oxidation. *Geoderma, 122,* 167–175.

Soil Survey Staff (2006). *Keys to Soil Taxonomy*. USA: Natural Resources Conservation Service, US Department of Agriculture.

Steinke, S., Hanebuth, T.J.J., Vogt, C., & Stattegger, K. (2008). Sea level induced variations in clay mineral composition in the Southwestern South China Sea over the past 17,000 year. *International Journal of Marine Geology, Geochemistry and Geophysics, 250,* 199 – 210.

Stevenson, N.J. (1997). Disused shrimp ponds: options for redevelopment of mangroves. *Coastal Management, 25(4)*, 425-435.

Stone, Y., Ahern, C. R., & Blunden, B. (1998). *Acid Sulfate Soils Manual 1998*. Wollongbar, NSW, Australia: Acid Sulfate Soil Management Advisory Committee.

Storm, J.E.A., Hoogendoom, R.M., Dam, R.A., Hoitink, A.J.F., & Kreenenberg, S.B. (2005). Late-holocene evolution of the Mahakam Delta, East Kalimantan, Indonesia. *Sedimentary Geology, 180 (3-4),* 149-166.

Strahler, A. (2003). *Physical Geography*. New York: John Willey & Sons.

Strobl, R.O., & Forte., F. (2007). Artificial Neural Network Exploration of the Influential Factors in Drainage Network Derivation, *Hydrological Processes, 21,* 2965–2978.

Su Rito, Hardoyo. (1982). The Kampung Laut of the Segara Anakan: A study of socio-economic problems. In E. C. F. Bird, A. Soegiarto, and K. A. Soegiarto, (Eds.), *Workshop on Coastal Resources Management in the Cilacap Region* (pp. 172-182). Jakarta: Indonesian Institute of Sciences and the United Nations University.

Sugeng, S.S., Sukandarrumidi, Pramumijoyo, S., & Karnawati, D. (2002). *The Environmental Changes in the Coastal Area: Case Study of Congot Beach, Kulonprogo Regency, Yogyakarta Province, Java, Indonesia* (pp. 369 – 377). In Omar, R., (Eds.), Proceedings of the Regional Symposium on Environment and Natural Resources, Malaysia.

Sukanto. (1969). Climate of Indonesia. In H. Arakawa (Eds.), *Climates of Northern and Eastern Asia* (pp. 215-229). Amsterdam.

Sukarjo, S. (2000). Indonesia: Mangrove-friendly aquaculture. In Primavera, J.H., *Mangrove-friendly Aquaculture*. Philippines: SEAFDEC Aquaculture Department.

Sulaeman, Y., Minasny, McBratney, A.B., Sarwani, M., & Sutandi, A. (2013). Harmonizing legacy soil data for digital soil mapping in Indonesia. *Geoderma, 192*, 77–85.

Sumosusastro, P.A., Tjia, H.D., Fortuin, H.D., & Van Der Plicht, J. (1989). Quaternary reef record of differential uplift at Luwuk, Sulawesi East Arm, Indonesia. *Netherlands Journal of Sea Research, 24,* 277 – 285.

Sunarto (2003). *Geomorfologi Pantai: Dinamika Pantai*. Yogyakarta: Fakultas Geografi, Universitas Gadjah Mada.

Sunarto (2004). Perubahan fenomena geomorfik daerah kepesisiran di sekeliling gunung api Muria Jawa Tengah. *Dissertation*. Indonesia: Yogyakarta, Universitas Gadjah Mada.

Sundstrom, R., Astrom, N., & Osterholm, P. (2002). Comparison of the metal content in acid sulfate soil runoff and industrial effluent in Finland, *Environmental Science and Technology*, *36 (20),* 4269 – 4272.

Suswanto, T.J., Shamshuddin, S.R., Syed, O., & Teh, C.B.S. (2007). Effect of lime and fertilizer, application in combination with water management on rice (*Oryza sativa*) cultivated on an acid sulfate soil. *Malaysian Journal of Soil Science*, *11,* 1-16.

Susilohadi, S., Gaedicke, C., & Djadjadihardja, Y. (2008). Structure and sedimentary deposition in the Sunda Strait, Indonesia. *Tectonophysic, 467*, 55-71.

Sylla, M., Stein, A., & Van Mensvoort, M.E.F. (1996). Spatial variability of soil actual and potential acidity in the mangrove agro-ecosystem of West Africa. *Soil Science Society of American Journal*, *60,* 219-229.

Takano, B., Suzuki, K., Sugimori, K., Ohba, T., Fazlullin, S.M., Bernard, A., Sumarti, S., Sukhyar, R., & Hirabayashi, M. (2004). Bathymetric and geochemical investigation of Kawah Ijen Crater Lake, East Java, Indonesia. *Journal of Volcanology and Geothermal Research*, *135*, 299 – 329.

Tarunamulia (2008). Application of fuzzy logic, GIS and remote sensing to the assessment of environmental factors for extensive brackishwater aquaculture in Indonesia. *Master of Science Thesis*. Sydney, Faculty of Science. Australia: University of New South Wales.

Thomas, B.P., Fitzpatrick, R.W., Merry, R.H., & Hicks, W.S. (2003). *Coastal Acid Sulfate Soil Management Guidelines, Barker Inlet, Version 1.2*. Urrbrae, SA: CSIRO Land and Water.

Thomas, P., & Varley, J.A. (2003). *Soil Survey of Tidal Sulphidic Soils in The Tropics: A Case Study*, *Land Resources Development Centre*. London: Overseas Development Administration.

Thom, B.G., & Roy, P.S. (1985). Relative sea levels and coastal sedimentation in Southeast Australia in the Holocene. *Journal of Sedimentary Research, 55 (2),* 257-264.

Tien, Steven J. (1979). Soil texture test. *Journal of Agronomy Education, 8*, 54-55.

Tiner, R. W. (2009). *Ecology of Wetlands: Classification Systems*. Amsterdam: Elsevier Science Publisher.

Tjia, H.D. (1987). *Ancient Shorelines in Peninsular Malaysia* (pp. 239-257). Spafa Final Report Seminar in Prehistoric of Southeast Asia, Thailand.

Tjia, H.D. (1996). Sea-level changes in the tectonically stable Malay – Thai Peninsula. *Quaternary International*, *31*, 95 – 101.

Tjia, H.D., Fujii, S., Kigoshi, K., & Sugimura, A. (1974). Late quaternary uplift in Eastern Indonesia. *Tectonophysics*, *23*, 427 – 433.

Tjia, H.D., Fujii, S., Kigoshi, K., Sugimura, A., & Zakaria, T. (1977). Radiocarbon Dates of Elevated Shorelines, Indonesia and Malaysia (Part 1), *Quaternary Research*, 2 : 487 – 495.

Triatmodjo, B. (1998). Penyusunan Skala Prioritas Pengendalian Banjir Sungai-Sungai di Jawa Tengah Selatan. *Forum Teknik, 22 (3),* 23-30.

Triatmodjo, B. (2000). Studi penanggulangan endapan di muara-muara sungai di pantai selatan Daerah Istimewa Yogyakarta dan Jawa Tengah. *Forum Teknik, 26 (3),* 1-9.

Triatmodjo, B. (2010). *Hidraulika II*. Yogyakarta: Beta Offset.

Turner, L., Tracey, D., Tilden, J., and Dennison, W.C. (2004). *Where River Meets Sea: Exploring Australia's Estuaries*. Brisbane, Australia: Cooperative Research Centre for Coastal Zone Estuary and Waterway Management.

Urushibara-Yoshino, K., & Yoshino, M. (1997). Palaeoenvironmental change in Java Island and its surrounding areas. *Journal of Quaternary Science*, *12 (5),* 435-442.

USDA (1971). *Soil Taxonomy, Natural Resources Conservation Service Soil*. USA: Unites State Department of Agriculture.

USDA (2007). *Indonesia Fishery Products Shrimp Report 2007*. Foreign Agriculture Service USDA.

USDA (2010). *Field Indicators of Hydric Soils in the United States, Version 7.0, 2010*. USA.

US NAVY (1977). *U.S. Navy Marine Climatic Atlas of the World, Volume II, North Pacific Ocean*. The Director Naval Oceanography and Meteorology.

van Breemen, N., Mulder, J., & Driscoll, C.T. (1983). Acidification and alkalinization of Soils, *Plant and Soil, 75,* 283 – 308.

van Breemen, N., & Harmsen, K. (1975). Translocation of iron in acid sulfate soils: I. Soil morphology, and the chemistry and mineralogy of iron in a chronosequence of acid sulfate soils. *Soil Science Society of America Journal, 39*, 1140-1148.

van Breemen, N. (1975). Acidification and deacidification of coastal plain soils as a result of periodic flooding. *Soil Science Society of America Journal, 39 (6),* 1153-1157.

van Breemen, N. (1982). Genesis, morphology, and classification of acid sulfate soils in coastal plains. In Kittrick, J.A., Fanning, D.S., Hossner, L.R. (Eds.), *Acid Sulfate Weathering* (pp. 95-108), Soil Science Society, America Special Publications, Madison, USA.

van der Kevie, W. (1972). *Physiography, Classification, and Mapping of Acid Sulphate Soils*. Proceedings of the International Symposium on Acid Sulphate Soils, Wageningen, The Netherlands, pp 204-222.

van Oploo, P. (2000). Soil and pore-water relations on a coastal acid sulfate soil in Northern New South Wales, Australia. *PhD Thesis*. Australia: University of New South Wales.

van Oploo, P., White, I., Ford, P., Melville, M.D., & Macdonald, B.C.T. (2008). Pore water chemistry of acid sulfate soils: Chemical flux and oxidation rates. *Geoderma*, *146*, 32–39.

Vegas-Vilarrubia, T., Baritto, F., & Melean, G. (2008). Critical examination of some common field tests to assess the acid-sulphate condition in soils. *Soil Use and Management 24*, 60-68.

Velasco, F., Alvaro, A., Suarez, S., & Herrero, J.M. (2005). Mapping Fe-bearing hydrated sulphate minerals with short wave infrared (SWIR) spectral analysis at San Miguel mine environment, Iberian Pyrite Belt (SW Spain). *Journal of Geochemical Exploration*, *87(2)*, 45–72.

Verburg, P.H., Veldkamp, T., & Bouma, J. (1999). Land use change under conditions of high population pressure: The case of Java. *Global Environmental Change*, *9*, 303 – 312.

Verstappen, H.T. (1997). The effect of climatic change on Southeast Asian Geomorphology. *Journal of Quaternary Science*, *12*, 413 – 418.

Verstappen, H.T. (2000). *Outline of the Geomorphology of Indonesia: A Case Study on Tropical Geomorphology of A Tectogene Region with A Geomorphological Map 1:5,000,000*. The Netherland: International Institute for Aerospace Survey and Earth Sciences.

Vinatea, L., Galvez, A.O., Browdy, C.L., Stokes, A., Venero, J., & Haveman, J. (2010). Photosynthesis, water respiration and growth performance of *Litopenaeus vannamei* in a super-intensive raceway culture with zero water exchange: Interaction of water quality variables. *Aquaculture Engineering, 42(1),* 17-24.

Vithana, C.L., Sullivan, L.A, Burton, E.D., Bush, R.T., Lewis, B.L., Lawson, A., Shuler, A., & Leffer, J.W. (2015). Stability of schwertmannite and jarosite in an acidic landscape: Prolonged field incubation. *Geoderma*, *239-240*, 47-57.

Walker, P.H. (1989). Contribution to the understanding of soil and landscape relationships. *Soil Genesis, Morphology and Classification*, *27*, 589 – 605.

Walsh, S.J., Butler, D.R., & Malanson, G.P. (1998). An overview of scale, pattern, process relationships in geomorphology: A remote sensing and GIS perspective. *Geomorphology, 21 (3-4)*, 18-205.

Ward, I.A.K., & Larcombe, P. (1996). Modern and holocene mangrove sediments: A geochemical comparison of modern and holocene mangrove sediment Twonsville Region, North Queensland. *Wetland (Australia), 15 (1),* 1996.

Water Resources Study Centre. (2008). *Review Rencana Strategi, Pusat Litbang Sumber Daya Air*. Indonesia: Department of Public Work.

Webster, R., & Oliver, M. (2001). *Geostatistics for Environmental Scientist*. Chichester: Wiley and Sons.

Welch, S. A. (2007). Jarosite dissolution I – trace cation flux in acid sulfate soils. *Chemical Geology*, *245*, 183 – 197.

Wells, F.E. (1983). An analysis of marine invertebrate distributions in a mangrove swamp in Northwestern Australia. *Bulletin Marine Science, 33,* 736 –44.

Werner, A.D., & Lockington, D.A. (2006). Tidal impacts on riparian salinities near estuaries. *Journal of Hydrology, 328,* 511 – 522.

Wetland International (2002). *Coastal Degradation Due to Shrimp Farming in Java*, Indonesia: Wetland International Indonesia Program.

White, I., Melville, M.D., B.P., Wilson, & Sammut, J. (1997). Reducing acidic discharges from coastal wetlands in Eastern Australia. *Wetland Ecology and Management*, *5(1),* 55-72.

White, I., Melville, M.D., Lin, C., van Oploo, P., Sammut, J. & Wilson, B.P. (1995). Identification and management of acid sulphate soils. In Hazelton, P.A. and Koppi, A.J., (Eds.), *Soil Technology—Applied Soil Science*. A course of Lectures 3rd Edition. Australian Soil Science Society, New South Wales Branch and Department of Agricultural Chemistry and Soil Science, University of Sydney, Australia, Chapter 30, 463–497.

White, I., Melville, M., MacDonald, B., Quirk, R., Hawken, R., Tunks, M., Buckley, D., Battie, R., Williams, J., & Heath, L. (2007). From conflict to wise practise agreement and national strategy: cooperative learning and coastal stewardship in estuarine floodplain management, Tweed River, Eastern Australia. *Journal of Cleaner Production*, *15 (16)*, 1545-1558.

Whitten, T., & Soeriaatmadja, R.E. (1996). *The Ecology of Java and Bali*. Dalhouise, Salhousie: University Perplus Editions.

Wijffels, S.E., Meyers, G., & Godfrey, J.S. (2008). A 20-year average of the Indonesian throughflow: Regional currents and the interbasin exchange. *Journal of Physical Oceanography, 38,* 1965 – 1978.

Wilcox, A.C., Peckarsky, B.L., Taylor, B.W., & Encalada, A.C. (2008). Hydraulic and geomorphic effects on mayfly drift in high–gradient streams at moderate discharge. *Ecohydrology*, *1*, 176 – 186.

Willett, I.R., Crockford, R.H., Milnes, A.R. (1992). Transformations of iron, manganese and aluminium during oxidation of a sulfidic material from an acid sulfate soil. *Catena*, *21*, 297–302.

Wilson, B.P. (2005). Elevations of sulfurous layers in acid sulfate soils: What do they indicate about sea levels during the Holocene in Eastern Australia? *Catena*, *62*, 45–56.

Wilson, J.P. (2012). *Digital Terrain Model.* Spatial Science Institute. United States: California.

Winegardner, D.L. (1996). *An Introduction to Soils for Environmental Professionals*. USA: Lewis Publisher.

Woodroffe, C.D. (1989). Mangrove swamp stratigraphy and holocene transgression, Grand Cayman Island, West Indies. *Marine Geology*, *41,* 271 – 294.

Woodroffe, C.D. (1999). Late quaternary evolution of coastal and lowland riverine plains of Southeast Asia and Noerthern Australia: An overview. *Sedimentary Geology*, *83,* 163-175. Amsterdam: Elsevier Science Publication.

Woodroffe, C.D. (2000). Deltaic and estuarine environment and their late quaternary dynamics on the Sunda and Sahul Shelves. *Journal of Asian Earth Science*, *18,* 303-413.

Woodroffe, C.D. (2005). Late quaternary sea–level high stands in the Central and Eastern Indian Ocean: An overview. *Global and Planetary Change*, *49,* 121 – 138.

Woodroffe, C.D., & Horton, B.P. (2005). Holocene sea-level changes in the Indo-Pacific. *Journal of Asian Earth Scienc*e, *25,* 29 – 43.

WRM (2002). *Mangrove: Local Livelihood vs Corporate Profit*. World Rainforest Movement Bulletin, December.

Yuanita, N. & Tawatchai, T. (2008). Development of a river delta: A case study of Cimanuk River Mouth, Indonesia. *Hydrological Processes*, *Interscience Publisher*, *22,* 3785 – 3801.

Yulianto, Eko, Rahardjo, A.T., Noeradi, D., Siregar, D.A., & Hirakawa, K. (2005). A holocene pollen record of vegetation and coastal environmental changes in the coastal swamp forest at Batulicin, South Kalimantan, Indonesia. *Journal of Asian Earth Science*, *25,* 1 – 8.

Yulianto, Eko, Sukapti, W.S., Rahardjo, A.T., Noeradi, D., Siregar, D.A., & Hirakawa, K. (2004). Mangrove shoreline responses to Holocene environmental change, Makassar Strait, Indonesia. *Review of Palaeobotany and Palynology*, *131*, 251 – 268.

Yulistiyanto, B., & Bambang, A. K. (2005). *Study of Water Resources Management Development in Progo-Opak-Serang River Basin using RIBASIM*. Indonesia: Gadjah Mada University.

Yusuf, D. (1995). Aquaculture in Indonesia. In: T.U. Bagarinao & E.E.C., Flores (Eds.). *Towards Sustainable Aquaculture in Southeast Asia and Japan* (pp. 109-115). Iloilo, Philippines: SEAFDEC Aquaculture Department.

Zavalloni, M., Groeneveld, R.A., van Zwieten, P.A.M. (2014). The role of spatial information in the preservation of the shrimp nursery function of mangroves: A spatially explicit bio-economic model for the assessment of land use trade-offs. *Journal of Environmental Management, 143*, 17-25.

Zhai, Y. (2006). Soil texture classification with artificial neural networks operating on remote sensing data. *Computers and Electronics in Agriculture*, *54*, 53 – 68.

Zhi-Guang, L. (1985). Oxidation-reduction potential. In Y. Tianren (Ed). *Physical Chemistry of Paddy Soils* (pp. 1-26). Berlin: Springer.

Zhu, A.X., Hudson, B., Burt, J., Lubich, K., & Simonson, D. (2001). Soil mapping using GIS, expert knowledge, and fuzzy logic. *Soil Science Society of American Journal. 65(5),* 1463-1472.

Zuidam, R.A. van (1986). *Aerial Photo-interpretation in Terrain Analysis and Geomorphologic Mapping*. The Hague, The Netherlands: Smiths Publication.

Zuidam, R.A. van, Farifteh, J., Eleveld, M.A., & Tao, C. (1998). Development in remote sensing: Dynamic modeling and GIS application for integrated coastal zone management. *Journal of Coastal Conservation, 4*, 191 – 202.